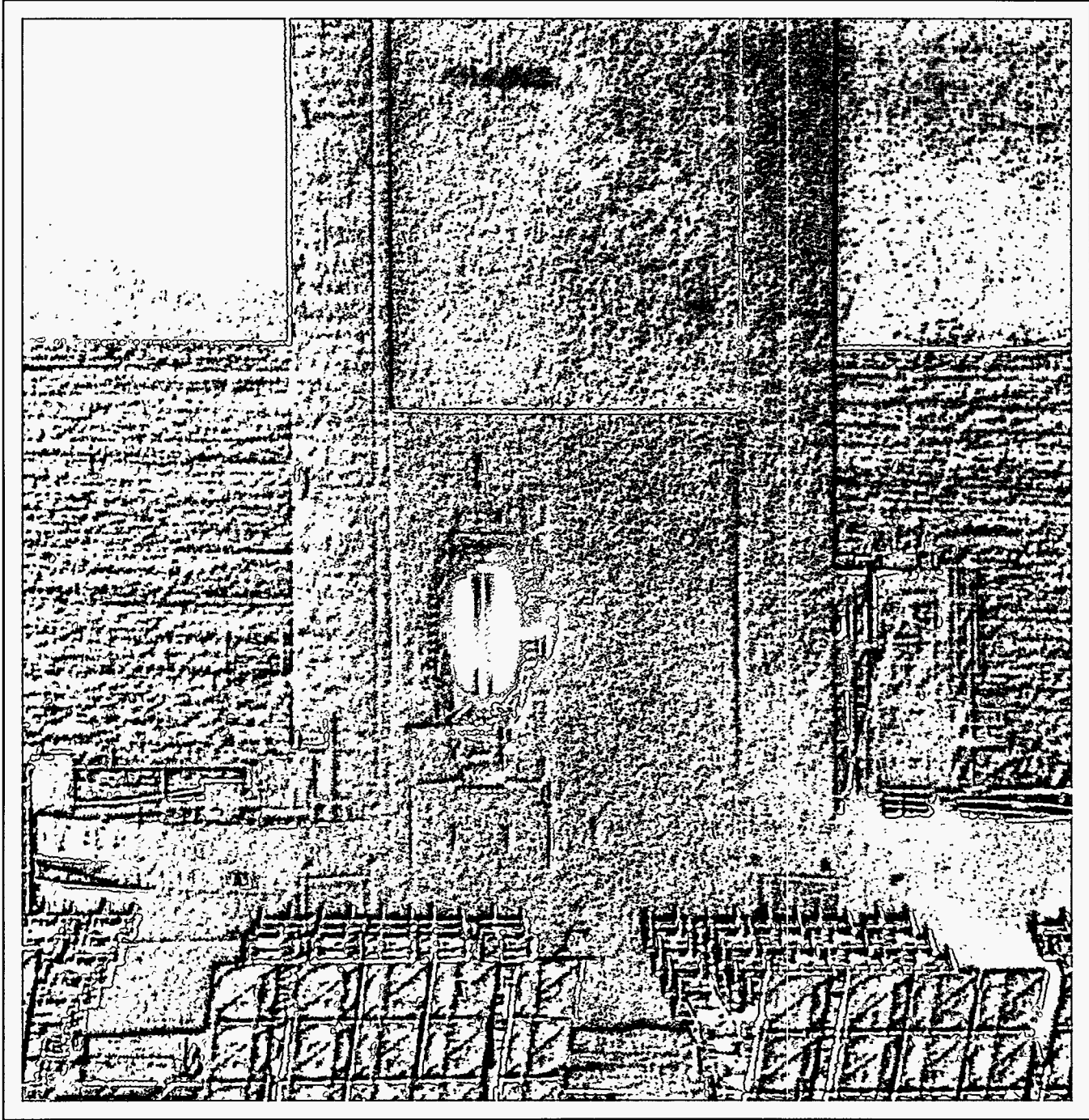


Results of Molten Salt Panel and Component Experiments for Solar Central Receivers: Cold Fill, Freeze/Thaw, Thermal Cycling and Shock, and Instrumentation Tests

James E. Pacheco, Mark E. Ralph, James M. Chavez,
Sam R. Dunkin, Earl E. Rush, Cheryl M. Ghanbari and Matt W. Matthews
Solar Thermal Technology and Test Departments

SAND94-2525

Printed January 1995



Issued by Sandia National Laboratories, operated for the United States Department of Energy by Sandia Corporation.

NOTICE: This report was prepared as an account of work sponsored by an agency of the United States Government. Neither the United States Government nor any agency thereof, nor any of their employees, nor any of their contractors, subcontractors, or their employees, makes any warranty, express or implied, or assumes any legal liability or responsibility for the accuracy, completeness, or usefulness or any information, apparatus, product, or process disclosed, or represents that its use would not infringe privately owned rights. Reference herein to any specific commercial product, process, or service by trade name, trademark, manufacturer, or otherwise, does not necessarily constitute or imply its endorsement, recommendation, or favoring by the United States Government, any agency thereof, or any of their contractors or subcontractors. The views and opinions expressed herein do not necessarily state or reflect those of the United States Government, any agency thereof, or any of their contractors.

Printed in the United States of America. This report has been reproduced directly from the best available copy.

Available to DOE and DOE contractors from
Office of Scientific and Technical Information
PO Box 62
Oak Ridge, TN 37831

Prices available from (615) 576-8401, FTS 626-8401

Available to the public from
National Technical Information Service
US Department of Commerce
5285 Port Royal Rd
Springfield, VA 22161

NTIS price codes
Printed copy: A16
Microfiche copy: A01

DISCLAIMER

Portions of this document may be illegible in electronic image products. Images are produced from the best available original document.

SAND94-2525
Unlimited Release
Printed January 1995

Distribution Category
UC-1301

**RESULTS OF MOLTEN SALT PANEL AND COMPONENT EXPERIMENTS FOR
SOLAR CENTRAL RECEIVERS: COLD FILL, FREEZE/THAW,
THERMAL CYCLING AND SHOCK, AND INSTRUMENTATION TESTS**

James E. Pacheco, Mark E. Ralph, James M. Chavez,
Sam R. Dunkin, Earl E. Rush, Cheryl M. Ghanbari and Matt W. Matthews
Solar Thermal Technology and Test Departments

RECEIVED
APR 03 1995
OSTI

Abstract

Experiments have been conducted with a molten salt loop at Sandia National Laboratories in Albuquerque, NM to resolve issues associated with the operation of the 10MW_e Solar Two Central Receiver Power Plant located near Barstow, CA. The salt loop contained two receiver panels, components such as flanges and a check valve, vortex shedding and ultrasonic flow meters, and an impedance pressure transducer. Tests were conducted on procedures for filling and thawing a panel, and assessing components and instrumentation in a molten salt environment. Four categories of experiments were conducted: 1) cold filling procedures, 2) freeze/thaw procedures, 3) component tests, and 4) instrumentation tests. Cold-panel and -piping fill experiments are described, in which the panels and piping were preheated to temperatures below the salt freezing point prior to initiating flow, to determine the feasibility of cold filling the receiver and piping. The transient thermal response was measured, and heat transfer coefficients and transient stresses were calculated from the data. Analysis is presented which quantifies the thermal stresses in a pipe undergoing thermal shock. In addition, penetration depths were calculated to determine the distances salt could flow in cold pipes prior to freezing shut and validated with panel tests. Freeze/thaw experiments were conducted with the panels, in which the salt was intentionally allowed to freeze in the receiver tubes, then thawed with heliostat beams to assess permanent deformation in the tubes, and to develop procedures to thaw a panel so minimal damage occurs. Slow thermal cycling tests were conducted to measure both how well various designs of flanges (e.g., tapered flanges or clamp type flanges) hold a seal under thermal conditions typical of nightly shut down, and the practicality of using these flanges on high maintenance components. In addition, the flanges were thermally shocked to simulate cold starting the system. Instrumentation such as vortex shedding and ultrasonic flow meters were tested alongside each other, and compared with flow measurements from calibration tanks in the flow loop.

MASTER

DISTRIBUTION OF THIS DOCUMENT IS UNLIMITED *n/w*

ACKNOWLEDGMENT

We would like to acknowledge the following for their contribution to the molten salt panel and component experiments:

Greg Kolb
Scott Rawlinson
Craig Tyner
-Roy Tucker
John Kelton
Darrell Johnson
Clifford Hilliard
Albert Mitchusson.

We would also like to thank Ann Van Arsdall for providing helpful suggestions to the report and acknowledge Tech Reps for formatting the manuscript.

Contents

I. BACKGROUND	1
II. SYSTEM DESCRIPTION	3
III. TEST RESULTS	7
COLD FILL TESTS	7
Results of Cold Fill Panel, Manifold, and Piping Tests	7
Thermal Analysis During Cold Fill	10
Transient Stress Analysis of Piping and Tubes Undergoing Thermal Shock - Nondimensional Analysis	12
Calculations of Penetration Distances - Transient Freezing in Pipes	20
Summary of Cold Fill Tests	22
FREEZE/THAW EXPERIMENTS	23
COMPONENT TESTS	28
Check Valve Cycling	28
Slow Thermal Cycling of Flanges	29
Thermal Shocking of Flanges	33
INSTRUMENTATION TESTS: FLOWMETERS AND PRESSURE TRANSDUCER	34
Flowmeters	34
Pressure Transducer	40
IV. ONGOING AND FURTHER RESEARCH.....	41
SIMPLE ELEMENT FREEZE/THAW TESTS (ONGOING).....	41
BALL VALVES TEST	41
TRANSIENT FREEZING EXPERIMENTS	41
IMPEDANCE HEATING SYSTEM.....	42
MULTIPORT VALVE.....	42
V. REFERENCES	43
APPENDIX A. FINITE ELEMENT ANALYSIS OF FLANGE UNDERGOING THERMAL SHOCK	45
APPENDIX B. FABRICATION OF HEAT TRACE CIRCUITS	81
APPENDIX C. HEAT TRANSFER COEFFICIENT FOR CIRCUMFERENTIALLY VARYING HEAT FLUX	91
APPENDIX D. STRAIN EQUATIONS FOR A RECEIVER TUBE UNDER HIGH FLUX	95
APPENDIX E. MOLTEN AND SOLID NITRATE SALT PROPERTIES	97
Molten Nitrate Salt.....	97
Phase Change Nitrate Salt Properties.....	97
Solid Salt.....	98
APPENDIX F. SELECTED SETS OF DATA AND OTHER INFORMATION.....	99

List of Figures

1.	Flow schematic of the system and the wing panels.	4
2.	Molten salt panels and flow loop at the base of the Central Receiver Test Facility at Sandia National Laboratories in Albuquerque, NM.....	5
3.	Temperature response of the cold tubes and manifolds as they are filled with 550°F (288°C) salt.....	8
4.	Temperature ramp rates of first, second, third, and fourth pass tubes	9
5.	Outside wall temperature as a function of time of a 2 inch schedule 40 pipe undergoing thermal shock.....	10
6.	Nondimensional circumferential thermal stresses in pipe undergoing thermal shock as function of the nondimensional radius for several times (Fo) using thirty terms in of the nondimensional temperature equation (Eq. 1) for $r_i/r_o=0.8$ and $Bi=100$	14
7.	Nondimensional radial thermal stresses in pipe undergoing thermal shock as function of the nondimensional radius for several times (Fo) using thirty terms in of the nondimensional temperature equation (Eq. 1) for $r_i/r_o=0.8$ and $Bi=100$	14
8.	Nondimensional axial thermal stresses in pipe undergoing thermal shock as function of the nondimensional radius for several times (Fo) using thirty terms in the nondimensional transient temperature equation (Eq. 1) for $r_i/r_o=0.8$ and $Bi=100$	15
9.	Effect of the Biot number on the nondimensional circumferential thermal stress distribution for a specific time ($Fo=0.2$) and $r_i/r_o=0.8$	15
10.	Nondimensional thermal (circumferential or axial) stress at the inner surface of the pipe undergoing thermal shock as a function of time (Fo) for several Biot numbers using 30 terms of the series in the nondimensional transient temperature equation (Eq. 1) for $r_i/r_o=0.8$	16
11.	The maximum nondimensional thermal stress as a function of the Biot number for a pipe undergoing thermal shock for $r_i/r_o=0.8$. These are the maxima of Figure 10	17
12.	The time (Fo) when the maximum thermal stress occurs as a function of the Biot number	17
13.	Maximum stress at the inside wall as a function of velocity for 6 inch piping.....	18
14.	Maximum stress at the inside wall as a function of velocity for 16 inch piping.....	19
15.	The penetration depths for several pipe diameters as a function flow velocity	21
16.	Temperatures receiver panels and header as they cool when filled with molten salt which freezes in the panel at approximately 430°F (221°C)	24
17.	Permanent strain induced in the east panel tubes as a function of the panel height after two freeze/thaw cycles.....	25
18.	Permanent strain induced in the west panel tubes as a function of the panel height after two freeze/thaw cycles.....	25
19.	Permanent strain as a function of the width (tube number) for the east panel.....	26
20.	Permanent strain as a function of the width (tube number) for the west panel.....	26
21.	Photograph of the 3 inch check valve (V-CON model manufactured by Reflange, Inc.) tested in the salt loop	29
22.	Pressure and flow as a function of time during a typical check valve cycle.....	30
23.	Typical slow thermal cycle of flanges simulating nightly cool down of components followed by slow heatup with heat trace.....	31
24.	Schematic of ECON and RCON flanges.....	32
25.	Typical temperature transient of the flanges during a shock.....	33
26.	Response of vortex and ultrasonic flowmeters during a varying flow condition	36

27.	Comparison of the vortex and ultrasonic flowmeters against the calibration tank flowrate	38
28.	Measured bias errors (relative to the calibration tank flowrate) for each flowmeter as a function of flow.....	38
29.	Measured random errors for each flowmeter as a function of flow.....	39

List of Tables

1.	Components and instrumentation tested in molten salt loop	6
2.	Biot numbers and heat transfer coefficients during cold fill experiments	12
3.	Calculated Maximum Stresses at the Inner Wall of Piping or Tubes Initially at 25°C Undergoing Thermal Shock with Molten Salt at 290°C based on the Biot Numbers from Experiments.....	18
4.	Maximum velocities during cold fill where maximum thermal stresses are below endurance limit of the material for $T_{wall} = 25^{\circ}\text{C}$ and $T_{salt} = 288^{\circ}\text{C}$	19
5.	Penetration depths for molten salt for various pipe diameters, velocities, and salt inlet temperatures for a wall temperature $T_w = 68^{\circ}\text{F}$ (20°C).....	20
6.	Results for cold start experiments with the MSEE external receiver along with the correlation results	22
7.	Estimated penetration depths for Rockwell's Solar Two receiver	22
8.	Pre- and Post-Measurements of Tube Diameters in East and West Panel after two Freeze/Thaw Cycles	27
9.	Bias Limit Sources for Calibration Tank Flow Measurements.....	37
10.	Root-sum-square Uncertainty (U_{RSS}) for Each Flowmeter.....	39

Nomenclature

Bi = Biot number
Cp_s = specific heat of solid
Cp_m = specific heat of liquid
D = diameter of pipe
E = modulus of elasticity
Fo = Fourier number
h = heat transfer coefficient
h_f = heat of fusion
k = thermal conductivity of pipe (Eq. 5)
L = wall thickness
Nu = Nusselt number
Pr = Prandtl number
r = radial coordinate of pipe
r_i = inner radius of pipe
r_o = outer radius of pipe
r* = nondimensional pipe radius
R = radial coordinate of inner radius of pipe
R_o = radial coordinate of frozen layer
Re = Reynolds number
T = temperature
T_f = freezing point
T_i = initial wall temperature
T_o = inlet liquid temperature
T_w = wall temperature
T_∞ = fluid temperature
x* = nondimensional distance from insulated surface
z = distance to freeze closed
α = thermal diffusivity (Eq. 3) or coefficient of thermal expansion (Eq. 9)
α_m = thermal diffusivity of liquid
α_s = thermal diffusivity of solid
δ = 1 - r_i* = nondimensional wall thickness
λ_n = characteristic values of transient conduction equation
γ = parameter measuring the relative importance of sensible to latent heat, assumed to be 0.7 (water)
θ* = nondimensional temperature
θ_o* = nondimensional temperature at the insulated surface
σ_θ = circumferential stress
σ_r = radial stress
σ_z = axial stress
σ* = nondimensional thermal stress
ν = Poisson's ratio

Executive Summary

This report summarizes experiments we conducted with a molten salt flow loop, located at the Central Receiver Test Facility at Sandia National Laboratories in Albuquerque, New Mexico, under the US DOE Central Receiver Development Program. Experiments were conducted to test hardware and instrumentation in a molten salt environment and to develop procedures that support the design and operation Solar Two. Solar Two is a 10 MW_e Solar Central Receiver Pilot plant in Daggett, California, which is undergoing retrofit with a receiver and storage system which use molten salt as the heat transfer fluid. The major conclusions and recommendations from our experiments with the molten salt loop are summarized below.

Cold Fill Tests

We successfully showed that molten salt can flow through ambient temperature piping without freezing shut provided the flow rate is high enough. These results were scaled to the riser and down comer of the Solar Two and a 100 MW_e molten salt power plant using a correlation. These large diameter pipes should not freeze closed during the cold filling procedure (e.g., at morning startup). The thermal stresses during this thermal shock were calculated to be lower than the material's endurance limit for vertical runs of the piping. We recommend testing the cold filling method in the riser and downcomer of Solar Two and if it proves favorable, implemented as a mode of operation in commercial plants to reduced parasitic power consumption and increase availability.

We found every region of the receiver does not have to be above the salt freezing point before flow is initiated. The minimum temperature to avoid freezing during startup for the Solar Two receiver is estimated to be 200°F (93°C). We found the best method for preheating a panel was to use moving heliostats to avoid hot or cold spots.

Freeze/Thaw Tests

A receiver panel which becomes frozen with salt could require hours to thaw and could damage the tubes. We measured permanent strains as high as 4% after two freeze/thaw cycles. Monitoring the temperatures during the thawing process was also difficult with a limited number of thermocouples, but an infrared camera would simplify the monitoring.

Component Tests

We found that check valves work well in a molten salt environment after repeated pressure cycling and recommend their use. Flanges held up well to slow thermal cycling and to thermal shocking without major failures. All the flanges tested, though, began to leak slowly. Flanges should be minimized in a molten salt loop. Hot torquing the flanges, periodically, may help reduce the leaks.

Instrumentation Tests

Vortex shedding flow meters worked exceedingly well with molten salt and are the preferred flow meter for this application. Overall flow rate uncertainties of less than $\pm 5\%$ can be obtained with a proper calibration. The impedance-type pressure transducer we tested was responsive and performed well. It could replace hard to find NaK filled pressure transducers. The impedance type is relatively expensive, though.

I. Background

In a molten salt central receiver power plant, the parasitic electrical power consumption can be a significant percentage of the total power production if it is not properly managed. Good management also involves careful assessment of operating strategies to minimize the parasitics. Since the nitrate salt, which serves as the heat transfer medium between the receiver and the steam generator, has a freezing point of 430°F (221°C), the associated piping, valves, instrumentation, and tanks must be kept above this temperature (typically at 550°F, 288°C) to assure the salt will not freeze. During inclement weather and during the night the plant does not operate, but the heat trace is kept energized to maintain the temperature of the empty lines at 550°F (288°C). This operating strategy is not an economically advantageous method of conditioning a highly cyclic power plant. One strategy of reducing the nightly parasitic power consumption is to turn off the heat trace at night, allowing the piping to cool down to ambient, then fill the piping cold at start up the next morning.

There has been very little data collected on cold starting the receiver and piping at temperatures below the molten salt freezing point. The Molten Salt Electric Experiment receiver in the external configuration was cold started at temperatures below the freezing point. In one of three cases, the receiver partially froze [1]. No detailed analysis was done on the transient freezing phenomenon. In this report we describe experiments where we cold started receiver panels and piping.

Due to the nitrate salt's high freezing point and the fact that the salt expands upon melting, we were concerned with the damage that could occur in receiver tubes if the salt were to freeze in the receiver and then thaw out. This situation could occur during shut down of the receiver. If one of the drain valves failed to open and went undetected during the drain process, molten salt would be trapped in the associated panel, and the salt would subsequently freeze. Upon thawing, the expanding salt could damage the tube. In previous experiments, detailed assessments of the freezing and thawing of the panel tubes were not conducted. The Martin Marietta molten salt receiver became frozen with salt and was successfully thawed, though no data on tube deformation was available.

Three molten salt receivers and large-scale pump and valve loops have been tested at Sandia National Laboratories to determine the viability of molten salt as a heat transport fluid and storage medium for central receiver solar power plants. The Category B receiver was a 5 MWt cavity molten nitrate salt receiver. The testing of this receiver in 1988 [2] showed the feasibility of fabricating and operating a molten salt receiver consisting of serpentine flow panels. However, there are some components and instrumentation that need further evaluation.

Check valves have not previously been used in molten salt. Check valves are required when pumps are connected in series to a common manifold, or to the base of a riser to prevent back spin and damage to a pump during a sudden shut off of one pump while the others are flowing. Experiments with flanges in the Pump and Valve Loop show that they were a significant source of leaks.

The purpose of the current molten salt experiments is to verify the operation and reliability of components, instrumentation, and procedures proposed for implementation in the Solar Two project. Many of the components have been proven in a molten salt environment, but additional information is required. Other components were not tested sufficiently or at all in previous molten

salt experiments. The goal of these tests was to reduce uncertainties concerning the performance of untested components and operating procedures (e.g., cold filling the receiver or piping, and thawing a frozen panel.)

We conducted these tests to address concerns by the Solar Two Technical Advisory Committee - a committee of utilities, industries, the U.S. Department of Energy, and Sandia National Laboratories overseeing the technical issue of the Solar Two Project. The technical needs and concerns were prioritized, and a test program was developed. Consequently, some issues, such as thermal cycling of full scale valves, could not be implemented. However, this test program did address all the high priority issues.

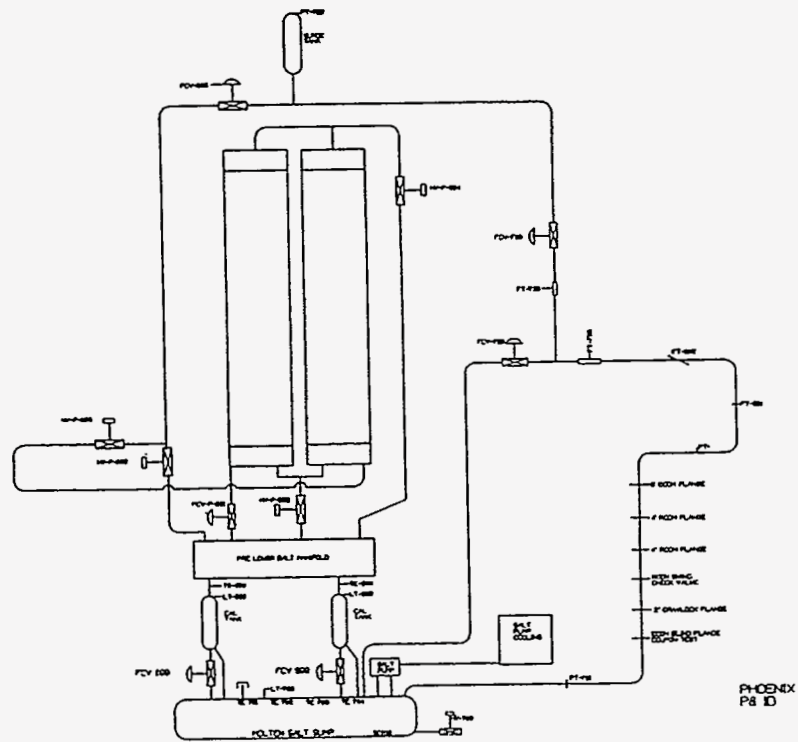
II. System Description

The experiments were conducted with an existing molten salt loop initially built for a direct absorption receiver [3]. It was modified to accommodate two wing panels (fabricated by Foster Wheeler Corporation) removed from a salt-in-tube receiver (the Category B receiver) to evaluate a cold receiver startup procedure and conduct freeze/thaw experiments. Each panel consists of two serpentine flow passes which have six 1 inch (2.5 cm) OD 304 stainless steel tubes with 0.065 inch (1.65 mm) thick walls. The two passes are connected to a common 6 inch (15 cm) diameter manifold (schedule 80 piping) at the top of the panel. Each panel vent connects to a common 1 inch vent line, in which a hand valve is located to vary the venting flow rate. The experiment was located at the base of the Solar Tower at the National Solar Thermal Test Facility in Albuquerque, NM. Figure 1 is a schematic of the system and the wing panels. Figure 2 is a photograph of the panels and flow loop.

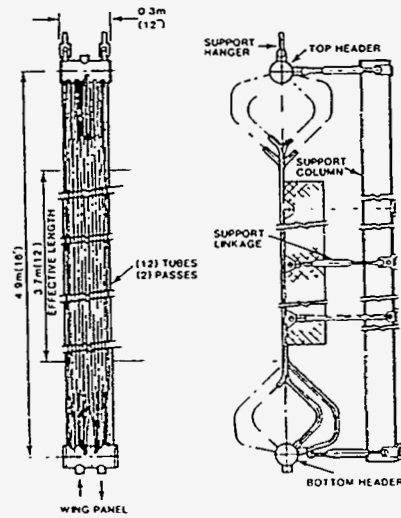
In this flow loop, salt is pumped from the salt sump, through the components, then either returned to the sump or diverted up the riser. At the top of the riser is the pressurized accumulator (surge) tank. The flow goes through the down comer, and can either be diverted to the panel or a manifold. The outlet of the panel flows into the manifold. The manifold drains into two calibration tanks. Flow from the calibration tanks returns to the sump. The pump can flow salt at 100 gallons per minute (380 liters/min) through the 2 inch (5.1 cm) piping.

We added flanges, a check valve, flow meters, and pressure transducers to test their performance. Three types of flanges were tested: 1) clamped, compressive metal-seal type flanges made by Reflange (R-CON) and by Grayloc, 2) bolted, compressive metal-seal flanges (E-CON) also made by Reflange, and 3) a standard ANSI ring-joint flange. The check valve, manufactured by Reflange (V-CON), was a spring-loaded, swing-type check valve. Two types of flow meters were tested: 1) vortex shedding flow meters made by Engineering Measurements Company, and 2) ultrasonic flow meters (wetted type and clamp on type transducers) manufactured by Panametrics. In addition, we installed pieces of performed fiberglass insulation to determine their viability as another insulation material. This insulation is easier to install than the wool blanket or calcium silicate insulation previously used. Its upper temperature limit is approximately 850°F. Table 1 lists the components we tested.

Although we were not able operate the flow loop at the pressures expected to be encountered in the cold side of a typical molten salt system, we were able to simulate operational and thermal cycling expected on the cold side of the system where the thermal ramp rates and stresses are typical of nightly conditioning. The ramp rates on the hot side of a molten salt system (down stream of a receiver) are very difficult to simulate with the existing loop, and therefore were not simulated with this test setup.



a)



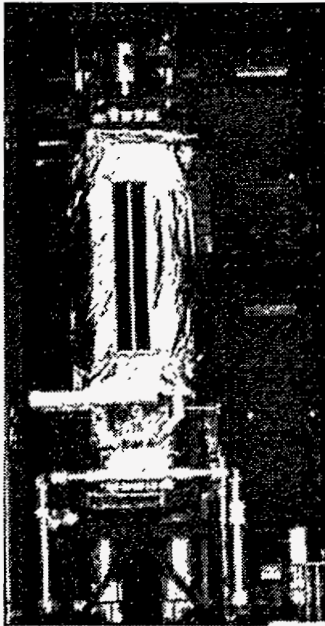
b)

c)

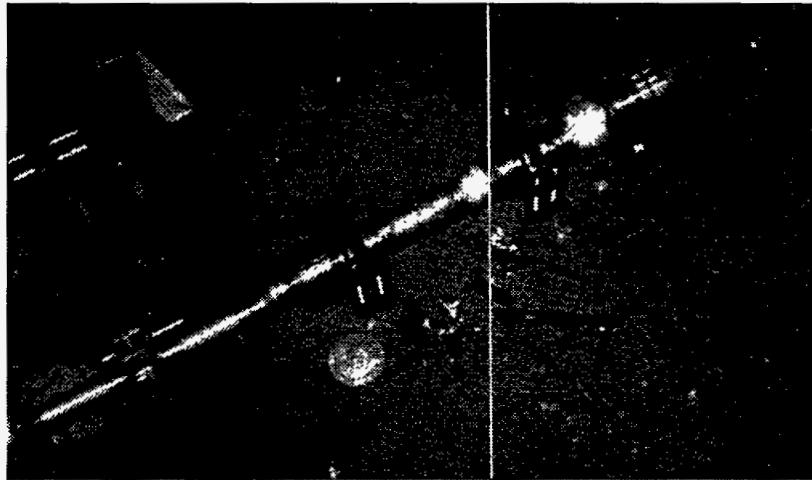
Figure 1. Flow schematic of the system (a) and a wing panel front (b) and side view (c).



a)



b)



c)

Figure 2. Photographs of molten salt panels (a and b) and flow loop test section (c) at the base of the Central Receiver Test Facility at Sandia National Laboratories.

Table 1. Components and instrumentation tested in molten salt loop.

Component or instrumentation	Type	Size	Manufacturer
Flange	Clamped, compressive metal seal type	2 inch and two 4 inch	Reflange (R-CON) and Grayloc (2 inch)
Flange	Bolted, compressive metal seal type	6 inch	Reflange (R-CON)
Flange	ANSI ring type flange	4 inch	standard
Check valve	Spring loaded swing	3 inch	Reflange (V-CON)
Flow meter	Vortex shedding	2 inch	Engineering Measurements Co.
Flow meter	Ultrasonic - wetted transducer	2 inch	Panametrics
Flow meter	Ultrasonic - clamp on transducer	any sized pipe up to 10 feet dia.	Panametrics
Pressure transducer	High temperature Impedance	0-250 psi range	Kaman

III. Test Results

Cold Fill Tests

Cold filling involves flowing molten salt through piping or the receiver when all or part is below the salt freezing point. Cold filling has several advantages in the operation of a plant that experiences cyclic operation. If the molten salt can flow through parts of the system which are below the freezing point, parasitics could be reduced, since the heat trace would not have to be used on those lines. In addition, the operation of the plant could be more flexible if the plant could be brought on line faster by not having to wait for the heat trace to heat the lines to operating temperatures resulting in increased availability. Also, during morning startup, it is difficult to uniformly preheat the entire receiver. Some spots will experience much more heating than others due to non-uniform flux profiles from heliostats. This is a particular concern for the east side of a cylindrical receiver during morning start up. Localized convection will add to the problem. A roving aiming strategy, where the heliostat aim points are periodically changed, could provide more uniform heating of the receiver panels, thus avoiding severe hot or cold spots. Also, if the receiver can be filled with molten salt when areas of the receiver are below the salt freezing point, the receiver start up procedure would be much simpler, and could occur sooner. These strategies will boost performance and reduce operating expenses, resulting in lower energy costs. There are two major concerns with cold filling components and piping: freezing of the flowing salt, and transient thermal stresses.

We conducted cold fill experiments on the panels and on a section of piping. We measured the thermal response as the panel or piping underwent the rapid change in temperature, and estimated the heat transfer coefficients during this transition. We also derived expressions describing the transient stresses a pipe or tube will experience during a thermal shock. Using a correlation which describes the penetration distance of a liquid as a function of the fluid properties and flow conditions, we estimated the distance salt could flow through cold piping before freezing shut.

Results of Cold Fill Panel, Manifold, and Piping Tests. We conducted tests varying the initial panel temperature to determine whether salt could flow through all four passes of the panel before freezing shut. The flow velocity was approximately the same for each test, 2 ft/s (0.6 m/s). The purposes of these tests were to 1) determine if salt flow could be established in "cold" manifolds, panels, and piping, 2) measure the thermal responses of the tubes and manifolds undergoing thermal shock, and 3) estimate the corresponding stresses in the materials.

We conducted a series of tests trying lower and lower panel preheat temperatures ranging from 550 °F (288°C) to ambient before initiating salt flow. Next, we tried flowing salt through cold (near ambient) manifolds (heat trace off) with the panels preheated to 550°F. Then we tried flowing through cold manifolds and cold panels. Each scenario was repeated several times.

We found we were able to consistently flow through ambient temperature manifolds and panels without freezing salt or blocking tubes. In our test loop, we were able to fill the panels only in a serpentine fashion. To prevent entrapment of air, we had to fill the panel slowly (~2 ft/s, 0.6 m/s). Figure 3 shows the temperature response of the tubes and upper manifold as they are filled with 550°F (288°C) salt. The receiver tubes were initially at 50°F (10°C). The header was

Temperatures During Cold Fill

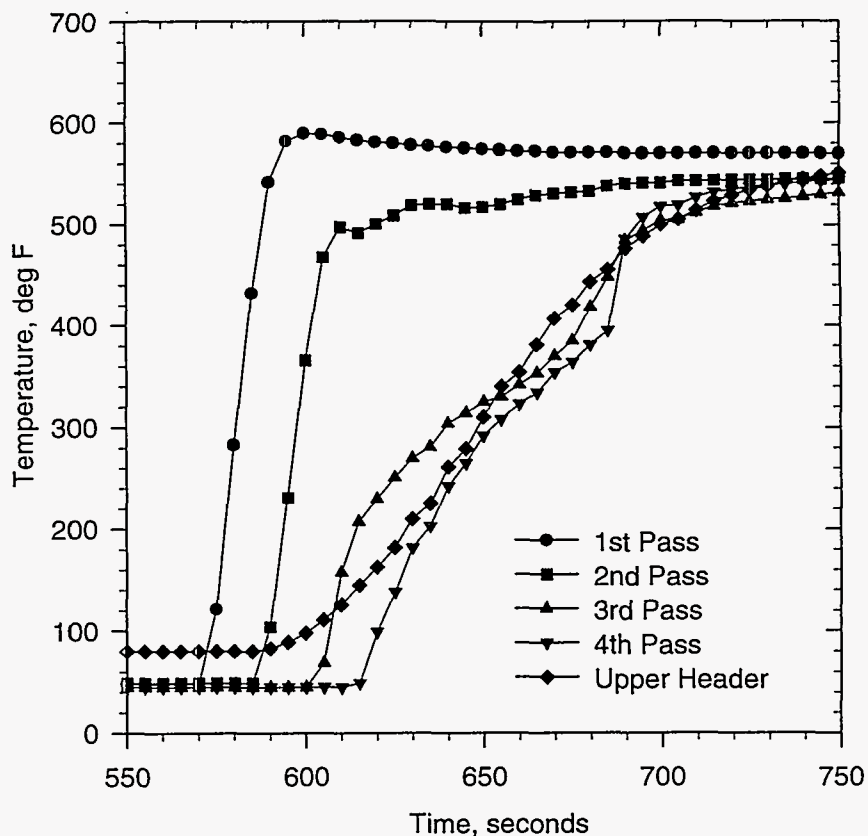


Figure 3. Temperature response of the cold receiver tubes and upper header as they are filled with 550°F (288°C) salt.

initially hotter than the panels, since an adjacent heat trace zone conducted heat to the header. The header and first pass receiver tubes experienced the greatest thermal shock. As the salt continued through the other passes, the temperature of the initial slug of salt decreased, resulting in the deposition of a frozen layer of salt on the tube wall, which reduced the shock, then melted away. This can be inferred from the change in slope of the fourth pass tube temperature and the upper header temperature. Figure 4 shows the temperature ramp rates of first, second, third, and fourth pass tubes. Note how the third and fourth passes show lower peak ramp rates. A frozen layer of salt is likely responsible for the reduced peak ramp rates, since as the initial slug of salt comes in contact with the cold tube surface, a frozen layer develops which limits the rate at which the temperature can rise, and provides some thermal capacitance. The outside tube temperature corresponding to the peak ramp rate in the fourth pass is approximately 395°F (202°C).

A thermal analysis was conducted on a receiver tube and header during this thermal shock, and is described in the Thermal Analysis section. The estimated heat transfer coefficients were calculated. In addition, calculations on the penetration depths—the distance a fluid flows through cold piping before freezing shut—are also discussed in the Calculation of Penetration Distances section.

Ramp Rates

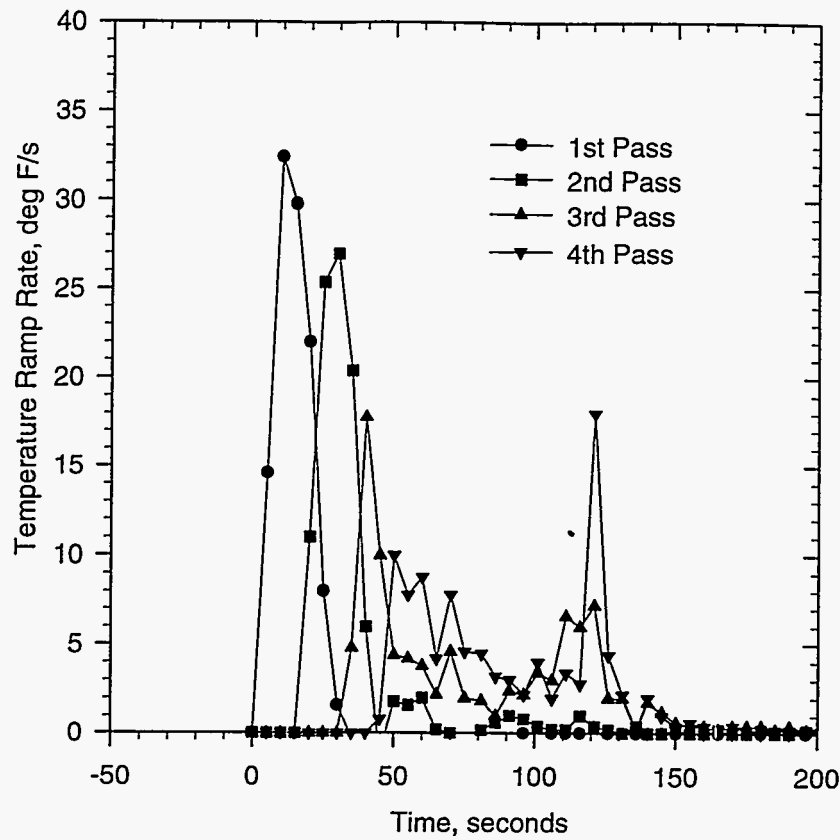


Figure 4. Temperature ramp rates of first, second, third, and fourth pass tubes.

The stresses in the receiver tube were calculated using the heat transfer coefficients obtained from the experiment. A stress model is described in the Transient Stress Analysis section. Stresses in the tube-to-header junction are more complicated, and are dictated by the temperature gradients at the transition.

In addition to cold filling the panels and manifolds, we conducted similar tests on a section of piping. We turned off the heat trace to a section of piping and let it cool to ambient, then initiated salt flow to determine its thermal response and estimate heat transfer coefficients and stresses. We measured the thermal response of an insulated 40 foot (12 m) long, 2 inch (5.1 cm) diameter 316 SS, schedule 40 pipe undergoing thermal shock. The piping was part of the riser. We turned off the heat trace, and allowed it to cool to ambient. When the piping was cold (at ambient), we pumped salt through it at approximately 9.5 ft/s (2.9 m/s) and measured the temperature outside of the pipe. Figure 5 is a plot of the outside wall temperature as a function of time. With this data, we calculated the heat transfer coefficient at the inner wall using a first eigenvalue approximation to an analytical solution of plane wall conduction. These procedures are discussed in the next section.

2" sch40 Pipe

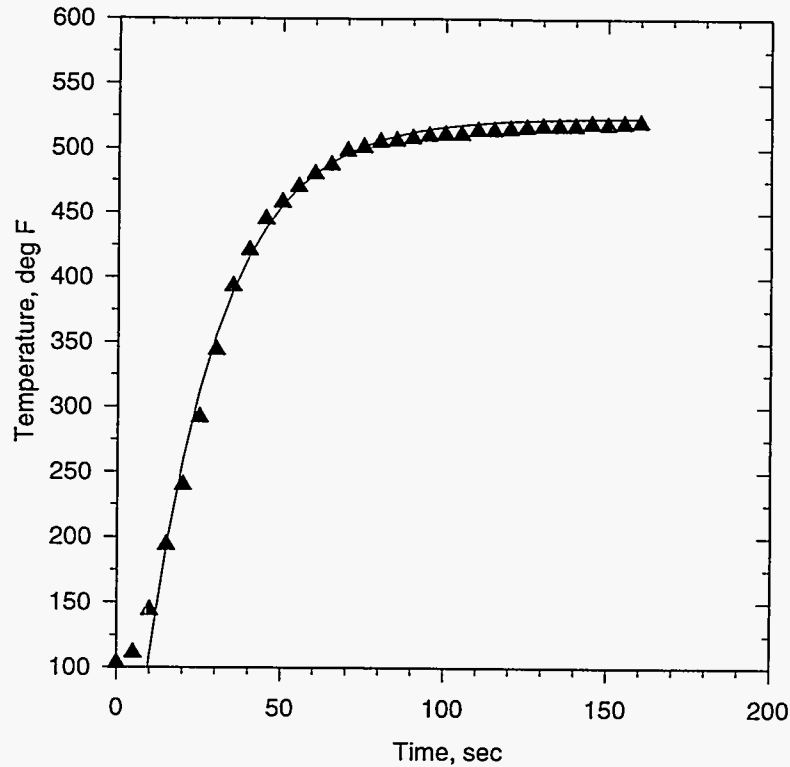


Figure 5. Outside wall temperature as a function of time of a 2 inch schedule 40 pipe undergoing thermal shock. The symbols are actual data points. The solid line is a fit of the data using the thermal model for $Bi = 0.444$.

Thermal Analysis During Cold Fill. In the cold-fill experiment on the panel, manifolds, and piping, we measured the outside wall temperatures as they are thermally shocked. From that data we wanted to obtain the inside wall temperature and the average heat transfer coefficient. The heat transfer coefficient allowed us to calculate the stresses developing in the wall of the pipe or tube as it rapidly heats up.

Assuming that the tube or pipe wall can be approximated as a plane wall, we can use an analytical solution to estimate the inside wall temperature and heat transfer coefficient. Since the receiver tube and piping have relatively thin walls, the plane wall assumption is a good approximation. In our tests, the outside of the pipe, manifolds, and the receiver tubes were insulated. (In actuality, only half of the receiver tube is insulated and the other side is exposed, but this should have minor bearing on the result, since initially the outside natural convective heat transfer to the air is relatively small, and the time scales are short for thermal shock.)

The solution to the energy equation for a plane wall suddenly subjected to a convection boundary condition describes the temperature distribution in the wall as a function of time [4]. Its form is:

$$\theta^*(x^*, t^*) = \frac{T(x, t) - T_\infty}{T_i - T_\infty} = \sum_{n=1}^{\infty} C_n \exp(-\lambda_n Fo) \cos(\lambda_n x^*) \quad (1)$$

where the coefficient C_n :

$$C_n = \frac{4 \sin(\lambda_n)}{2\lambda_n + \sin(2\lambda_n)}, \quad (2)$$

Fo (the Fourier number) is the nondimensional time and x^* is referenced from the insulated surface:

$$Fo = \frac{\alpha t}{L^2}, \quad x^* = \frac{x}{L}. \quad (3, 4)$$

The discrete characteristic values (eigenvalues) of λ_n are the positive roots of the transcendental equation:

$$\lambda_n \tan(\lambda_n) = Bi = \frac{hL}{k}. \quad (5)$$

The length, L , is half the thickness of the plane wall since convection occurs on both faces, but in the case of a pipe or tube wall it is equal to the wall thickness, since one face has convection and the other is insulated. Note the midplane of a plane wall behaves like an insulated surface. The infinite series solution can be approximated by the first term in the series for values of $Fo \geq 0.2$. The solution becomes:

$$\theta^* = C_1 \exp(-\lambda_1^2 Fo) \cos(\lambda_1 x^*) \quad (6)$$

or

$$\theta^* = \theta_o^* \cos(\lambda_1 x^*) \quad (7)$$

where θ_o^* is the temperature at the midplane, $x^*=0$ (the insulated boundary, in our case the outside tube wall). The coefficients C_1 and λ_1 are determined from the equations 2 and 5. Since we measured the outside wall temperature (insulated surface) as a function of time and we knew the approximate salt bulk-fluid-temperature (initial salt temperature), we calculated measured values for θ_o^* and Fo . By iterating on λ_1 until the calculated value of θ_o^* converged on the measured value of θ_o^* , we obtained the Biot number, Bi . From the Biot number we obtained the heat transfer coefficient.

The average heat transfer coefficients determined during the thermal shock for each pass, for the upper header, and for a 2 inch pipe are shown in Table 2. The solid line in Figure 5 is a fit of the data to the model for a constant heat transfer coefficient. Note that initially the temperature changes gradually (the first three data points). In order to get a good fit of the data with the model, the initial starting time of the model had to be adjusted, since the actual heat transfer coefficient is not constant with time. Assuming a constant heat transfer coefficient will yield higher stresses than one which gradually increases to its final value, and thus will be conservative. Stress analyses for an insulated circular pipe undergoing thermal shock are discussed in the next section.

For heat transfer in fully developed pipe flow when applied to freezing with turbulent flow, the following correlation has been suggested to estimate heat transfer coefficients between the fluid and the frozen layer [5]:

$$Nu = 0.0155 Re^{0.83} Pr^{0.5} (R_o/R)^{0.83} \quad (8)$$

Table 2. Biot numbers and heat transfer coefficients during cold fill experiments.

Location	Approx. Velocity m/s	Bi (from data using the model)	h (from Bi) W/m ² K
2" sch40 Pipe	2.9	0.444	1700
6" sch80 Header	0.11	0.881	1200
First Pass Tube	0.67	0.296	2700
Second Pass Tube	0.67	0.243	2200
Third Pass Tube	0.67	0.124	1100
Fourth Pass Tube	0.67	0.114	1000

where R_o is the inner pipe radius and R is the radial coordinate of the frozen layer. This correlation is applicable beyond the thermal entrance length (approximately 10 tube diameters), and provides a conservative estimate of the heat transfer to the pipe, since the frozen layer will act as an insulator.

It should be noted that the heat transfer that occurs when the receiver is under high flux is quite different for a cold start scenario. A description of the heat transfer under high flux is presented in Appendix C.

Transient Stress Analysis of Piping and Tubes Undergoing Thermal Shock - Nondimensional Analysis. The stress calculations are important in determining the material behavior in a severe transient condition. For an insulated pipe, we can use the temperature distribution from the thermal analysis to calculate the circumferential, radial, and axial stresses. These thermal stresses should be superimposed on existing pipe loads due to structural factors. If the temperature is a function of the radial component only, then each component of stress is [6,11]:

$$\sigma_{\theta}(r) = \frac{E\alpha}{(1-\nu)r^2} \left(\frac{r^2 + r_i^2}{r_o^2 - r_i^2} \int_{r_i}^{r_o} T(r)rdr + \int_{r_i}^r T(r)rdr - T(r)r^2 \right) \quad (9)$$

$$\sigma_r(r) = \frac{E\alpha}{(1-\nu)r^2} \left(\frac{r^2 - r_i^2}{r_o^2 - r_i^2} \int_{r_i}^{r_o} T(r)rdr - \int_{r_i}^r T(r)rdr \right) \quad (10)$$

$$\sigma_z(r) = \frac{E\alpha}{(1-\nu)} \left(\frac{2}{r_o^2 - r_i^2} \int_{r_i}^{r_o} T(r)rdr - T(r) \right) \quad (11)$$

The temperature profile at a given time, Fo , can be found from Equation 7:

$$T(r) = \theta_o^* (T_i - T_{\infty}) \cos(\lambda_1 x^*) + T_{\infty} \quad (12)$$

The nondimensional length x^* is referenced from the insulated surface (the outside radius) and can be transformed into the nondimensional radial coordinates, $r^* = r/r_o$ and $r_i^* = r_i/r_o$, from:

$$x^* = (1 - r^*) / (1 - r_i^*) = (1 - r^*) / \delta.$$

In carrying out the integration, the stress components can be expressed in a nondimensional thermal stress format:

$$\sigma^*(r^*) = \frac{\sigma(r)(1-\nu)}{E\alpha(T_1 - T_\infty)} \quad (13)$$

Which for the three stress components are:

$$\begin{aligned} \sigma_\theta^*(r^*) = & \frac{r^{*2} + r_i^{*2}}{1 - r_i^{*2}} \frac{\theta_o^*}{r^{*2}} \left\{ \frac{\delta^2}{\lambda_1^2} [1 - \cos(\lambda_1)] + \frac{\delta r_i^*}{\lambda_1} \sin(\lambda_1) \right\} \\ & + \frac{\delta^2 \theta_o^*}{\lambda_1^2 r^{*2}} \{ \cos(A) - \cos(\lambda_1) \} \\ & - \frac{\delta \theta_o^*}{\lambda_1 r^{*2}} \{ r^* \sin(A) - r_i^* \sin(\lambda_1) \} - \theta_o^* \cos(A) \end{aligned} \quad (14)$$

$$\begin{aligned} \sigma_r^*(r^*) = & \frac{r^{*2} - r_i^{*2}}{1 - r_i^{*2}} \frac{\theta_o^*}{r^{*2}} \left\{ \frac{\delta^2}{\lambda_1^2} [1 - \cos(\lambda_1)] + \frac{\delta r_i^*}{\lambda_1} \sin(\lambda_1) \right\} \\ & - \frac{\delta^2 \theta_o^*}{\lambda_1^2 r^{*2}} \{ \cos(A) - \cos(\lambda_1) \} \\ & + \frac{\delta \theta_o^*}{\lambda_1 r^{*2}} \{ r^* \sin(A) - r_i^* \sin(\lambda_1) \} \end{aligned} \quad (15)$$

$$\begin{aligned} \sigma_z^*(r^*) = & \frac{2\theta_o^*}{1 - r_i^{*2}} \left\{ \frac{\delta^2}{\lambda_1^2} [1 - \cos(\lambda_1)] + \frac{\delta r_i^*}{\lambda_1} \sin(\lambda_1) \right\} \\ & - \theta_o^* \cos(A) \end{aligned} \quad (16)$$

$$A = \frac{\lambda_1}{\delta} (1 - r^*) \quad (17)$$

The characteristic value, λ_1 , is found from the solution to Equation 5 and is a function of the Biot number, Bi , which indicates the relative importance of surface heat transfer to conduction. Equations 14 to 16 are valid for $Fo \geq 0.2$. For smaller times ($Fo < 0.2$), several terms in the series in Equation 1 must be used to calculate the temperature distribution. The temperature distribution is then used in Equations 9-11 to calculate the stresses. These equations can be used to calculate the transient stresses as a function of the Biot number and the pipe geometry. Figures 6, 7, and 8 show the nondimensional circumferential, radial, and axial thermal stresses as function of the nondimensional radius for several times (Fo) for a specific geometry. Note that in Figure 6 a skin stress develops at the inner surface. When the pipe is cold relative to the fluid—"up shock"—the stresses at the inner surface are compressive and tensile on the outer surface during the thermal shock. When it is hot relative to the fluid—"down shock"—the stresses are tensile on the inner surface. Figure 9 shows the effect of the Biot number on the stress distribution for a specific time. Figure 10 shows the nondimensional thermal (circumferential or axial) stress at the inner surface of the pipe as a function of time (Fo) for several Biot numbers using 30 terms of the series in Equation 1. When the heat transfer coefficient is large relative to the pipe thermal conductivity (large Bi numbers), there will be significant temperature gradients across the pipe wall and larger thermal stresses will develop during a thermal shock. At small Biot numbers, conductivity dominates relative to surface heat transfer and there are small thermal gradients across the wall

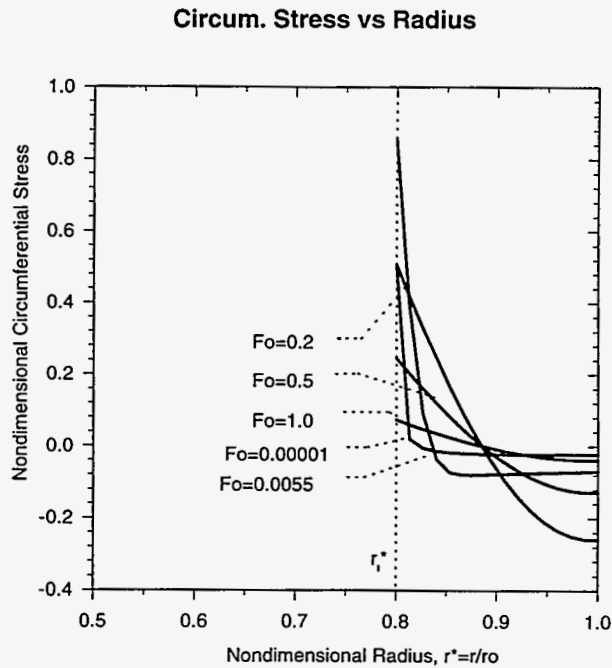


Figure 6 . Nondimensional circumferential thermal stresses in pipe undergoing thermal shock as function of the nondimensional radius for several times (Fo) using thirty terms in of the nondimensional temperature equation (Eq. 1) for $r_i/r_o=0.8$ and $Bi=100$.

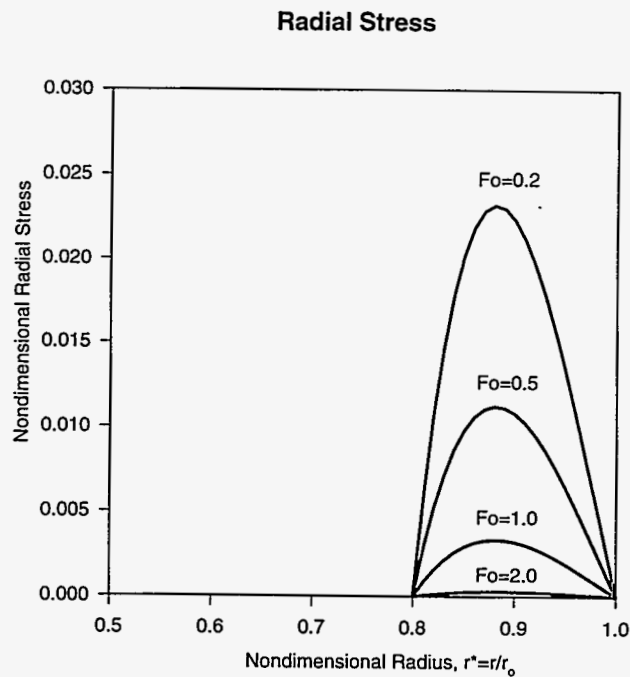


Figure 7 . Nondimensional radial thermal stresses in pipe undergoing thermal shock as function of the nondimensional radius for several times (Fo) using thirty terms in of the nondimensional temperature equation (Eq. 1) for $r_i/r_o = 0.8$ and $Bi=100$.

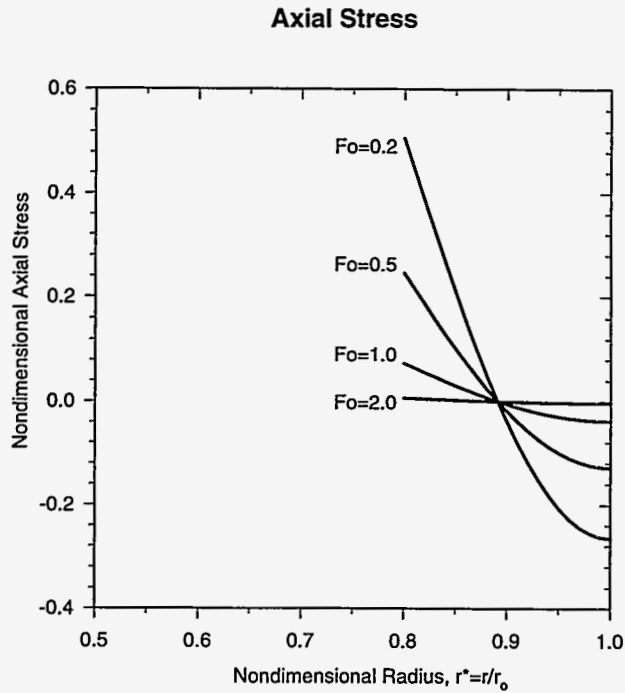


Figure 8. Nondimensional axial thermal stresses in pipe undergoing thermal shock as function of the nondimensional radius for several times (Fo) using thirty terms in the nondimensional transient temperature equation (Eq. 1) for $r_i/r_o = 0.8$ and $Bi=100$.

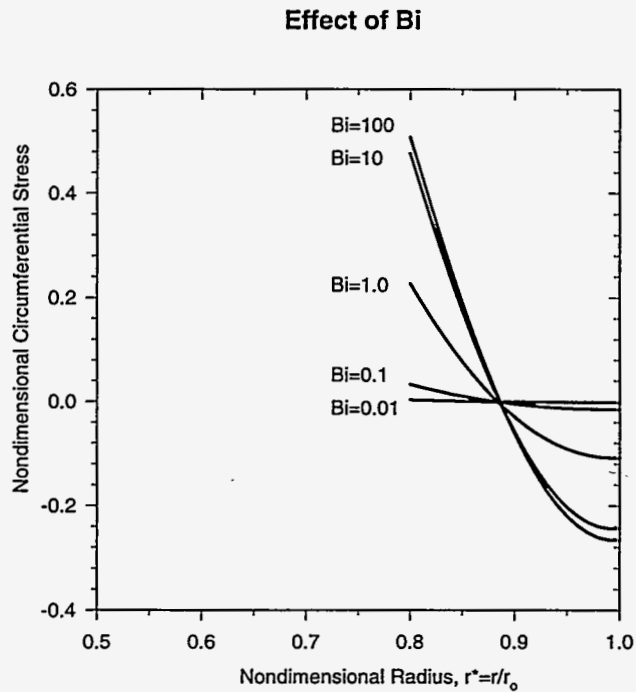


Figure 9. Effect of the Biot number on the nondimensional circumferential thermal stress distribution for a specific time ($Fo=0.2$) and $r_i/r_o = 0.8$.

Stress vs Time (Fo)

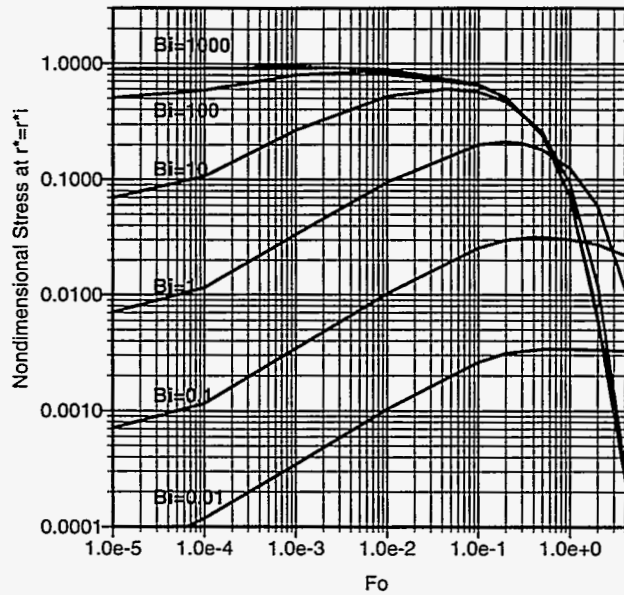


Figure 10. Nondimensional thermal (circumferential or axial) stress at the inner surface of the pipe undergoing thermal shock as a function of time (Fo) for several Biot numbers using 30 terms of the series in the nondimensional transient temperature equation (Eq. 1) for $r_i/r_o=0.8$.

resulting in small thermal stresses. The stresses build with time, reaching a peak, then finally drop as the wall reaches a uniform temperature. Each curve has a maximum thermal stress. These maximum stresses are shown in Figure 11 as a function of the Biot number. Figure 12 shows the time (Fo) when the maximum stress occurs as a function of Biot number.

From the data we gathered during the shock tests, we determined the Biot numbers are relatively small. We used these Biot numbers to calculate the stresses in piping or tubes we thermally shocked: a 2-inch schedule 40 316SS pipe, a 6-in schedule 40 304SS header and a 1-inch 0.065 inch wall 304SS receiver tube. Table 3 shows the maximum equivalent stress based on the maximum energy distortion theory of failure [7], sometimes referred to as the von Mises stress, for each case. In each case the stresses were calculated to be lower than the endurance limit of the material ($\sigma_e \approx 270$ MPa for stainless steel [8]) for these tests indicating that for the test conditions the piping itself can handle these stresses over the life of the system. It is likely these stresses are conservative, since the heat transfer coefficients are not constant, but gradually increase to the equilibrium value.

Maximum Stress vs Bi

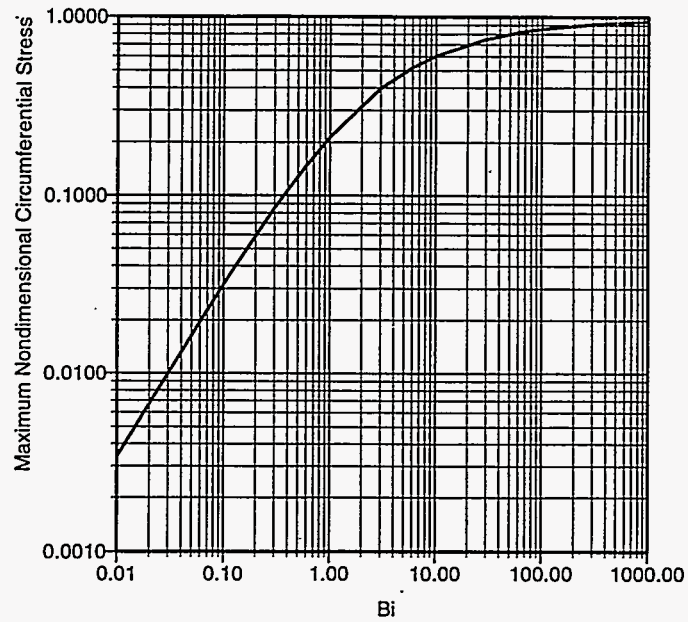


Figure 11. The maximum nondimensional thermal stress as a function of the Biot number for a pipe undergoing thermal shock for $r_i/r_o=0.8$. These are the maxima of Figure 10.

Time When Max. Stress Occurs

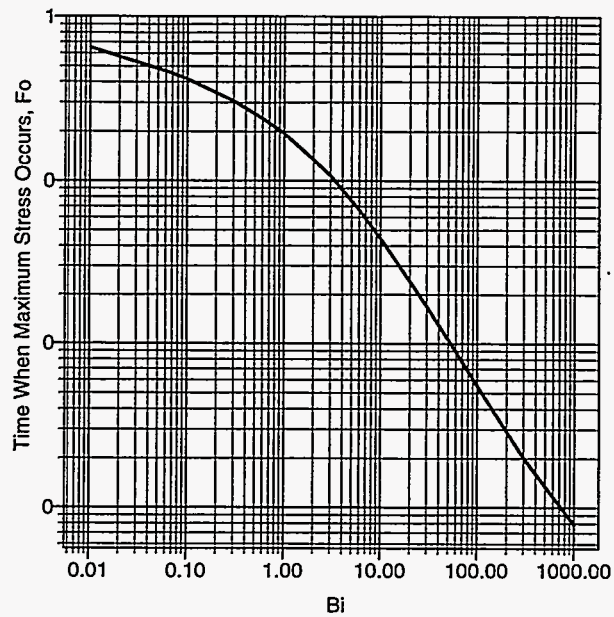


Figure 12. The time (F_o) when the maximum thermal stress occurs as a function of the Biot number.

Table 3. Calculated Maximum Stresses at the Inner Wall of Piping or Tubes Initially at 25°C Undergoing Thermal Shock with Molten Salt at 290°C based on the Biot Numbers from Experiments.

Pipe or Tube Size	$\sigma_{\text{Equivalent}}$, MPa
1 inch receiver tube, 0.065 inch wall, 304 SS	-100
2 inch schedule 40, 316 SS	-140
6 inch schedule 80 header, 304 SS	-240

Using Equation 9, a conservative estimate of the peak circumferential stresses at the inner surface of a pipe or tube can be calculated as a function of salt velocity. Plots of these relations are shown in Figures 13 and 14 for 6 inch and 16 inch piping proposed for handling molten salt in the Solar Two and Commercial scale systems, respectively. There is a critical velocity at which the stresses exceed the endurance limit of the material. These velocities are listed in Table 4 for several pipe schedules and materials proposed for handling molten salt. Carbon steel is able to handle thermal stresses better than stainless steel, because carbon steel has a much lower coefficient of thermal expansion, even though its endurance limit is lower.

Thermal Stresses in 6" Pipe (Stainless Steel)

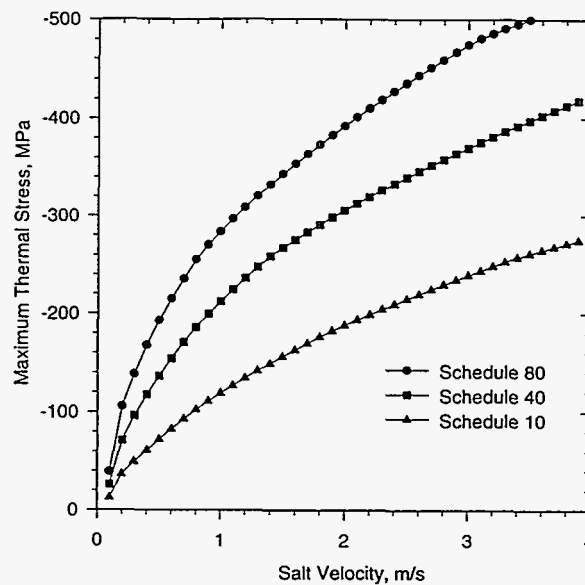


Figure 13. Maximum stress at the inside wall as a function of velocity for 6 inch piping.

Thermal Stresses in Stainless Steel 16 inch Pipe

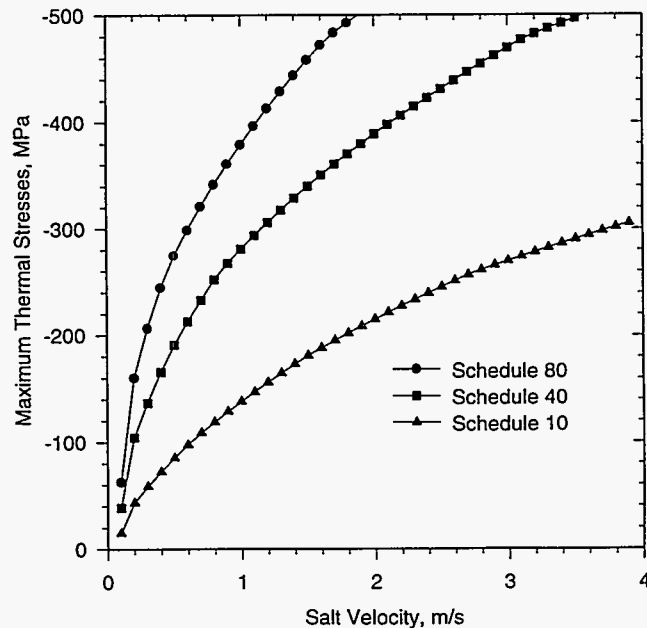


Figure 14. Maximum stress at the inside wall as a function of velocity for 16 inch piping.

Table 4. Maximum Velocities During Cold Fill Where Maximum Thermal Stresses are Below Endurance Limit of the Material for $T_{wall} = 25^{\circ}\text{C}$ and $T_{salt} = 288^{\circ}\text{C}$.

Pipe Size	Schedule	Material	Maximum Velocity, m/s
6 inch	80	Stainless 316	0.9
6 inch	80	Carbon	3.7
6 inch	40	Stainless 316	1.5
6 inch	40	Carbon	6.3
6 inch	10	Stainless 316	3.8
16 inch	80	Carbon	1.9
16 inch	40	Carbon	3.7
16 inch	10	Carbon	12.2
16 inch	10	Stainless 316	5.7

Even though the stresses in the walls of piping or tubes were low when thermally shocked in our tests, high stresses could develop where there are large loads already existing in the piping due to structural considerations, where there is a sudden change in wall thickness, or where there is abrupt changes in contour resulting stress concentrations. It should be noted this analysis applies only to vertical runs of piping or tubes where the temperature gradient is a function of the radial coordinate. In horizontal pipes, the leading edge of the fluid could have a sloped profile resulting in circumferential temperature gradient, in addition to the radial gradient. This would result in stress condition. Most of the piping in the risers and downcomers of molten-salt central-receiver solar power plants is in vertical runs.

For a receiver illuminated with high flux, the stresses are quite different from the stresses during thermal shock. In addition to a through-wall stress, there is a front-to-back tube stress. Appendix D shows the strain equations applicable to receiver tubes under high flux.

Calculations of Penetration Distances - Transient Freezing in Pipes. Another issue pertaining to cold starting piping is how far the molten salt can flow through a cold pipe before freezing shut. This length is known as the penetration distance. There are several models which describe transient freezing in pipes, but one model correlates data from several experiments and a variety of fluids into a single equation that describes the penetration depth as a function of the fluid properties, the Reynolds number, the wall temperature, and fluid temperature [9]. The correlation, Equation 18, describes the axial distance a fluid will flow through a cold pipe whose temperature is held below the fluid's freezing point before the pipe freezes shut. The wall temperature is held constant.

$$\frac{z}{D} = 0.23 \text{Pr}^{1/2} \text{Re}^{3/4} (\alpha_m / \alpha_s)^{1/9} [h_f / (Cp_s(T_f - T_w))]^{1/3} [1 + \gamma Cp_m(T_o - T_f) / h_f] \quad (18)$$

The penetration depths were calculated for molten salt properties at several pipe diameters and flow velocities. These results are shown in Table 5 and in Figure 15. For large diameter piping, such as used with the riser or downcomer in the Solar Two central receiver power plant, we could theoretically flow through hundreds or thousands of feet of piping. In a commercial scale plant, we may be able to flow through *miles* of cold piping. We expect these values to be conservative, since the correlation was developed for a constant wall temperature.

Table 5. Penetration depths for molten salt for various pipe diameters, velocities, and salt inlet temperatures for a wall temperature $T_w = 68^\circ\text{F}$ (20°C).

Diameter	Flow Velocity	Salt Inlet Temperature	Penetration Depth
0.75 in	3 m/s (9.8 ft/s)	288°C (550°F)	39 m (129 ft)
0.75	1 m/s (3.3 ft/s)	288°C (550°F)	17 m (57 ft)
0.75	1 m/s	371°C (700°F)	27 m (87 ft)
1.5 in	3 m/s	288°C (550°F)	132 m (435 ft)
1.5	1 m/s	288°C (550°F)	58 m (191 ft)
1.5	1 m/s	371°C (700°F)	90 m (294 ft)
6 in	3 m/s	288°C (550°F)	1498 m (4920 ft)
6	1 m/s	288°C (550°F)	657 m (2160 ft)
16 in	3 m/s	288°C (550°F)	8340 m (27400 ft)
16	1 m/s	288°C (550°F)	3660 m (12000 ft)

For the panel experiments described previously, we were able to flow through four passes and the associated headers and jumper tubes all at ambient temperature with a salt velocity of 2 ft/s (0.6 m/s). The total length of tubing is about 60 feet (18 m). The correlation predicts the fluid should freeze in about 50 feet (15 m). This means we were probably on the border of freezing.

Penetration Depths vs Salt Flow Rate

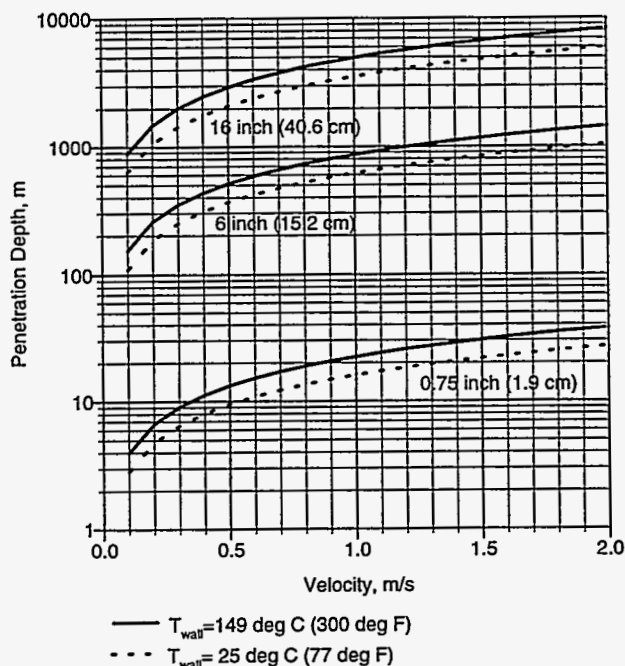


Figure 15. The penetration depths for several pipe diameters as a function flow velocity.

In addition, we were able to flow through over 155 feet (47 m) of ambient temperature ($<100^{\circ}\text{F}$) 2 in piping without freezing the pipe shut. The correlation predicted we would be able flow at least twice that distance. It should be noted that the correlation was developed for piping that was submerged in a bath of fluid to hold the pipe outer surface at a constant temperature. In the cold fill tests described in the previous section, the piping or receiver tubing was not held at a constant temperature, but allowed to heat up. The correlation may be conservative, because an insulated pipe has a finite heat capacitance.

When tried filling the panels at lower velocities (0.4 m/s), we were not able to flow through all the passes. We detected salt in the second and part of the third pass, but it is unclear whether the flow stopped in third pass due to freezing, or a systematic problem. The correlation predicted we should have frozen in the third pass. Unfortunately, we could not verify the accuracy of the correlation very well with the panels, because they are connected with a common vent line which allows the flow to bypass the second and third pass and enter the fourth pass. We postulate that when the flow through the tubes in the second and third pass becomes restricted due to a buildup of a frozen layer of salt, the preferential path of least resistance is the bypass line. This could effectively cut off the venting of air through the second and third passes, resulting the panel becoming air bound.

In a report on the Molten Salt Electric Experiment of a receiver in the external configuration [1], experiments are described in which the receiver was started cold in a flood fill mode (all the panels in a receiver are filled from the bottom up). In two cases they succeeded in filling the panel, but in one case they froze part of it. For this case, the correlation predicts that salt would have barely made it through the 11.5 foot (3.5 m) high panel, which is consistent with the results.

The data are summarized in Table 6. (The flow rate was not given in the report, but was calculated from information about the system. The fact that third test in the series has a higher penetration distance than the second one may be attributed the uncertainty in the flow assumption and average panel temperature measurement.)

Table 6. Results for cold start experiments with the MSEE external receiver along with the correlation results. The panel height is 11.5 feet (3.5 m), tube diameter 0.62 inches (1.6 cm), salt flow rate approximately 0.4 ft/s (0.1 m/s).

Wall Temp	Salt Temp	Penetration Distance	MSEE Result
325°F (163°C)	700°F (371°C)	19.0 ft (5.8 m)	Fill OK
240°F (116°C)	650°F (343°C)	13.6 ft (4.2 m)	Fill OK
210°F (99°C)	700°F (371°C)	14.7 ft (4.5 m)	Partially frozen panel

For the Solar Two receiver designed by Rockwell, in order to prevent freezing, the receiver panels should be heated (with heliostats) to temperatures above 200°F (93°C) with headers and jumper tubes preheated with heat trace to the salt temperature, assuming the panels are flood filled at the design flow rate. The panels should be heated to at least 390°F (199°C) with jumper tubes initially at ambient temperature. These results are shown in Table 7.

Table 7. Estimated penetration depths for Rockwell's Solar Two receiver. Panel height is approximately 21 feet (6.4 m), jumper tube length: approximately 10 ft (3.0 m), tube inside diameter: 0.7145 inches (1.81 cm), salt velocity during flood fill: 0.87 ft/s (0.27 m/s).

Tube Temp	Penetration depth
10°F (-12°C)	18.35 ft (5.6 m)
100°F (38°C)	19.9 ft (6.1 m)
200°F (93°C)	22.4 ft (6.8 m)
400°F (204°C)	44.3 ft (13.5 m)

Summary of Cold Fill Tests

The following conclusions can be made about the cold fill tests:

- Cold filling the panel and/or manifolds is feasible. In normal operation it would not be necessary to cold fill the panel. As a minimum, our results show that the entire panel does not have to be above the salt freezing temperature before salt flow is established.
- Results from the stress analysis show that the stresses in the header and receiver tubes were below the endurance limit during a thermal shock. Analysis should be done for a particular design of the tube-to-header junction and transitions in piping cross section to make sure there are not any localized stress concentrations, and to estimate the life based on fatigue of these areas.
- The best combination of reduced parasitics and increased availability might be partial preheating (e.g., preheating to 300°F).

- We recommend that even if the piping is cold started, valves, flanges, and instrumentation should be kept near the salt temperature to minimize reliability issues that could arise if these components were thermally stressed.
- Our experience has shown that the most successful method for uniformly preheating the panels is to use a roving aiming pattern where the heliostat aim points change every few seconds to avoid localized under- and overheating.
- Although our results show that we can successfully flow through cold piping and tubes, care must be taken to avoid freezing of salt past slow leaking valves in unheated piping.

Freeze/Thaw Experiments

In a molten salt receiver, there are multiple drain valves. During the nightly shut down of the receiver, a drain valve might fail to actuate. If a valve fails to actuate once in a thousand times, a receiver—which has 14 drain valves—will fail to drain approximately once every two and a half months. That does not necessarily mean a panel will freeze that often. Only if this failure is not detected in time and corrective action (such as manually opening the valve) is not taken will the salt trapped in the associated panels freeze. Since the volume of salt increase when it goes from the solid to the liquid state for a fixed mass, damage can occur to the panel if the salt is thawed in a section of tubing or piping which is constrained at both ends.

The objectives of these tests were to determine the procedure required to thaw a receiver panel if it became frozen with salt, and to determine what amount of damage were done to the receiver tubes during the thawing process. A total of five freeze/thaw cycles were conducted. Prior to installation of the panels, all the tubes' outside diameters were measured at various locations along its length, so we could determine the permanent strain induced during the freeze/thaw tests. The freeze/thaw test procedures we used are described below.

First, we established flow in all tubes of the panels to allow the panels to reach thermal equilibrium. After flowing salt through the panels for several minutes, we shut off all drain and outlet valves to prevent salt from draining out of the panel. We then allowed the panels to cool so their temperatures' dropped below salt the freezing point. Figure 16 shows panel and header temperatures as they cool. Note how the slopes of the curves change at the salt freezing temperature, 430°F (221°C). When the salt becomes solid, the slopes change again. The header temperature is maintained above 460°F (238°C) by heat trace. The panels cooled to the salt's freezing point only 25 minutes after the pump stopped in the shielded environment of the solar tower. An exposed external central receiver (e.g., the Solar Two receiver) will cool much faster.

After the average panel temperature was less than 280°F (138°C), we opened the drain and panel outlet valves to empty the lower header of salt. Heat trace was kept on in the headers and on the jumper tubes to maintain the temperature above the freezing point. Once the headers had drained, we initiated thawing with heliostats. The only way for salt to leave the panel as it thaws is through the drain. Therefore, we started thawing from the bottom by putting on one heliostat and allowing it to heat that area of the panel to > 500°F (260°C). We continued to add heliostats, one at a time above the previous one, raising the panel temperature. One test was interrupted by weather and had to be continued the next sunny day. Once all thermocouple readings on the panel were above the salt freezing point, we tried to establish flow through the panel. On the first attempt, we were

Panel Freeze Test: 01/04/94

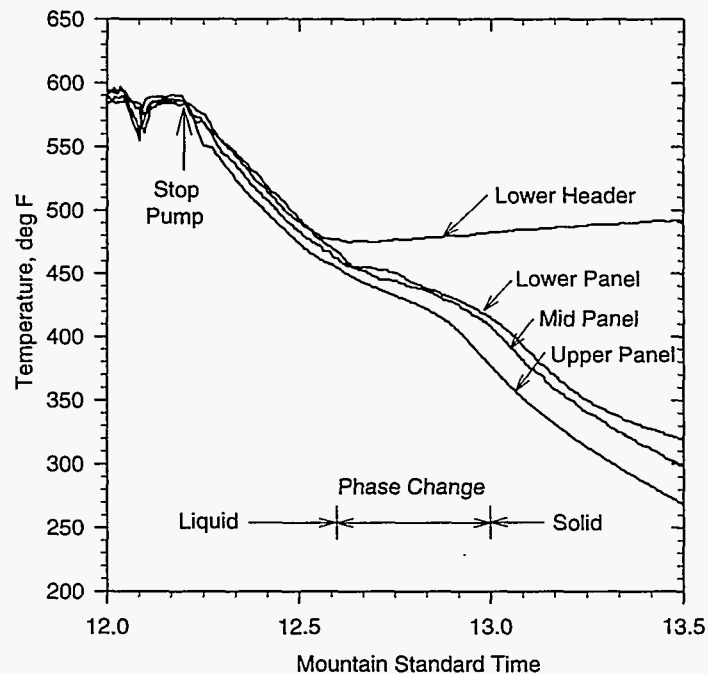


Figure 16. Temperatures receiver panels and header as they cool when filled with molten salt which freezes in the panel at approximately 430°F (221°C).

unable to flow through the majority of the panel because there were sections of tubes under the insulation where the heat trace could not heat it up enough, and we could not heat it with solar. In these regions we had to rely on conduction to melt the salt. Once we achieved flow through part of the panel we continued to flow salt, which helped thaw the frozen areas. After several hours we were able clear all tubes.

After two freeze/thaw cycles we measured the tube diameters. Plots of the permanent (plastic) strain as a function of the panel height are shown in Figure 17 for the east panel and 18 for the west panel. There did not seem to be any pattern to the damage. The maximum permanent strain induced in the tubes was over 4%. Figures 19 and 20 show the plastic permanent strain as a function of the horizontal location (tube number). The values of tube deformations are also shown in Table 8. Tubes 3, 4, and 5 in the east panel have much lower permanent strains than the other tubes in the panel. The west panel does not show this behavior. These results indicate the freezing phenomenon is complex, and requires further study.

Some observations and conclusions can be made regarding these tests:

- Thawing a frozen panel can require several hours, and could result in significant down time.
- The major problem with thawing the panel was a lack of sufficient heat under the insulation, particularly in the upper header where beneficial natural convection within the header oven cavity is not significant. It may be necessary to install additional heat trace in the regions where the insulation meets the panel to assure those areas can heat up to above the salt melting point.

East Panel Deformation

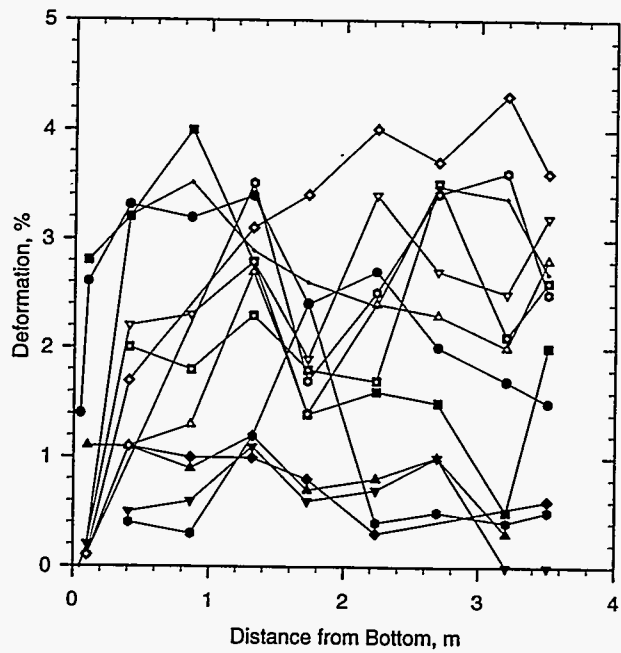


Figure 17. Permanent strain induced in the east panel tubes as a function of the panel height after two freeze/thaw cycles.

West Panel Deformation

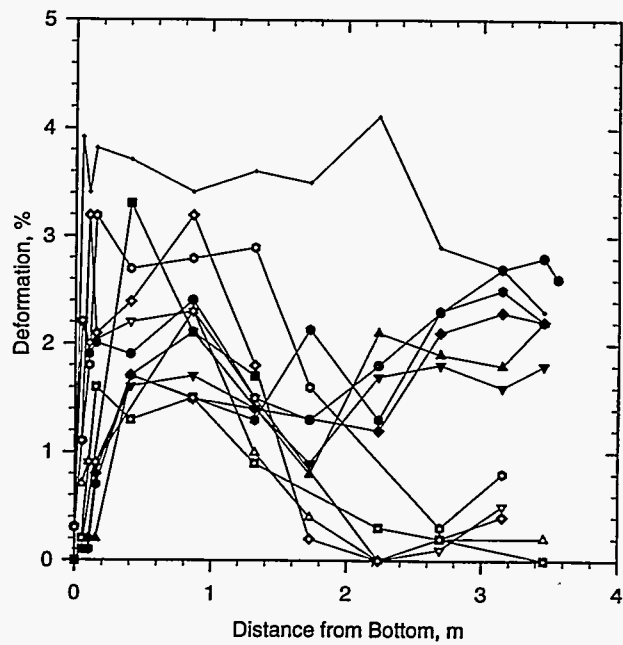


Figure 18. Permanent strain induced in the west panel tubes as a function of the panel height after two freeze/thaw cycles.

Side View: East Panel Deform.

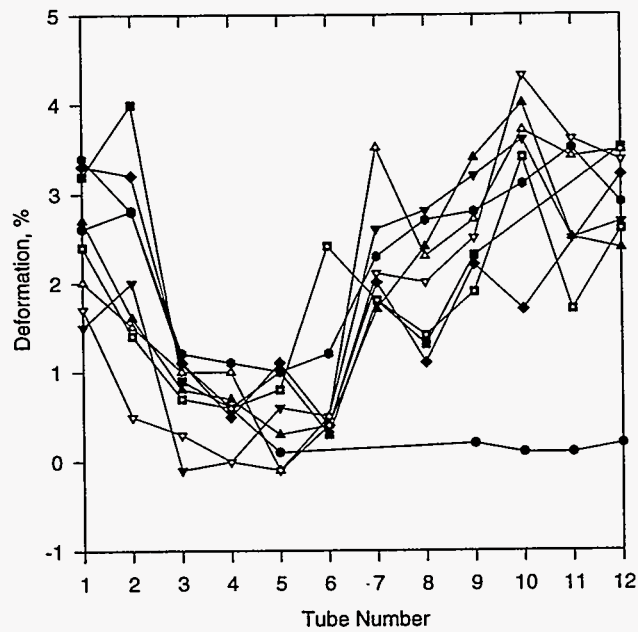


Figure 19. Permanent strain as a function of the width (tube number) for the east panel.

Side View: West Panel Deformation

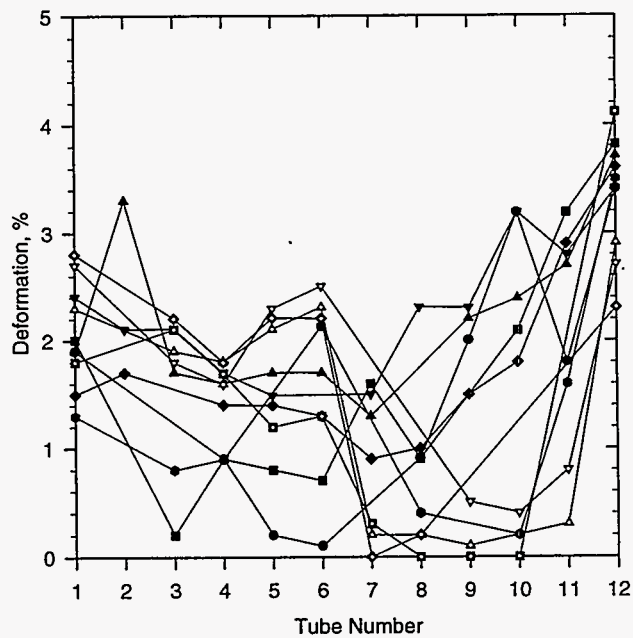


Figure 20. Permanent strain as a function of the width (tube number) for the west panel.

Table 8. Pre- and Post-Measurements of Tube Diameters in East and West Panel after 2 Freeze/Thaw Cycles.

Molten Salt Panel Deformation Measurements
 Pretest Measurements: 02/02/93
 Post Measurements: 02/07/94-02/08/94

dist from bottom	Station No.	dist. from bottom inches	Pre E1 inches	Post E1 inches	Diff. E1 %	Pre E2 inches	Post E2 inches	Diff. E2 %	Pre E3 inches	Post E3 inches	Diff. E3 %	Pre E4 inches	Post E4 inches	Diff. E4 %	Pre E5 inches	Post E5 inches	Diff. E5 %	Pre E6 inches	Post E6 inches	Diff. E6 %	Pre E7 inches	Post E7 inches	Diff. E7 %	Pre E8 inches	Post E8 inches	Diff. E8 %	Pre E9 inches	Post E9 inches	Diff. E9 %	Pre E10 inches	Post E10 inches	Diff. E10 %	Pre E11 inches	Post E11 inches	Diff. E11 %	Pre E12 inches	Post E12 inches	Diff. E12 %	
0	1	0	0.997			0.997			0.999			1.001			1.000			1.002			1.014			0.998			0.998			0.998			0.998			1.000			
0.051	2	2	0.999	1.013	1.401	0.999			0.998			0.999			1.000			0.999			1.003			0.998			0.998			0.998			0.999			1.000	1.000	0.000	
0.102	3	4	0.997	1.023	2.608	0.998	1.026	2.806	0.999	1.010	1.101	0.997			0.999	1.000	1.000	1.003			1.000	0.998			0.999			0.997	0.999	0.201	0.997	0.998	0.100	0.999	0.999	0.100	0.999	1.001	0.200
0.152	4	6	0.997			0.999			0.999			1.002			0.999			1.003			0.999			0.998			0.998			0.999			0.999			0.997			
0.203	5	8	1.000			0.997			0.997			1.000			0.998			1.003			1.001			0.998			0.998			0.998			0.999			0.996			
0.254	6	10																																					
0.305	7	12																																					
0.356	8	14	0.999			1.001			1.000			1.000			1.002			1.002			1.003			1.000			1.001			1.002			0.998			0.999			
0.406	9	16	0.997	1.030	3.310	0.999	1.031	3.203	1.001	1.012	1.099	1.000	1.005	0.500	1.001	1.012	1.099	1.002	1.006	0.399	0.999	1.019	2.002	0.999	1.010	1.101	0.998	1.020	2.204	1.001	1.018	1.698	0.998		0.997	1.029	3.210		
0.864	10	34	1.001	1.033	3.197	1.001	1.041	3.996	0.999	1.008	0.901	1.000	1.006	0.600	0.999	1.009	1.001	1.002	1.005	0.299	1.001	1.019	1.798	0.997	1.010	1.304	0.997	1.020	2.307	0.997		1.000		0.996	1.031	3.514			
1.321	11	52	1.001	1.035	3.397	1.001	1.028	2.800	0.997	1.009	1.204	0.998	1.009	1.102	1.000	1.010	1.000	1.002	1.200	1.002	1.025	2.295	0.999	1.026	2.703	1.001	1.029	2.797	0.997	1.028	3.109	0.997	1.032	3.511	0.999	1.028	2.903		
1.727	12	68	1.000	1.024	2.400	1.001	1.015	1.399	0.998	1.005	0.701	1.001	1.007	0.599	1.001	1.009	0.799	0.996	1.020	2.410	1.001	1.019	1.798	0.998	1.022	2.405	1.000	1.020	1.898	0.998	1.032	3.407	1.000	1.017	1.700	0.999	1.025	2.603	
2.235	13	88	0.999	1.026	2.703	0.999	1.015	1.602	0.997	1.005	0.802	1.000	1.007	0.700	0.999	1.002	0.300	1.000	1.004	0.400	1.001	1.018	1.698	0.998	1.022	2.405	1.000	1.034	3.400	0.998	1.038	4.008	0.997	1.022	2.508	1.007	1.031	2.983	
2.692	14	106	0.998	1.018	2.004	0.999	1.014	1.502	0.999	1.009	1.001	1.001	1.010	1.000	1.001	1.000	-0.100	1.000	1.005	0.500	0.997	1.032	3.511	1.000	1.023	2.300	0.997	1.024	2.708	0.998	1.035	3.707	0.996	1.030	3.414	1.005	1.040	3.483	
3.15	15	124	0.999			0.998			1.000			0.998			1.001			1.001			0.998			0.997			0.999			0.997			0.998			1.005			
3.2	16	126	1.001	1.018	1.698	1.000	1.005	0.500	0.999	1.002	0.300	0.998	0.998	0.000	1.001	1.000	-0.100	1.001	1.005	0.400	0.998	1.019	2.104	0.998	1.018	2.004	1.001	1.024	2.503	0.996	1.039	4.317	0.998	1.034	3.607	1.008	1.042	3.373	
3.251	17	128	1.000			1.000			0.999			0.998			1.001			1.001			0.998			1.000			1.001			0.999			0.998			1.007			
3.302	18	130																																					
3.353	19	132																																					
3.404	20	134	1.001			1.000			0.998			0.997			1.000			1.001			1.000			0.999			1.000			0.997			0.997			1.006			
3.454	21	136	1.001			0.999			1.000			0.998			1.001			1.000			1.000			0.997			0.999			0.997			1.000			1.006			
3.505	22	138	1.002	1.017	1.497	0.999	1.019	2.002	1.001	1.000	-0.100	1.000	1.000	0.000	0.999	1.005	0.601	0.998	1.003	0.501	0.999	1.025	2.603	0.997	1.025	2.808	1.000	1.032	3.200	0.999	1.035	3.604	1.001	1.026	2.498	1.006	1.033	2.684	
3.556	23	140	1.002			0.998			1.000			0.996			0.999			0.998			0.999			0.997			0.998			0.997			1.000			1.003			
Average			1.000	1.024	2.421	0.999	1.022	2.201	0.999	1.007	0.779	0.999	1.005	0.563	1.000	1.005	0.522	1.001	1.008	0.764	1.001	1.022	2.226	0.998	1.018	2.004	0.999	1.022	2.358	0.998	1.028	2.994	0.998	1.023	2.477	1.002	1.026	2.435	
Std Dev			0.002	0.007	0.749	0.001	0.011	1.083	0.001	0.004	0.424	0.002	0.004	0.404	0.001	0.005	0.484	0.002	0.006	0.722	0.004	0.005	0.598	0.001	0.007	0.660	0.002	0.010	0.937	0.001	0.014	1.409	0.001	0.012	1.257	0.004	0.014	1.290	
Max			1.002	1.035	3.397	1.001	1.041	3.996	1.001	1.012	1.204	1.002	1.010	1.102	1.002	1.012	0.999	1.003	1.020	2.410	1.014	1.032	3.511	1.000	1.026	2.808	1.001	1.034	3.400	1.002	1.039	4.317	1.000	1.034	3.607	1.008	1.042	3.514	
Min			0.997	1.013	1.401	0.997	1.005	0.500	0.997	1.000	-0.100	0.996	0.998	0.000	0.998	1.000	-0.100	0.996	1.003	0.299	0.997	1.018	1.698	0.996	1.010	1.101	0.997	0.999	0.201	0.996	0.998	0.100	0.996	0.999	0.100	0.996	1.000	0.000	
Max. change %				4.317																																			

27

dist from bottom	Station No.	dist. from bottom inches	Pre W1 inches	Post W1 inches	Diff. W1 %	Pre W2 inches	Post W2 inches	Diff. W2 %	Pre W3 inches	Post W3 inches	Diff. W3 %	Pre W4 inches	Post W4 inches	Diff. W4 %	Pre W5 inches	Post W5 inches	Diff. W5 %	Pre W6 inches	Post W6 inches	Diff. W6 %	Pre W7 inches	Post W7 inches	Diff. W7 %	Pre W8 inches	Post W8 inches	Diff. W8 %	Pre W9 inches	Post W9 inches	Diff. W9 %	Pre W10 inches	Post W10 inches	Diff. W10 %	Pre W11 inches	Post W11 inches	Diff. W11 %	Pre W12 inches	Post W12 inches	Diff. W12 %
0	1	0	1.001	1.004	0.300	0.999	0.999	0.000	1.000			0.997			0.999			1.003			1.000			0.996			1.001	1.004	0.300	0.999			1.001	1.004	0.300	0.998	0.999	0.100
0.051	2	2	1.001	1.023	2.198	1.000	1.001	0.100	0.999			0.998			1.000	0.999	-0.100	1.003			1.001	1.003	0.200	0.993	1.000	0.705	0.996	1.018	2.209	1.000	1.011	1.100	0.998	1.009	1.102	0.996	1.035	3.916
0.102	3	4	1.000	1.019	1.900	1.000			1.000	0.999	-0.100	0.999	1.008	0.901	1.000	1.002	0.200	1.001	1.002	0.100	1.002	1.000	-0.200	0.993	1.002	0.906	1.000	1.020	2.000	1.003	1.035	3.180	1.001	1.019	1.788	0.998	1.032	3.407
0.152	4	6	0.998	1.018	2.004	0.999	0.998	-0.100	1.000	1.002	0.200	0.999	1.008	0.901	1.001	1.009	0.799	1.000	1.007	0.700	1.000	1.016	1.600	0.997	1.006	0.903	0.998			1.004	1.025	2.092	1.004	1.036	3.187	0.996	1.034	3.815
0.203	5	8	1.000			-1.002			1.000			0.997			1.001			1.002			1.002			1.001			1.003			1.005			1.002			0.999		
0.254	6	10																																				
0.305	7	12																																				
0.356	8	14	1.001			1.001			0.999			0.999			0.998			1.002			1.002			0.994			1.002			1.005			1.002			0.999		
0.406	9	16	1.000	1.019	1.900	0.999	1.032	3.303	0.997	1.014	1.705	0.996	1.012	1.606	0.997	1.014	1.705	0.998	1.015	1.703	1.001	1.014	1.299	0.997			0.999	1.021	2.202	1.003	1.027	2.393	1.001	1.028	2.697	0.997	1.034	3.711
0.864	10	34	0.997	1.021	2.407	0.998	1.019	2.104	0.996	1.017	2.108	0.998	1.015	1.703	1.005	1.020	1.493	0.999			0.999	1.014	1.502	0.996	1.019	2.309	0.998	1.021	2.305	1.002	1.034	3.194	1.001	1.029	2.797	0.997	1.031	3.410
1.321	11	52	1.001	1.016	1.499	0																																

- Although we had over 41 thermocouples on the 24 receiver tubes and 4 headers, we were unable to determine where the blockages were. Even when all the thermocouples indicated that the temperatures were above the salt melting point, we still had plugs of salt. In the Solar Two and commercial receivers there will be even less instrumentation. If a panel becomes frozen, temporary thermocouples should be installed to monitor the panel temperatures more thoroughly. They could be mounted on the outside of the tubes. Another option is to monitor the temperatures with an IR camera.
- The heat trace should be designed to heat the headers and jumper tubes above 500°F within 10 hours when they are *full* of salt.

Component Tests

The main objectives of the component tests were to test unproven hardware and determine how well they perform in a molten salt environment, and to reduce uncertainties of the performance of untested components and operating procedures. Many of the flanges were tested in a molten salt environment, but additional information is required. Check valves were not tested previously in molten salt. The component tests were broken down into three areas: 1) check valve cycling, 2) slow thermal cycling of flanges, and 3) thermal shocking of flanges.

Check valves are needed at the pump outlet to prevent damage to the pump from the static "head" of salt when the pump stops, or to prevent pressure surges caused by redundant pumps on a common header when one pump stops. Serious damage to the pump can result if it is not protected from the strong inertial forces of the salt coming from the other pump and from the salt head in the riser.

It is desirable to use flanges that facilitate service of certain high maintenance components in molten salt loops. The flanges used in the molten salt pump and valve test loops were a constant source of salt leaks. The purpose of these tests was to test various other designs of flanges (e.g., tapered flanges or clamp type flanges) to measure how well they held a seal under thermal cycling, and to determine if it is practical to use flanges around the high maintenance components. We tested five flanges: a 2 inch Grayloc, two 4 inch R-CONs, a 6 inch E-CON, and a 4 inch ANSI ring type.

Check Valve Cycling. The purpose of the experiments with the check valve were to test their operation in a molten salt environment and to determine how to drain the salt from the check valve. A 3 inch spring loaded swing check valve was tested in a section of piping between flanges in the loop. Although we could not simulate the pressures expected to be encountered in cold side of a molten salt loop, we did simulate the flow velocities and the temperature cycles on the cold loop.

Figure 21 is a photograph of the check valve we tested (V-CON model manufactured by ReFlange, Inc.). A drain hole was drilled in the flapper to allow a short section of piping downstream of the check valve to drain.

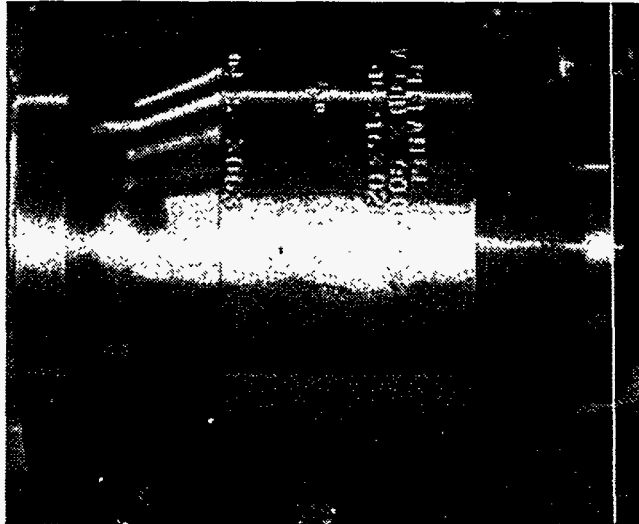


Figure 21. Photograph of the 3 inch check valve (V-CON model manufactured by Reflange, Inc.) tested in the salt loop.

In these tests we pressure cycled the check valve by flowing salt at the maximum flow rate - approximately 100 gallons/min (380 l/min) and establishing pressure in the accumulator to 30 psi, then shutting a bypass valve (FCV 720) and turning off the pump. Shutting the valve before turning off the pump caused a momentary spike in the pressure, but assured the check valve would receive positive pressure on the downstream side of the flapper. We monitored the pressure decay in the accumulator tank. After waiting approximately 30 minutes to allow the pump motor to cool, we repeated the cycling. Figure 22 shows the pressure and flow as a function of time for several cycles. There were no problems with its operation after over 300 cycles (approximately 1 year of operation). The flapper was inspected after the 300 cycles, and found to be in good condition with no signs of wear.

Slow Thermal Cycling of Flanges. Flanges in a molten salt environment have been known to leak significantly after being thermally cycled [12]. It is desirable to use flanges to facilitate service of high maintenance components, such as the pumps, in molten salt loops. The flanges used in the molten salt pump and valve experiments were a constant source of salt leaks. We tested various flanges to determine how well they hold a seal under the slow thermal cycling expected during nightly shut down of the plant followed by morning preheat with heat trace. We slow cycled four flanges: a Grayloc 2 inch with clamp type connectors, two 4 inch R-CON flanges with clamp type connectors manufactured by Reflange, and one 6 inch E-CON bolted flange also manufactured by Reflange. The Reflange flanges have a unique metal gasket that is radially compressed (elastically) when the two faces are brought together, providing a tight seal.

Checkvalve Cycling

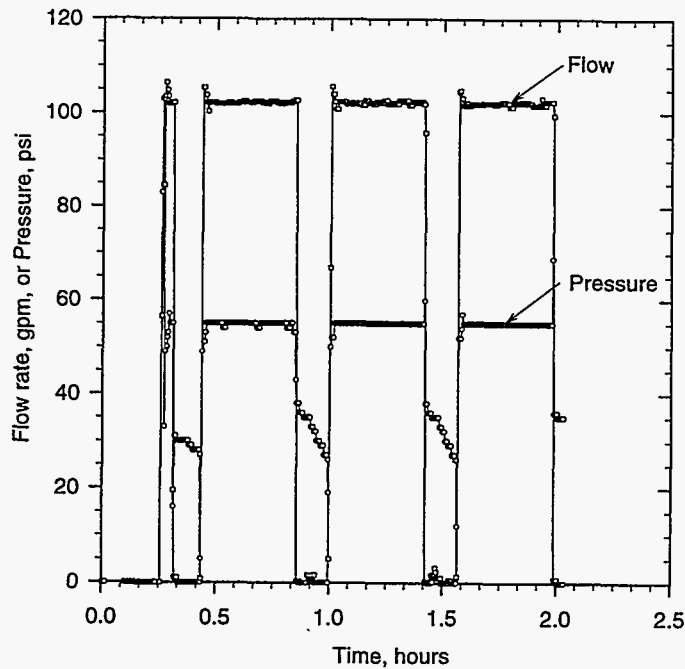
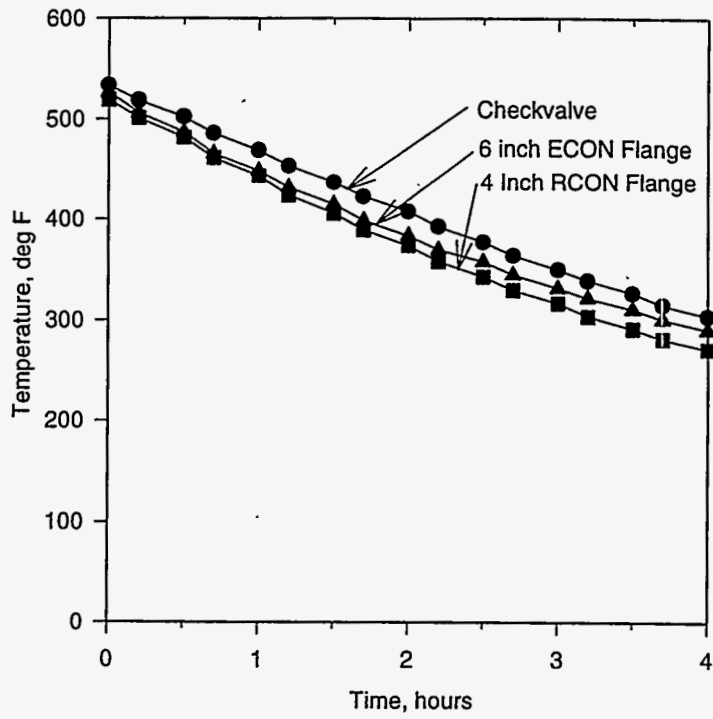


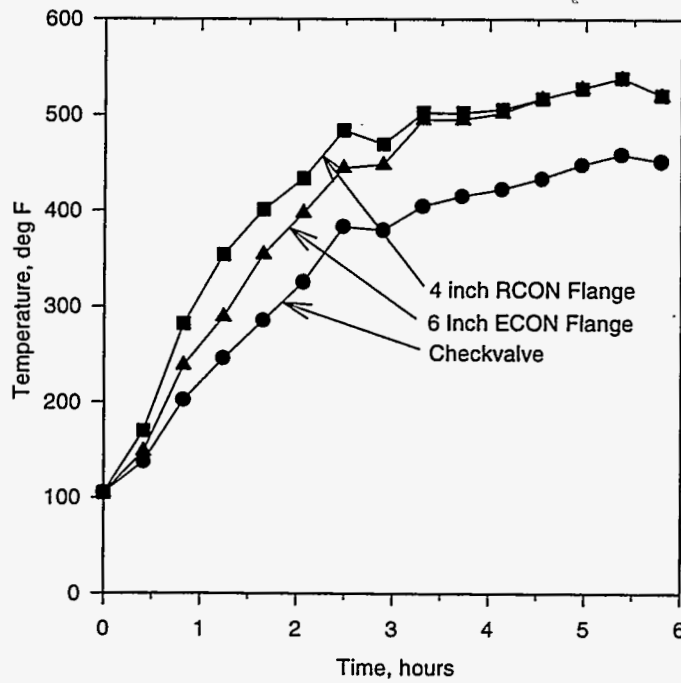
Figure 22. Pressure and flow as a function of time during a typical check valve cycle.

In these tests we simulated the nightly shut down and cooling of the components (assuming the heat trace were turned off) by using a fan and removing some of the insulation to enhance the cooling and match the temperature profiles we had expected to see in service at Solar Two. We cycled between 200 and 500°F. Each cycle took between six and eight hours. Figure 23 shows a typical slow thermal cycle. After approximately 180 slow thermal cycles, one of the 4 inch flanges started leaking very slightly. (We realized the torque on the bolts for the first 180 cycles was lower than the recommended value for the size of bolts we were using, and may have resulted in a less than optimum compression on the gasket.) We inspected all the flanges (we disassembled the two 4 inch flanges) and noticed they had all leaked to some extent, except the bolted 6 inch E-CON which showed no visible signs of salt. The bolted flange may provide a more uniform compression on the faces of the flange and gasket as compared to the clamp type flanges. See Figure 24. Since the salt is very wetting, it tends to get into cracks and seeps past gaskets, soaking and degrading the insulation. The continuous thermal cycling adds to its migration. Even though the flanges leaked a small amount (approximately 1 drop per hour), they would not likely fail catastrophically, since the gaskets are metal.

We retorqued the bolts to their recommended torque and continued the slow thermal cycling for an additional 120 cycles (a total of 300 cycles -- approximately one year of service) without any failures.

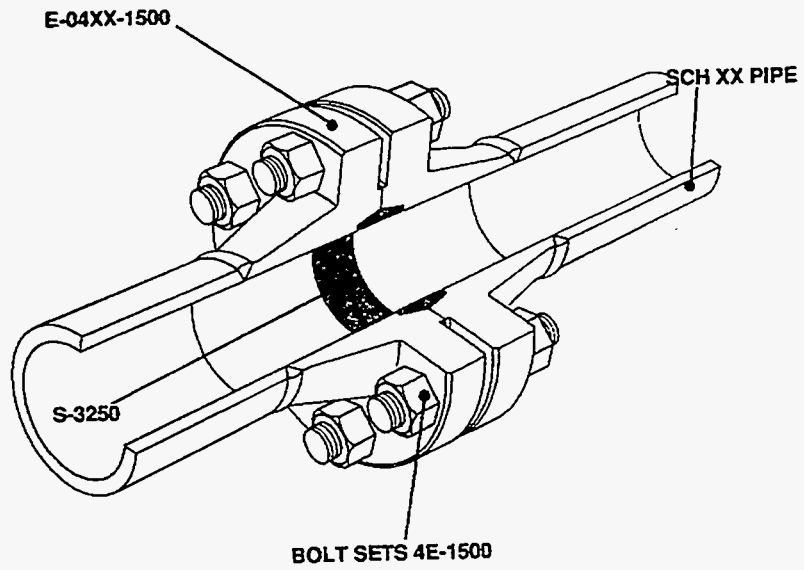


a)

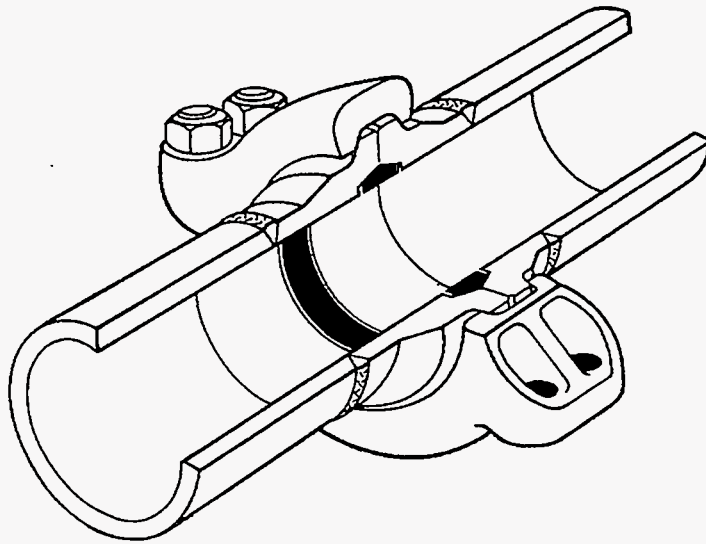


b)

Figure 23. Typical slow thermal cycle of flanges simulating nightly cool down of components followed by slow heatup with heat trace.



a)



b)

Figure 24. Schematic of a) ECON and b) RCON flanges.

Thermal Shocking of Flanges. The most severe thermal cycling a flange could experience in a molten salt system would be a thermal shock where the flange is at one temperature and it is suddenly subjected to salt at a different temperature. This situation could occur in one of two ways: 1) when the salt temperature at the outlet of the receiver suddenly drops due to a cloud transient, or 2) at startup if the flanges were at a temperature below the salt temperature. In the first case, the salt temperature transient could be from 1050 to 550°F (566 to 288°C) in approximately five minutes. In the second case, the flange could be as cold as ambient with the salt at approximately 550°F (288°C). This situation could arise if the parasitic power consumption were being minimized at nightly shut down by turning off the heat trace followed by cold filling of the piping. In our test loop we only simulated the second thermal shock case, since it would be very difficult to simulate the transient salt temperature at the receiver outlet. We conducted these tests at two initial flange temperatures either: 300°F or ambient (~100°F) with the salt at 550°F.

Prior to the start of the thermal shock tests we installed a 4 inch ring-type flange to test alongside the other flanges. In these tests we allowed the flanges to cool for several hours or overnight by lowering set point temperature of the heat trace or by turning off the heat trace completely. After the flanges had cooled to the desired temperature, we shock them by pumping 550°F salt through them. Figure 25 shows a typical temperature profile of the flanges and check valve during a shock.

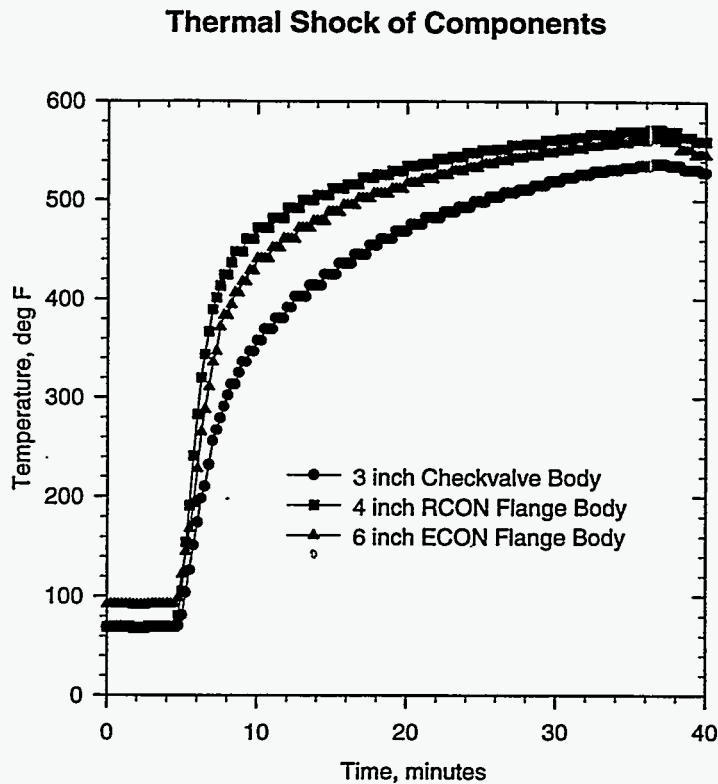


Figure 25. Typical temperature transient of the flanges during a shock.

After 25 cycles at 300°F, we inspected the flanges. There did not appear to be any visible breaches of integrity. We continued the thermal shocks with the flanges at ambient temperature. The flanges experienced 146 shocks without failure, although the flanges continued to leak at a very slight rate. After all these thermal shocks, none of the flanges failed catastrophically. With continuous operation and exposure to pressurized salt, all except one of the flanges showed only minor leaking (wetting between the interfaces of the flange faces or actually dripping of salt at a rate of approximately one drop per hour). The exception is the Grayloc flange which leaked significantly, enough to form a stalagmite of salt on the floor. Leaks over a long period of time can soak the insulation and increase the thermal losses. Exposure of salt to heat trace can also cause an electrical short in the heat trace.

A finite element analysis was done on the 6 inch E-CON flange to determine the stresses that developed in this flange undergoing thermal shock with salt at 550°F and the flange either initially at 77°F (25°C) or at 300°F (149°C). The details of this analysis are included in the appendix. There were two areas of concern in the flange where the stresses reached a maximum: 1) at the interface of the two flange faces at the outer most radius, and 2) on the inner surface of the flange adjacent to the gasket. The stresses developed at the interface between the two flange faces during either initial condition (77 or 300°F) were highly localized and were in excess of the yield for the material, but a chamfer exists at this location. The actual stress should be much lower with the chamfer, so that region is not a concern. On the other hand, the stresses in second region are in excess of the yield when the flange is shocked from an initial temperature of 77°F (25°C) but not in excess when shocked at 300°F (149°C). Based on this analysis, we recommend that flanges are preheated at least to 300°F (149°C) prior to initiating salt flow.

These flanges are an improvement over the flanges used in the pump and valve test loops which were raised-faced flanges with a Flexitalic type gasket. Those flanges tended to leak severely under cyclic conditions.

Our observations and recommendations regarding these flanges are:

- The flanges held up remarkably well to the conditions to which we subjected them. There were no severe failures. The majority of the salt leaks were very slight.
- Flanges should be minimized in a salt system. They should be used only for removal of high maintenance equipment such as the pumps, if at all. All welded construction is preferred, especially on hot loops.
- If the piping is cold started, the flanges should be preheated to at least 300°F (149°C) prior to flowing salt through them.
- The flanges tend to seal better if they are not thermally cycled.
- Hot retorquing the bolts periodically may reduce the leaks.
- Heat trace zones should be designed so that flanges and valves are not part of the same heat trace circuit as the rest of the riser or down comer, so that cold starting the rest of the piping can be done.

Instrumentation Tests: Flowmeters and Pressure Transducer

Flowmeters. Flowmeters were a considerable source of problems in previous molten salt experiments [2]. For example, the Category B receiver used venturi type flowmeters with differential pressure transducers using silicone oil as an intermediate fluid to measure flow. The

pressure transducers had problems with silicone oil volatilizing at the cold salt temperature. In addition, venturi flowmeters only have a range of about 4:1. Because of the limited range and silicone oil problems, we investigated other designs of flow meters that could be more reliable, provide higher accuracy, and have a greater range.

We chose to test two types of flowmeters: vortex shedding and ultrasonic. These flowmeters were selected because they are common, commercially available products which can withstand the temperatures we expected to encounter in the cold side of a salt system. The vortex shedding flowmeter has wedge in the flow field and senses oscillations of the vortices which are shed from the wedge. The frequency of the oscillations is proportional to the flow rate. The ultrasonic flowmeter sends a sound wave through the moving fluid from one transducer to the other, with and against the flow. It measures the time difference between the traverses. We tested two types of ultrasonic flowmeters: a wetted type where the transducers actually send the sound wave directly into the fluid, and a clamp-on type where the transducers simply mount on the outside of the pipe and propagate the sound wave through the pipe wall. The vortex shedding flowmeter we tested was manufactured by Engineering Measurement Company, and the ultrasonics by Panametrics. Both have temperature limitations and are only rated for the cold side of a molten salt system. The ultrasonic flowmeters were calibrated with water at the factory prior to installation in the salt loop. The vortex shedding flowmeters had been calibrated under the Direct Absorption Receiver Program.

We have operated the flowmeters since the beginning of this test program. The first clamp-on transducers were not made for the cold salt temperatures and their bodies (made of a "high" temperature phenolic material) melted. The manufacturer replaced them with all metal transducers. We also experienced some problems with the cables to the wetted transducers. Once we worked through the bugs in the hardware and programming, the ultrasonic flow meters worked reasonably well. The clamp-on flowmeter uses a petroleum couplant between the transducer and the pipe wall which allows the sound wave to penetrate through the pipe and into the fluid. After approximately a week or two of intermittent service at the cold salt temperatures (above 500°F), the couplant dried out and caused inaccuracies in its readings. A new application of couplant restored the contact between the transducer and the pipe wall.

A comparison between the flowmeters is shown in Figure 26 during a varying flow condition. The vortex shedding responds much faster and stabilizes better to changes in flow rate. For control purposes, the vortex shedding would be the preferred flowmeter. The ultrasonic flowmeter took some time to tune and to get operating properly, partly due to the faulty cable. By changing the parameters (such as the number of samples it averages for a reading) in the software of the electronics for the ultrasonic flowmeters, we were able to change its response.

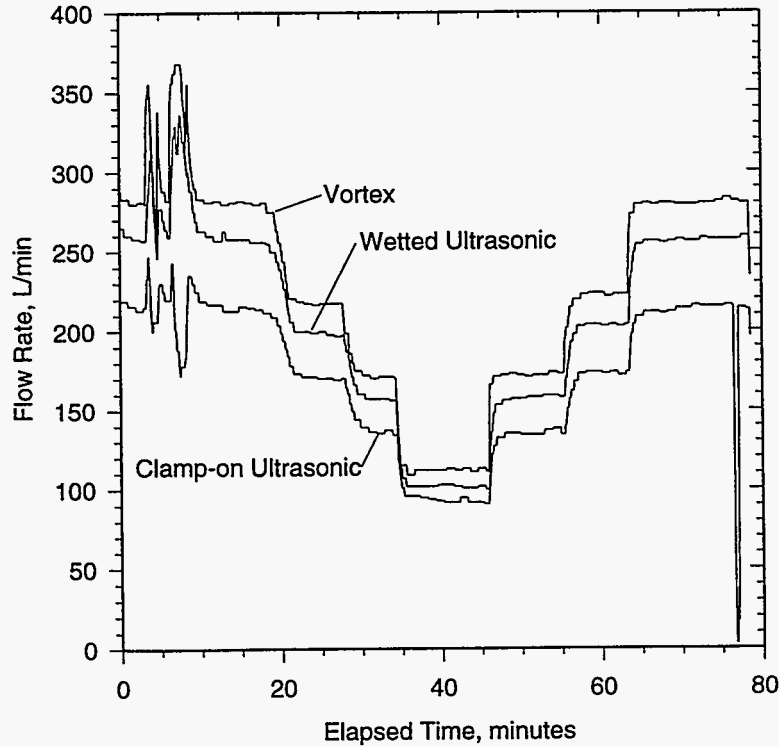


Figure 26. Response of vortex and ultrasonic flowmeters during a varying flow condition.

The flowmeters were compared with calibration tanks in the salt loop. Since the volumes of the calibration tanks are essentially constant with time, and the accuracy of the bubbler level measurement devices is good ($\pm 3.8\%$), we chose to compare the flowmeters with the calibration tank flow.

The uncertainty of the flow measurement has two components: the bias (also called systematic) errors and the random errors [10]. The bias errors affect each measurement the same amount (at a given condition) and represent the offset from the “true” value. Random errors are the errors that change in a random fashion with repeated measurement. The random errors are not correlated with each other, and their limit can be measured if several data points are taken. Since the true bias and random errors are not known, their estimates are approximated by limits of each. The bias limit equals the square root of the sum of squares of each elemental bias limit (b_i):

$$B = [\sum b_i^2]^{1/2} \quad (19)$$

The random limit equals:

$$S = \left(\frac{t_{95} S_x}{\sqrt{N}} \right) \quad (20)$$

where t_{95} is the Student’s t statistic at 95% confidence, S_x is the standard deviation of the data set, and N is the number of data points [10]. For the root-sum-square uncertainty model, the uncertainty is found by combining the bias and random limits as follows:

$$U_{RSS} = \pm [B^2 + S^2]^{1/2} \quad (21)$$

This model provides an interval around the test average that will contain the true value $\approx 95\%$ of the time. In the flow tests, the flowmeter readings were compared with a reference—the calibration tanks. The bias errors relative to the reference can be measured. However, the reference (the calibration tanks) also has bias errors which we could not measure.

Table 9 lists each bias error source and estimated magnitude for the calibration tank flow measurement. The calibration tanks use bubblers to sense level. The amount of time to fill between two levels in each tank is measured and the flow rate calculated. Since the volumes of calibration tanks were not measured when the Panel Research Experiment was fabricated, exact volumes are not known. However, the dimensions were determined from drawings of the tanks. The volume was calculated, accounting for an overflow standpipe. Even if the tanks have significant amounts of eccentricity (5% change in the diameter) causing the tank to become elliptical, the volume of each is not significantly affected (it changes by less than 0.5%). Other bias sources of errors are thermal expansion of the tank volume between ambient and 550°F, salt density variations due to temperature, and the bubbler calibration.

Table 9. Bias Limit Sources for Calibration Tank Flow Measurement.

Error Source	Magnitude
1. Tank Eccentricity (tank cross section is elliptical: minor axis is 95% tank radius, major axis 105% radius).	0.5%
2. Tank Thermal Expansion (change in tank volume from ambient to 550°F).	1.5%
3. Salt Property Variations (change in density and thus level between 550 and 650°F).	1.8%
4. Bubbler Calibration (approximately 0.5 inch in 18 inches).	<u>3.0%</u>
Total Bias Limit Calibration Tank Flow (Root Sum Square)	3.8%

The flowmeters were compared with the calibration tanks at several flow rates. Starting at 100% flow, we allowed the flow to stabilize, then closed the drain valves to the calibration tanks. The bubblers measured the level in each tank as a function of time. The elapsed time for the salt to fill the tank between the lower and upper level settings is measured in each tank to calculate the flowrate. The total flowrate is the sum of the two calibration tank flows.

Figure 27 shows the results of the comparison of the flowmeters against the calibration tank flowrate. Each data point represents the average of several readings during the calibration run. Figure 28 shows the measured bias errors (relative to the calibration tank flowrate) for each flowmeter as a function of flow. The bias errors represent the systematic errors in the measurements. Note how the bias errors are a function of the flow rate. The implication of this dependency is that calibration constant for each flow meter is off by a fixed percentage. The random errors are shown in Figure 29. The random errors were calculated from the data using Equation 20. The random errors are quite small, indicating the flowmeters give consistent readings over the range of the flows tested. The root-sum-square uncertainties, U_{RSS} , for each flow meter as a function of flow rate are shown in Table 10. The U_{RSS} accounts for the bias errors of the reference source—the calibration tanks.

Flowmeter Calibration

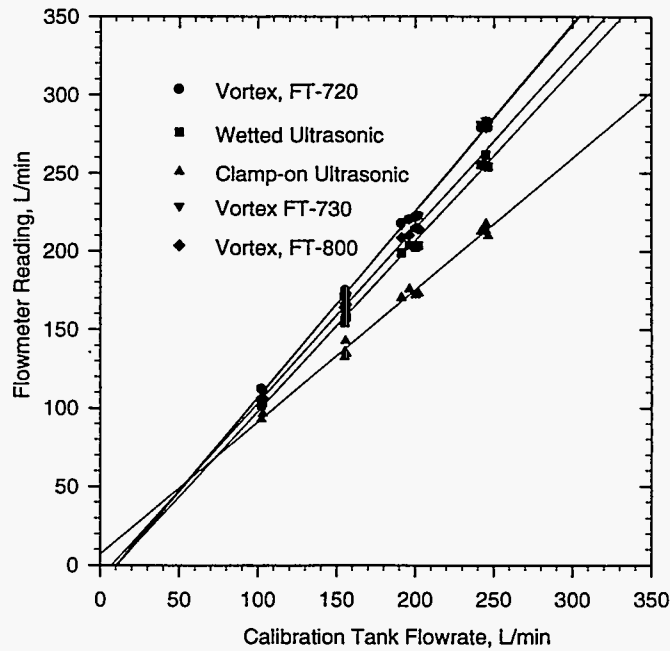


Figure 27. Comparison of the vortex and ultrasonic flowmeters against the calibration tank flowrate.

Bias Errors for Flowmeters

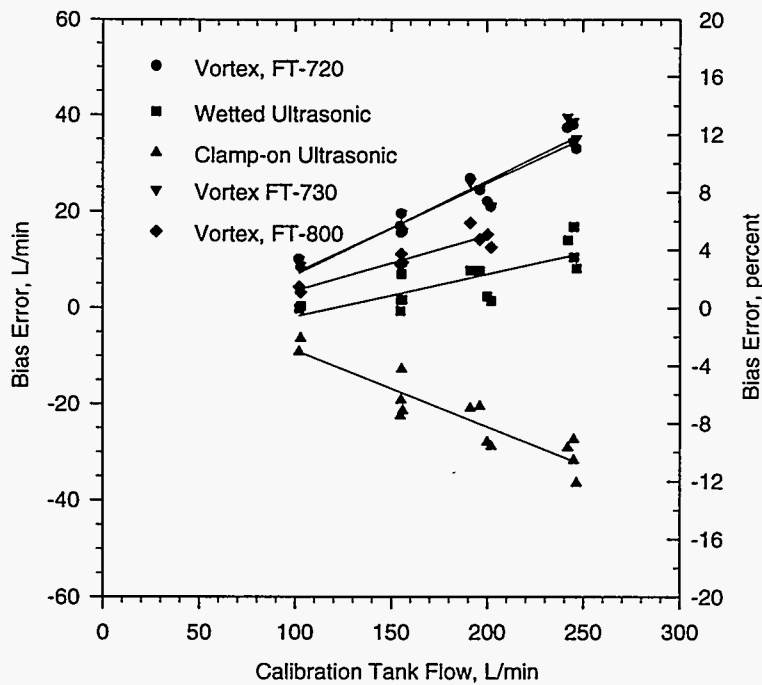


Figure 28. Measured bias errors (relative to the calibration tank flowrate) for each flowmeter as a function of flow.

Random Errors for Flowmeters

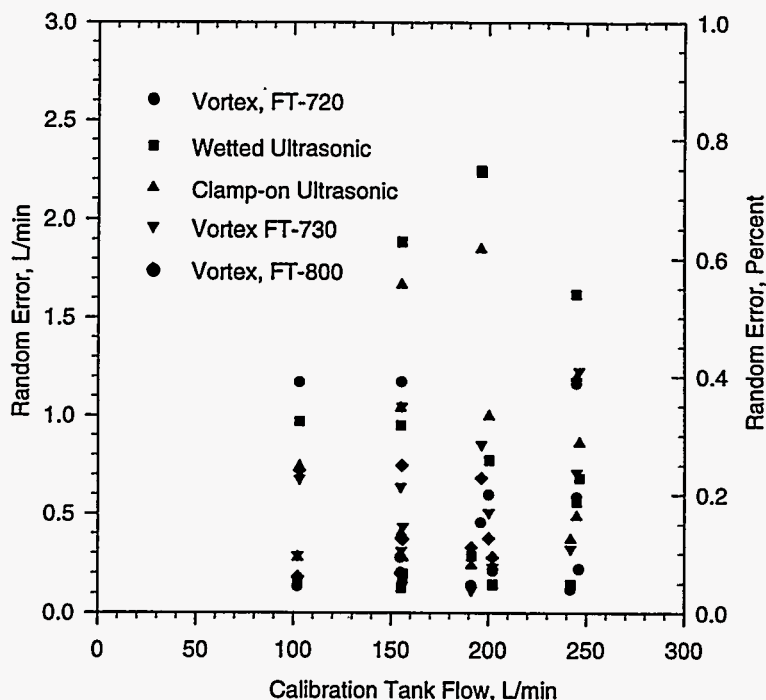


Figure 29. Measured random errors for each flowmeter as a function of flow.

Table 10. Root-sum-square Uncertainty (U_{RSS}) for Each Flowmeter.

Flowrate, L/min	Vortex, FT-720	Wetted Ultrasonic, PF-001	Clamp-on Ultrasonic, PF-002	Vortex, FT-730	Vortex, FT-800
102.6	± 9.8%	± 3.9%	± 8.5%	± 9.9%	± 5.3%
155.4	11.6	4.2	12.8	11.6	7.3
197.4	12.6	4.6	13.0	12.5	8.5
244.6	15.1	6.4	13.3	15.6	--

The large uncertainties observed are primarily due to the large bias errors. By periodically calibrating the flowmeters against a calibrated reference (such as calibration tanks or the cold surge tank of receiver with a *calibrated* bubbler - this is important), the majority of bias error limits can be calibrated out resulting in a root-sum-square uncertainty with a magnitude of the uncertainty equal to the calibrated reference. Overall uncertainties (U_{RSS}) of less than ±5% can be obtained with these flowmeters. The random error limits were much smaller and did not contribute significantly to the overall uncertainty under steady conditions.

Other observations and recommendations regarding flowmeters:

- The vortex shedding flowmeter worked exceedingly well (very reliable) in the molten salt environment and should be used whenever possible. The ultrasonic flowmeters were less reliable.

- It is essential that provisions to calibrate the flowmeters in situ are designed into a molten salt system (e.g., calibrated level indicators in the cold tanks).
- For calibration purposes, the tank volume should be measured before installation and the bubbler must be calibrated.
- The clamp-on ultrasonic flowmeters are useful for temporarily (< 1 week) measuring flow in areas where there is no flow measurement or to verify flow measurement of an existing flowmeter and where the effort or expense and down time does not justify installation of a welded in flowmeter. During the check out phase of the receiver and salt system or during performance monitoring may be the time when clamp-on ultrasonic flowmeters could be useful on a very temporary basis or as a temporary backup if one of the permanent flowmeters were to fail and the plant was ready to run.
- The flow rate only needs to be measured on the cold side. There should be no need to measure flow on the hot side.

Pressure Transducer. We have tested an impedance-type pressure transducer and a NaK-filled pressure transducer in the salt loop to determine how well they work in molten salt. The silicone oil used in pressure transducers in previous molten salt tests tended to volatilize. The NaK-filled pressure transducers made by Taylor worked well in the pump and valve loop once snubbers were used to eliminate pressure pulsations which fatigued the membrane. Unfortunately, NaK-filled pressure transducers are difficult to find anymore. The impedance-type pressure transducer we tested in our loop is made by Kaman, and is good for temperatures up to 1200°F. It senses small displacements in its membrane and correlates them to pressure. It is self temperature compensating. Although we don't have any method to calibrate the pressure transducers in our system, the impedance-type pressure transducer was calibrated at the factory at 550, 750, and 1050°F. The impedance-type pressure transducer in our loop experienced the same thermal cycling and shock as the flanges, and did not fail or give erroneous readings. The pressure measurement in Figure 22 was from the impedance-type pressure transducer.

Comments regarding pressure transducers:

- The impedance-type pressure transducers work well but are expensive (~\$5k each).
- NaK-filled pressure transducers are hard to find.
- To keep instrumentation costs down, minimize the number of salt pressure measurements needed.
- The pressure transducers should be oriented so the salt can drain from them. Experience from previous molten salt experiments has shown, that if salt is allowed to freeze on the membrane, then thawed, the thawing process causes the membrane to rupture.

IV. Ongoing and Further Research

The work conducted so far has answered many of the questions regarding how far salt can flow through cold pipes during a cold fill scenario and the thermal stresses that develop when components and piping are thermally shocked, and some of the effects of freezing and thawing. We have also tested instrumentation that are an improvement over previous instruments. Ongoing and further research is directed towards understanding the freeze/thaw phenomenon, validating transient freezing models, and testing improved components and instrumentation. A description of each of these follows.

Simple Element Freeze/Thaw Tests (Ongoing)

A two-chamber oven was built to investigate the salt freeze/thaw phenomenon in typical receiver tubes. The purpose of the simple-element freeze/thaw experiments is to quantitatively measure in a controlled setup the permanent deformation inflicted to samples of receiver tubes undergoing freezing and thawing. When nitrate salt changes from the solid to the liquid phase the volume increases, causing an expansion of a given mass of salt. During the expansion process, the tube material can yield resulting in a plastic deformation of the tube material. In these tests, several receiver tubes of various diameters and wall thicknesses filled with nitrate salt undergo several freeze/thaw cycles to measure the deformation of tubes. Preliminary results indicate under the most severe case (freezing the lower half of a tube, then freezing the upper half, followed by thawing the lower part with a stop in the upper half to prevent sliding of the solid salt) the tubes will rupture after 12 cycles.

Ball Valves Test

Ball valves are desirable for use as drain and fill valves because they are relatively compact and in the fully opened position the flow restriction is small relative to other types of valves, such as globe valves. We have pressure cycled a 2 inch Mogas ball valve to assess its functionality and leak rate in a molten salt environment. The valve was closed and pressurized to 60 psi (410 kPa) for five minutes followed by flow for five minutes. After each 50 cycles, the leak rate was measured with the valve in the closed position and pressure on the valve. The amount of salt that leaks by was measured every 0.5 hour. After 300 cycles the leak rate was measured to be approximately 15 grams of salt per half hour.

Transient Freezing Experiments

The correlation for transient freezing in pipes used to calculate penetration depths is based on experiments where the pipe wall is cooled externally to maintain a constant wall temperature. In reality, pipes have a finite heat capacitance. The effects of the pipe heat capacitance on the penetration depths for molten salt penetration depths is an area that could be investigated further.

Impedance Heating System

For long runs of piping, impedance heating could have advantages over mineral insulated (MI) cable. With impedance heating, the pipe wall becomes the heater by passing a low A-C voltage (<80 volts) through it. One lead of the electrical cables is connected to the electrical midpoint of the pipe, and the other is divided in two, with each of these connected to an end of the pipe that is to be heated. The cables run on the outside of the pipe and are easy to access. We plan to test an impedance heating system in our salt loop.

Multiport Valve

A multiport valve allows flow from one line to be distributed to several lines. It has a single actuator to control the valve. A multiport valve could be used in place of several drain and fill valves, thus reducing the complexity associated with controlling and maintaining several valves. Although this valve is not a commercial product, a small company in Colorado (TedCo) has designed such a valve for molten salt applications. This type of valve should be investigated further.

V. References

1. N. E. Bergan, *Testing of the Molten Salt Electric Experiment Solar Central Receiver in an External Configuration*, Sandia National Laboratories, SAND86- 8010, October 1986.
2. D. C. Smith and J. M. Chavez, *A Final Report on the Phase I Testing of a Molten Salt Cavity Receiver*, Volume II - The Main Report, Sandia National Laboratories, SAND87-2290, May 1992.
3. C. E. Tyner, *Status of the Direct Absorption Receiver Panel Research Experiment: Salt Flow and Solar Test Requirements and Plans*, Sandia National Laboratories, SAND88-2455, March 1989.
4. F. P. Incropera, D. P. De Witt, *Fundamentals of Heat and Mass Transfer*, second edition, John Wiley & Sons, pp. 181-191, 1985.
5. A. S. Mujumdar, R. A. Mashelkar, *Advances in Transport Processes*, John Wiley & Sons, Vol. III, pp. 35-117, 1984.
6. J. N. Goodier, "Thermal Stress," *ASME J. Appl. Mech.*, Vol. 4, no. 1, March 1937.
7. A. H. Burr, *Mechanical Analysis and Design*, Elsevier Science Publishing Co., Inc., 1982.
8. H. E. Boyer and T. L. Gail, editors, *Metals Handbook Desk Edition*, American Society for Metals, 1985.
9. F. B. Cheung and L. Baker, Jr., "Transient Freezing of Liquids in Tube Flow," *Nuclear Science and Engineering*, Vol. 60, pp. 1-9, 1976.
10. R. H. Dieck, *Measurement Uncertainty Methods and Applications*, Instrument Society of America, 1992.
11. W. C. Young, *Roark's Formulas for Stress and Strain*, sixth edition, McGraw-Hill, pp. 722-724, 1989.
12. E. E. Rush, J. M. Chavez, C. W. Matthews, P. Bator, *An Interim Report on Testing the Molten Salt Pump and Valve Loops*, Sandia National Laboratories, SAND89-2964, April

Appendix A. Finite Element Analysis of Flange Undergoing Thermal Shock

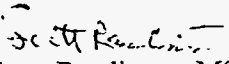
The following is memo written by Scott Rawlinson describing a finite element analysis of an ECON type 6 inch flange undergoing thermal shock at two different initial conditions: 25 and 149°C.

Sandia National Laboratories

Albuquerque, New Mexico 87185-1127

date: July 27, 1994

to: Jim Pacheco, MS-0703
Org. 6216


from: Scott Raylinson, MS-1127
Org. 6215 5-3137

subject: Finite Element Results for Salt Flange

To ensure the reliability of some aspects of Solar Two, you are concerned about stresses in several critical components, one of which is the flange coupling. As an alternate method of thermal conditioning at night, some of the salt line may be drained and allowed to cool. At startup these lines will be at ambient temperature or they will be preheated to a temperature below the salt freezing point and will undergo a significant thermal shock. The purpose of this memo is to document the finite element analysis (FEA) results on the flanges undergoing thermal shock that will be used in these molten salt loops.

I used the COSMOS/M finite element program to model the pipe flange. This program can be used on a PC and according to a survey done by our analysis group about three years ago, is one of the better FEA programs. The program has been continuously updated and improved since that time. I used the latest version, 1.70. The developers of this code, Structural Research and Analysis Corporation (SRAC), verify its results using numerous test case models.

The system being modeled is two E-CON flanges that are bolted together at 45 degree intervals. A step is machined into each of the mating flanges. A gasket is placed in this notch that is formed from these steps. The model was developed to determine: (1) stresses at steady-state conditions; (2) stresses that would occur if 290 °C salt suddenly flowed through this pipe connection without any heat trace (at ambient temperature); and (3) stresses that would occur if 290 °C salt suddenly flowed through this pipe connection after the flanges are preheated to 149 °C (300 °F). Therefore a transient solution is required for (2) and (3).

The envelope of the FEA model was developed from the sketch you supplied, using data from ReFlange. Several iterations of the model were developed. The first model was developed in an older version, 1.65A. Then the newer version arrived, and although it did not contain any changes that should affect this particular model, I developed the model in the newer version. In addition, after knowing what loading would occur, I decided that gap elements should be placed between the flange and the gasket. Otherwise, the gasket would appear to be part of the flange, adding to its strength -- this would not be realistic. Only the results using the gap elements, separating the gasket from the flanges, will be presented.

A summary of the parameters in the FEA model is given below:

- Element type (for flanges and gasket): 4-node planar, "PLANE2D", axisymmetric
- Average element size: 2-mm
- Element type (gap between flange and gasket): 2-node "GAP"
- Force/pressure boundary conditions: 28,300 N at bolt hole location
- Flux/Temperature boundary conditions:
 - Convection along entire length of inner pipe
 - Convection coeff = 550 W/m²-K
 - Bulk fluid temp: 290 °C
- Displacement boundary conditions: Zero displacement in y direction at midpoint of gasket
- Flange material properties (SS316) [1,2]:
 - Modulus of elasticity: 193 GPa
 - Poisson's ratio: 0.3
 - Coefficient of thermal expansion: 17.5 x 10⁻⁶ m/m-K
 - Density: 8000 kg/m³
 - Specific Heat at Constant Pressure: 505 J/kg-K
 - Thermal conductivity: 15.6 W/m-K
- Gasket material properties (17-4PH) [3]:
 - Modulus of elasticity: 193 GPa
 - Poisson's ratio: 0.3
 - Coefficient of thermal expansion: 12.1 x 10⁻⁶ m/m-K
 - Density: 7832 kg/m³
 - Specific Heat at Constant Pressure: 505 J/kg-K
 - Thermal conductivity: 12.1 W/m-K

Note: Material properties were taken as constant and were calculated at the average between an ambient temperature of 25 °C and the operating temperature of 290 °C.

The boundary conditions stated above require some explanation. Since the pipe flange is modeled axisymmetrically, the proper bolt load must be calculated. COSMOS/M assumes axisymmetric problems are based on one radian. Therefore the proper bolt load is:

$$F = F_b \frac{\#bolts}{2\pi}$$

The force in the bolt was given as 4000-5000 lb. from Bob Lathan at Reflange, Inc.. I used 5000 lb. = 22,242N, or an equivalent load of about 28,300N, using the above equation.

When I first developed the thermal model, I placed 290 °C boundary conditions (salt temperature) along the inside of the pipe. The resultant stresses were extremely high in this region. However, I realized that was not the proper boundary condition. The inside of the pipe will not instantaneously reach 290 °C -- it will reach that temperature much more slowly through the boundary layer. Therefore I re-analyzed the problem using convective boundary conditions.

The correlation I used to determine the convection coefficient is based on turbulent flow in circular tubes and is given as [4]:

$$\bar{h} = 0.023 \frac{k}{D} \text{Re}_D^{4/5} \text{Pr}^{0.3}$$

for

$$0.7 \leq \text{Pr} \leq 160$$

$$\text{Re}_D \geq 10,000$$

$$L/D \geq 60$$

where k = thermal conductivity
 D = pipe diameter
 L = pipe length
 Re_D = Reynolds number
 Pr = Prandtl number

Using your stated flowrate of 100 gpm and using the properties of salt at 290 °C from [5], I calculated a convection coefficient of 552 W/m²-K \cong 550 W/m²-K (the above assumptions were met). This number is very close to your calculated value based on experimental results from the smaller pipe flange at time \geq 90 seconds.

Since the problem is transient in nature, a timestep is needed. The critical timestep is calculated as (information supplied by SRAC):

$$\Delta t_{cr} \leq \frac{2}{1-2\theta} \frac{\Delta x^2 \rho c_p}{k}$$

where Δx = smallest mesh size
 ρ = density
 c_p = specific heat at constant pressure
 θ = stability parameter

Using the values of material properties and stability factor to give the smallest possible stable timestep, I calculated a critical timestep of 0.86 seconds. I used a 0.5 second timestep in the analysis.

My assumptions in the analysis were as follows:

- (1) Constant material properties (linear problem)
- (2) Constant convection coefficient
- (3) No external thermal losses (insulated)
- (4) Bolt load does not change with time or temperature
- (5) No friction at gasket/flange interface (it will become apparent later that this value is irrelevant)
- (6) Flowrate = 100 gpm

Steady-State Results (Ambient Temperature):

The results of the steady-state analysis for 25 °C are shown in Figures 1a through 1d. All stresses discussed below are Von-Mises stresses, a common stress criterion used to predict failure. Figure 1a illustrates the model's element mesh, force, and displacement boundary conditions. Two areas, regions A and B are also illustrated -- these will be referred to later. Figures 1b and 1c are exaggerated displacement plots. The pipe flanges tend to be clamped together due to the bolt loads. This plot appears to show that the gasket is separating from the lower pipe flange. However, remember that this is an exaggerated plot on a scale on the order of several hundred. I was concerned that the apparent non-symmetry indicated a problem, so I consulted personnel at SRAC -- they said that sometimes this happens in a deformed plot when the displacements are very small, resulting in a very distorted plot with the huge scale factor. This is what happened in this case. In fact, he checked the entire model and found no problems. Figure 1d is a Von-Mises stress plot of the center of the bolted connection. The maximum stress is 175 MPa, and occurs where the two flange bodies contact due to the bolt forces (region A). This stress is well below the yield point of SS316 at ambient temperature.

Transient Results for No Preheat:

Next, the convective boundary condition was applied along the inside of the pipe wall. Since the temperature distribution changes with time, the resultant stresses will also change. I examined the results at $t = 0.5, 1, 5, 10, 20, 30, 60, 120, 180,$ and 240 seconds. To observe how the stress patterns develop with time, I included the results at $t = 0.5, 5, 10, 30, 60, 120,$ and 240 seconds in Figures 2 through 8.

The maximum stress occurs at the same location as the steady-state results, but is higher due to the additive effect of the temperature or convective boundary conditions. Because the pipe is being heated from the inside of the pipe, this inner region expands faster than the outer region, which tends to compress the contact line even greater than with only bolt loads.

The following table summarizes the stresses in the two areas of concern:

Table I - FEA Results for Case Without Preheat

Time (seconds)	Von-Mises Stress, Region A (MPa)	Corresponding Temperature, Region A (°C)	Yield Strength, Region A (MPa)	Von-Mises Stress, Region B (MPa)	Corresponding Temperature, Region B (°C)	Yield Strength, Region B (MPa)
0.0	175	25	240	35	25	240
0.5	180	25	240	90	37	240
1.0	171	25	240	90	44	240
5.0	178	25	240	142	69	240
10.0	214	25	240	172	81	240
20.0	279	25	240	196	98	240
30.0	341	25	240	239	107	240
60.0	527	25	240	265	128	240
120.0	537	50	240	323	161	240
180.0	542	58	240	325	178	240
240.0	547	67	240	328	187	240

These results at the contact point (region A) indicate that the yield strength is easily exceeded. However, I asked if this was actually chamfered at this point. It turns out that it is, which would eliminate this high stress point. More of a concern is the stresses along the inner pipe adjacent to the gasket. For times > 30 seconds, stresses exceed the yield point in this region (the yield point is constant from 25-200 °C). Based on this, it is apparent that local yielding may occur if you thermally shock this bolted connection.

Notice that maximum stresses are nearly level at 240 seconds. As the temperature distribution evens out, the stresses will decrease and eventually return to the stresses with bolt loading only (since the expansion will be equal throughout the flange assembly). Therefore, the stresses at t= 240 seconds are about as high as can be expected.

Finally, I looked at any gap that may occur between the flange and gasket surfaces. There is a slight gap at t=240 seconds but is nearly undetectable -- less than $\cong 0.1$ -mm. Because of the effect of the bolt force and thermal loading, the gasket is never compressed. Any stresses in the gasket are only due to the thermal gradient. Because the gasket is never constrained, the coefficient of friction used is not relevant.

Transient Results with Preheat:

I re-ran the model assuming the entire flange was preheated to a uniform temperature of 149 °C (300 °F). I examined the results at t = 0.5, 30, 60, 120, 180, and 240 seconds. The results are displayed in Figures 9 through 14. The following table summarizes the Von-Mises stresses in regions A and B.

Table I - FEA Results for Case Without Preheat to 149 °C

Time (seconds)	Von-Mises Stress, Region A (MPa)	Corresponding Temperature, Region A (°C)	Yield Strength, Region A (MPa)	Von-Mises Stress, Region B (MPa)	Corresponding Temperature, Region B (°C)	Yield Strength, Region B (MPa)
0.5	177	150	240	18	150	240
30.0	266	150	240	133	193	240
60.0	361	150	240	145	204	240
120.0	454	162	240	182	221	$\cong 240$
180.0	495	170	240	198	230	$\cong 240$
240.0	504	180	240	202	235	$\cong 240$

As with the case with no preheat, the highest stresses occurred at the point of contact between the two flange bodies. Again, this point was ignored because there is actually a chamfer at this location. The other area of concern, region B, has much more acceptable stresses. A maximum Von-Mises stress of 202 MPa occurs at t=240 seconds. The corresponding temperature at that point and time is approximately 235 °C. The yield strength of SS316 at this temperature point is nearly 240 MPa, therefore the stress level is acceptable. Note that as with the case with no preheat, the stresses have very nearly peaked and would begin to decrease with time to the levels of that in the steady-state condition.

Conclusions:

Based on these results of this model, it appears that local yielding may occur (without preheat) along the inner pipe adjacent to the gasket. It is possible that a full 3-D model may indicate otherwise, but it is not likely since the region in question is far from the bolts. Therefore, it is not recommended that this flange connection be thermally shocked from ambient conditions. However if heat trace is used to preheat the flanges to 149 °C (300 °F), the stresses would remain below the yield point of the material..

References:

1. American Society for Metals, Engineering Properties of Steel, pp. 292-296, ASM, 1982.
2. Incropera, F. P., and DeWitt, D.P., Fundamentals of Heat Transfer, p765, Wiley, New York, 1981.
3. Kattus, J.R., Aerospace Structural Metals Handbook, code 1501, March, 1978.
4. Incropera, F. P., and DeWitt, D.P., Fundamentals of Heat Transfer, p406-407, Wiley, New York, 1981.
5. Smith, David C., Chavez, James M., Final Report on Phase I Testing of a Molten Salt Cavity Receiver, Vol II - The Main Report, Table 2-II, p 2-4, SAND 87-2290, May 1992.

Attachments with all copies: Figures 1 through 14

Copy to:

Chuck Lopez, SCE
Bill Gould, Bechtel
Alex Zavoico, Bechtel
Dick Holl, Jenna Baskets
Bob Lathan, Reflange
Mark Marko, Rockwell
Tom Tracey, Ted Co.

MS-0703 Jim Chavez, 6216
MS-0703 Craig Tyner, 6216
MS-0703 Greg Kolb, 6216
MS-0704 Paul Klimas, 6201
MS-1127 Chris Cameron, 6215
MS-1127 Scott Rawlinson, 6215 (2)
File K.3, 6215

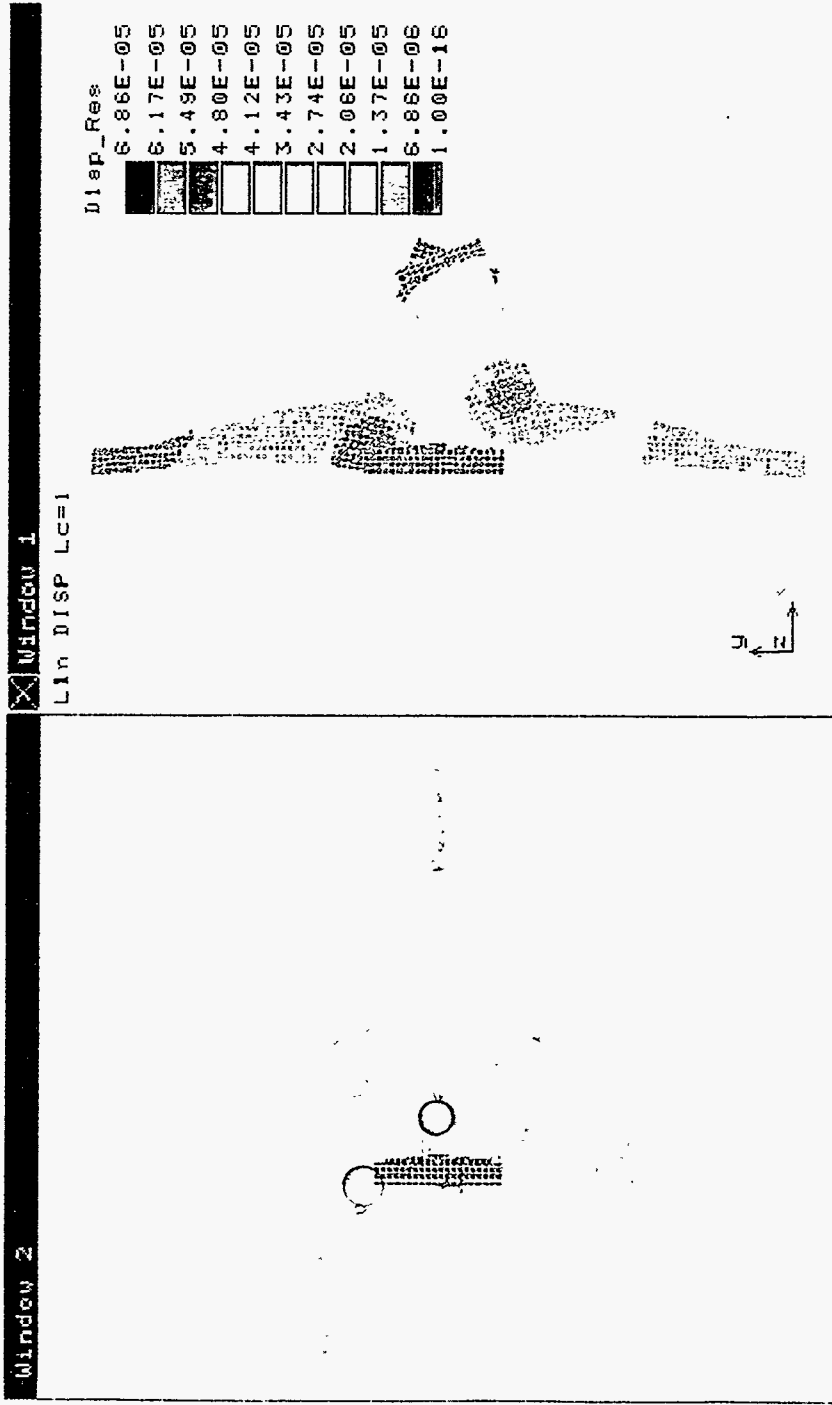


Figure 1a-
Element and boundary condition plot,
no thermal loads

Figure 1 b-
Displacement plot, no thermal loads

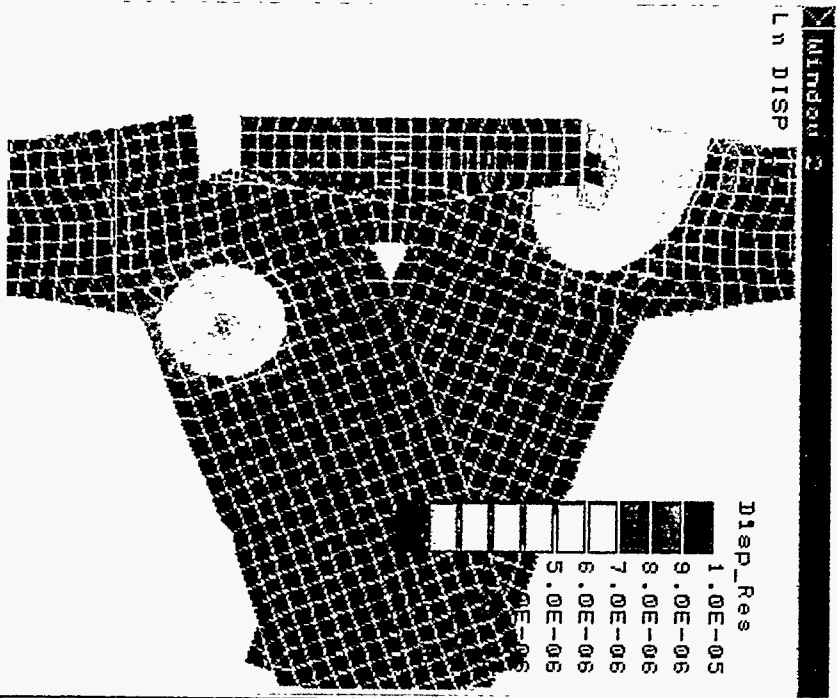


Figure 1c-
Displacement plot, closeup,
no thermal loads

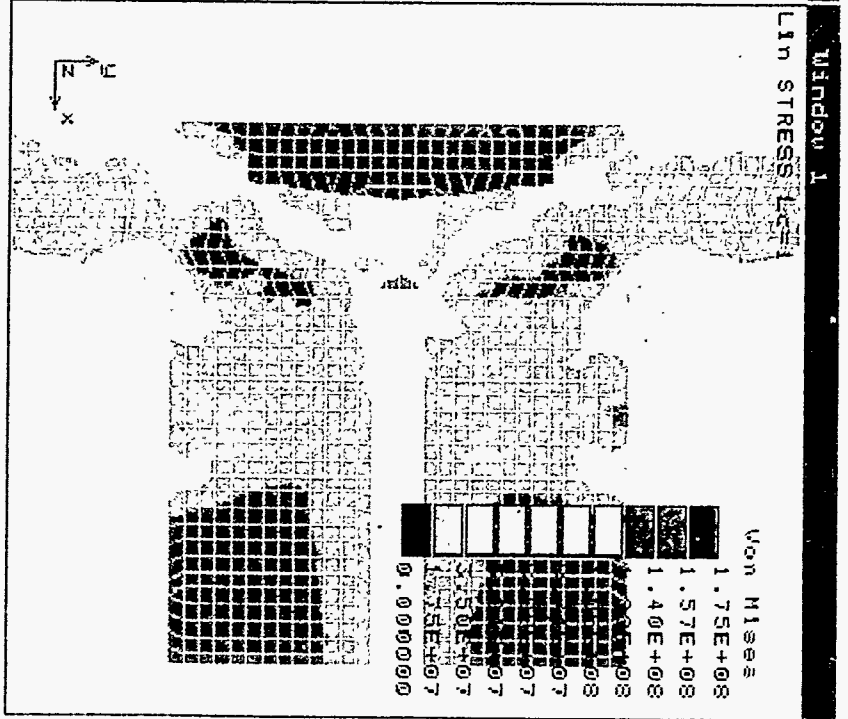


Figure 1d-
Stress plot, closeup,
no thermal loads

Window 2

THERMAL Step=1

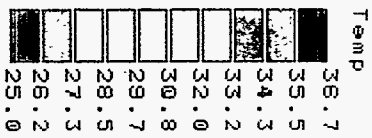


Figure 2a-
Temperature plot, no preheat
t=0.5 seconds

Window 1

LM DISP LC=1

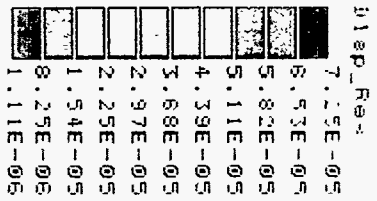
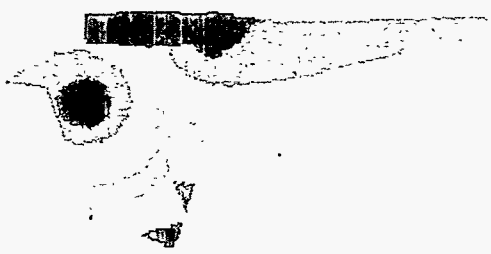
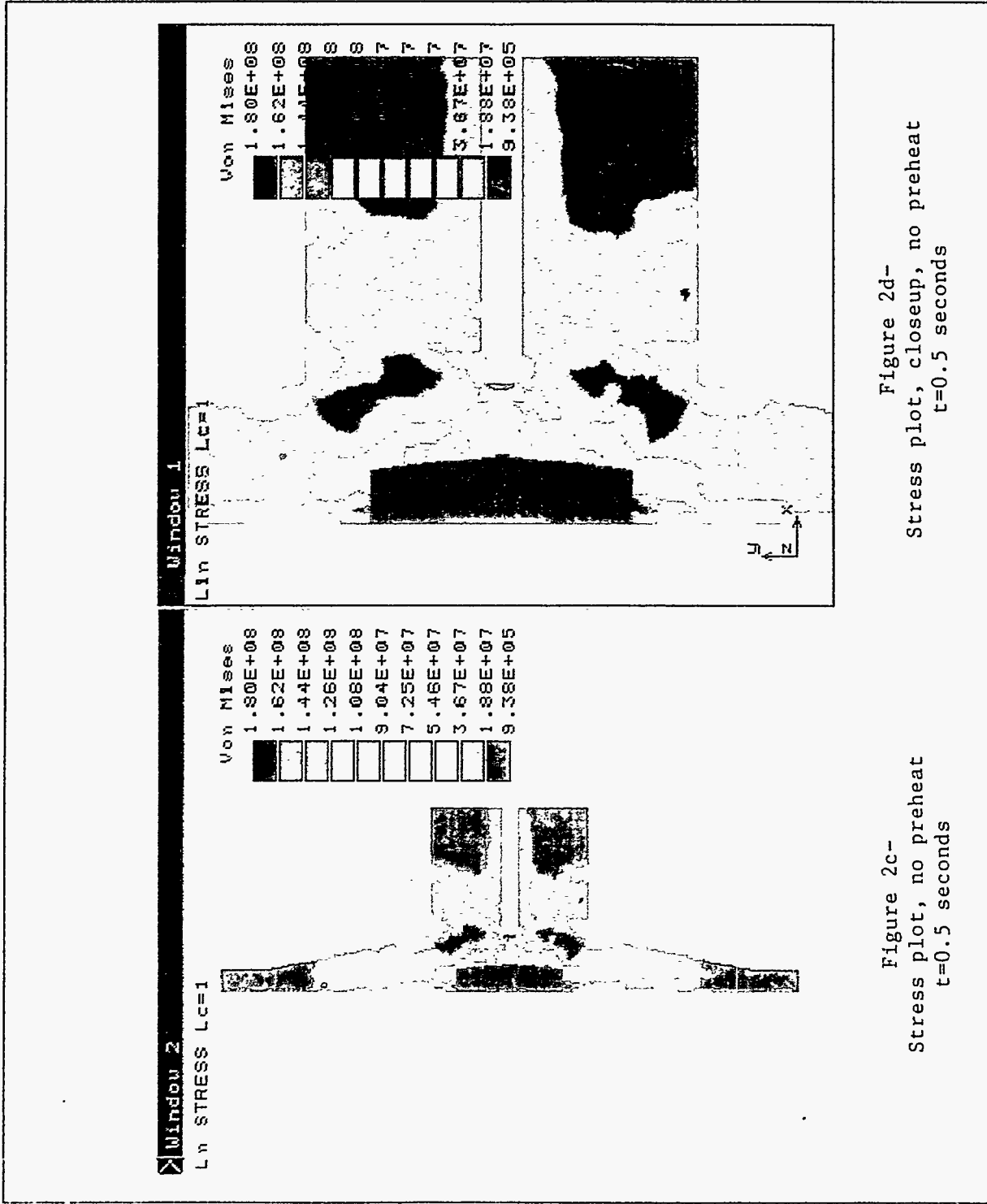
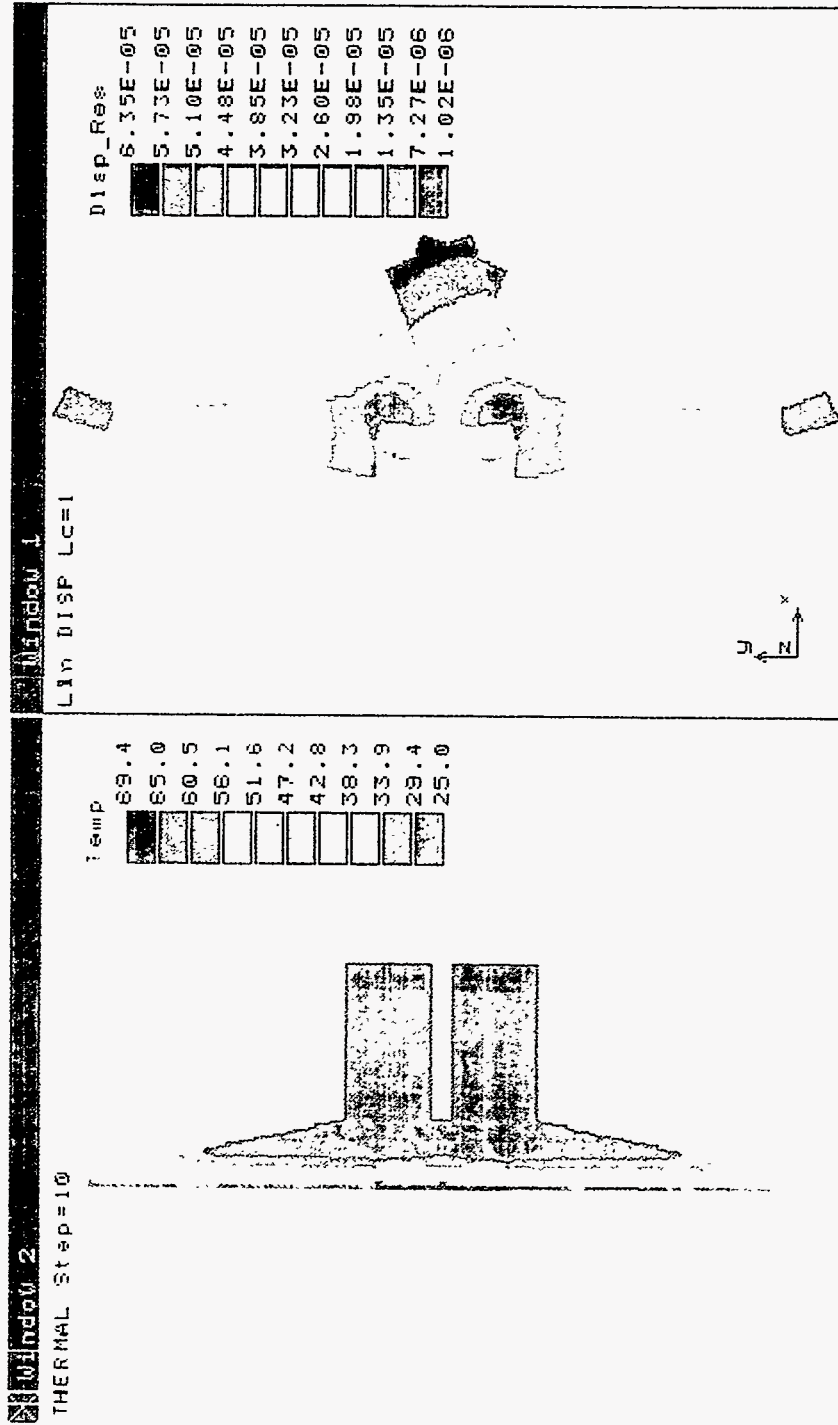


Figure 2b-
Displacement plot, no preheat
t=0.5 seconds





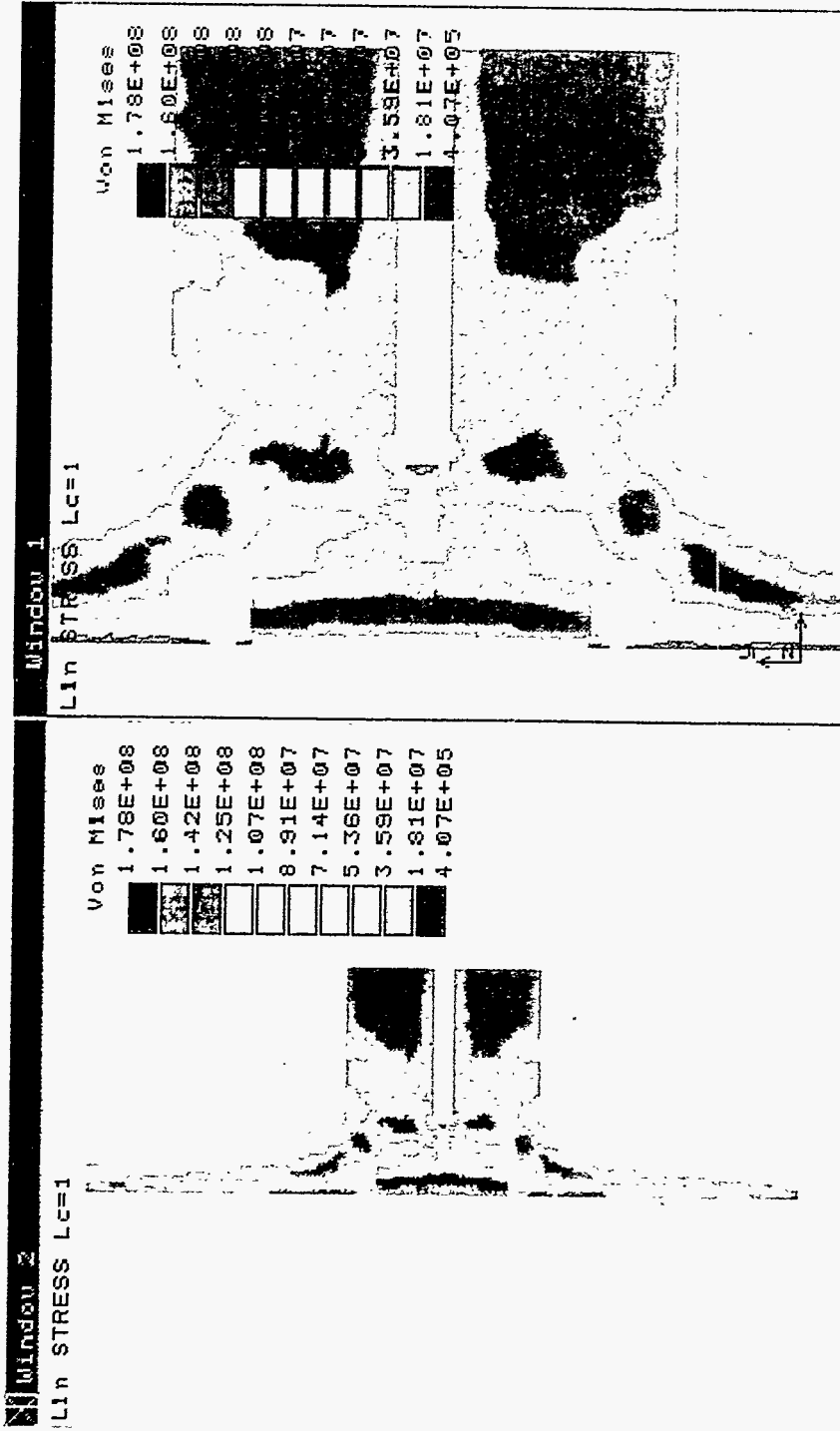


Figure 3c-
Stress plot, no preheat
t=5 seconds

Figure 3d-
Stress plot, closeup, no preheat
t=5 seconds

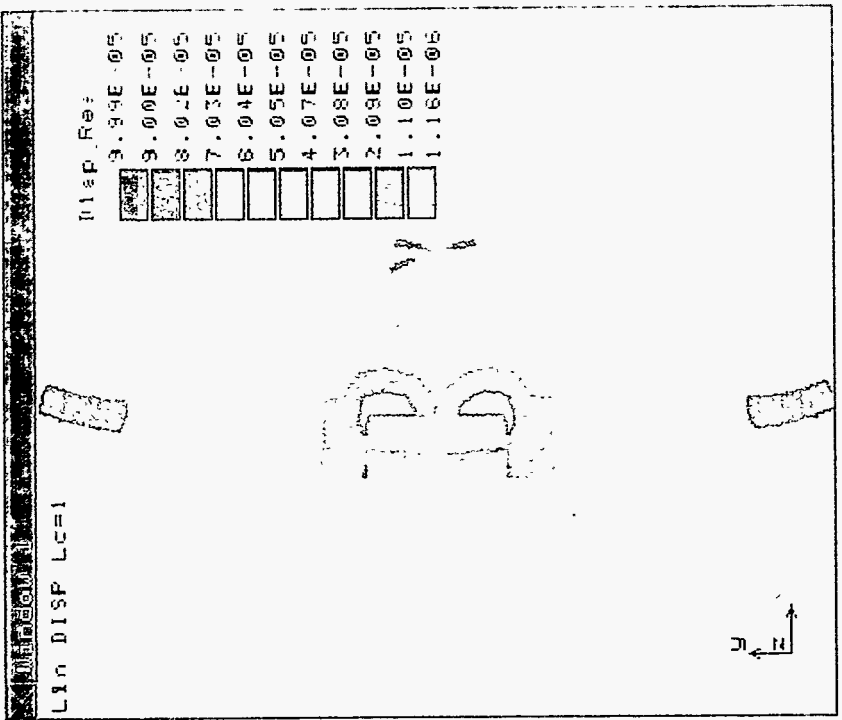


Figure 4b-
Displacement plot, no preheat
t=10 seconds

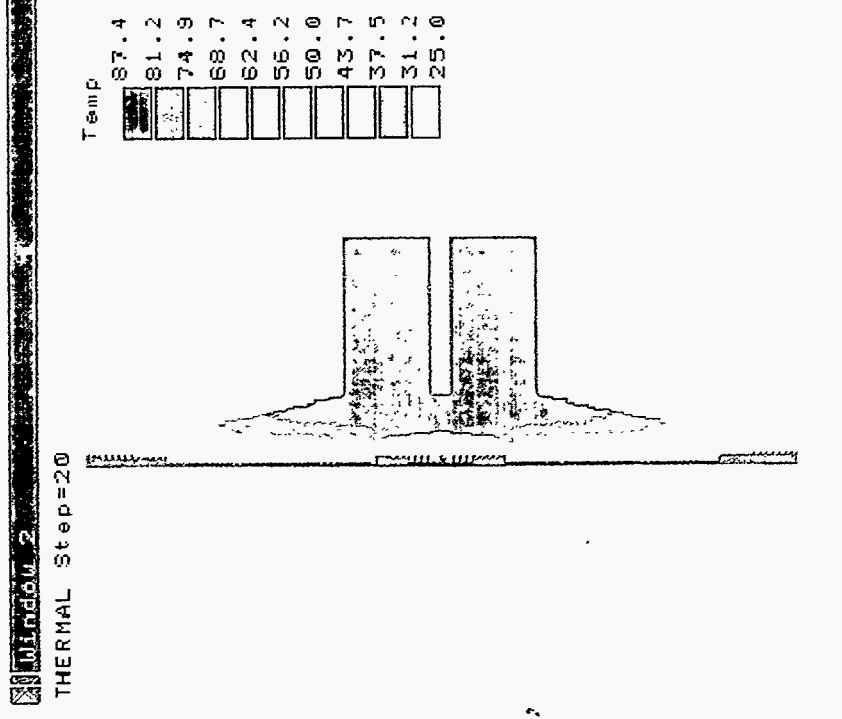


Figure 4a-
Temperature plot, no preheat
t=10 seconds

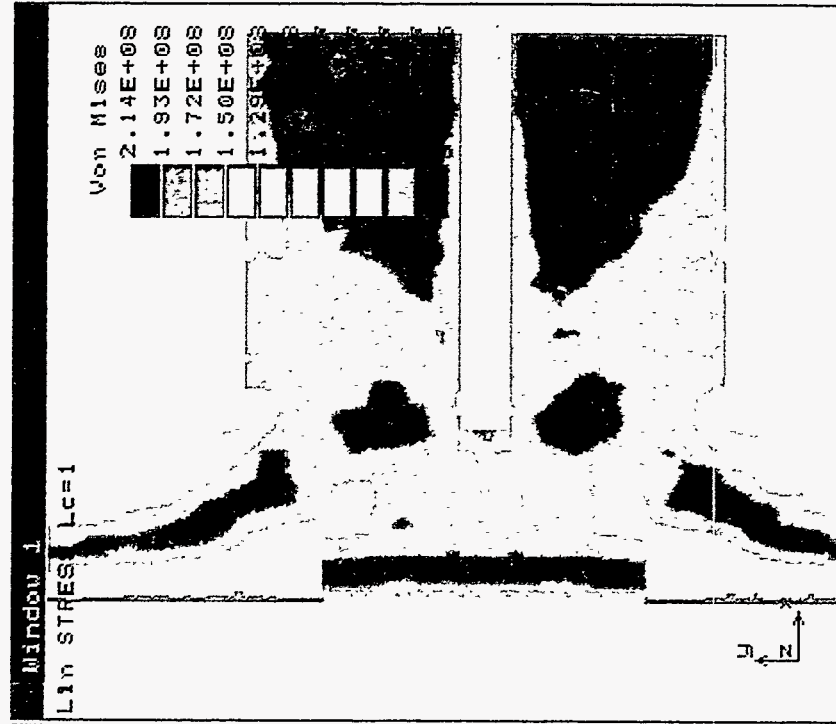


Figure 4c-
Stress plot, no preheat
t=10 seconds

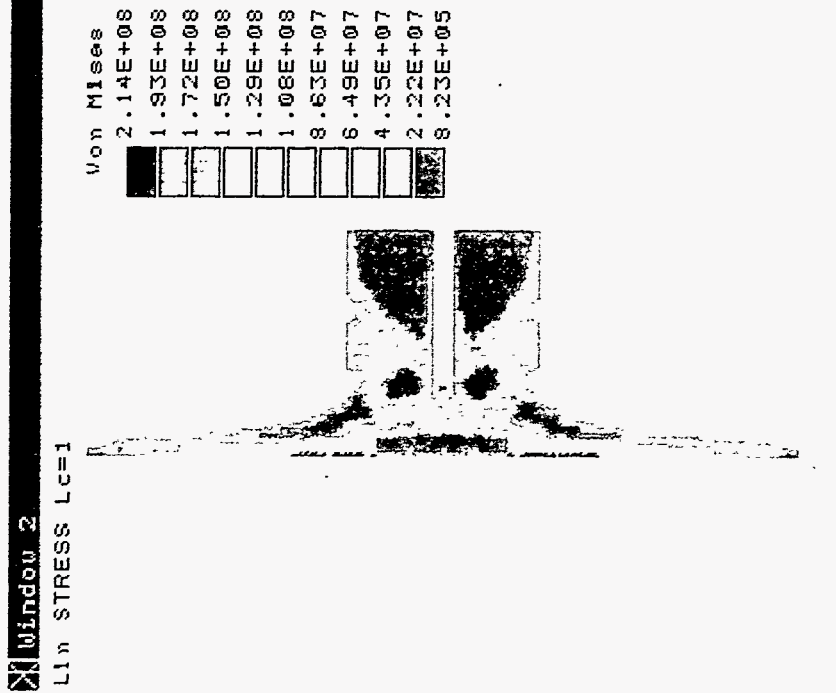


Figure 4d-
Stress plot, closeup, no preheat
t=10 seconds

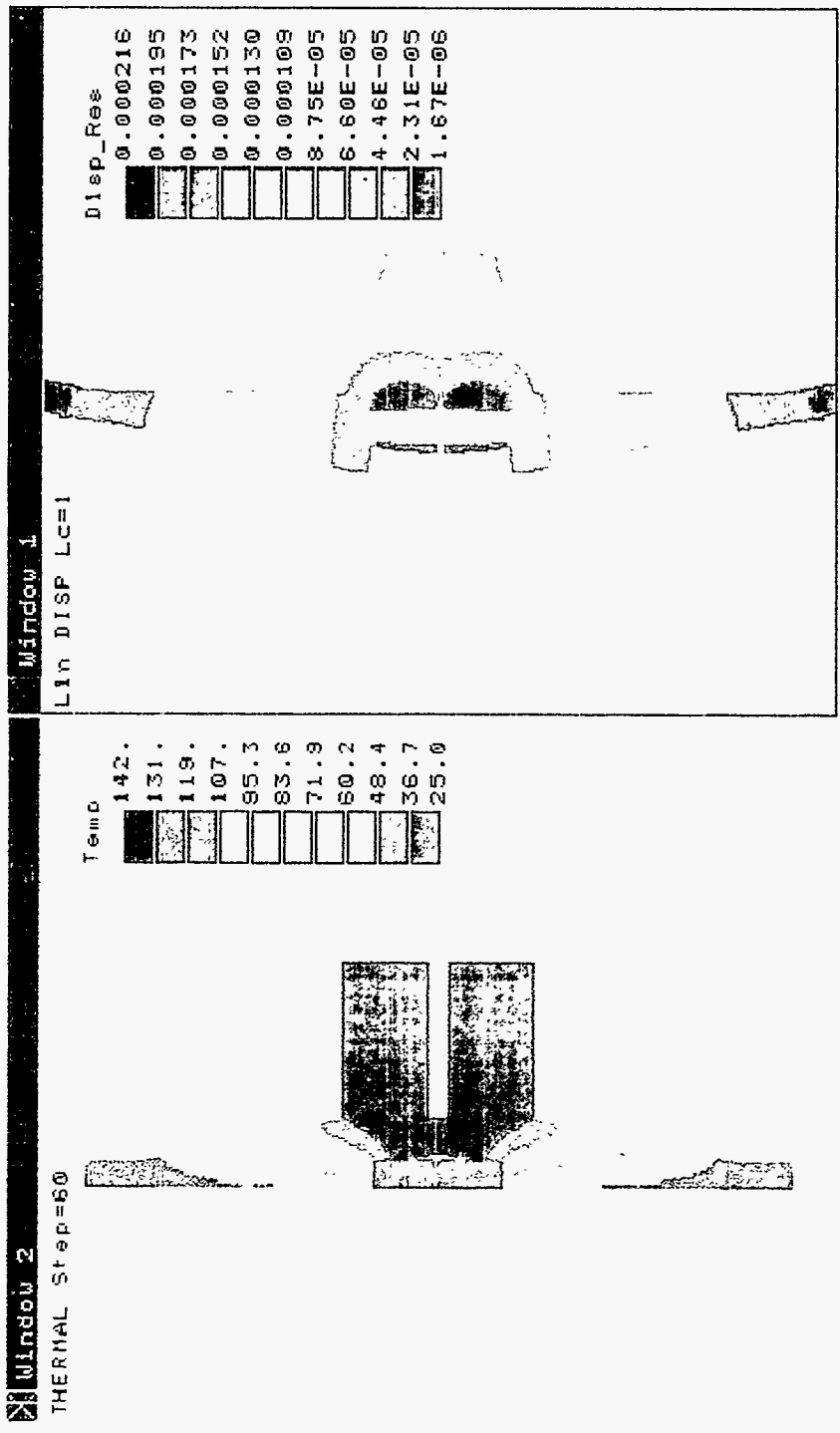


Figure 5a- Temperature plot, no preheat, t=30 seconds
 Figure 5b- Displacement plot, no preheat, t=30 seconds

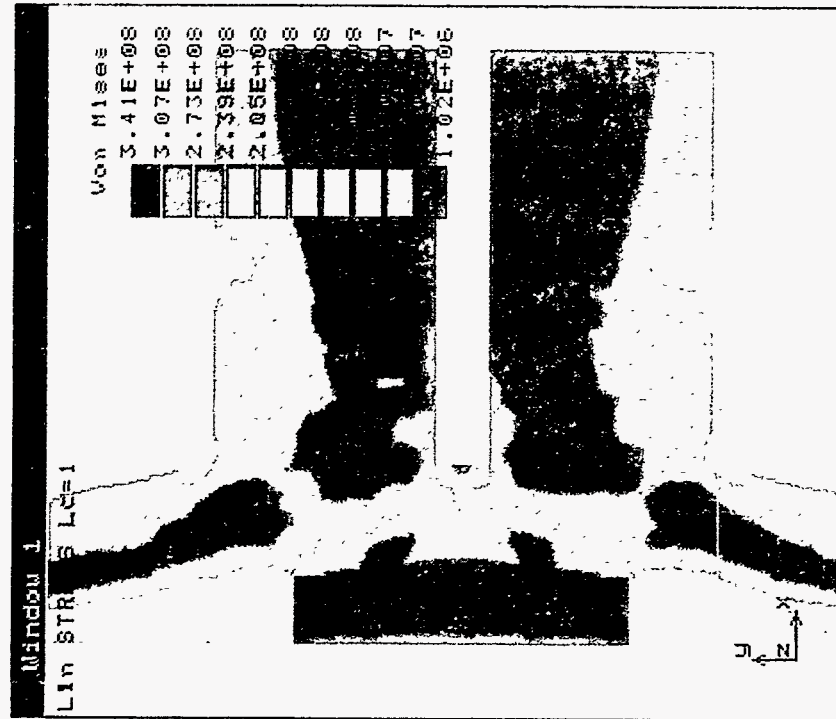


Figure 5c-
Stress plot, no preheat, t=30 seconds

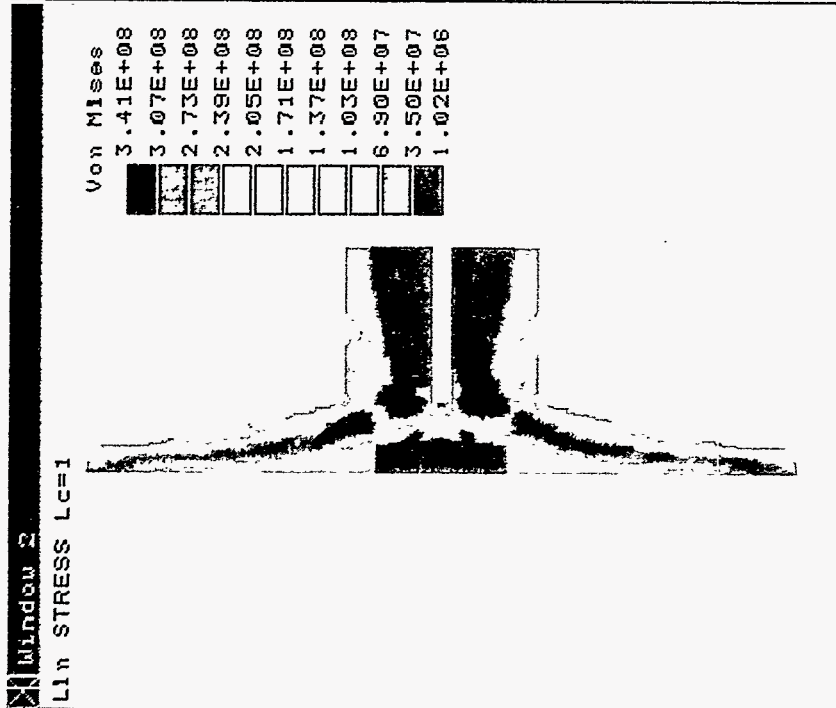


Figure 5d-
Stress plot, closeup, no preheat
t=30 seconds

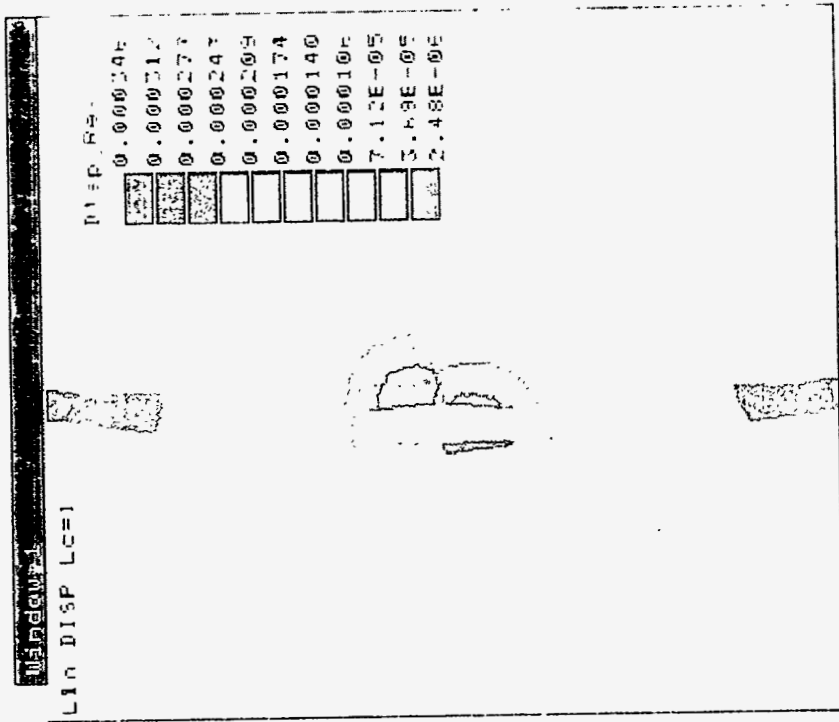


Figure 6a-
Temperature plot, no preheat
t=60 seconds

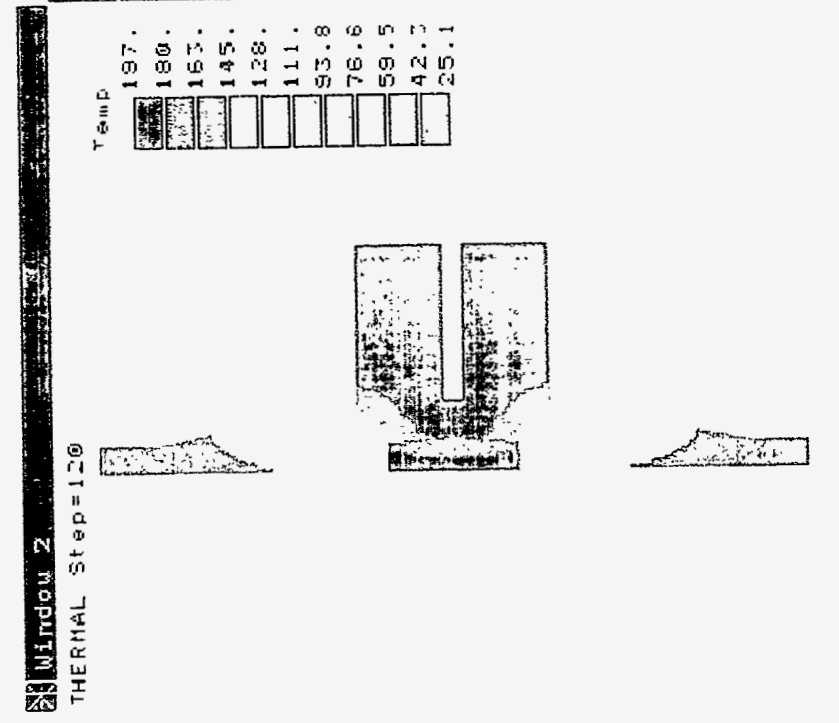


Figure 6b-
Displacement plot, no preheat
t=60 seconds

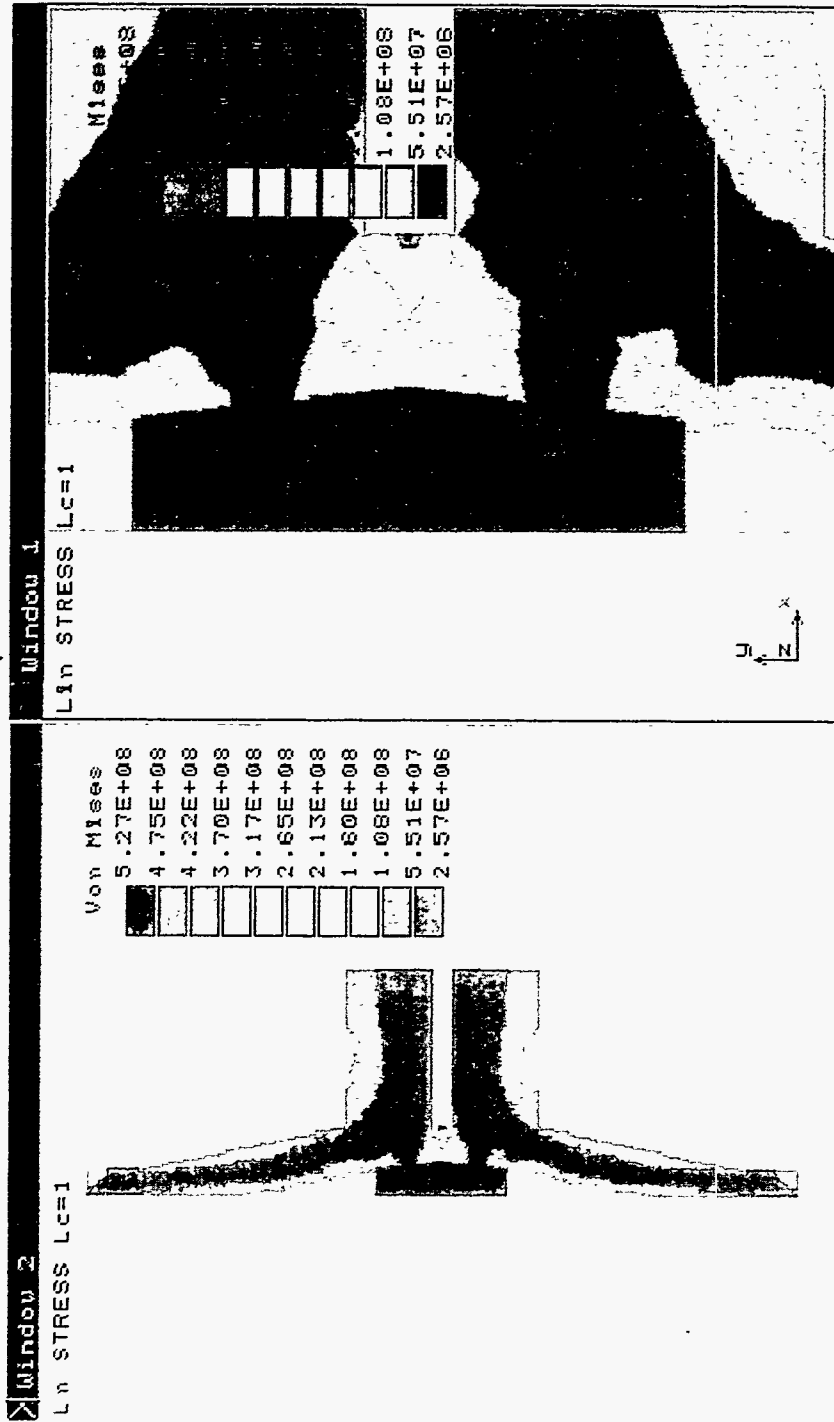


Figure 6c- Stress plot, no preheat, t=60 seconds

Figure 6d- Stress plot, closeup, no preheat, t=60 seconds

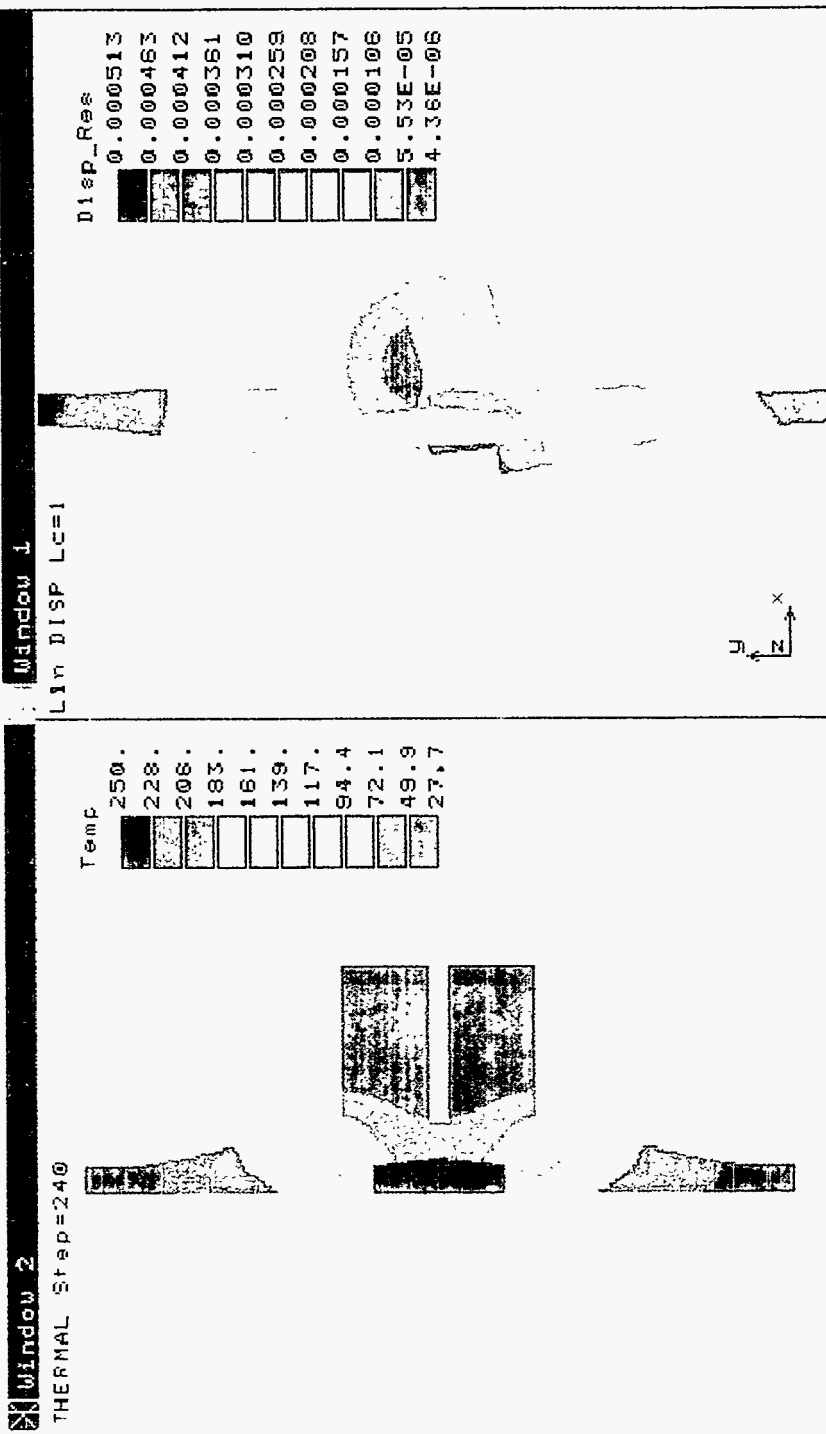


Figure 7a- Temperature plot, no preheat, t= 120 seconds

Figure 7b- Displacement plot, no preheat t=120 seconds

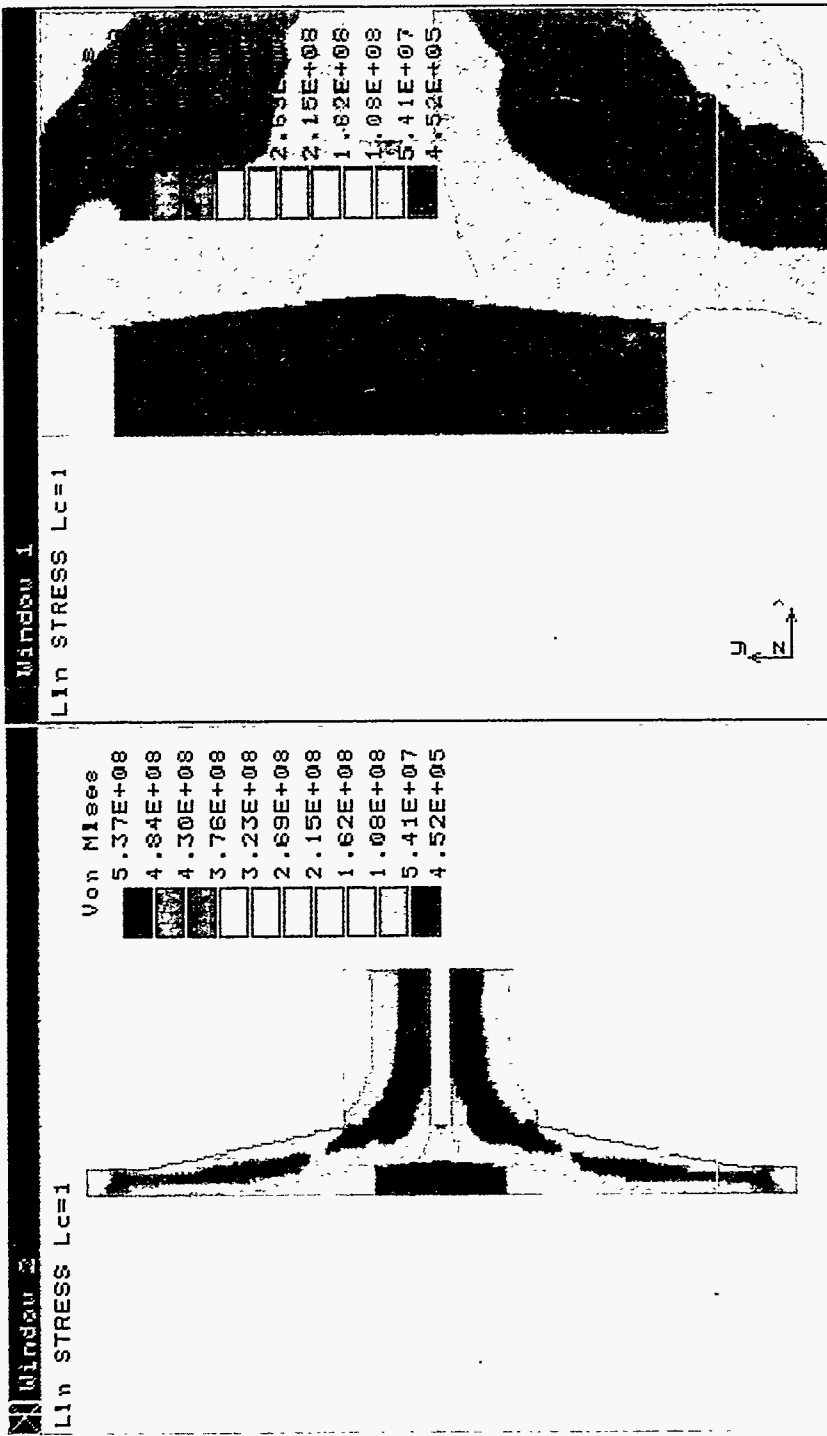


Figure 7c- Stress plot, no preheat, t=120 seconds

Figure 7d- Stress plot, closeup, no preheat, t=120 seconds

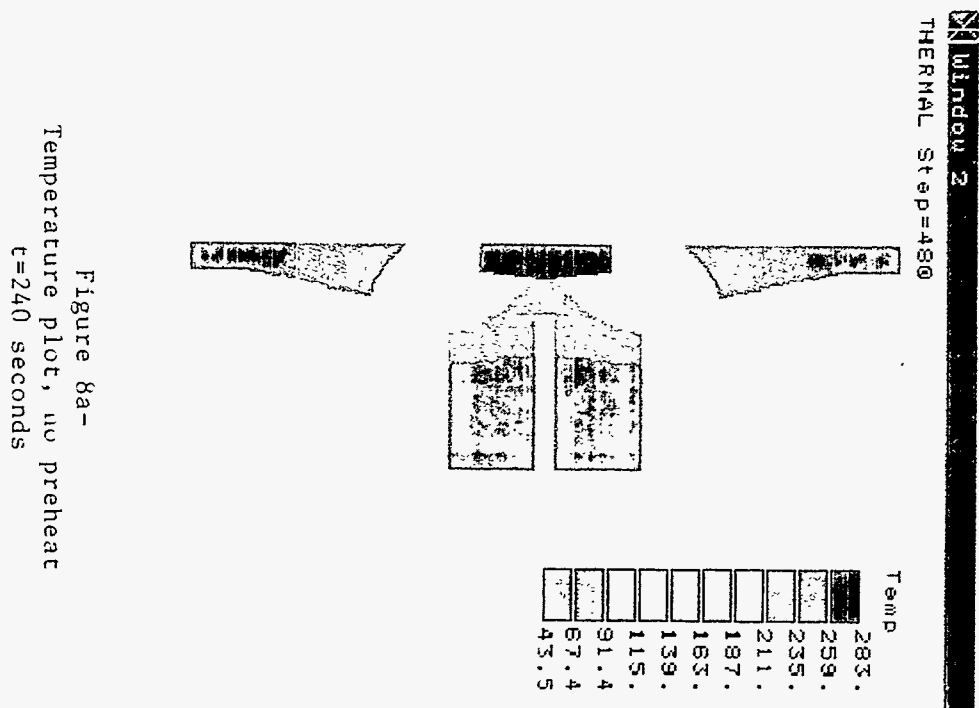


Figure 8a-
Temperature plot, no preheat
t=240 seconds

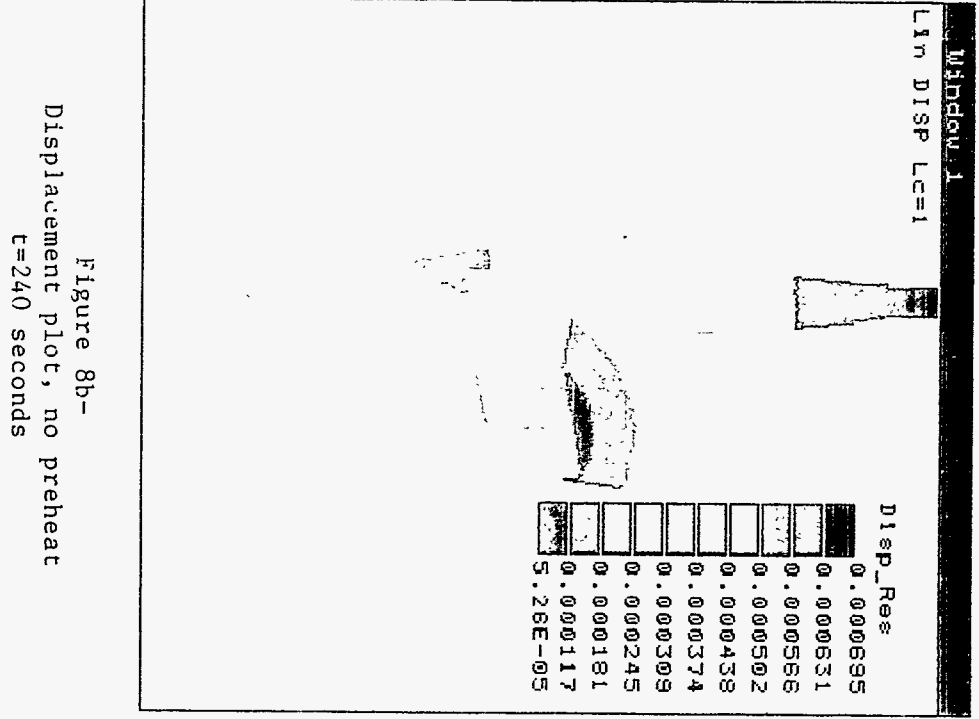


Figure 8b-
Displacement plot, no preheat
t=240 seconds

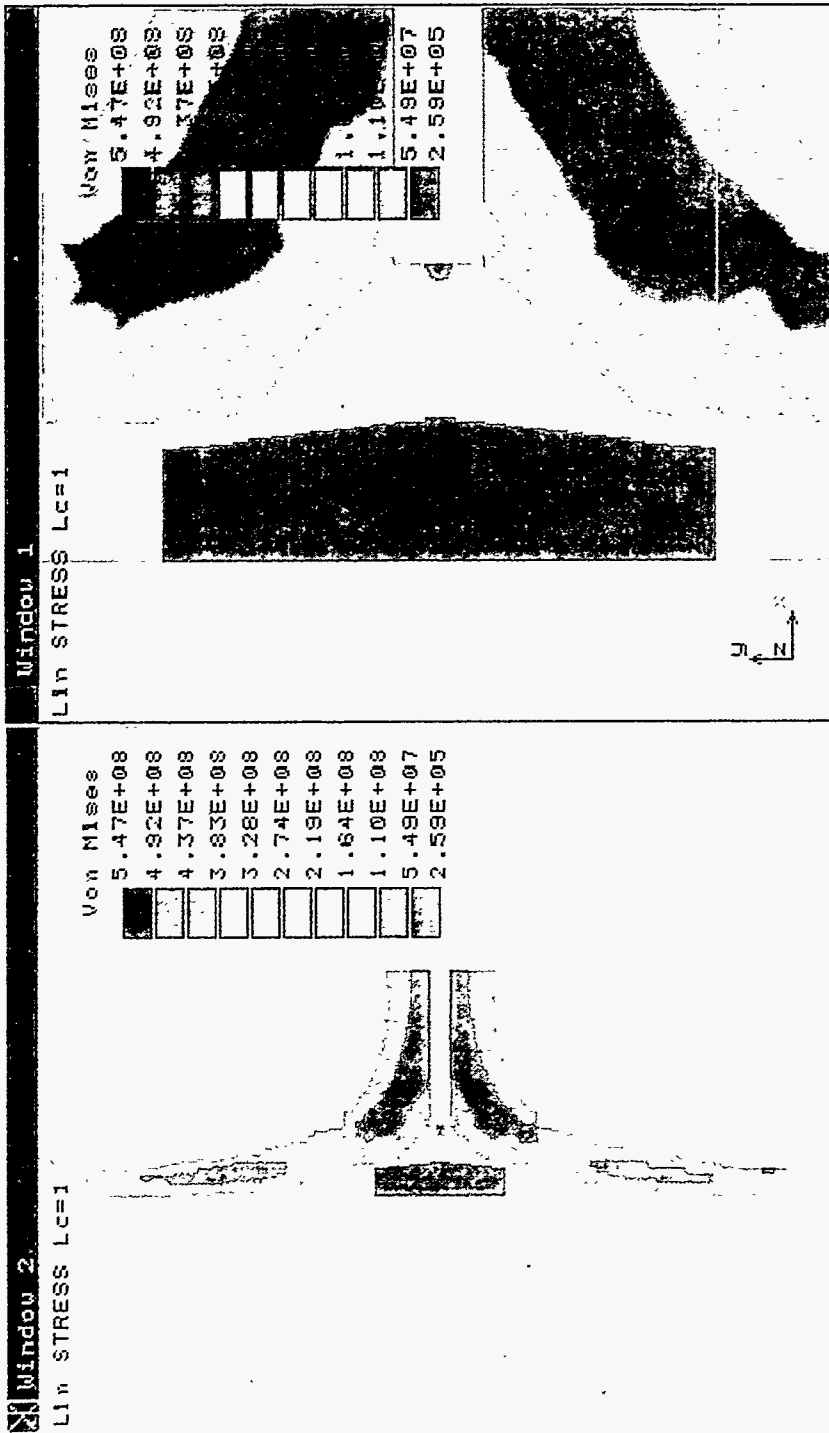


Figure 8c-
Stress plot, no preheat, t=240 seconds

Figure 8d-
Stress plot, closeup, t=240 seconds

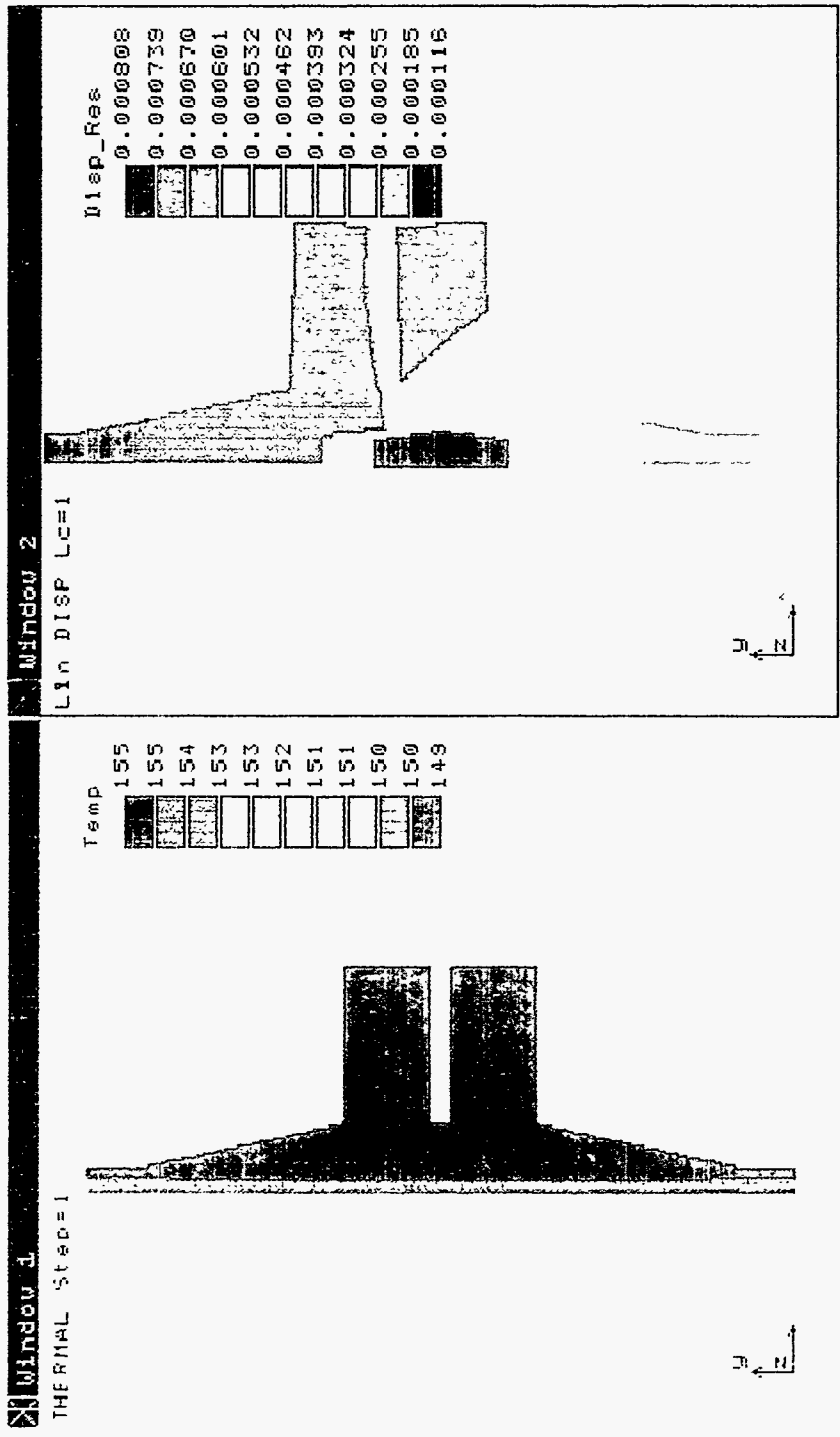


Figure 9a- Temperature plot, preheat to 149°C
t=0.5 seconds

Figure 9b- Displacement plot, preheat to 149°C
t=0.5 seconds

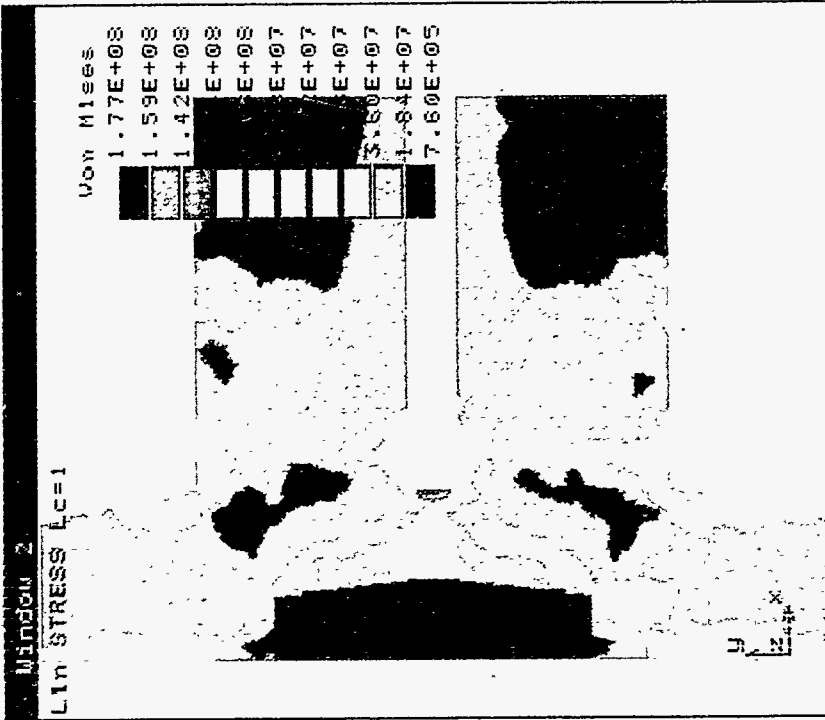


Figure 9d-
Stress plot, closeup, preheat to 149°C
t=0.5 seconds

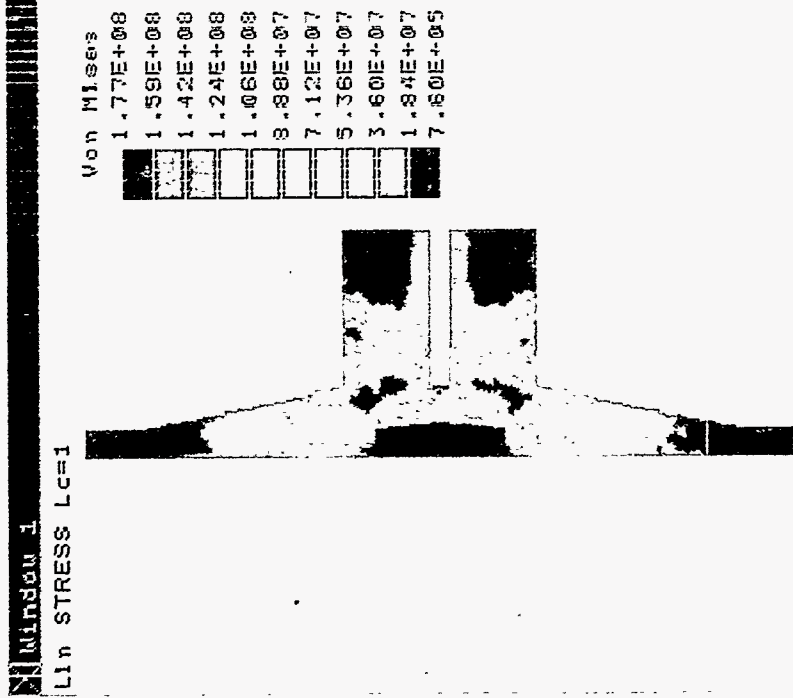
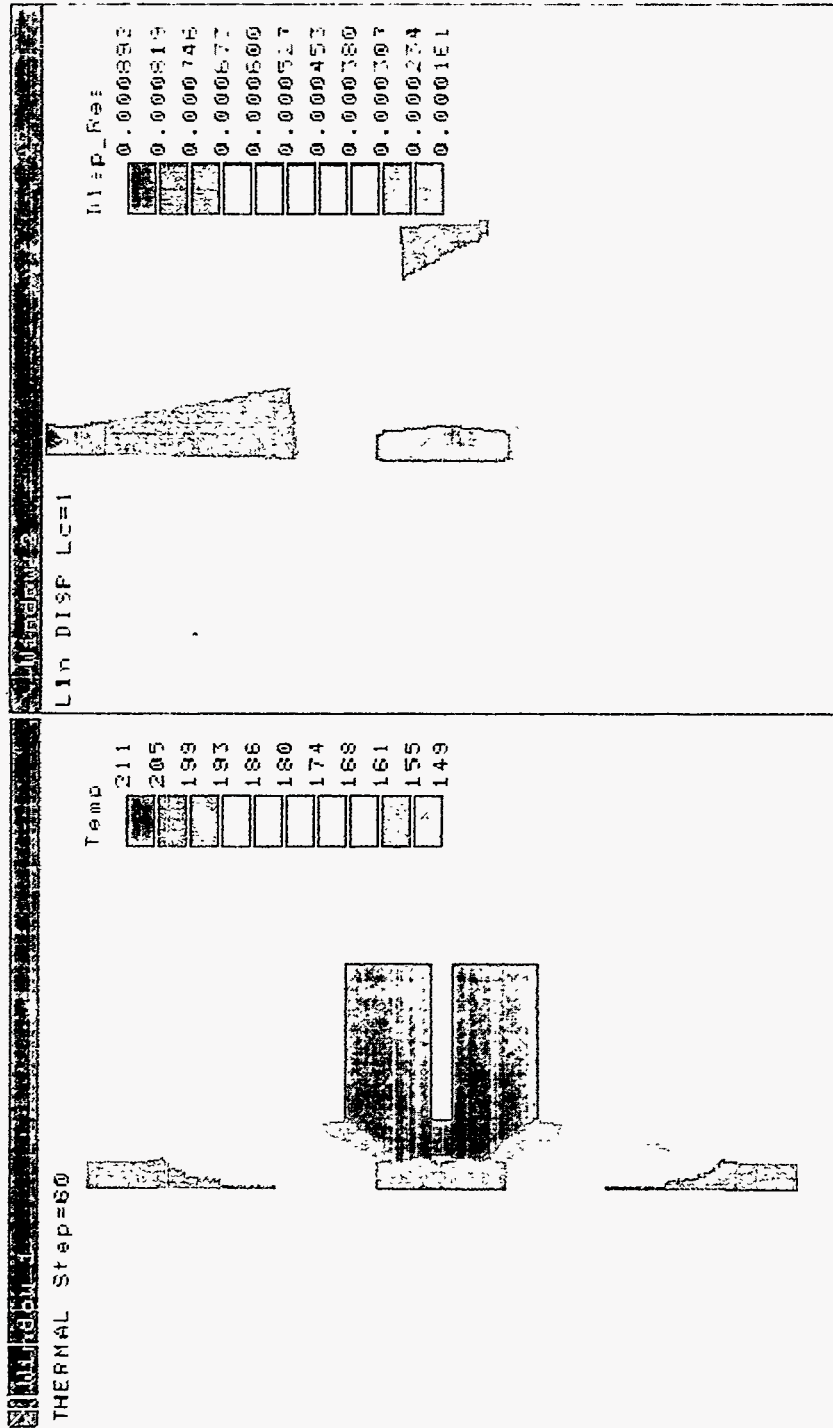


Figure 9c-
Stress plot, preheat to 149°C
t=0.5 seconds



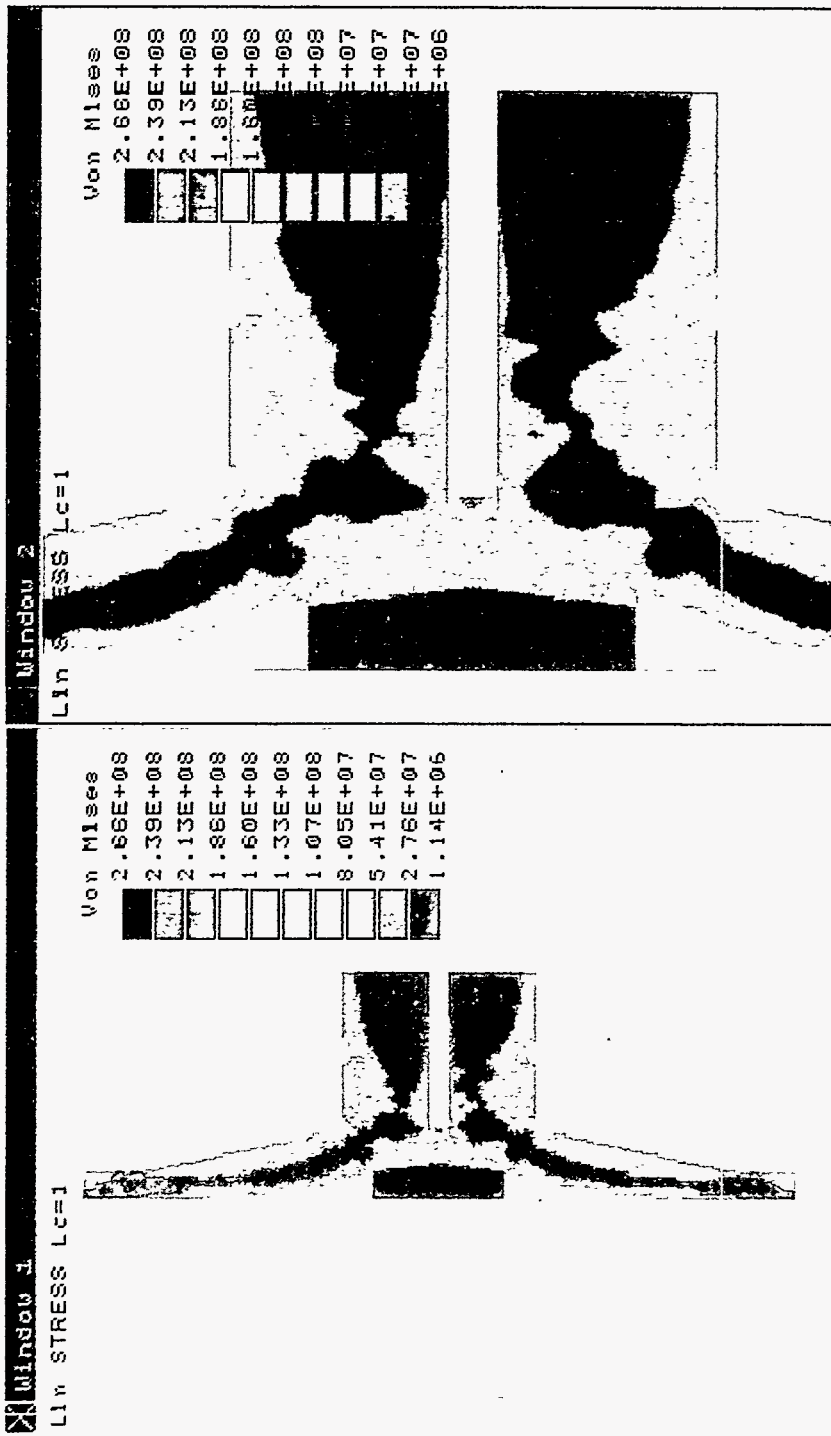


Figure 10c-
Stress plot, preheat to 149°C
t=30 seconds

Figure 10d-
Stress plot, closeup, and preheat to 149°C
t=30 seconds

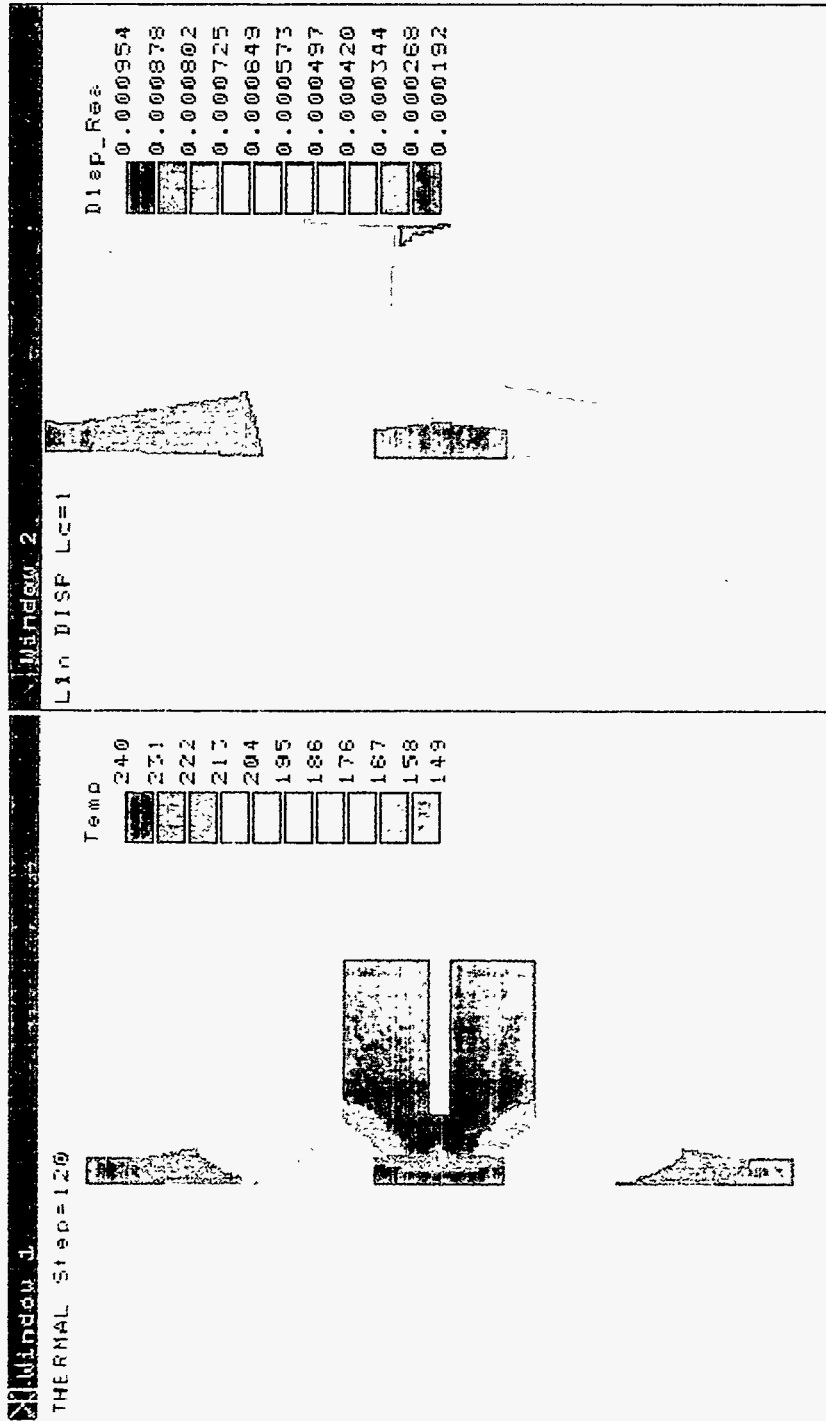


Figure 11a-
Temperature plot, preheat to 149°C
t=60 seconds

Figure 11b-
Displacement plot, preheat to 149°C
t=60 seconds

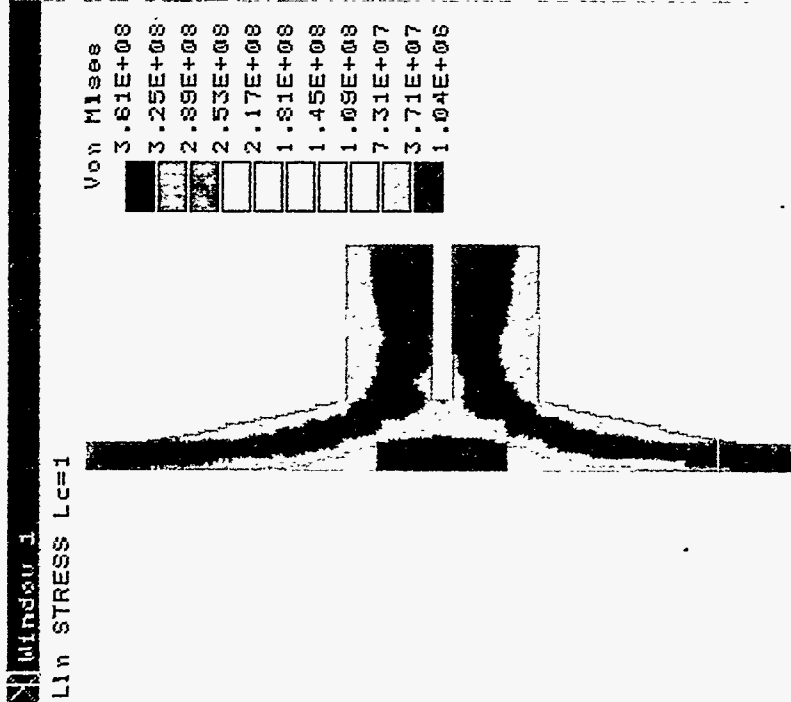


Figure 11c-
Stress plot, preheat to 149°C
t=60 seconds

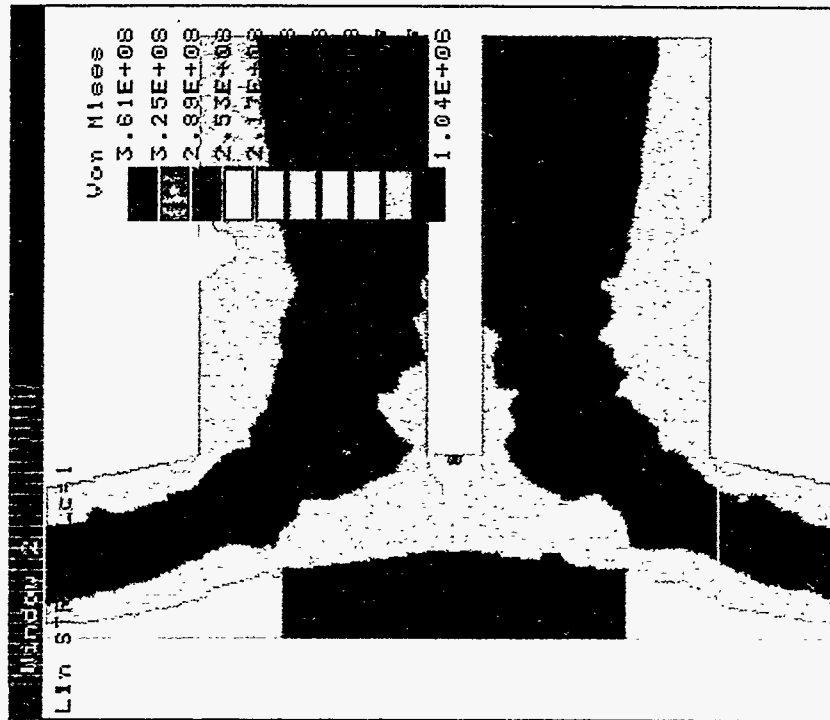


Figure 11d-
Stress plot, closeup, preheat to 149°C
t=60 seconds

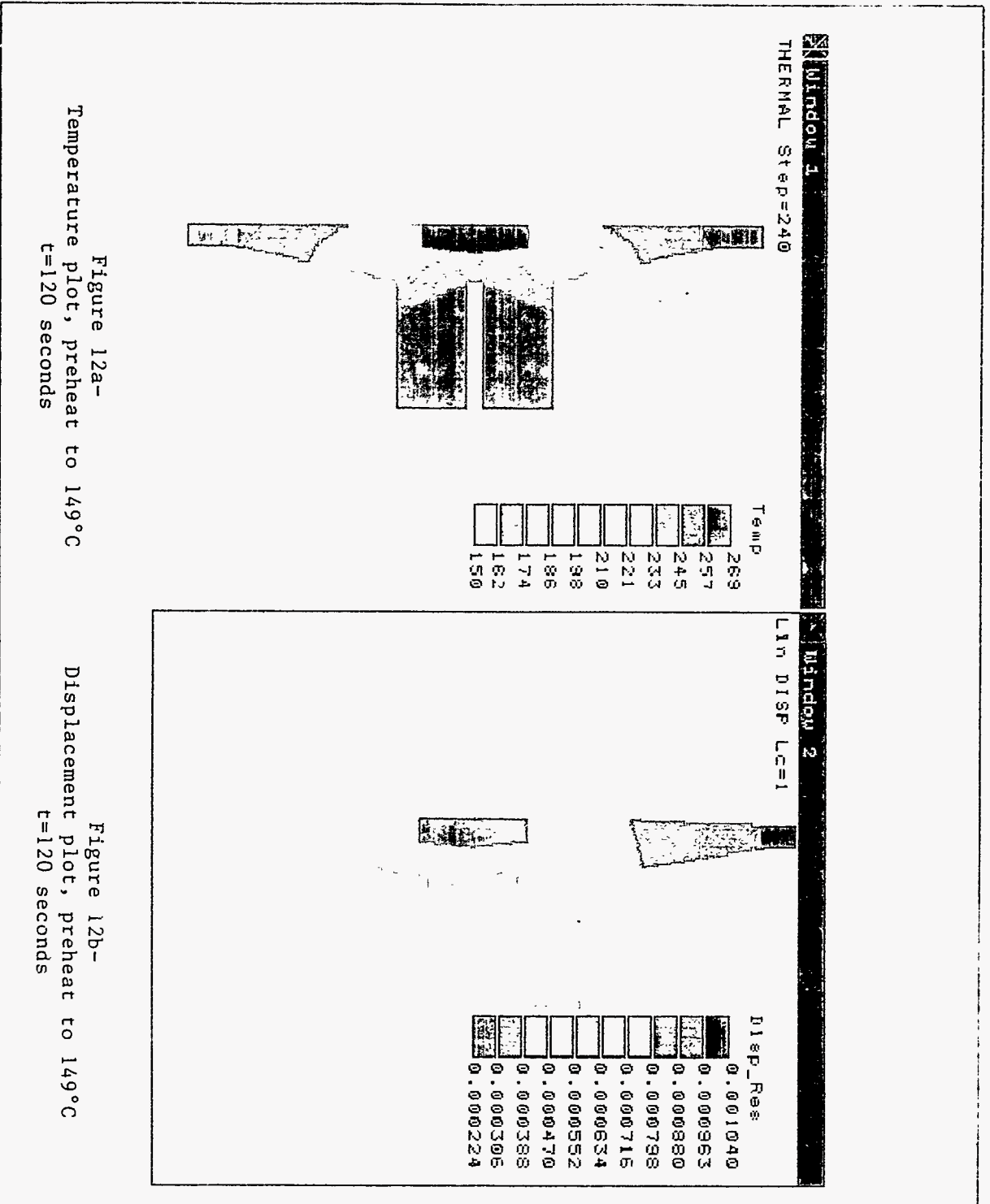


Figure 12a-
Temperature plot, preheat to 149°C
t=120 seconds

Figure 12b-
Displacement plot, preheat to 149°C
t=120 seconds

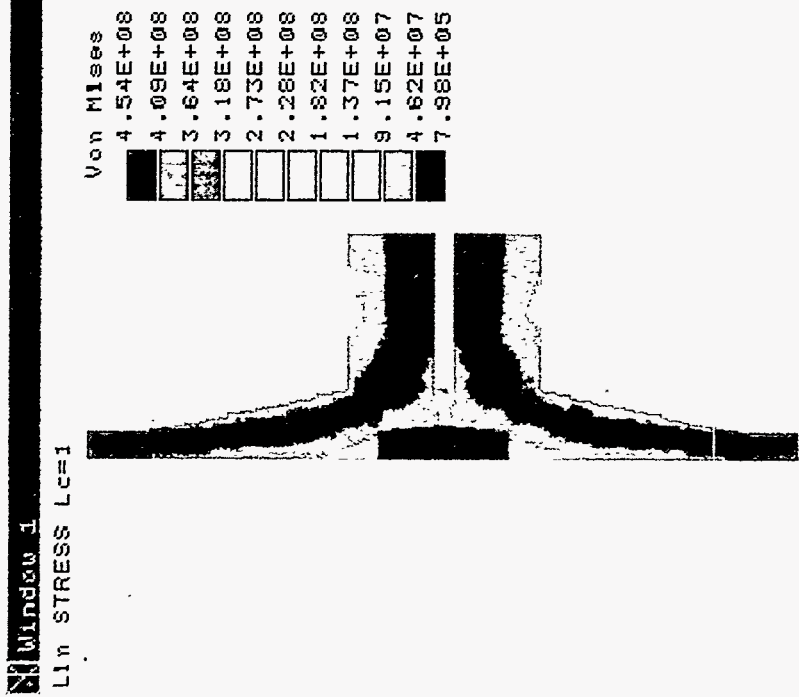


Figure 12c-
Stress plot, preheat to 149°C
t=120 seconds

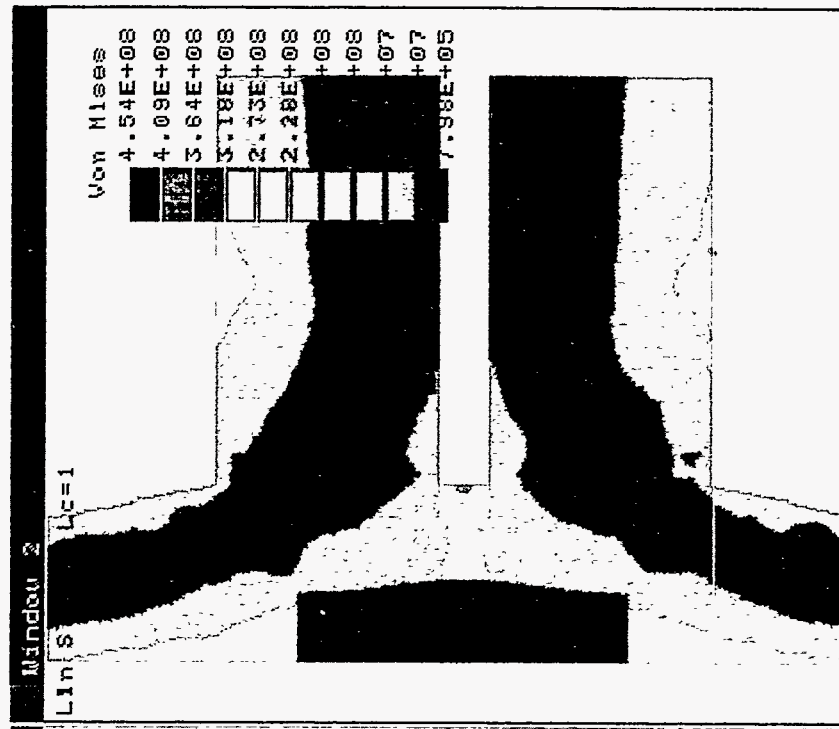


Figure 12d-
Stress plot, closeup, preheat to 149°C
t=120 seconds

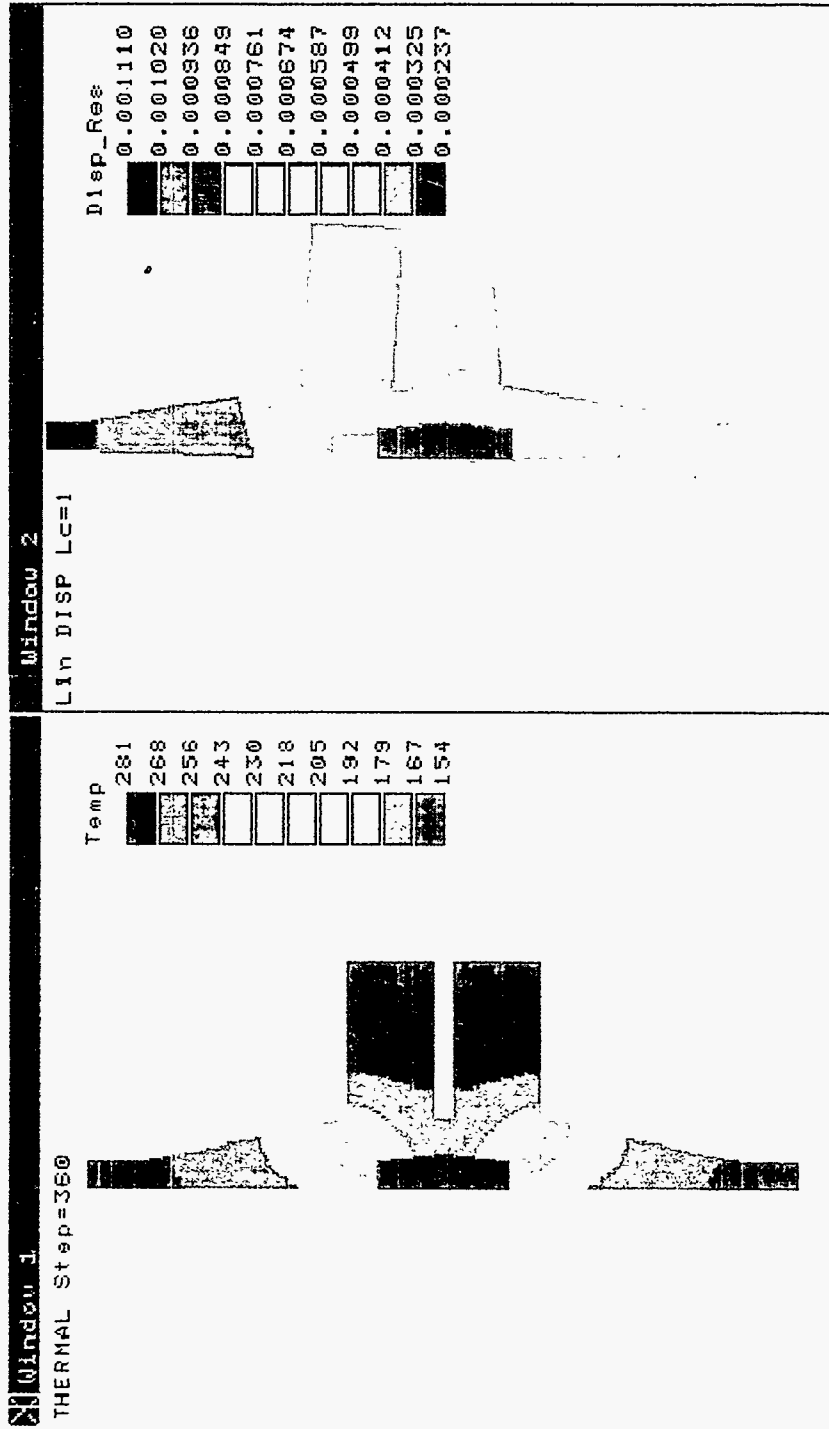
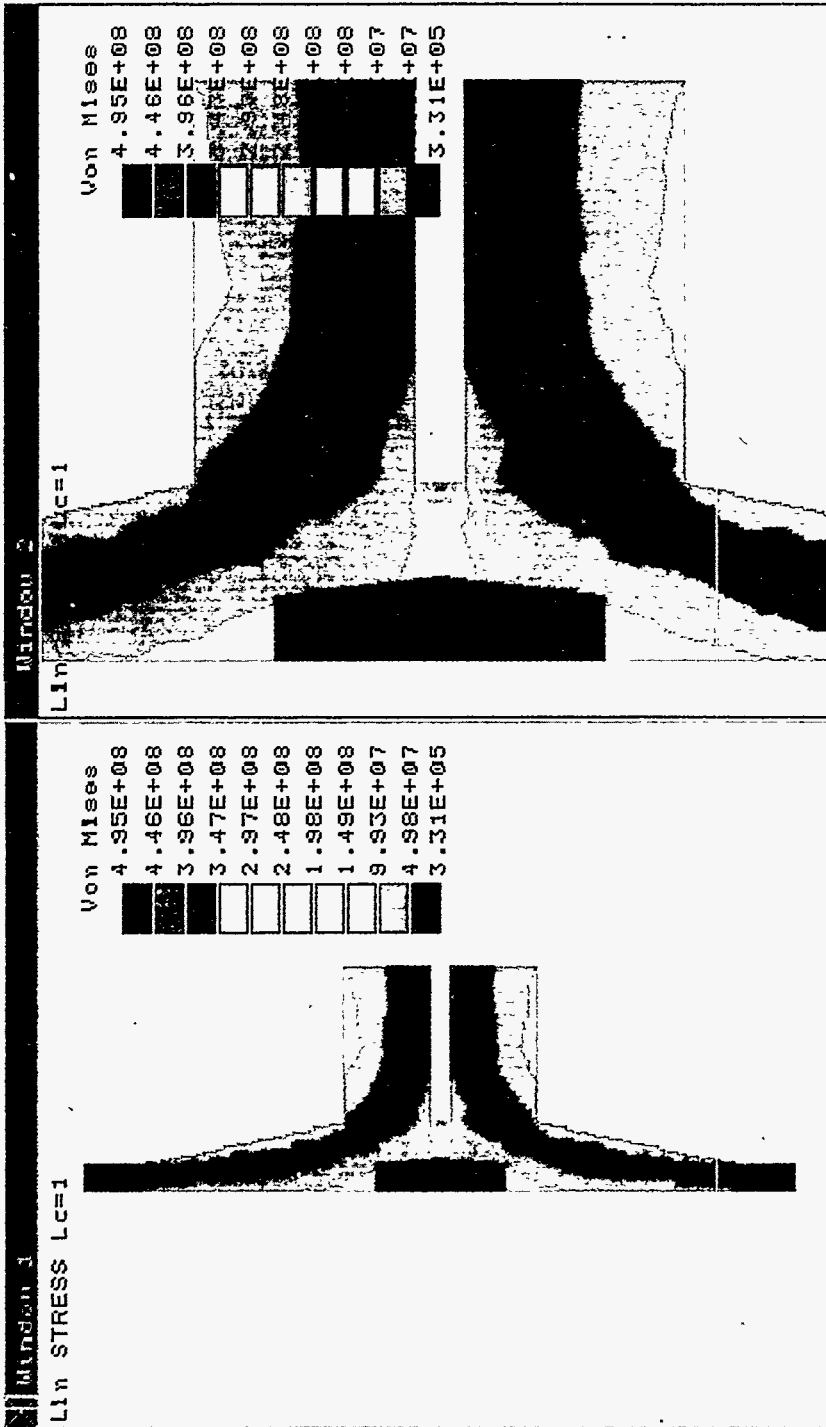


Figure 13a-
Temperature plot, preheat to 149°C
t=180 seconds

Figure 13b-
Displacement plot, preheat to 149°C
t=180 seconds



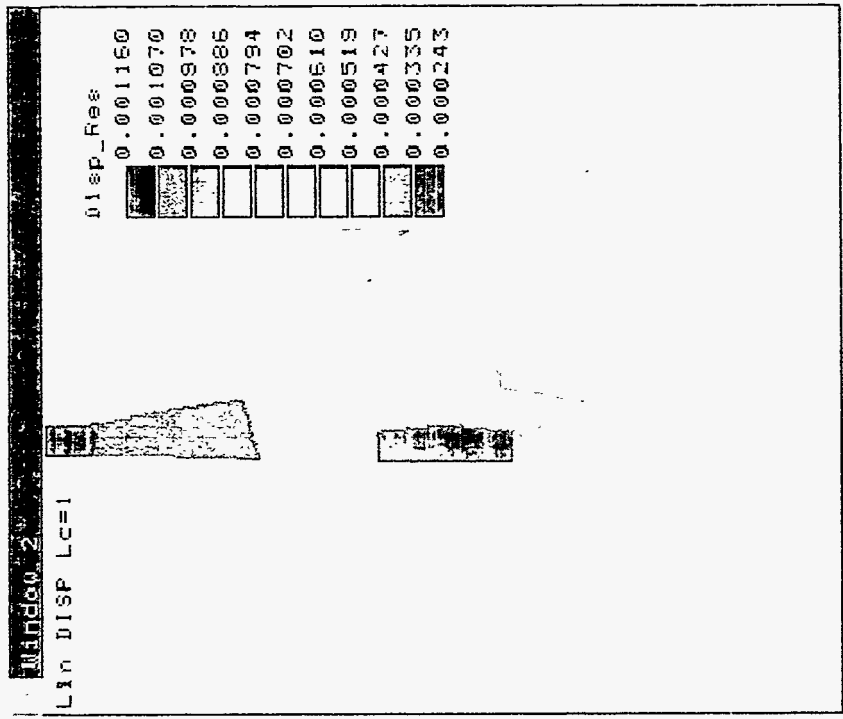


Figure 14b
displacement plot, preheat to 149°C
t=240 seconds

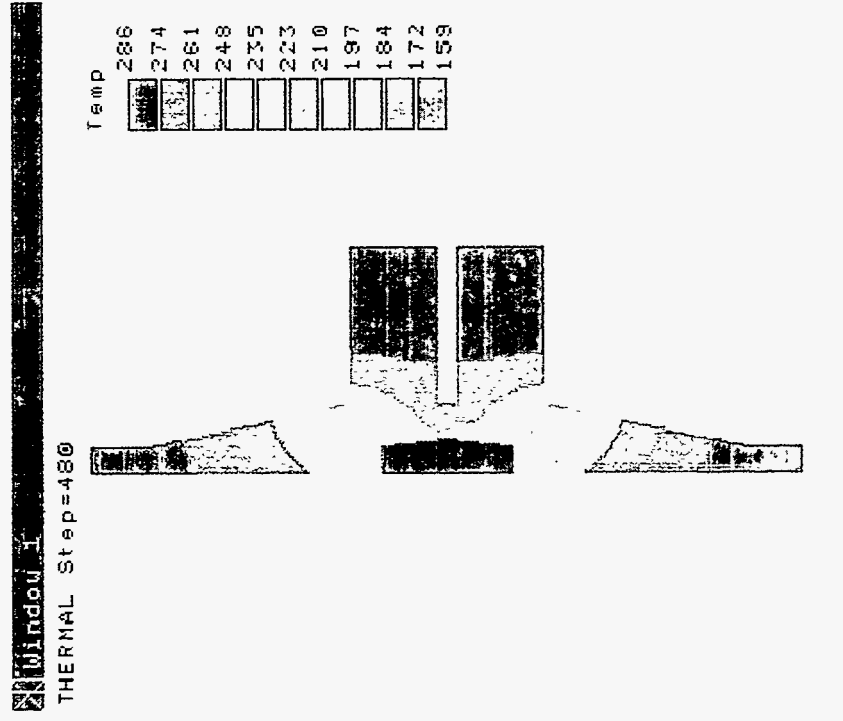


Figure 14a-
Temperature plot, preheat to 149°C
t=240 seconds

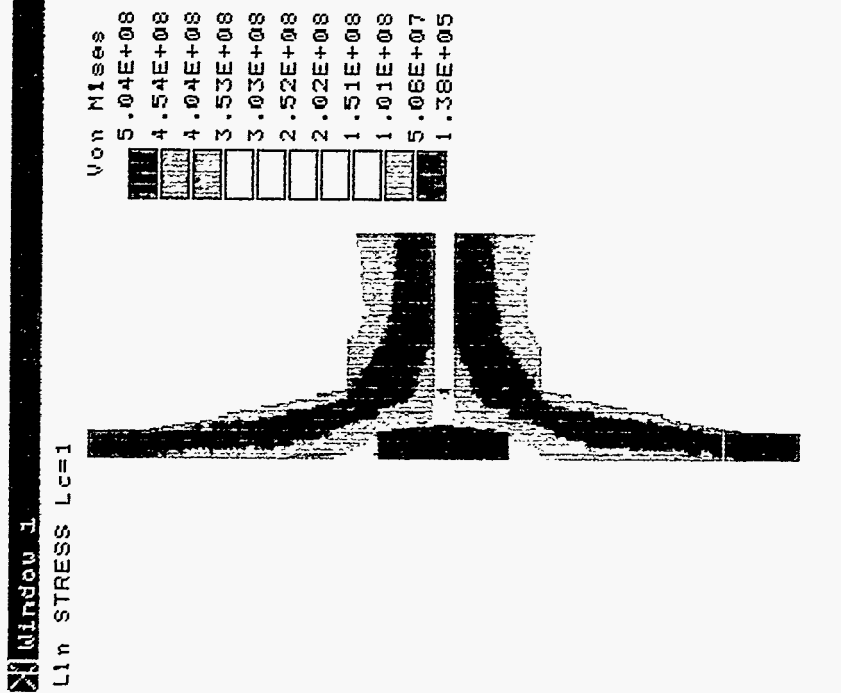
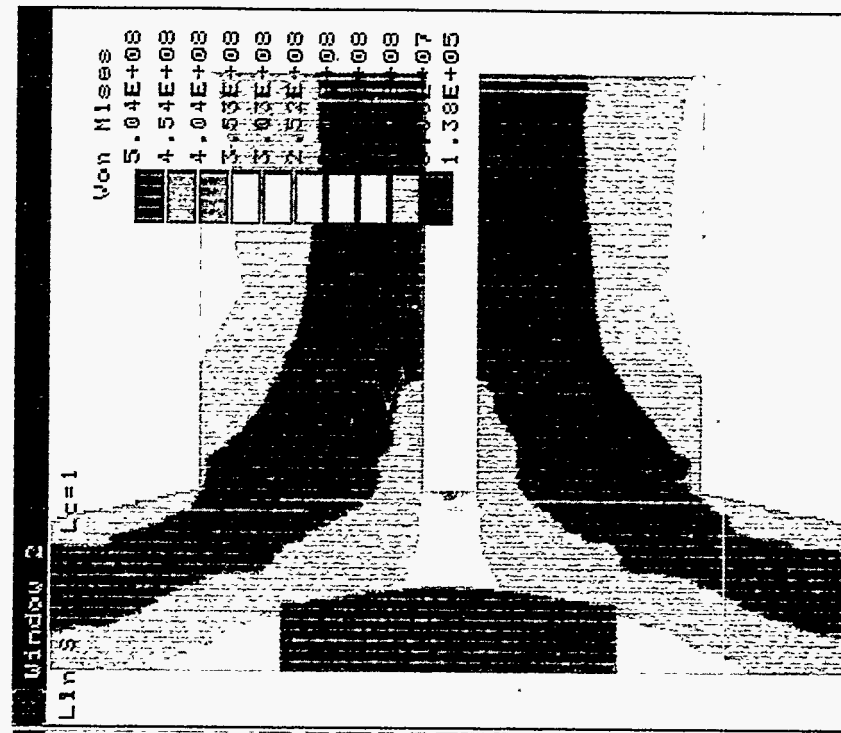


Figure 14c-
Stress plot, preheat to 149°C
t=180 seconds

Figure 14d-
Stress plot, closeup, preheat to 149°C
t= 40 seconds

Appendix B. Fabrication of Heat Trace Circuits

The heat trace for large systems is usually designed by the supplier. Each zone is sized based on the heating load and the piping diagrams. The length and power rating of a heat trace cable are sized based on the power required to maintain a pipe at given temperature and the power supply voltage. For a given voltage and heat trace cable length, the MI cable resistance density can be selected to provide the desired power. As a rule of thumb, we try to limit the power wattage density to less than 50 W/ft of MI cable length. Figures B-1 through B-4 are photographs of heat trace installed on a section of piping, a valve body, the header of a receiver panel, and above the jumper tubes in a receiver panel.

To maintain the integrity of the electrical circuit, only, tube benders should be used to bend the heat trace cable. See Figure B-5. After the heat trace is installed, it is covered with metal foil to prevent insulation from getting between the heater and the pipe causing the heater to overheat. The metal foil also helps to direct the radiant heat from the heat trace to the pipe or component. The metal foil can either be wrapped around the pipe and heat trace or tack welded over the heat trace to the pipe.

A critical area in heat trace circuit fabrication is the hot to cold junction. This junction makes a transition from the power lead (copper cable) to the heater (NiCr cable). Most of the failures of heat trace circuits can be attributed to a failure at the hot to cold junction. Below is an outline of the fabrication of hot-to-cold junctions.

1. First, a splice is drilled out to fit over the MI cable. See Figure B-6.
2. Cut the MI cable by scoring it three times, but not cutting it all the way through because it may cause a short of the conductor wire. Snap off the cut piece.
3. Remove 3/8 inch of the sheath to expose the inner wire of the MI cable. Peel the sheath to expose the Magnesium Oxide (MgO) and conductor wire (Figure B-7.)
4. File the inner conductor wire flat. Everything must be kept clean to make sure the silver solder adheres. Clean with emery cloth (Figure B-8).
5. Test (Meger Test) the insulation quality of each MgO MI cable by measuring the resistance between the conductor and the sheath. The resistance should be at least 5 M Ω preferably 20 M Ω .
6. Clean everything that has to be brazed: the conductors and sheath.
7. Check the splice and stress fitting for fit.
8. Slip the stress fitting and splice over the MI cable.
9. Put flux on the conductor of the cold lead (copper wire) to help the brazing process.
10. Put solder on with a torch.
11. Check the resistance again to make sure there are no shorts.
12. Line up the hot (NiCr) and cold (Cu) leads (Figure B-9).
13. Melt the solder from the cold (Cu) side and let it flow towards the hot (NiCr) side.
14. Remove flux residue with pliers. Check integrity of joint. Buff with emery cloth.
15. Check resistance again for shorts.
16. Clean any outgassing of flux residue on the surface of the MgO by taking out the top surface of the MgO. The MgO is very hydroscopic.
17. Slide the splice over the junction until the junction can be seen through the breather hole.



Figure B-1. Heat trace installed on 2 inch pipe before metal foil was installed. It is snaked to allow for thermal expansion.

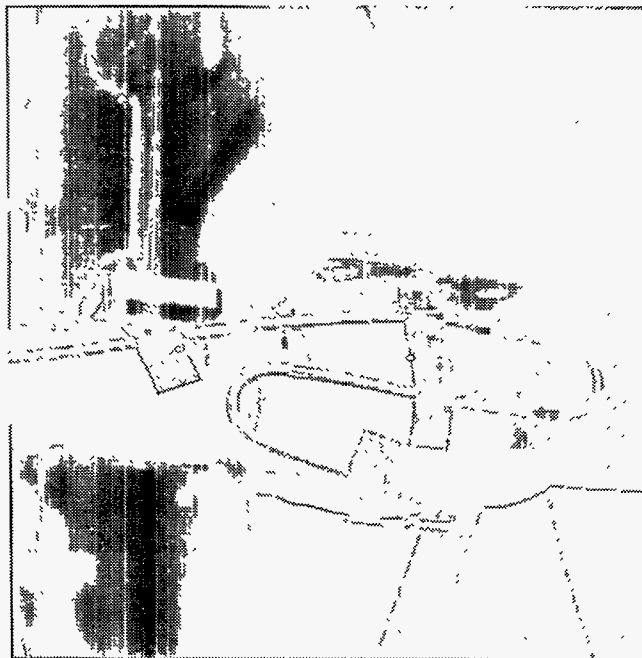


Figure B-2. Heat trace installed on valve body prior to being covered with metal foil.



Figure B-3. Heat trace on receiver panel header with metal foil covering the cable.

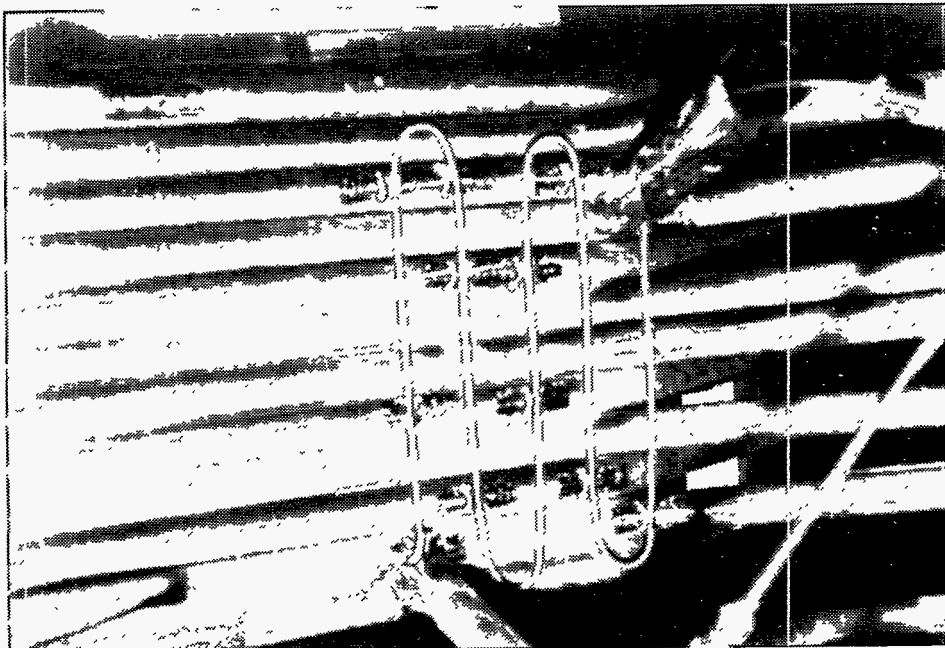


Figure B-4. Heat trace on jumper tubes in receiver panel.

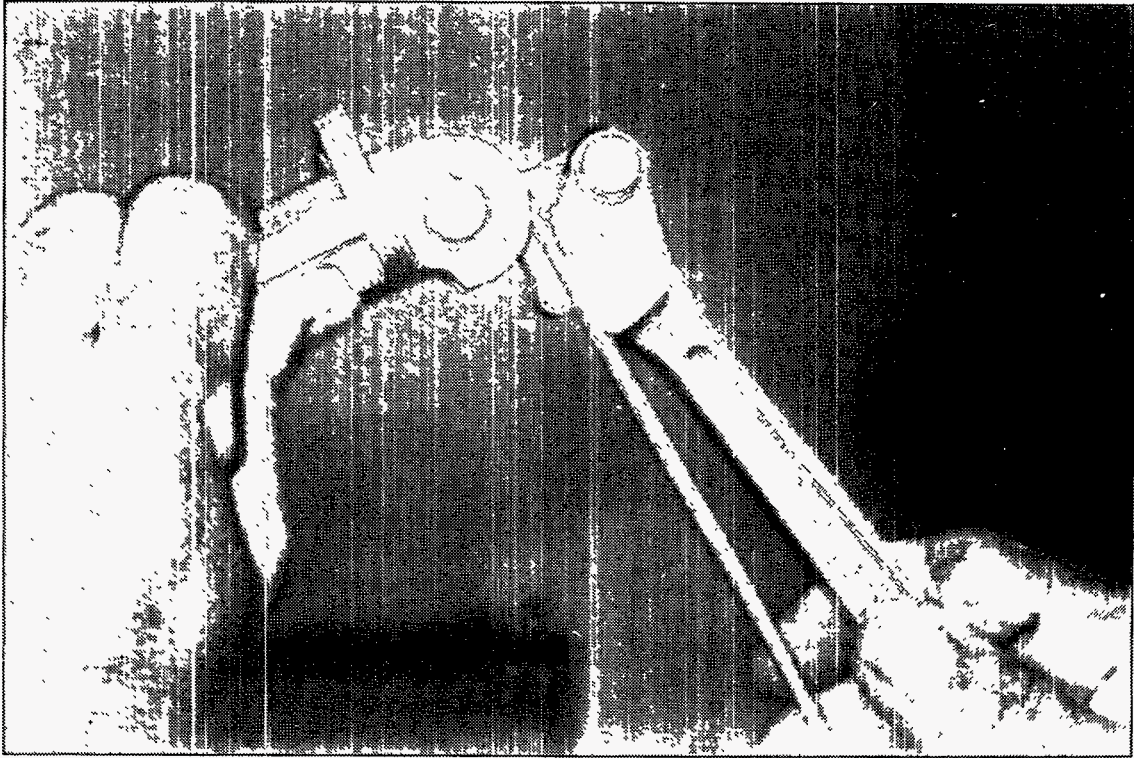


Figure B-5. Tube bender used for bending MI cable.

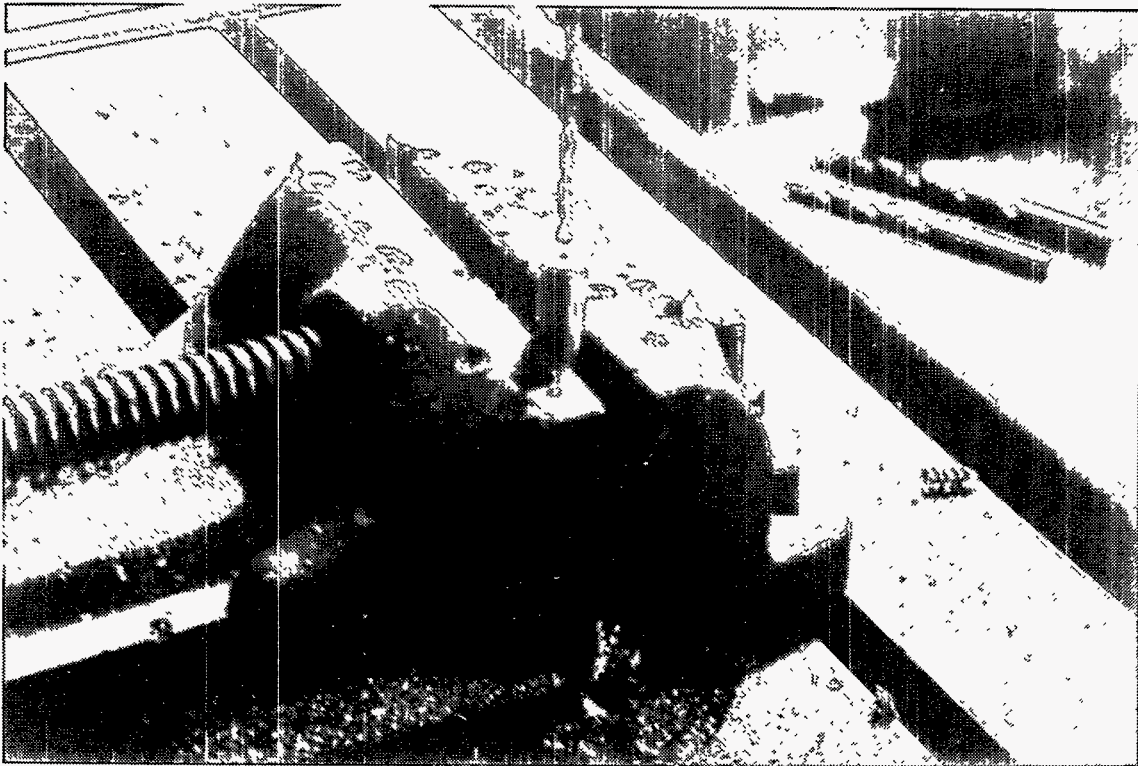


Figure B-6. Splice is drilled to fit over MI cable.

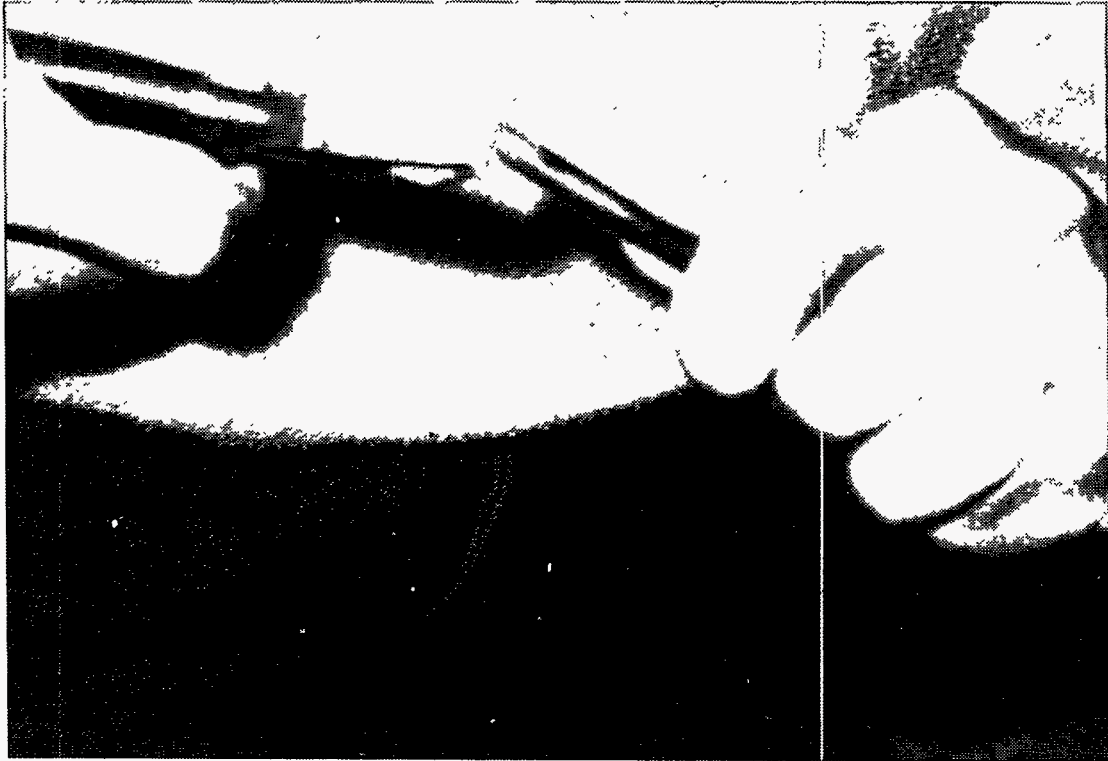


Figure B-7. Sheath is peeled away to expose magnesium oxide (MO) and the conductor wire.

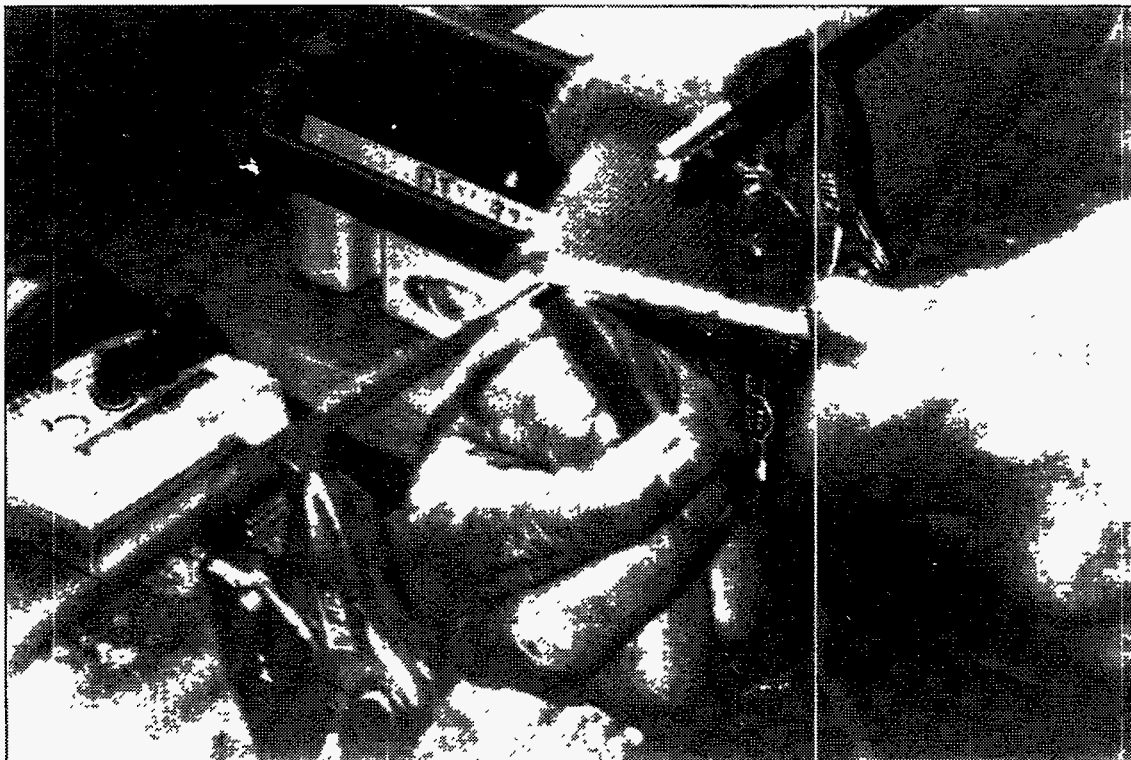


Figure B-8. The conductor wire must be cleaned so the silver solder will adhere.

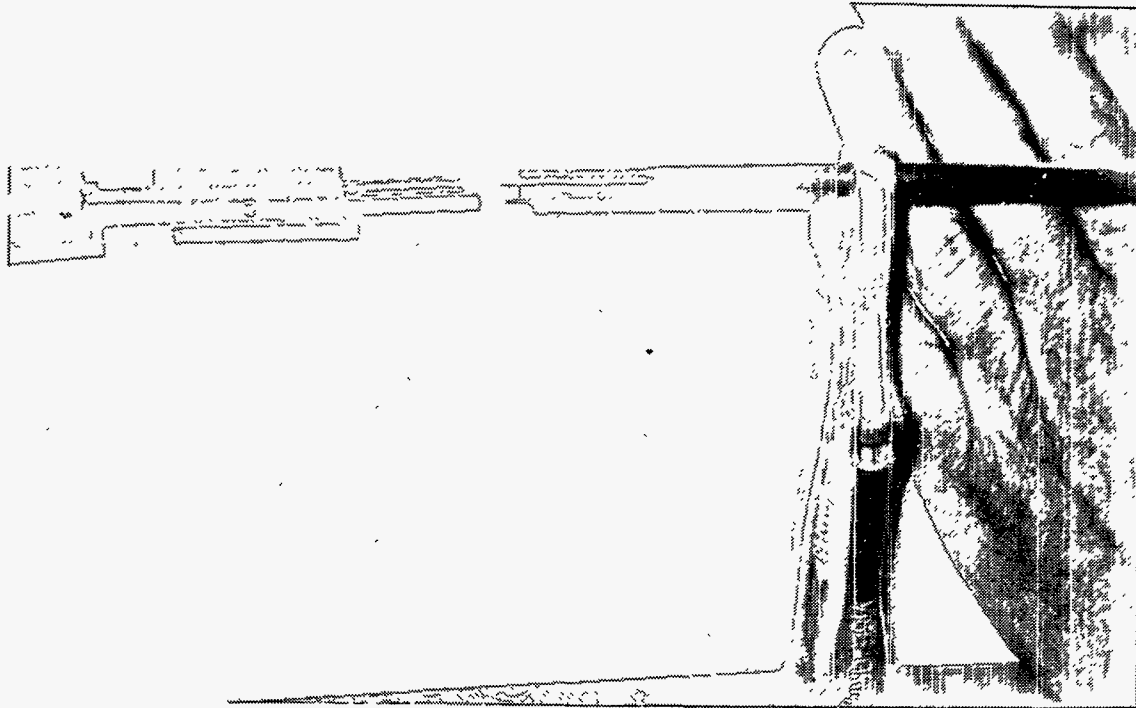


Figure B-9. The heater wire - NiCr, (on the left) and cold lead - Cu (on the right) are lined up.

18. Braze the heater side of the splice to the sheath first. Don't have both sides of the MI cable clamped tight otherwise stress will build in the joint. Allow the junction to grow. Braze the hot side by first heating the splice because it has more thermal mass than the sheath, then heating the surrounding cable to bring all parts to temperature at once. Flow solder around the splice. Repeat for cold side (Figure B-10).
19. Check resistance again.
20. Use a screw to cap off the breather hole in the slice by first putting a kink in the threads two or three threads up to prevent the screw from going in too far and screwing it in the breather hole. Clip off the screw flush with the surface of the splice. File it down. Use a round tail file to make grooves in splice for solder to adhere.
22. Flux area. Seal vent hole with solder.
22. Use a wet rag (Figure B-11) to determine if junction is sealed by measuring resistance. If water penetrated the seal, the resistance would decrease.

Don'ts with Heat Trace:

1. Don't weld near heat trace. Weld splatter could burn a hole in the sheath.
2. Don't hammer heat trace to fit it in tight spots (Figure B-12).
3. Don't use pliers or files to bend the MI cable (Figures B-13 and B-14). Use a tube bender (Figure B-5).

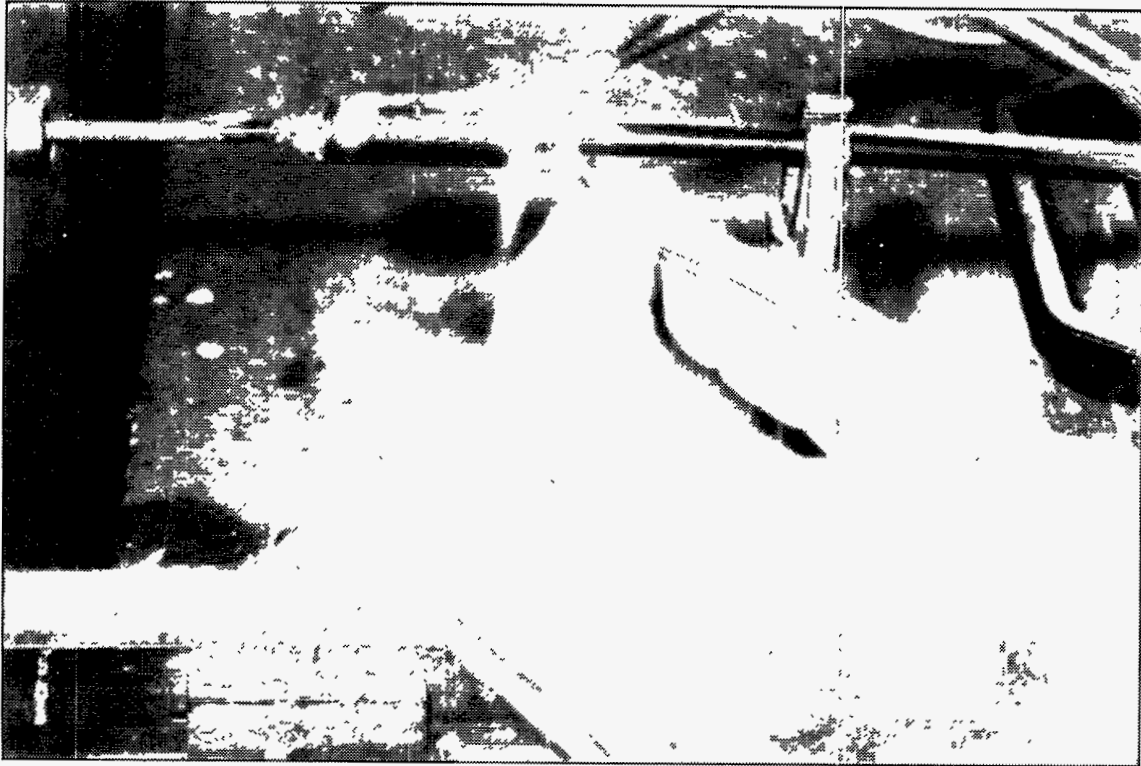


Figure B-10. The splice is brazed to the cable sheath.



Figure B-11. Use a wet rag to determine if the junction is sealed.

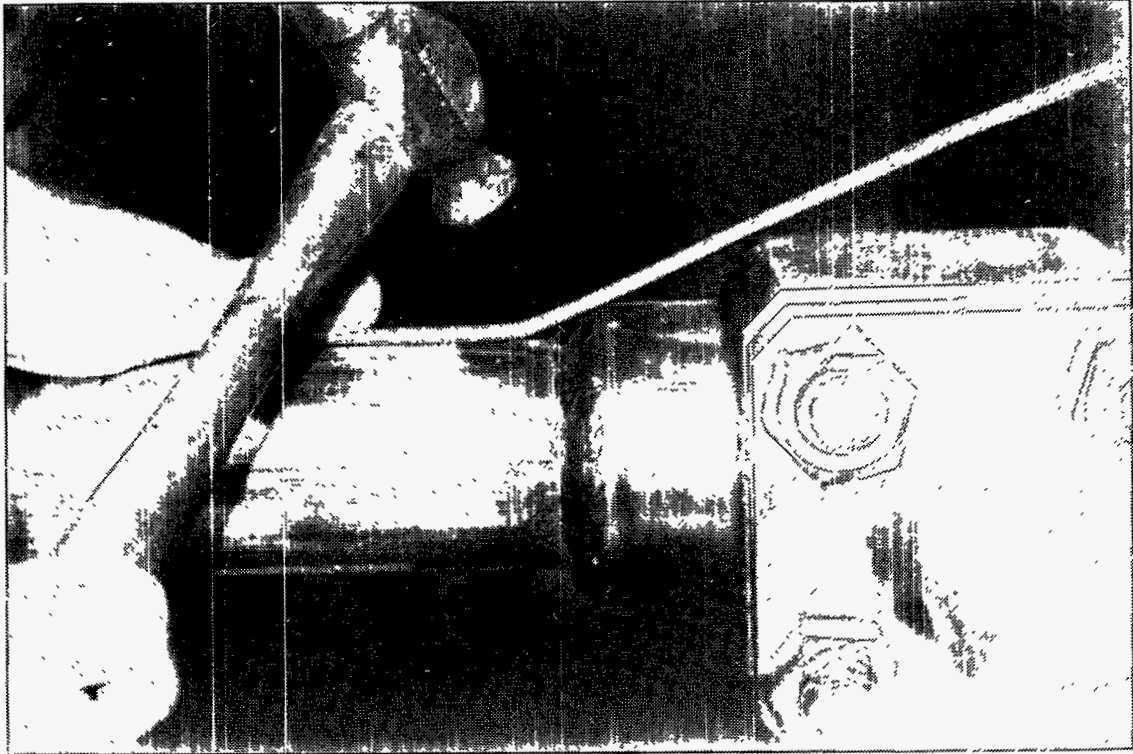


Figure B-12. Do not hammer heat trace.

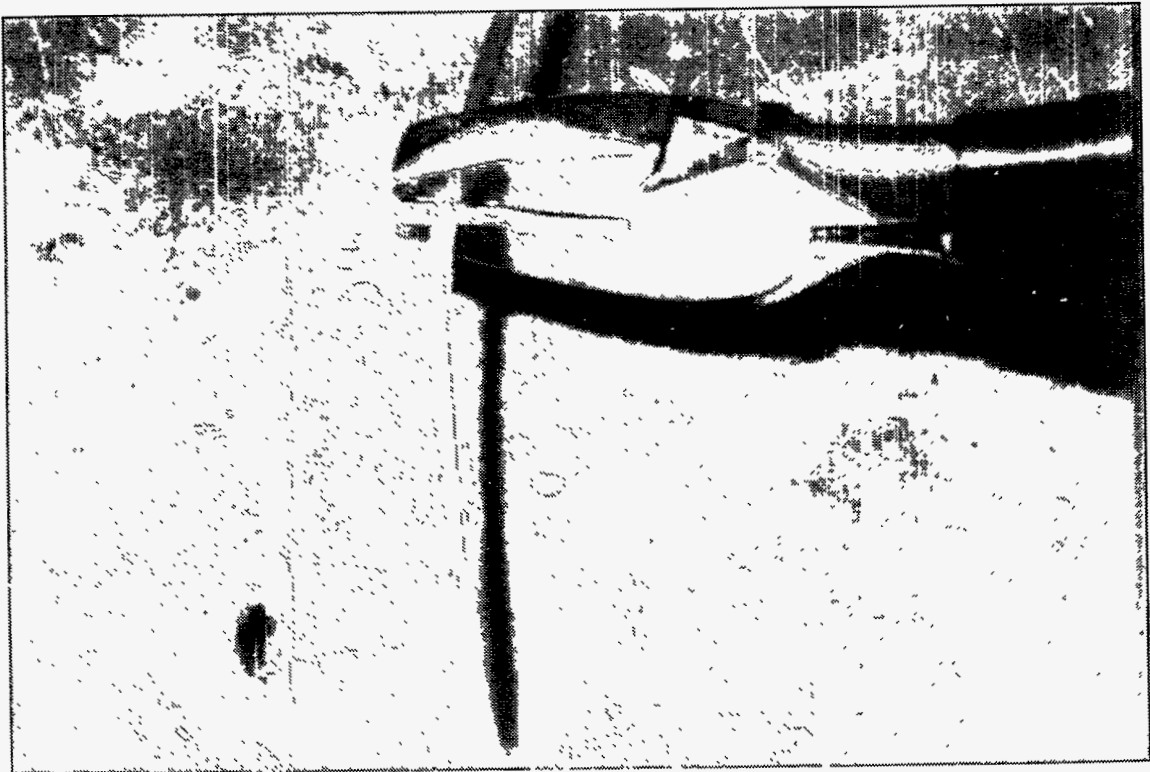
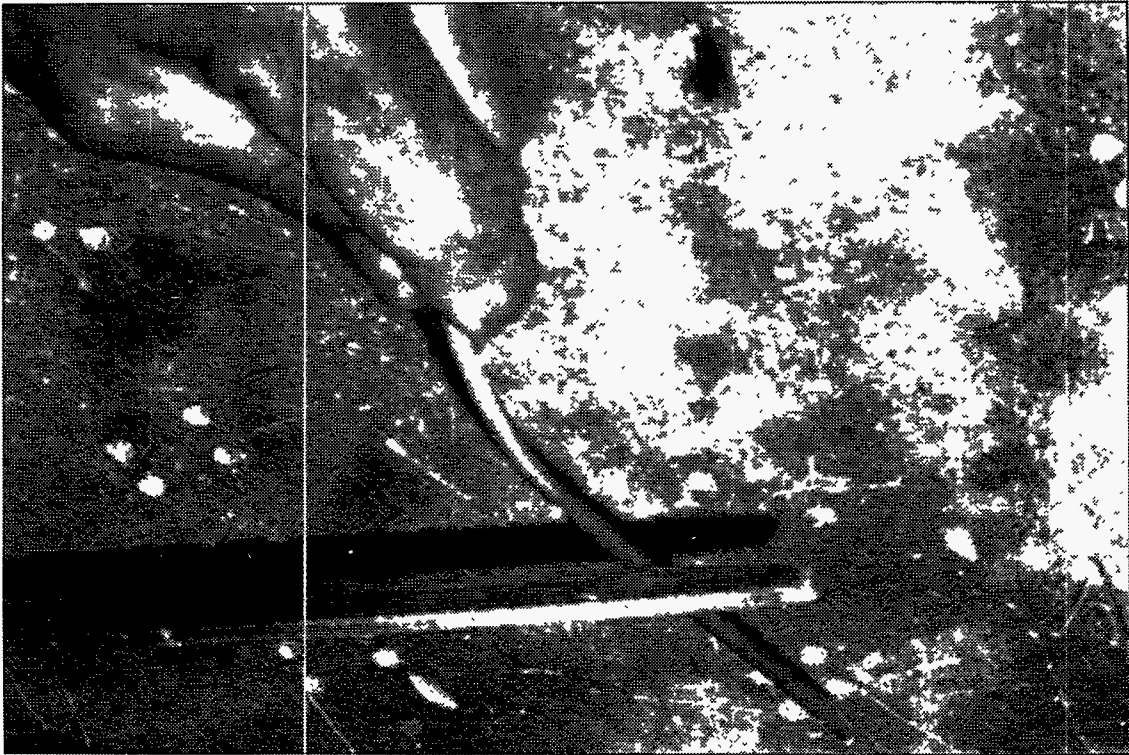


Figure B-13. Do not use pliers to bend heat trace.

Figure B-14. Do not use a file on the heat trace sheath.



Appendix C. Heat Transfer Coefficient for Circumferentially Varying Heat Flux

The impetus behind establishing a method to estimate accurately heat transfer coefficients is so that the flux limitations on receiver tubes can be set using thermal fatigue data based on the maximum temperature the tube material will experience during normal operation. Since the receiver tubes in a central receiver are heated on one side and insulated on the other, asymmetric heating will affect the heat transfer and thus the tube-temperature distribution. In the *Handbook of Heat Transfer Fundamentals* there is a description of the effects of circumferentially varying heat flux distribution on the Nusselt number (the nondimensional heat transfer coefficient, $Nu=hD/k$) for a specific flux distribution, but not a general case. In the journal article referenced by the handbook¹, the methodology to estimate the Nusselt number for an arbitrarily varying flux distribution is described. Basically, the authors describe an analytical derivation where they solve the energy equation by breaking the arbitrary flux distribution into the average flux around the tube plus the variation from the average. The authors claim the theoretical results are within 10% of experimental data for $0.7 \leq Pr \leq 75$. The model accounts for variations in the radial and circumferential thermal eddy diffusivities for turbulent flow ($\epsilon_{H\rho}$ and $\epsilon_{H\theta}$) which are based on experimental data. The local Nusselt number, $Nu(\theta)$, can be calculated if the flux variation can be expressed in terms of a Fourier series.

In the case of a receiver tube, the flux distribution varies approximately with cosine of the angle from the tube crown assuming the flux is specular (parallel rays). See Figure C-1a). Normalizing the flux distribution by the average flux, $q''_o = q''_{net}/\pi$, the distribution can be represented as $q''(\theta)/q''_o = 1 + F(\theta)$ where:

$$F(\theta) = \begin{cases} \pi \cos(\theta) & 0^\circ \leq \theta \leq 90^\circ \\ 0 & 90^\circ \leq \theta \leq 270^\circ \\ \pi \cos(\theta) & 270^\circ \leq \theta \leq 360^\circ. \end{cases}$$

$F(\theta)$ is represented by the Fourier series:

$$F(\theta) = \sum_{n=1}^{\infty} F_n(\theta) = \sum_{n=1}^{\infty} a_n \cos(n\theta)$$

where

$$a_1 = \pi/2$$

$$a_n = \frac{\sin((1-n)\pi/2)}{1-n} + \frac{\sin((1+n)\pi/2)}{1+n}$$

Figure C-1b) shows the comparison of the flux distribution to Fourier series representation ($n=0$ to 6). Once the Fourier series representation is known, the fully developed, local Nusselt number is calculated from:

$$Nu_{\infty}(\theta) = \frac{2(q''(\theta)/q''_o)}{G_o + \sum_{n=1}^{\infty} G_n F_n(\theta)} = h(\theta)D/k$$

¹"Turbulent Heat Transfer in a Circular Tube with Circumferentially varying Thermal Boundary Conditions," *J. Heat. Mass. Transfer*, Vol. 17, pp 1003-1018, (1974).

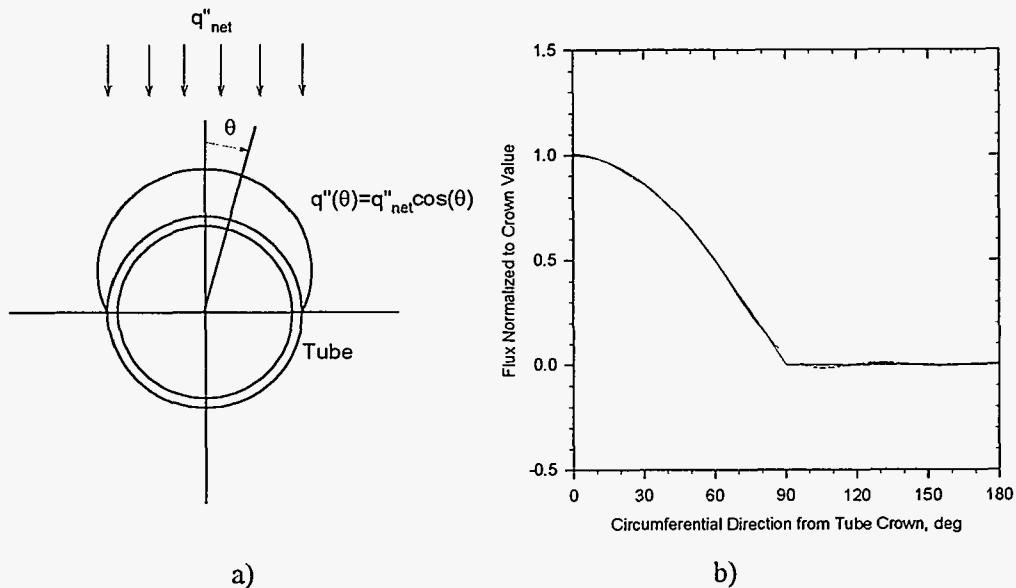


Figure C-1. a) Flux distribution around an asymmetrically heated tube with insulation on the unilluminated side, and b) comparison of flux distribution to Fourier series representation (six terms).

where G_o and G_n are found from solutions to the energy equation and are functions of the Prandtl, Pr , and Reynolds, Re , numbers. They are tabulated in the referenced article.

Figure C-2 shows a comparison of the Nusselt number computed by the above method to that computed by the Dittus Boelter equation - a commonly used correlation for uniformly heat tubes ($Nu = 0.023 Re^{0.8} Pr^{0.4}$). As can be seen, the analytical estimate of the heat transfer coefficient is greater in value. The authors also state for $Pr=8$, the dependence of the Nusselt number upon Reynolds number exceeds the power of 0.8 and thus the Dittus-Boelter equation tends to give more conservative results the higher the Reynolds number. This has been cited by other researchers. According to the referenced article, the deviations between the derivation and experimental data do not exceed 10% and are generally much less. Note, the Pr and Re number for nitrate salts vary from approximately 3.2 and 100,000, respectively, at 1050°F to 10.2 and 30,000, respectively, at 550°F.

This method will give an accurate estimate of localized heat transfer coefficients for a non-uniformly heated tube.

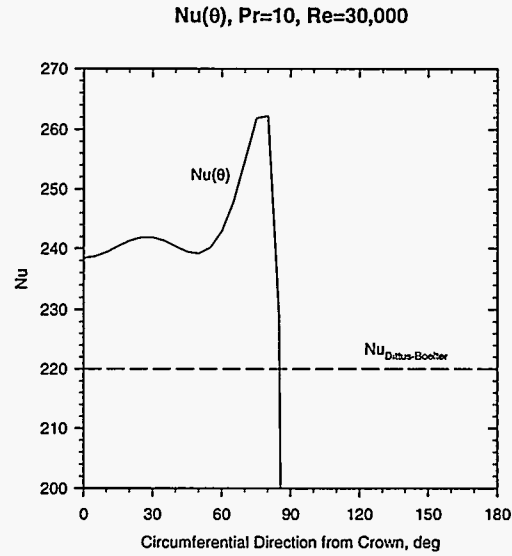


Figure C-2. Comparison of analytical calculation of Nusselt number which accounts for variations in flux to that determined by the Dittus-Boelter equation for $Pr=10$ and $Re=30,000$. $Nu(\theta)$ drops to zero between 90° to 180° .

Appendix D. Strain Equations for a Receiver Tube Under High Flux

Assuming a flux profile on the tube that follows a cosine function (Eq. D-1), a relation can be found between the tube strain and flux, tube material properties, and heat transfer coefficient. The plane strain in the tube is the sum of the strain in the tube wall due to the temperature difference across the wall and the strain due to the tube front-to-back temperature difference (Eq. D-2). The flux profile, strain equation, ε , and the tube inside and outside crown temperatures are defined below (assuming thin walled tubes):

$$q''(\theta) = q''_{net} \cos(\theta) \quad (D-1)$$

$$\varepsilon = \alpha \left[\left(\frac{T_{o,c} - T_{i,c}}{2(1-\nu)} \right) + \left(\frac{T_{o,c} + T_{i,c}}{2} - T_{avg} \right) \right] \quad (D-2)$$

$$T_{o,c} = \frac{q''_{net} t_{wall}}{k} + T_{i,c} \quad (D-3)$$

$$T_{i,c} = T_s + \frac{q''_{net}}{h_c} \quad (D-4)$$

The average tube temperature can be approximated by:

$$T_{avg} = \frac{q''_{net}}{\pi h_c} + \frac{q''_{net} t_{wall}}{2 \pi k} + T_s \quad (D-5)$$

Substituting these into the strain equation yields:

$$\varepsilon = \frac{\alpha q''_{net}}{\pi} \left[\frac{t_{wall}}{2k} \left(\frac{\pi(2-\nu) - (1-\nu)}{(1-\nu)} \right) + \frac{(\pi+1)}{h_c} \right] \quad (D-6)$$

Eq. D-6 shows how the flux, tube thickness, material properties and heat transfer coefficient at the crown affect the strain. Also note that the heat transfer coefficient is a function of the salt velocity and temperature. Assuming the control system has anticipatory capabilities, the flow rate and thus the heat transfer coefficient will be tied to the incident flux. At nominal operating conditions, a deviation in the heat transfer coefficient of 10% will only result in a 5% change in strain.

Appendix E. Molten and Solid Nitrate Salt Properties

The following properties are for molten and solid nitrate salt. Table E-1 shows the density, heat capacity, thermal conductivity, absolute and kinematic viscosities, Prandtl number, and thermal diffusivity as a function of temperature for molten salt. These data were compiled from various sources. Many properties were obtained for an equimolar ratio of sodium nitrate (46% by weight) and potassium nitrate (54% by weight). We have assumed the difference is not significant. For further details on salt properties please refer to *A Review of the Chemical and Physical Properties of Molten Alkali Nitrate Salts and Their Effect on Materials Used for Solar Central Receivers*, R.W. Bradshaw and R.W. Carling, SAND87-8005, printed April 1987.

Molten Nitrate Salt

Composition:

Sodium Nitrate	NaNO ₃	60% by weight
Potassium Nitrate	KNO ₃	40% by weight

Physical Properties (300-600°C, T is in °C):

Density (kg/m³):

$$\rho = 2090 - 0.636 T$$

Heat Capacity (J/kg·K):

$$C_p = 1443 + 0.172 T$$

Thermal Conductivity (W/m·K):

$$k = 0.443 + 1.9 \times 10^{-4} T$$

Absolute Viscosity (mPa·s):

$$\mu = 22.714 - 0.120 T + 2.281 \times 10^{-4} T^2 - 1.474 \times 10^{-7} T^3$$

Other Molten Salt Properties:

Isotropic Compressibility (NaNO₃) at the melting point:

$$2 \times 10^{-10} \text{ m}^2/\text{N}$$

Speed of Sound:

NaNO₃: 1763.3 m/s (5785.1 ft/s) at 336°C (637°F)

KNO₃: 1740.1 m/s (5709 ft/s) at 352°C (666°F)

Change in Sound Speed with Temperature:

NaNO₃: 0.74 m/s·K

KNO₃: 1.1 m/s·K

Phase Change Nitrate Salt Properties

Freezing Point:

Solidifies at 221°C (430°F)

Start to crystallize at 238°C (460°F)

Heat of Fusion - (based on molecular average of heat of fusion of each component):

$$h_{sl} = 161 \text{ kJ/kg}$$

Change in Density Upon Melting:

$$\Delta V/V_{\text{solid}} = 4.6\% \Rightarrow V_{\text{liquid}} = 1.046 V_{\text{solid}}$$

Solid Salt

Density, ρ :

NaNO_3 : 2260 kg/m^3 at room temperature

KNO_3 : 2190 kg/m^3 at room temperature

Heat Capacitance, C_p :

NaNO_3 : 37.0 $\text{cal/K}\cdot\text{mol} = 1820 \text{ J/kg}\cdot\text{K}$ near melting point

KNO_3 : 28.0 $\text{cal/K}\cdot\text{mol} = 1160 \text{ J/kg}\cdot\text{K}$ near melting point

Thermal Conductivity, k :

KNO_3 : 2.1 $\text{W/m}\cdot\text{K}$

Table E-1. Molten Nitrate Salt Properties: 60% NaNO₃, 40% KNO₃.

T		ρ		Cp		k		μ		ν		Pr	α	
Temperature		Density		Heat Capacity		Thermal Conductivity		Absolute Viscosity		Kinematic Viscosity		Prandtl	Thermal Diffusivity	
C	F	Kg/m ³	lbm/ft ³	J/kg/K	Btu/lbm/F	W/m/K	Btu/h/ft/F	Pa s	lbm/ft/h	m ² /s	ft ² /h		m ² /s	ft ² /h
270	518	1918	119.8	1489	0.3558	0.493	0.2850	0.00404	9.78	2.11E-06	0.082	12.20	1.73E-07	0.00669
280	536	1912	119.4	1491	0.3562	0.495	0.2861	0.00376	9.10	1.97E-06	0.076	11.33	1.74E-07	0.00673
290	554	1906	119.0	1493	0.3566	0.497	0.2872	0.00350	8.47	1.84E-06	0.071	10.52	1.75E-07	0.00677
300	572	1899	118.6	1495	0.3570	0.499	0.2883	0.00326	7.89	1.72E-06	0.067	9.77	1.76E-07	0.00681
310	590	1893	118.2	1496	0.3574	0.501	0.2894	0.00304	7.36	1.61E-06	0.062	9.09	1.77E-07	0.00685
320	608	1886	117.8	1498	0.3578	0.503	0.2905	0.00284	6.87	1.51E-06	0.058	8.47	1.78E-07	0.00689
330	626	1880	117.4	1500	0.3582	0.505	0.2916	0.00266	6.43	1.41E-06	0.055	7.90	1.79E-07	0.00694
340	644	1874	117.0	1501	0.3586	0.507	0.2927	0.00249	6.02	1.33E-06	0.051	7.38	1.80E-07	0.00698
350	662	1867	116.6	1503	0.3591	0.509	0.2938	0.00234	5.65	1.25E-06	0.048	6.91	1.81E-07	0.00702
360	680	1861	116.2	1505	0.3595	0.510	0.2949	0.00220	5.32	1.18E-06	0.046	6.48	1.82E-07	0.00706
370	698	1855	115.8	1507	0.3599	0.512	0.2960	0.00207	5.02	1.12E-06	0.043	6.10	1.83E-07	0.00710
380	716	1848	115.4	1508	0.3603	0.514	0.2971	0.00196	4.75	1.06E-06	0.041	5.76	1.84E-07	0.00715
390	734	1842	115.0	1510	0.3607	0.516	0.2982	0.00186	4.51	1.01E-06	0.039	5.46	1.86E-07	0.00719
400	752	1836	114.6	1512	0.3611	0.518	0.2993	0.00178	4.30	9.68E-07	0.038	5.18	1.87E-07	0.00723
410	770	1829	114.2	1514	0.3615	0.520	0.3004	0.00170	4.11	9.29E-07	0.036	4.95	1.88E-07	0.00728
420	788	1823	113.8	1515	0.3619	0.522	0.3015	0.00163	3.94	8.94E-07	0.035	4.73	1.89E-07	0.00732
430	806	1817	113.4	1517	0.3623	0.524	0.3026	0.00157	3.80	8.64E-07	0.033	4.55	1.90E-07	0.00736
440	824	1810	113.0	1519	0.3628	0.526	0.3037	0.00152	3.67	8.39E-07	0.032	4.39	1.91E-07	0.00741
450	842	1804	112.6	1520	0.3632	0.528	0.3048	0.00147	3.56	8.16E-07	0.032	4.24	1.92E-07	0.00745
460	860	1797	112.2	1522	0.3636	0.529	0.3059	0.00143	3.47	7.97E-07	0.031	4.12	1.93E-07	0.00750
470	878	1791	111.8	1524	0.3640	0.531	0.3070	0.00140	3.38	7.80E-07	0.030	4.01	1.95E-07	0.00754
480	896	1785	111.4	1526	0.3644	0.533	0.3081	0.00137	3.31	7.66E-07	0.030	3.91	1.96E-07	0.00759
490	914	1778	111.0	1527	0.3648	0.535	0.3092	0.00134	3.24	7.53E-07	0.029	3.82	1.97E-07	0.00763
500	932	1772	110.6	1529	0.3652	0.537	0.3103	0.00131	3.18	7.42E-07	0.029	3.74	1.98E-07	0.00768
510	950	1766	110.2	1531	0.3656	0.539	0.3114	0.00129	3.12	7.31E-07	0.028	3.66	1.99E-07	0.00773
520	968	1759	109.8	1532	0.3660	0.541	0.3125	0.00127	3.06	7.20E-07	0.028	3.59	2.01E-07	0.00777
530	986	1753	109.4	1534	0.3664	0.543	0.3136	0.00124	3.01	7.09E-07	0.027	3.51	2.02E-07	0.00782
540	1004	1747	109.0	1536	0.3669	0.545	0.3147	0.00122	2.95	6.97E-07	0.027	3.43	2.03E-07	0.00787
550	1022	1740	108.6	1538	0.3673	0.547	0.3158	0.00119	2.88	6.84E-07	0.027	3.35	2.04E-07	0.00791
560	1040	1734	108.2	1539	0.3677	0.548	0.3169	0.00116	2.81	6.69E-07	0.026	3.26	2.05E-07	0.00796
570	1058	1727	107.8	1541	0.3681	0.550	0.3180	0.00113	2.72	6.52E-07	0.025	3.15	2.07E-07	0.00801
580	1076	1721	107.4	1543	0.3685	0.552	0.3191	0.00109	2.63	6.32E-07	0.024	3.04	2.08E-07	0.00806
590	1094	1715	107.0	1544	0.3689	0.554	0.3202	0.00104	2.52	6.08E-07	0.024	2.91	2.09E-07	0.00811
600	1112	1708	106.7	1546	0.3693	0.556	0.3213	0.00099	2.40	5.80E-07	0.022	2.76	2.10E-07	0.00816

Appendix F. Selected Sets of Data and Other Information

Thermocouple Layout on Panels	101
Thermocouple Layout on Components	102
Ultrasonic Flow Meter Parameters	103
Component Part Numbers and Weights	105
Selected Sets of Data:	
- Panel Cold Fill Test	107
- Cold Fill Test of 2 inch Pipe	112
- Flow Meter Calibration Data Summary	114
- Flow Meter Calibration Data	118
- Panel Temperature Data During Freezing	130
- Checkvalve Cycling Data	142
- Thermal Shock Data for Components	149
- Data for Slow Cool Down of Components with Fan	152
- Data Slow Heat Up of Components with Heat Trace Circuits	153

ELH-17
X

WUH-19
X

Panel Thermocouple
Layout

1 2 3 4 5 6 7 8 9 10 11 12

1 2 3 4 5 6 7 8 9 10 11 12

E-15
X

E-16
X

W-17
X

W-18
X

FG-3



E-13
X

E-14
X

W-15
X

W-16
X

E-11
X

E-12
X

W-13
X

W-14
X

W-11
X

W-12
X

E-9
X

E-10
X

FG-2



W-9
X

W-10
X

E-7
X

E-8
X

W-7
X

W-8
X

E-5
X

E-6
X

W-5
X

W-6
X

E-3
X

E-4
X

W-3
X

W-4
X

FG-1



W-1
X

W-2
X

ELH-18
X

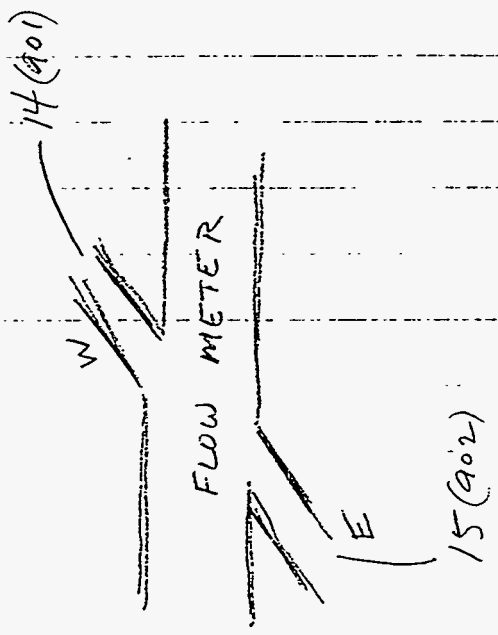
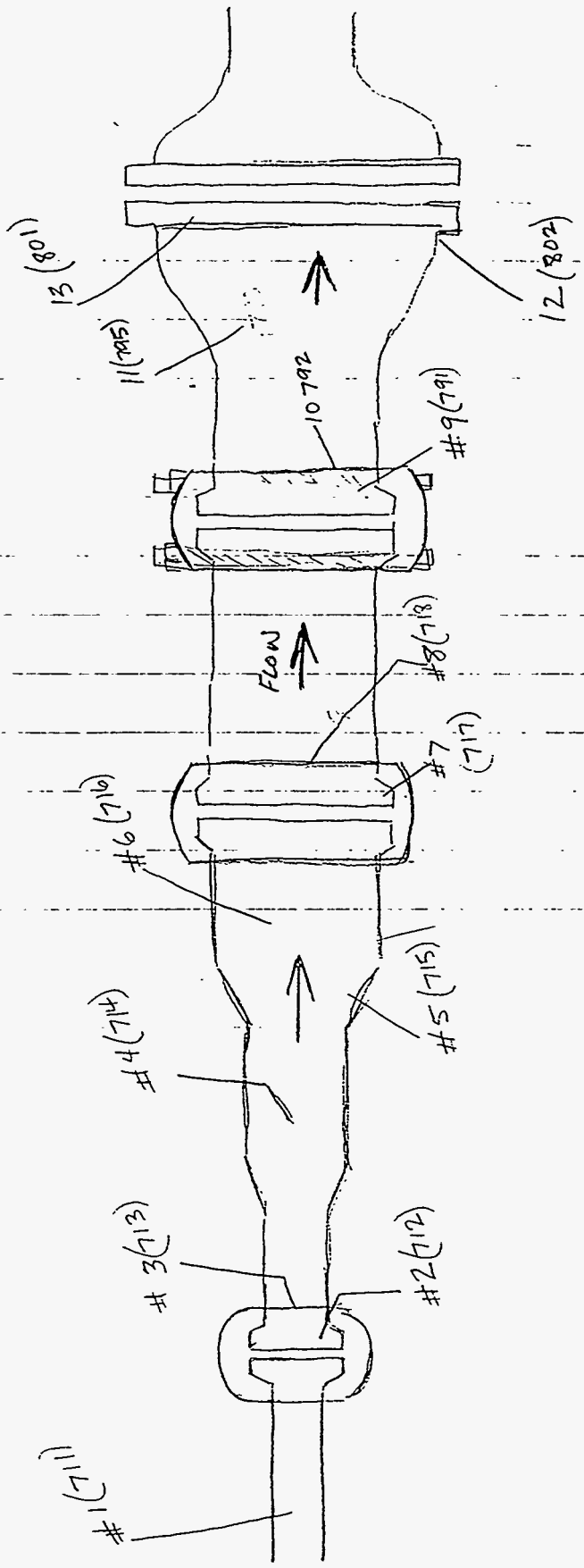
ELH-19
X

WLH-20
X

WLH-21
X

PANEL TC
LOCATION

Thermocouple Layout on Components



SETUP INFORMATION FOR THE PANAMETRICS ULTRASONIC FLOWMETER

PROMPT	SETTING
System Units	METRIC
Volumetric Units	liters
Time Units	minutes
Decimal Digits	2
Totalizer Units	liters
Decimal Digits	2
Analog Out Units	Volumetric
Analog Out Zero	0.0 liters/min (4 mA)
Full Scale	500.0 liters/min (20 mA)
Error Handling	Force Low
Response Time	30 readings
Fluid Type	Other (for Molten Sodium Nitrate-60% and Potassium Nitrate-40%)
Fluid Sound Speed	1800.0 m/s (nitrate salt, 1812 m/s was measured when clamp on flowmeter was work)
Reynolds Correction	Active
Kin. Viscosity	1.863 E-6 m ² /s @ 288 C (550F) nitrate salt
Meter Factor K	1.000
Transducer #	91 for the wetted flow cell (Channel 1) 116 for the clamp on transducer (Channel 2)

The setup for each type of transducer is different and continues on the next page.

The Following Apply to the CLAMP ON TRANSDUCERS. (Note the clamp on transducer temperature should not exceed 288 C (550 F). It should be removed before operating at higher temperatures.)

Pipe Temperature	93 C (Wedge Temperature - measured half way up wedge)
Wall Thickness	3.91 mm (0.154 in for 2" dia SCH 40 SS piping)
Pipe I.D.	52.50 mm (2.067 in)
# Traverses	2
Pipe Material	Stainless Steel
Pipe Type	Round
Zero Cutoff	0.3 m/s
Xducer Spacing S	58.00 mm (enter actual dimension)

This is the space needed for the clamp on transducers as computed from the parameters entered into the computer. If the actual spacing doesn't match this value, the value can be overwritten to match the actual physical spacing.

The Following Apply to the WETTED TRANSDUCERS. (Note the wetted transducer temperature should be monitored and the sensor itself - which is out of the fluid - should not exceed 288 C (550 F). It should be removed before operating at higher temperatures.)

Path Length P	256.4816 mm (10.0977 in from Panametrics)
Axial Dimension L	157.5054 mm (6.2010 in from Panametrics)
Pipe I.D.	52.50 mm (2.067 in)
Pipe Type	Round
Zero Cutoff	0.3 m/s

Type Parameter 909 to enter parameters for wetted transducer 91:

Transducer Number	91
Transducer type	Wetted
Tranducer Frequency	1.0 MHz
Transducer Tw (delay)	36 µsec (or 36.7 per Mike Pougla of Panametrics)
Transducer THETA 1	N/A
Transducer Wedge Soundspeed	N/A m/sec (ft/sec)

Metal Clamp-on Flow transducers Numbers:

CTS-1.0-HT 1192256 1.0 MHz XDCR#21 on elbow: 2R0308	CTS-1.0-HT CTS. 1.0 MHz S/N 693286 XDCR #21
-----------------------------------------------------------------	------------------------------------------------------

Part Numbers on Components in Molten Salt Experiments

Tee and cap for Corrosion Experiments:

E-CON E0204-300 S-2063 316 ISZ

E-CON E0204-300 S-2063 316 ISZ

2" Flange:

Clamp: GRAYLOC 2
182F304 GNS0218
CANADA SN48302

Body (2 of these):

PN115405 GRAYLOC® 2GR20 BW
2SCH40 SA182-F316L G1316 S07037700

Checkvalve: REFLANGE V-CON 3-900
316 216302

(Clamp side): F04 S-3063

4" Flange (on checkvalve):

(Clamp): REFLANGE C-04

(Body): R-CON F04-0304 S-3063 316 216302

4" Flange:

(Clamp): REFLANGE C-04

(Body, 2): R-CON S4063 316 91461

6" Flange (8 bolt):

(Body, 2): E-CON E0604-300 S-6065 316 AJM

E-CON E0604-300 S-6065 316 LDI

Panametrics Flow Meter - Electronics

Model 6468-22-1000-0

Serial Number 791

Software Version 4.D

Weight of Components

31 lbs: from elbow to blind flange for corrosion coupons to first half of 2" grayloc flange

14.5 lbs: 2" grayloc clamp

39 lbs: 2nd half of 2" grayloc flange + 2x3 reducer + 3" V-CON checkvalve + half of 3" inner 4" outer R-CON flange

27 lbs: 2nd half of 3" inner, 4" outer R-CON flange to 1st half of 4" R-CON flange

27 lbs: 1st R-CON 4" clamp

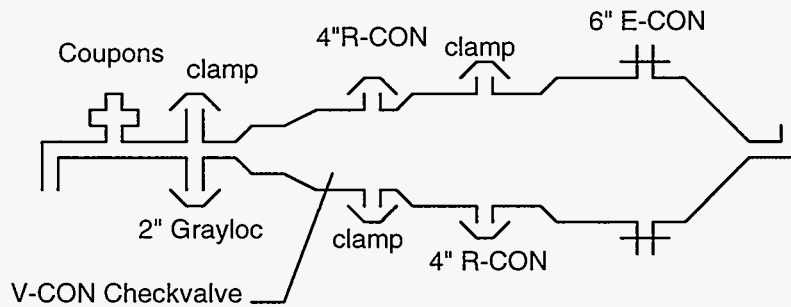
29 lbs: 2nd R-CON 4" clamp

42 lbs: 2nd half of 4" R-CON flange + 4x6 reducer + 1st half of 6" E-CON flange.

42 lbs: 2nd half of 6" E-CON flange + 6"x2" reducer + elbow

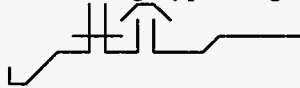
Total weight: 251 lbs

Total length outer edge of elbow to outer edge of elbow: 100"



Added 2-1-94

4" ANSI Ring Type flange, 300#, oval groove, oval ring, stainless steel



Ring Type Flange

added between 4" R-CON Flanges

43.1 lbs: 2nd half of 3" inner, 4" outer R-CON flange to 1st half of 4" Ring-type flange

36.5 lbs: 2nd half of 4" Ring-type flange to 1st half of 4" R-CON flange

New Total Weight: 303.6 lbs

Panel Cold Fill Test: 12/01/93

Panel Cold Fill Test, 12/01/93						
CRTF	TEST	1st pass	2nd pass	3rd pass	4th pass	Upper he
Time	Time	TEW4	TEW17	TEE12	TEE9	TEWUH19
hour	Time	DEG F	DEG F	DEG F	DEG F	DEG F
9.4494	475	48	48	46	46	80
9.4508	480	48	48	46	46	80
9.4522	485	48	48	46	46	80
9.4536	490	48	48	46	46	80
9.455	495	48	48	46	46	80
9.4564	500	48	48	46	46	80
9.4581	505	48	48	46	46	80
9.4594	510	48	48	46	46	80
9.4608	515	48	48	45	46	80
9.4622	520	48	48	45	45	80
9.4636	525	48	48	45	45	80
9.465	530	48	48	45	45	80
9.4664	535	48	49	45	45	80
9.4678	540	48	49	45	45	80
9.4692	545	48	49	45	45	80
9.4706	550	48	49	45	45	80
9.4717	555	48	49	45	45	80
9.4731	560	48	49	45	45	80
9.4744	565	48	49	45	45	80
9.4758	570	48	49	45	45	80
9.4772	575	121	49	45	45	80
9.4786	580	283	49	45	45	80
9.48	585	432	49	45	45	80
9.4814	590	542	104	45	45	83
9.4828	595	582	231	45	45	89
9.4842	600	590	366	45	45	98
9.4856	605	589	468	69	45	111
9.4869	610	586	498	158	45	126
9.4883	615	583	492	208	49	145
9.4897	620	581	501	230	99	163
9.4911	625	580	509	251	138	182
9.4925	630	578	519	270	182	210
9.4939	635	577	520	281	203	225
9.4953	640	576	520	304	242	261
9.4967	645	575	516	314	265	279
9.4983	650	574	517	325	292	310
9.4997	655	573	520	330	308	340
9.5011	660	572	525	342	323	354
9.5025	665	572	529	353	334	381
9.5039	670	571	531	370	354	407
9.5053	675	571	532	385	364	420
9.5067	680	571	533	418	381	443
9.5081	685	571	538	448	395	455
9.5094	690	570	540	484	485	476
9.5108	695	570	541	494	507	488

Panel Cold Fill Test: 12/01/93

CRTF Panel Cold Fill Test, 12/01/93						
TEST	1st pass	2nd pass	3rd pass	4th pass	Upper head	
Time	TEW4	TEW17	TEE12	TEE9	TEWUH19	
hour	Time	DEG F	DEG F	DEG F	DEG F	DEG F
9.5122	700	570	541	504	518	500
9.5136	705	570	543	505	519	505
9.5147	710	570	543	512	527	514
9.5161	715	570	543	518	532	523
9.5175	720	570	544	521	534	529
9.5189	725	570	544	523	537	534
9.5203	730	570	544	525	539	538
9.5217	735	570	545	526	540	543
9.5231	740	570	545	528	542	545
9.5244	745	570	545	530	543	548
9.5258	750	570	546	532	544	551
9.5272	755	570	546	533	545	553
9.5286	760	570	546	535	546	555
9.5303	765	570	547	536	547	557
9.5317	770	570	547	537	549	558
9.5331	775	569	547	538	550	559
9.5344	780	569	547	538	550	559
9.5358	785	569	548	539	551	561
9.5372	790	569	548	540	551	562
9.5386	795	569	548	540	551	562
9.54	800	569	548	542	552	563
9.5414	805	569	548	542	552	563
9.5425	810	569	550	543	553	564
9.5439	815	569	550	543	553	564
9.5453	820	569	550	543	553	564
9.5467	825	569	550	544	553	564
9.5481	830	569	550	544	555	564
9.5494	835	569	550	544	555	566
9.5508	840	569	550	545	555	566
9.5522	845	569	550	545	555	566
9.5536	850	569	550	545	555	566
9.555	855	569	550	545	555	566
9.5564	860	569	550	545	556	566
9.5581	865	569	550	546	556	566
9.5594	870	568	550	546	556	566
9.5608	875	568	550	546	556	566
9.5622	880	568	550	546	556	566
9.5636	885	568	550	546	556	566
9.565	890	568	550	546	556	566
9.5664	895	567	550	548	556	567
9.5678	900	567	550	548	557	567
9.5689	905	567	550	548	557	567
9.5703	910	567	550	548	557	567
9.5717	915	567	550	548	557	567
9.5731	920	567	550	548	557	567

Panel Cold Fill Test: 12/01/93

CRTF Panel Cold Fill Test, 12/01/93						
TEST	1st pass	2nd pass	3rd pass	4th pass	Upper he	
Time	TEW4	TEW17	TEE12	TEE9	TEWUH19	
hour	Time	DEG F	DEG F	DEG F	DEG F	DEG F
9.5744	925	567	550	548	557	567
9.5758	930	567	550	548	557	567
9.5772	935	567	550	548	556	567
9.5786	940	567	550	548	554	567
9.58	945	567	550	548	552	567
9.5814	950	567	550	548	549	567
9.5831	955	567	550	548	548	567
9.5844	960	567	550	548	547	567
9.5858	965	567	550	548	546	567
9.5872	970	567	550	548	546	567
9.5886	975	567	550	548	545	567
9.59	980	566	550	548	545	567
9.5914	985	566	550	548	545	567
9.5928	990	566	550	550	545	567
9.5942	995	565	550	550	543	567
9.5953	1000	565	550	550	543	567
9.5967	1005	565	550	550	548	567
9.5981	1010	565	550	550	555	567
9.5994	1015	564	550	550	557	567
9.6008	1020	564	550	550	557	566
9.6022	1025	564	550	550	557	566
9.6036	1030	564	550	550	557	566
9.605	1035	564	550	550	557	566
9.6064	1040	564	550	550	557	566
9.6078	1045	564	550	550	557	566
9.6092	1050	564	550	549	557	566
9.6106	1055	564	550	549	557	566
9.6122	1060	564	550	549	557	566
9.6136	1065	564	550	549	557	566
9.615	1070	564	550	549	557	566
9.6164	1075	564	550	549	557	566
9.6178	1080	564	550	549	557	565
9.6192	1085	564	550	549	557	565
9.6206	1090	564	550	549	557	565
9.6219	1095	564	550	549	557	565
9.6233	1100	564	550	549	557	565
9.6244	1105	564	550	549	557	565
9.6258	1110	564	550	550	557	565
9.6272	1115	564	549	550	557	565
9.6286	1120	564	549	550	557	565
9.63	1125	564	549	550	557	565
9.6314	1130	564	549	550	557	565
9.6328	1135	564	549	550	558	565
9.6342	1140	564	549	550	558	566
9.6356	1145	564	550	550	558	566

Panel Cold Fill Test: 12/01/93

CRTF Panel Cold Fill Test, 12/01/93						
TEST	1st pass	2nd pass	3rd pass	4th pass	Upper head	
Time	TEW4	TEW17	TEE12	TEE9	TEWUH19	
hour	Time	DEG F	DEG F	DEG F	DEG F	DEG F
9.6369	1150	564	550	550	558	566
9.6383	1155	564	550	551	558	566
9.64	1160	564	550	551	558	566
9.6414	1165	564	550	551	558	566
9.6428	1170	564	550	551	558	566
9.6442	1175	564	550	551	558	566
9.6456	1180	564	550	551	558	566
9.6469	1185	564	550	551	558	566
9.6483	1190	564	550	551	558	566
9.6497	1195	564	550	551	559	566
9.6511	1200	564	550	551	559	566
9.6522	1205	564	550	551	559	566
9.6536	1210	564	550	551	559	566
9.6553	1215	564	550	551	559	566
9.6567	1220	568	550	551	559	566
9.6578	1225	571	551	551	559	566
9.6592	1230	574	555	551	559	566
9.6606	1235	576	557	551	559	566
9.6619	1240	577	559	551	560	567
9.6633	1245	578	561	554	561	568
9.6647	1250	579	562	555	562	570
9.6661	1255	579	562	558	563	571
9.6675	1260	580	563	558	566	572
9.6689	1265	580	563	559	566	573
9.6703	1270	580	565	560	567	574
9.6717	1275	580	565	560	568	574
9.6731	1280	580	565	561	568	575
9.6744	1285	580	565	561	570	576
9.6761	1290	580	565	563	570	578
9.6775	1295	580	565	563	571	578
9.6789	1300	580	566	563	571	578
9.6803	1305	580	566	564	571	579
9.6817	1310	577	566	564	571	579
9.6831	1315	574	565	564	571	579
9.6844	1320	570	562	564	571	579
9.6858	1325	568	560	564	571	579
9.6872	1330	566	557	564	571	579
9.6886	1335	565	554	563	571	578
9.69	1340	565	553	560	570	577
9.6911	1345	564	552	559	567	576
9.6925	1350	564	552	556	565	575
9.6939	1355	564	550	555	563	573
9.6953	1360	564	550	554	562	572
9.6967	1365	564	550	554	561	571
9.6981	1370	564	550	553	560	571

Panel Cold Fill Test: 12/01/93

CRTF		Panel Cold Fill Test, 12/01/93				
TEST		1st pass	2nd pass	3rd pass	4th pass	Upper he
Time		TEW4	TEW17	TEE12	TEE9	TEWUH19
hour	Time	DEG F	DEG F	DEG F	DEG F	DEG F
9.6994	1375	564	550	553	560	570
9.7008	1380	564	550	553	560	569
9.7022	1385	564	550	552	559	569
9.7036	1390	564	550	552	559	568
9.705	1395	564	550	552	559	568
9.7064	1400	564	550	552	559	568

Cold Fill Test of 2 inch Pipe

Cold Pipe Test		Schedule 40, 2in pipe					
Sept. 24, 1993		Salt Temperature, 524 F					
Outside Pipe Temperature, deg F							
Channel	439	440	441	442	443	444	445
Hrs:Min:Sec							
9:16:55	367	262	103	99	96	126	613
9:17:00	363	263	104	99	96	126	613
9:17:05	362	263	103	99	96	125	613
9:17:10	362	263	103	99	96	126	613
9:17:15	362	263	103	98	96	126	613
9:17:20	361	263	104	99	96	125	613
9:17:25	363	263	102	99	96	125	613
9:17:30	363	262	103	99	96	126	613
9:17:35	361	262	103	99	96	125	613
9:17:40	383	268	111	100	95	125	613
9:17:45	415	281	144	122	100	125	613
9:17:50	444	302	194	157	124	141	607
9:17:55	462	320	240	191	152	164	592
9:18:00	475	341	292	230	186	194	572
9:18:05	485	358	344	275	222	227	555
9:18:10	493	377	393	334	277	280	540
9:18:15	496	391	421	377	335	331	532
9:18:20	496	405	445	416	395	384	528
9:18:25	499	415	458	440	431	420	527
9:18:30	500	425	470	460	460	451	527
9:18:35	502	434	480	473	478	469	529
9:18:40	504	441	487	483	490	482	529
9:18:50	507	455	498	498	503	499	531
9:18:55	507	460	501	501	506	503	532
9:19:00	508	465	505	506	509	507	532
9:19:05	509	468	506	508	510	508	532
9:19:10	508	472	508	510	513	510	532
9:19:15	509	475	510	512	514	512	532
9:19:20	509	478	511	513	515	512	532
9:19:25	511	480	511	513	515	512	532
9:19:30	511	483	514	515	517	514	532
9:19:35	511	485	514	517	518	515	532
9:19:40	511	487	515	517	519	516	532
9:19:45	510	488	516	519	519	515	532
9:19:50	513	490	517	519	519	517	532
9:19:55	511	491	517	518	520	516	532
9:20:00	513	493	517	519	520	519	532
9:20:05	513	495	519	520	520	519	532
9:20:10	515	495	518	521	521	519	532
9:20:15	514	497	519	522	523	520	532
9:20:20	514	497	520	521	522	520	533
9:20:25	516	498	519	521	522	520	533
9:20:30	514	499	521	522	522	521	532
9:20:35	515	499	519	521	521	520	532

Cold Fill Test of 2 inch Pipe

Cold Pipe Test		Schedule 40, 2in pipe					
Sept. 24, 1993		Salt Temperature, 524 F					
Outside Pipe Temperature, deg F							
Channel	439	440	441	442	443	444	445
Hrs:Min:Sec							
9:20:40	516	501	520	522	523	521	532
9:20:45	517	502	520	523	523	522	532
9:20:50	516	503	521	524	523	521	533
9:20:55	516	503	520	524	524	522	533
9:21:00	517	503	521	524	524	523	533
9:21:05	516	504	521	524	524	523	533
9:21:10	519	504	522	525	524	523	533
9:21:15	518	505	522	524	524	522	533
9:21:20	516	505	522	525	524	523	533
9:21:25	517	505	522	525	525	523	533
9:21:30	517	507	523	526	525	523	533
9:21:35	517	507	523	526	525	524	533
9:21:40	518	507	523	525	525	524	533
9:21:45	517	507	523	525	526	524	534
9:21:50	516	507	523	526	525	524	533
9:21:55	518	508	523	526	525	525	533
9:22:00	517	508	523	526	525	524	533
9:22:05	519	508	523	526	526	525	533
9:22:10	518	509	523	527	526	525	533
9:22:15	519	507	523	526	525	523	532
9:22:20	519	509	524	526	527	525	533
9:22:25	518	510	524	527	527	525	533
9:22:30	518	509	523	526	525	524	533

Flow meter calibration data summary.

Total Bias and Random Uncertainty Percents and Urss Uncertainties											
Flow L/min	FT-720 Vortex Flow		PF-001 Wetted Ultra		PF-002 Clampon Ultr		FT-730 Vortex		FT-800 Vortex		
	Bias Bi	Random t95S/N ^{.5}	Bias Bi	Random t95S/N ^{.5}	Bias Bi	Random t95S/N ^{.5}	Bias Bi	Random t95S/N ^{.5}	Bias Bi	Random t95S/N ^{.5}	
Average											
Flow, lt/min	%	%	%	%	%	%	%	%	%	%	%
102.58	9.76	0.63	3.84	0.55	8.47	0.50	9.90	0.47	5.29	0.44	
155.40	11.58	0.29	4.14	0.51	12.78	0.55	11.55	0.39	7.29	0.27	
197.41	12.56	0.18	4.56	0.44	12.97	0.42	12.50	0.22	8.48	0.21	
244.65	15.09	0.21	6.35	0.31	13.27	0.30	15.62	0.35			
Flow	Urss		Urss		Urss		Urss		Urss		
102.5759	9.77976		3.878089		8.485958		9.91473		5.310453		
155.3991	11.58529		4.168351		12.79488		11.55541		7.295545		
197.4063	12.55799		4.581304		12.97705		12.49935		8.48723		
244.6471	15.08722		6.358041		13.27571		15.62751				

Flow meter calibration data summary.

Bias and Random Uncertainty Percents Relative to Bubbler Reference											
Flow L/min	FT-720 Vortex Flow		PF-001 Wetted Ultra		PF-002 Clampon Ultr		FT-730 Vortex		FT-800 Vortex		
	Bias	Random	Bias	Random	Bias	Random	Bias	Random	Bias	Random	
Lt/min	Bi	t95S/N [^] .5	Bi	t95S/N [^] .5	Bi	t95S/N [^] .5	Bi	t95S/N [^] .5	Bi	t95S/N [^] .5	
	%	%	%	%	%	%	%	%	%	%	
245.07	15.52159	0.475089	6.862377	0.662462	-11.1397	0.488859	15.82366	0.481864			
245.07	13.99688	0.239153	4.261886	0.230269	-12.9097	0.200013	14.08849	0.290354			
196.22	12.42478	0.232202	3.896936	1.145752	-10.4407	0.944796	12.56068	0.435271	7.226531	0.348303	
191.20	13.99572	0.071855	4.027049	0.149455	-10.8986	0.125255	13.66786	0.060468	9.22606	0.171739	
155.47	12.56275	0.753997	4.490394	1.213737	-8.18096	1.074611	12.56275	0.674396	7.159739	0.480827	
155.19	10.07565	0.12859	1.012406	0.081947	-12.3653	0.25961	10.29978	0.201509	5.663095	0.24198	
102.99	8.110337	1.133905	0.300727	0.940323	-6.15803	0.721195	8.490264	0.658884	3.086858	0.699224	
102.16	9.834467	0.130553	-0.22997	0.152059	-8.94488	0.272782	9.767941	0.282077	4.198763	0.17449	
154.91	10.90267	0.179409	-0.45872	0.614047	-14.4883	0.671667	10.51535	0.412473	5.932066	0.129107	
156.03	10.16607	0.099755	1.122052	0.125268	-13.7377	0.177755	10.1898	0.27912	6.035729	0.236388	
200.13	11.02	0.299602	1.208081	0.386784	-13.964	0.498647	10.88372	0.25495	7.597939	0.187905	
202.08	10.38117	0.10355	0.711803	0.070636	-14.2525	0.116727	10.46034	0.114129	6.214532	0.137835	
246.46	13.39638	0.089405	3.323362	0.277316	-14.7587	0.349742	14.27843	0.499605			
242.00	15.44113	0.048174	5.7871	0.059108	-12.0118	0.152921	16.38737	0.134167			

Flow meter calibration data summary.

Bias and Random Uncertainty Levels Relative to Bubbler Reference											
Flow L/min	FT-720 Vortex Flow		PF-001 Wetted Ultra		PF-002 Clampon Ultr		FT-730 Vortex		FT-800 Vortex		
	Bias Bi	Random $t_{95S}/N^{.5}$	Bias Bi	Random $t_{95S}/N^{.5}$	Bias Bi	Random $t_{95S}/N^{.5}$	Bias Bi	Random $t_{95S}/N^{.5}$	Bias Bi	Random $t_{95S}/N^{.5}$	
Lt/min	Lt/min	Lt/min	Lt/min	Lt/min	Lt/min	Lt/min	Lt/min	Lt/min	Lt/min	Lt/min	
245.07	38.04	1.164281	16.82	1.623467	-27.30	1.198025	38.78	1.180883			
245.07	34.30	0.586083	10.44	0.564311	-31.64	0.490163	34.53	0.711559			
196.22	24.38	0.455627	7.65	2.248196	-20.49	1.853879	24.65	0.85409	14.18	0.68344	
191.20	26.76	0.137384	7.70	0.285752	-20.84	0.239483	26.13	0.115611	17.64	0.328358	
155.47	19.53	1.172231	6.98	1.886982	-12.72	1.670686	19.53	1.048475	11.13	0.747537	
155.19	15.64	0.199558	1.57	0.127173	-19.19	0.402888	15.98	0.312721	8.79	0.375527	
102.99	8.35	1.167861	0.31	0.968482	-6.34	0.742792	8.74	0.678615	3.18	0.720163	
102.16	10.05	0.133369	-0.23	0.15534	-9.14	0.278667	9.98	0.288162	4.29	0.178255	
154.91	16.89	0.277923	-0.71	0.951224	-22.44	1.040483	16.29	0.638965	9.19	0.2	
156.03	15.86	0.155645	1.75	0.195453	-21.43	0.277347	15.90	0.435503	9.42	0.36883	
200.13	22.05	0.599587	2.42	0.774063	-27.95	0.997932	21.78	0.510226	15.21	0.376051	
202.08	20.98	0.209255	1.44	0.142743	-28.80	0.235883	21.14	0.230634	12.56	0.278538	
246.46	33.02	0.220348	8.19	0.683476	-36.37	0.86198	35.19	1.231332			
242.00	37.37	0.11658	14.00	0.14304	-29.07	0.370062	39.66	0.324677			

Flow meter calibration data.

CRTF		NET-90		99: POINT		DATA		FILE:						
TEST	DATE:	Tue	May	3	1994	11:28:42	am:							
Time	Time	Time	Time	FT720	PF-001	PF-002	FT730	FT800	PT720	CALE.FLCCALW.FL	FCV800	LT700	LT899	
MST	hour	min	sec	L/min	L/min	L/min	L/min	L/min	PSIG		L/min	Inch	Inch	
11.53417	11	32	3	288	265	219	288	57	56	0	0	55	22	0
11.53556	11	32	8	288	265	219	288	60	56	0	0	55	22	0
11.53694	11	32	13	288	265	219	288	57	56	0	0	55	22	0
11.53833	11	32	18	283	265	219	288	64	56	0	0	61	22	0
11.53972	11	32	23	283	265	219	282	56	57	0	0	61	22	0
11.54111	11	32	28	283	265	219	282	62	57	0	0	61	22	0
11.5425	11	32	33	283	265	219	282	62	57	0	0	61	22	0
11.54389	11	32	38	283	260	219	282	62	57	0	0	61	22	0
11.54528	11	32	43	283	260	219	282	56	57	0	0	55	22	0
11.54667	11	32	48	283	260	219	282	59	57	0	0	62	21	2
11.54806	11	32	53	283	260	219	282	63	57	0	0	62	21	3
11.54944	11	32	58	283	260	219	282	60	57	0	0	62	21	6
11.55083	11	33	3	283	260	216	282	63	57	0	0	62	20	8
11.55222	11	33	8	283	260	216	282	59	57	0	0	62	20	11
11.55361	11	33	13	283	260	216	282	61	57	0	0	62	20	13
11.555	11	33	18	280	260	216	282	57	57	0	0	55	19	16
11.55639	11	33	23	280	260	216	282	62	57	0	0	62	19	18
11.55778	11	33	28	280	260	216	281	59	57	0	0	62	19	19
11.55917	11	33	33	280	260	216	281	57	57	0	0	62	18	21
11.56056	11	33	38	280	258	216	281	62	57	0	0	62	18	24
11.56194	11	33	43	280	258	216	281	65	57	0	0	62	18	27
11.56333	11	33	48	280	258	216	281	61	57	0	0	62	18	27
11.56472	11	33	53	280	258	216	281	60	57	0	0	62	18	28
11.56611	11	33	58	280	258	216	281	59	57	0	0	56	18	29
11.5675	11	34	3	280	258	213	281	63	57	0	0	63	18	30
11.56889	11	34	8	280	258	213	281	60	57	0	0	57	18	30
11.57028	11	34	13	280	258	213	281	62	57	0	0	62	18	31
11.57194	11	34	19	281	258	213	281	53	57	0	0	53	18	30
11.57333	11	34	24	281	258	213	282	66	57	0	0	66	18	28
11.57472	11	34	29	281	258	213	282	64	57	0	0	66	19	23
11.57611	11	34	34	281	258	213	282	61	57	0	0	66	19	19
11.5775	11	34	39	281	257	213	282	61	57	0	0	57	20	15
11.57889	11	34	44	281	257	213	282	61	57	0	0	63	20	11
11.58028	11	34	49	281	257	213	282	61	57	0	0	57	20	7
11.58167	11	34	54	281	257	213	282	60	57	0	0	57	21	4
11.58306	11	34	59	281	257	215	282	60	57	0	0	63	21	0
11.58444	11	35	4	281	257	215	282	63	57	0	0	63	21	0
11.58583	11	35	9	281	257	215	282	60	57	0	0	63	21	0
11.58722	11	35	14	280	257	215	282	61	57	0	0	63	21	0
11.58861	11	35	19	300	257	220	243	61	56	0	0	63	22	0
11.59	11	35	24	335	264	233	129	61	43	0	0	57	22	0
11.59139	11	35	29	343	275	233	151	52	38	0	0	57	22	0
11.59278	11	35	34	349	281	242	157	57	34	0	0	57	22	0
11.59417	11	35	39	349	287	247	163	57	32	0	0	50	23	0
11.59556	11	35	44	355	287	240	163	47	30	0	0	50	23	0
11.59694	11	35	49	355	301	228	169	47	31	0	0	24	23	0
11.59833	11	35	54	342	308	216	144	2	41	0	0	5	23	0
11.59972	11	35	59	328	308	207	126	2	48	0	0	5	23	0
11.60111	11	36	4	315	301	200	99	2	57	0	0	5	23	0
11.6025	11	36	9	303	301	200	82	2	64	0	0	5	23	0
11.60389	11	36	14	289	301	206	59	2	71	0	0	5	23	0
11.60528	11	36	19	277	294	206	46	2	75	0	0	5	23	0
11.60667	11	36	24	271	283	206	21	2	80	0	0	5	23	0
11.60806	11	36	29	265	273	206	11	2	82	0	0	5	23	0
11.60944	11	36	34	265	257	206	5	2	85	0	0	5	23	0
11.61083	11	36	39	258	252	206	16	2	86	0	0	5	24	0
11.61222	11	36	44	268	246	206	32	26	66	0	0	44	24	0
11.61361	11	36	49	323	251	212	116	63	50	0	0	63	24	0
11.615	11	36	54	338	269	225	139	58	41	0	0	57	23	0
11.61639	11	36	59	313	277	230	300	54	43	0	0	51	23	0
11.61778	11	37	4	305	277	230	300	61	48	0	0	57	23	0
11.61917	11	37	9	299	277	230	293	57	50	0	0	57	23	0
11.62056	11	37	14	293	277	230	288	62	53	0	0	65	23	1
11.62194	11	37	19	288	277	230	288	63	54	0	0	58	22	4
11.62333	11	37	24	288	270	225	288	63	55	0	0	63	22	4
11.62472	11	37	29	288	270	225	288	59	55	0	0	63	22	6
11.62611	11	37	34	288	270	225	282	66	56	0	0	63	22	6
11.6275	11	37	39	288	264	220	282	62	57	0	0	63	22	8
11.62889	11	37	44	288	264	220	282	62	57	0	0	63	22	9
11.63028	11	37	49	282	264	220	282	62	57	0	0	63	22	10
11.63167	11	37	54	282	264	220	282	65	57	0	0	63	22	12
11.63306	11	37	59	282	264	220	282	59	57	0	0	63	22	13
11.63444	11	38	4	282	259	220	282	63	57	0	0	63	22	15
11.63583	11	38	9	282	259	220	282	63	57	0	0	63	22	15

Flow meter calibration data.

11.63722	11	38	14	282	259	220	282	59	57	0	0	63	22	16
11.63861	11	38	19	303	259	220	235	67	56	0	0	68	22	17
11.64	11	38	24	342	277	220	103	58	40	0	0	60	22	17
11.64139	11	38	29	350	288	237	121	54	35	0	0	53	22	18
11.64278	11	38	34	356	295	243	135	53	31	0	0	53	22	18
11.64417	11	38	39	356	306	243	141	53	29	0	0	53	22	19
11.64556	11	38	44	356	311	234	146	49	27	0	0	47	22	19
11.64694	11	38	49	362	323	214	146	46	26	0	0	47	22	20
11.64833	11	38	54	362	323	201	152	46	24	0	0	47	22	20
11.64972	11	38	59	362	323	201	152	42	24	0	0	41	23	21
11.65111	11	39	4	362	329	196	158	34	23	0	0	35	23	21
11.6525	11	39	9	368	317	188	158	50	22	0	0	47	23	20
11.65389	11	39	14	368	312	188	164	45	22	0	0	47	23	19
11.65528	11	39	19	368	312	188	164	41	21	0	0	40	23	17
11.65667	11	39	24	368	312	178	164	44	20	0	0	40	23	15
11.65806	11	39	29	368	331	172	164	47	20	0	0	46	23	14
11.65944	11	39	34	368	331	172	169	48	20	0	0	46	24	11
11.66083	11	39	39	368	336	178	169	66	20	0	0	63	24	10
11.66222	11	39	44	368	329	178	162	5	23	0	0	4	24	8
11.66361	11	39	49	362	329	178	148	1	28	0	0	4	24	4
11.665	11	39	54	362	319	178	135	1	32	0	0	4	24	0
11.66639	11	39	59	349	319	178	120	1	38	0	0	4	24	0
11.66778	11	40	4	343	319	178	106	1	42	0	0	4	24	0
11.66917	11	40	9	338	319	183	94	1	47	0	0	4	24	0
11.67056	11	40	14	330	312	183	82	1	51	0	0	4	24	0
11.67194	11	40	19	316	309	196	68	1	56	0	0	0	24	0
11.67333	11	40	24	325	303	213	74	36	50	0	0	39	24	0
11.67472	11	40	29	348	298	221	118	42	38	0	0	42	24	0
11.67611	11	40	34	355	298	230	131	47	34	0	0	48	24	0
11.6775	11	40	39	328	300	235	291	51	32	0	0	48	24	0
11.67889	11	40	44	322	294	235	313	54	36	0	0	54	23	0
11.68028	11	40	49	314	288	235	313	51	41	0	0	54	23	0
11.68167	11	40	54	308	288	235	307	54	43	0	0	54	23	0
11.68306	11	40	59	301	288	235	307	54	46	0	0	54	23	0
11.68444	11	41	4	301	288	230	301	54	49	0	0	55	23	0
11.68583	11	41	9	295	282	230	295	57	50	0	0	55	23	0
11.68722	11	41	14	295	275	230	295	57	52	0	0	56	23	0
11.68861	11	41	19	290	275	230	289	57	53	0	0	56	23	0
11.69	11	41	24	290	275	225	289	60	54	0	0	56	23	0
11.69139	11	41	29	290	269	225	289	60	54	0	0	62	23	0
11.69278	11	41	34	290	269	225	289	60	55	0	0	62	23	0
11.69417	11	41	39	283	269	225	289	60	55	0	0	62	22	0
11.69556	11	41	44	283	263	225	283	63	56	0	0	62	22	0
11.69694	11	41	49	283	263	225	283	60	56	0	0	62	22	0
11.69833	11	41	54	283	263	219	283	62	56	0	0	62	22	0
11.69972	11	41	59	283	263	219	283	65	56	0	0	62	22	0
11.70111	11	42	4	283	263	219	283	63	56	0	0	62	22	0
11.7025	11	42	9	283	263	219	283	63	56	0	0	62	22	0
11.70389	11	42	14	283	263	219	283	59	57	0	0	62	22	0
11.70528	11	42	19	283	263	219	283	66	57	0	0	62	22	0
11.70667	11	42	24	283	263	219	283	62	57	0	0	62	22	0
11.70806	11	42	29	283	263	219	283	59	57	0	0	59	22	0
11.70944	11	42	34	283	263	219	283	66	57	0	0	67	22	0
11.71083	11	42	39	281	263	219	283	63	57	0	0	60	22	0
11.71222	11	42	44	281	263	219	282	59	57	0	0	60	22	0
11.71361	11	42	49	281	260	219	282	62	58	0	0	66	22	0
11.715	11	42	54	281	260	217	282	61	58	0	0	58	22	0
11.71639	11	42	59	281	260	217	282	56	58	0	0	58	22	0
11.71778	11	43	4	281	260	217	282	63	58	0	0	58	22	0
11.71917	11	43	9	281	260	217	282	63	58	0	0	65	22	0
11.72056	11	43	14	281	260	217	282	66	58	0	0	65	22	0
11.72194	11	43	19	281	260	217	282	64	58	0	0	65	22	0
11.72333	11	43	24	281	260	217	282	64	58	0	0	65	22	0
11.72472	11	43	29	281	260	217	282	64	58	0	0	65	22	0
11.72583	11	43	33	281	260	217	282	61	58	0	0	65	22	0
11.72722	11	43	38	281	260	217	282	64	58	0	0	65	22	0
11.72861	11	43	43	282	260	217	282	60	58	0	0	59	22	0
11.73	11	43	48	282	257	217	282	60	58	0	0	59	22	0
11.73139	11	43	53	282	257	217	282	57	58	0	0	59	22	0
11.73278	11	43	58	282	257	217	282	61	58	0	0	65	22	0
11.73417	11	44	3	282	257	217	282	60	58	0	0	59	21	4
11.73556	11	44	8	282	257	217	282	64	58	0	0	59	21	6
11.73694	11	44	13	282	257	217	282	57	58	0	0	59	20	8
11.73833	11	44	18	282	257	217	282	59	58	0	0	59	20	10
11.73972	11	44	23	282	257	217	282	62	58	0	0	66	20	13
11.74111	11	44	28	282	257	217	282	58	58	0	0	59	19	15
11.7425	11	44	33	282	257	217	282	60	58	0	0	59	19	19
11.74389	11	44	38	282	257	217	282	67	58	0	0	66	19	20
11.74528	11	44	43	280	257	217	284	62	58	0	0	60	18	22

Flow meter calibration data.

11.74667	11	44	48	280	257	217	284	64	57	0	0	60	18	24
11.74806	11	44	53	280	263	213	284	61	57	0	0	60	18	27
11.74944	11	44	58	280	263	213	284	57	57	0	0	60	18	27
11.75083	11	45	3	280	263	213	284	61	57	0	0	60	18	27
11.75222	11	45	8	280	263	213	284	66	57	0	0	66	19	25
11.75361	11	45	13	280	263	213	284	66	57	0	0	66	19	21
11.755	11	45	18	280	258	213	284	62	57	0	0	60	19	18
11.75639	11	45	23	280	258	213	284	62	57	0	0	60	20	13
11.75778	11	45	28	280	258	213	284	62	57	0	0	60	20	10
11.75917	11	45	33	280	258	213	284	58	57	0	0	60	21	7
11.76056	11	45	38	280	258	213	284	59	57	0	0	60	21	3
11.76194	11	45	43	281	258	213	280	59	57	0	0	60	21	1
11.76333	11	45	48	281	258	213	280	59	58	0	0	60	21	0
11.76472	11	45	53	281	258	213	280	63	58	0	0	60	22	0
11.76611	11	45	58	281	258	213	280	62	58	0	0	60	22	0
11.7675	11	46	3	281	258	213	280	59	58	0	0	60	22	0
11.76889	11	46	8	281	258	213	280	59	58	0	0	60	22	0
11.77028	11	46	13	281	258	213	280	60	58	0	0	60	22	0
11.77167	11	46	18	281	258	213	280	55	58	0	0	58	22	0
11.77306	11	46	23	281	258	213	280	59	58	0	0	58	22	0
11.77444	11	46	28	281	258	213	280	63	58	0	0	65	22	0
11.77583	11	46	33	281	258	213	280	60	58	0	0	58	22	0
11.77722	11	46	38	281	258	213	280	60	58	0	0	58	22	0
11.77861	11	46	43	282	258	213	282	60	58	0	0	58	22	0
11.78	11	46	48	282	258	213	282	65	58	0	0	65	22	0
11.78139	11	46	53	282	258	216	282	60	58	0	0	59	22	0
11.78278	11	46	58	282	258	216	282	57	58	0	0	59	22	0
11.78417	11	47	3	282	258	216	282	62	58	0	0	59	22	0
11.78556	11	47	8	282	258	216	282	58	58	0	0	59	22	0
11.78694	11	47	13	282	258	216	282	62	58	0	0	65	22	0
11.78833	11	47	18	282	258	216	282	61	58	0	0	65	22	0
11.78972	11	47	23	282	258	216	282	61	58	0	0	65	22	0
11.79111	11	47	28	282	258	216	282	62	58	0	0	58	22	0
11.79278	11	47	34	282	258	216	282	63	58	0	0	58	22	0
11.79417	11	47	39	281	258	216	282	60	58	0	0	58	22	0
11.79556	11	47	44	281	258	216	282	59	58	0	0	58	21	2
11.79694	11	47	49	281	258	216	282	56	58	0	0	58	21	5
11.79833	11	47	54	281	258	215	282	63	58	0	0	64	21	7
11.79972	11	47	59	281	258	215	282	57	58	0	0	57	20	9
11.80111	11	48	4	281	258	215	282	57	58	0	0	57	20	12
11.8025	11	48	9	281	258	215	282	60	58	0	0	57	19	14
11.80389	11	48	14	281	258	215	282	59	58	0	0	62	19	16
11.80528	11	48	19	281	256	215	282	57	58	0	0	62	19	18
11.80667	11	48	24	281	256	215	282	60	58	0	0	62	18	20
11.80806	11	48	29	281	256	215	282	63	58	0	0	62	18	23
11.80944	11	48	34	281	256	215	282	59	58	0	0	62	18	25
11.81083	11	48	39	280	256	215	282	64	58	0	0	62	18	27
11.81222	11	48	44	280	256	215	281	64	58	0	0	62	18	28
11.81361	11	48	49	280	256	215	281	64	57	0	0	62	18	26
11.815	11	48	54	280	256	214	281	59	57	0	0	62	18	27
11.81639	11	48	59	280	256	214	281	63	57	0	0	61	19	24
11.81778	11	49	4	280	256	214	281	60	57	0	0	59	19	21
11.81917	11	49	9	280	256	214	281	57	57	0	0	59	19	17
11.82056	11	49	14	280	256	214	281	60	57	0	0	60	20	14
11.82194	11	49	19	280	256	214	281	60	57	0	0	60	20	9
11.82333	11	49	24	280	256	214	281	98	57	0	0	98	21	5
11.82472	11	49	29	280	256	214	281	123	57	0	0	123	21	2
11.82611	11	49	34	280	256	214	281	127	57	0	0	127	21	0
11.8275	11	49	39	281	256	214	281	125	58	0	0	121	21	0
11.82889	11	49	44	281	256	214	280	120	58	0	0	121	22	0
11.83028	11	49	49	281	256	214	280	211	58	0	0	188	22	0
11.83167	11	49	54	281	256	212	280	226	59	0	0	223	22	0
11.83306	11	49	59	281	256	212	280	236	59	0	0	231	22	0
11.83444	11	50	4	281	256	212	280	236	59	0	0	236	22	0
11.83583	11	50	9	281	256	212	280	239	59	0	0	236	22	0
11.83722	11	50	14	281	256	212	280	237	59	0	0	242	22	0
11.83861	11	50	19	281	255	212	280	260	60	0	0	254	22	0
11.84	11	50	24	275	255	212	280	270	61	0	0	270	22	0
11.84139	11	50	29	275	255	212	274	270	61	0	0	270	22	0
11.84278	11	50	34	275	255	212	274	272	62	0	0	270	22	0
11.84417	11	50	39	275	255	212	274	272	62	0	0	270	22	0
11.84556	11	50	44	275	255	212	274	272	62	0	0	270	22	0
11.84694	11	50	49	275	250	212	274	272	62	0	0	270	22	0
11.84833	11	50	54	275	250	209	274	272	62	0	0	270	22	0
11.84972	11	50	59	275	250	209	274	272	62	0	0	270	22	0
11.85111	11	51	4	275	250	209	274	268	63	0	0	268	22	0
11.8525	11	51	9	275	250	209	274	257	63	0	0	257	22	0
11.85389	11	51	14	275	250	209	274	257	63	0	0	257	22	0
11.85528	11	51	19	275	250	209	274	244	65	0	0	244	22	0

Flow meter calibration data.

11.85667	11	51	24	268	250	209	268	244	66	0	0	244	22	0
11.85806	11	51	29	268	250	209	268	244	67	0	0	244	22	0
11.85944	11	51	34	263	244	209	268	244	68	0	0	245	22	0
11.86083	11	51	39	263	244	204	262	239	70	0	0	238	22	0
11.86222	11	51	44	263	244	204	262	239	71	0	0	238	22	0
11.86361	11	51	49	256	244	204	256	239	72	0	0	238	22	0
11.865	11	51	54	256	239	204	256	239	73	0	0	238	22	0
11.86639	11	51	59	256	239	204	256	242	73	0	0	238	22	0
11.86778	11	52	4	256	239	199	256	239	74	0	0	236	22	0
11.86917	11	52	9	251	239	199	250	228	76	0	0	228	22	0
11.87056	11	52	14	251	233	199	250	228	78	0	0	228	22	0
11.87194	11	52	19	244	233	194	243	228	79	0	0	228	22	0
11.87333	11	52	24	244	233	194	243	228	80	0	0	228	22	0
11.87472	11	52	29	244	227	194	243	228	80	0	0	228	22	0
11.87611	11	52	34	244	227	194	243	228	81	0	0	223	22	0
11.8775	11	52	39	238	227	189	243	218	83	0	0	216	22	0
11.87889	11	52	44	232	222	189	238	216	85	0	0	216	22	0
11.88028	11	52	49	232	222	189	231	213	87	0	0	209	22	0
11.88167	11	52	54	226	216	184	225	208	89	0	0	209	22	0
11.88306	11	52	59	226	216	184	225	208	90	0	0	209	22	0
11.88444	11	53	4	221	211	184	225	208	90	0	0	209	22	0
11.88583	11	53	9	221	211	178	221	208	91	0	0	209	22	0
11.88722	11	53	14	221	206	178	221	208	91	0	0	209	22	0
11.88861	11	53	19	221	206	178	221	211	91	0	0	209	22	0
11.89	11	53	24	221	206	178	221	211	91	0	0	209	22	0
11.89139	11	53	29	221	206	178	221	211	91	0	0	209	22	0
11.89278	11	53	34	221	206	178	221	211	91	0	0	212	22	0
11.89417	11	53	39	221	206	173	221	211	91	0	0	212	22	0
11.89556	11	53	44	221	200	173	221	211	91	0	0	212	22	0
11.89694	11	53	49	221	200	173	221	211	91	0	0	212	22	0
11.89833	11	53	54	221	200	173	221	211	91	0	0	212	22	0
11.89972	11	53	59	221	200	173	221	211	92	0	0	212	22	0
11.90111	11	54	4	219	200	173	221	211	92	0	0	212	22	0
11.9025	11	54	9	219	200	173	218	211	92	0	0	212	22	0
11.90361	11	54	13	219	200	173	218	211	92	0	0	212	22	0
11.905	11	54	18	219	200	173	218	211	92	0	0	212	22	0
11.90639	11	54	23	219	200	173	218	211	92	0	0	212	22	0
11.90778	11	54	28	219	200	173	218	211	92	0	0	212	22	0
11.90917	11	54	33	219	200	173	218	211	92	0	0	210	22	0
11.91056	11	54	38	219	200	171	218	211	92	0	0	210	22	0
11.91194	11	54	43	219	200	171	218	211	92	0	0	210	22	0
11.91333	11	54	48	219	200	171	218	211	92	0	0	210	22	0
11.91472	11	54	53	219	200	171	218	211	92	0	0	210	22	0
11.91611	11	54	58	219	200	171	218	211	92	0	0	210	21	2
11.9175	11	55	3	218	200	171	218	211	92	0	0	210	21	4
11.91889	11	55	8	218	200	171	218	210	92	0	0	210	21	7
11.92028	11	55	13	218	200	171	218	210	92	0	0	210	20	8
11.92167	11	55	18	218	200	171	218	210	92	0	0	210	20	11
11.92306	11	55	23	218	200	171	218	210	92	0	0	210	20	12
11.92444	11	55	28	218	200	171	218	210	92	0	0	210	20	15
11.92583	11	55	33	218	200	171	218	210	92	0	0	209	19	16
11.92722	11	55	38	218	200	171	218	210	92	0	0	209	19	18
11.92861	11	55	43	218	200	171	218	210	92	0	0	209	19	20
11.93	11	55	48	218	199	171	218	210	92	0	0	209	19	23
11.93139	11	55	53	218	199	171	218	210	92	0	0	209	18	25
11.93278	11	55	58	218	199	171	218	210	92	0	0	209	18	27
11.93417	11	56	3	217	199	171	218	207	92	0	0	209	18	27
11.93556	11	56	8	217	199	171	217	207	92	0	0	209	18	26
11.93694	11	56	13	217	199	171	217	210	92	0	0	209	19	21
11.93833	11	56	18	217	199	171	217	210	92	0	0	209	19	17
11.93972	11	56	23	217	199	171	217	207	92	0	0	209	20	13
11.94111	11	56	28	217	199	171	217	207	92	0	0	209	20	8
11.9425	11	56	33	217	199	171	217	207	92	0	0	207	21	5
11.94389	11	56	38	217	199	170	217	207	92	0	0	207	21	1
11.94528	11	56	43	217	199	170	217	207	92	0	0	207	21	1
11.94667	11	56	48	217	200	170	217	210	92	0	0	207	22	1
11.94806	11	56	53	217	200	170	217	210	92	0	0	207	22	1
11.94944	11	56	58	217	200	170	217	208	92	0	0	207	22	1
11.95083	11	57	3	218	200	170	217	208	92	0	0	207	22	1
11.95222	11	57	8	218	200	170	217	208	92	0	0	207	22	1
11.95361	11	57	13	218	200	170	217	208	92	0	0	207	22	1
11.955	11	57	18	218	200	170	217	208	92	0	0	207	22	1
11.95639	11	57	23	218	200	170	217	208	92	0	0	207	22	1
11.95778	11	57	28	218	200	170	217	208	92	0	0	207	22	1
11.95917	11	57	33	218	200	170	217	208	92	0	0	209	22	1
11.96056	11	57	38	218	200	170	217	208	92	0	0	209	22	0
11.96194	11	57	43	218	200	170	217	208	92	0	0	209	22	0
11.96333	11	57	48	218	198	170	217	208	92	0	0	209	22	0
11.96472	11	57	53	218	198	170	217	211	93	0	0	209	22	0

Flow meter calibration data.

11.96611	11	57	58	218	198	170	217	208	93	0	0	209	22	0
11.9675	11	58	3	218	198	170	217	208	93	0	0	209	22	0
11.96889	11	58	8	218	198	170	217	208	93	0	0	209	22	0
11.97028	11	58	13	218	198	170	217	208	93	0	0	209	22	0
11.97167	11	58	18	218	198	170	217	208	93	0	0	209	22	0
11.97306	11	58	23	218	198	170	217	208	93	0	0	209	22	0
11.97444	11	58	28	218	198	170	217	208	93	0	0	209	22	0
11.97583	11	58	33	218	198	170	217	208	93	0	0	209	21	2
11.97722	11	58	38	218	198	169	217	208	93	0	0	209	21	3
11.97861	11	58	43	218	198	169	217	208	93	0	0	209	21	6
11.98	11	58	48	218	197	169	217	208	93	0	0	209	20	8
11.98139	11	58	53	218	197	169	217	208	92	0	0	209	20	10
11.98278	11	58	58	218	197	169	217	208	92	0	0	209	20	12
11.98417	11	59	3	218	197	169	217	208	92	0	0	209	20	14
11.98556	11	59	8	218	197	169	217	208	92	0	0	209	19	16
11.98694	11	59	13	218	197	169	217	208	92	0	0	209	19	18
11.98833	11	59	18	218	197	169	217	208	92	0	0	209	19	20
11.98972	11	59	23	218	197	169	217	208	92	0	0	209	19	23
11.99111	11	59	28	218	197	169	217	208	92	0	0	209	18	24
11.9925	11	59	33	218	197	169	217	208	92	0	0	209	18	27
11.99389	11	59	38	218	197	170	217	208	92	0	0	209	18	27
11.99528	11	59	43	218	197	170	217	208	92	0	0	209	18	27
11.99667	11	59	48	218	198	170	217	208	92	0	0	208	19	25
11.99806	11	59	53	211	198	170	210	187	96	0	0	187	19	19
11.99944	11	59	58	206	198	170	204	187	98	0	0	187	20	15
12.00083	12	0	3	199	192	170	204	187	99	0	0	187	20	10
12.00222	12	0	8	199	192	164	198	187	100	0	0	187	21	6
12.00361	12	0	13	199	187	164	198	187	101	0	0	187	21	2
12.005	12	0	18	199	187	164	198	189	101	0	0	187	21	0
12.00639	12	0	23	199	187	160	198	189	101	0	0	187	22	0
12.00778	12	0	28	199	187	160	198	180	102	0	0	176	22	0
12.00917	12	0	33	186	182	160	192	174	105	0	0	176	22	0
12.01056	12	0	38	186	182	154	186	176	105	0	0	176	22	0
12.01194	12	0	43	186	176	154	186	176	105	0	0	176	22	0
12.01333	12	0	48	186	176	154	186	174	106	0	0	176	22	0
12.01472	12	0	53	186	171	149	181	174	106	0	0	176	22	0
12.01611	12	0	58	180	171	149	181	171	107	0	0	168	22	0
12.0175	12	1	3	180	171	149	181	167	108	0	0	168	22	0
12.01889	12	1	8	180	166	149	175	167	108	0	0	168	22	0
12.02028	12	1	13	175	166	144	175	167	108	0	0	168	22	0
12.02167	12	1	18	175	166	144	175	167	109	0	0	168	22	0
12.02306	12	1	23	175	166	144	175	167	109	0	0	168	22	0
12.02444	12	1	28	175	166	144	175	167	109	0	0	168	22	0
12.02583	12	1	33	175	160	144	175	167	109	0	0	168	22	0
12.02722	12	1	38	175	160	144	175	167	109	0	0	168	22	0
12.02861	12	1	43	175	160	144	175	167	109	0	0	168	22	0
12.03	12	1	48	175	160	144	175	164	109	0	0	168	22	0
12.03139	12	1	53	175	160	144	175	167	109	0	0	168	22	0
12.03278	12	1	58	175	160	139	175	167	109	0	0	166	22	0
12.03417	12	2	3	175	160	139	175	167	109	0	0	166	22	0
12.03556	12	2	8	175	160	139	173	167	109	0	0	166	22	0
12.03694	12	2	13	172	160	139	173	167	109	0	0	166	21	2
12.03833	12	2	18	172	160	139	173	167	109	0	0	166	21	3
12.03972	12	2	23	172	160	139	173	164	109	0	0	166	21	5
12.04111	12	2	28	172	160	139	173	164	109	0	0	166	21	7
12.0425	12	2	33	172	157	139	173	164	109	0	0	166	21	9
12.04389	12	2	38	172	157	139	173	164	109	0	0	166	20	11
12.04528	12	2	43	172	157	139	173	164	109	0	0	166	20	13
12.04667	12	2	48	172	157	139	173	164	109	0	0	166	20	15
12.04833	12	2	54	172	157	139	173	164	109	0	0	166	20	18
12.04972	12	2	59	172	157	136	173	164	109	0	0	162	19	19
12.05111	12	3	4	172	157	136	173	164	109	0	0	162	19	21
12.0525	12	3	9	172	157	136	171	164	109	0	0	162	19	23
12.05389	12	3	14	170	157	136	171	164	109	0	0	162	19	25
12.05528	12	3	19	170	157	136	171	164	109	0	0	162	19	27
12.05667	12	3	24	170	157	136	171	165	109	0	0	162	18	29
12.05806	12	3	29	170	157	136	171	165	109	0	0	162	18	29
12.05944	12	3	34	170	157	136	171	165	109	0	0	162	19	27
12.06083	12	3	39	170	157	136	171	165	109	0	0	162	20	21
12.06222	12	3	44	170	157	136	171	165	109	0	0	162	20	16
12.06361	12	3	49	170	157	136	171	165	109	0	0	162	20	10
12.065	12	3	54	170	157	136	171	165	109	0	0	162	21	4
12.06639	12	3	59	170	157	135	171	165	109	0	0	165	21	1
12.06778	12	4	4	170	157	135	171	165	109	0	0	165	22	0
12.06917	12	4	9	170	157	135	172	162	109	0	0	165	22	0
12.07056	12	4	14	171	157	135	172	165	109	0	0	165	22	0
12.07194	12	4	19	171	157	135	172	165	109	0	0	165	22	0
12.07333	12	4	24	171	157	135	172	165	109	0	0	165	22	0
12.07472	12	4	29	171	157	135	172	165	109	0	0	165	22	0

Flow meter calibration data.

12.07611	12	4	34	171	157	135	172	165	109	0	0	165	22	0
12.0775	12	4	39	171	157	135	172	165	109	0	0	165	22	0
12.07889	12	4	44	171	157	135	172	165	109	0	0	165	22	0
12.08028	12	4	49	171	157	135	172	163	109	0	0	165	22	0
12.08167	12	4	54	171	157	135	172	163	109	0	0	165	21	2
12.08306	12	4	59	171	157	137	172	163	109	0	0	161	21	3
12.08444	12	5	4	171	157	137	172	163	109	0	0	161	21	6
12.08583	12	5	9	171	157	137	170	166	109	0	0	161	21	7
12.08722	12	5	14	171	157	137	170	163	109	0	0	161	21	9
12.08861	12	5	19	171	157	137	170	163	109	0	0	161	20	11
12.09	12	5	24	171	157	137	170	163	109	0	0	161	20	13
12.09139	12	5	29	171	157	137	170	163	109	0	0	161	20	15
12.09278	12	5	34	171	156	137	170	166	109	0	0	161	20	17
12.09417	12	5	39	171	156	137	170	163	109	0	0	161	19	19
12.09556	12	5	44	171	156	137	170	163	109	0	0	161	19	21
12.09694	12	5	49	171	156	137	170	163	109	0	0	161	19	22
12.09833	12	5	54	171	156	137	170	163	109	0	0	161	19	25
12.09972	12	5	59	171	156	134	170	163	109	0	0	165	19	26
12.10083	12	6	3	171	156	134	170	163	109	0	0	165	18	28
12.10222	12	6	8	171	156	134	170	163	109	0	0	165	18	29
12.10361	12	6	13	170	156	134	170	163	109	0	0	165	18	29
12.105	12	6	18	170	156	134	170	166	109	0	0	165	19	25
12.10639	12	6	23	170	156	134	170	159	109	0	0	150	19	20
12.10778	12	6	28	145	156	134	150	124	117	0	0	120	20	14
12.10917	12	6	33	127	145	128	127	118	118	0	0	120	21	10
12.11056	12	6	38	127	137	117	127	118	118	0	0	120	21	3
12.11194	12	6	43	127	130	117	127	118	118	0	0	120	22	0
12.11333	12	6	48	121	125	112	122	111	119	0	0	108	22	0
12.11472	12	6	53	115	119	106	116	108	120	0	0	108	22	0
12.11611	12	6	58	115	113	106	110	108	120	0	0	108	22	0
12.1175	12	7	3	115	113	101	110	105	120	0	0	108	22	0
12.11889	12	7	8	115	107	101	110	105	120	0	0	105	22	0
12.12028	12	7	13	115	107	101	110	107	120	0	0	105	22	0
12.12167	12	7	18	115	107	101	110	107	120	0	0	105	22	0
12.12306	12	7	23	115	107	96	110	107	120	0	0	105	22	0
12.12444	12	7	28	115	107	96	110	107	120	0	0	105	22	0
12.12583	12	7	33	115	107	96	110	104	120	0	0	105	22	0
12.12722	12	7	38	115	102	96	110	104	120	0	0	105	22	0
12.12861	12	7	43	109	102	96	110	104	120	0	0	105	22	0
12.13	12	7	48	109	102	96	110	104	120	0	0	105	22	0
12.13139	12	7	53	109	102	96	110	104	120	0	0	105	22	0
12.13278	12	7	58	109	102	96	113	108	120	0	0	105	22	0
12.13417	12	8	3	109	102	96	113	108	120	0	0	105	22	0
12.13556	12	8	8	109	102	96	113	108	120	0	0	106	22	0
12.13694	12	8	13	109	102	96	113	105	120	0	0	106	22	0
12.13833	12	8	18	109	102	96	113	105	120	0	0	106	22	0
12.13972	12	8	23	109	102	96	113	105	120	0	0	106	22	0
12.14111	12	8	28	109	102	96	113	105	120	0	0	106	22	0
12.1425	12	8	33	109	102	96	113	105	120	0	0	106	22	0
12.14389	12	8	38	109	102	96	113	108	120	0	0	106	22	0
12.14528	12	8	43	112	102	96	113	108	120	0	0	106	22	1
12.14667	12	8	48	112	102	96	113	108	120	0	0	106	22	3
12.14806	12	8	53	112	102	96	113	108	119	0	0	106	22	4
12.14944	12	8	58	112	102	96	114	108	119	0	0	106	21	6
12.15083	12	9	3	112	102	96	114	108	119	0	0	106	21	8
12.15222	12	9	8	112	102	96	114	108	119	0	0	108	21	10
12.15361	12	9	13	112	102	96	114	108	119	0	0	108	21	11
12.155	12	9	18	112	102	96	114	108	119	0	0	108	21	14
12.15639	12	9	23	112	102	95	114	108	119	0	0	108	21	15
12.15778	12	9	28	112	102	95	114	108	119	0	0	108	21	17
12.15917	12	9	33	112	102	95	114	108	119	0	0	108	20	18
12.16056	12	9	38	112	102	95	114	106	119	0	0	108	20	20
12.16194	12	10	4	112	102	95	112	106	119	0	0	108	20	30
12.16333	12	10	9	112	102	95	112	106	119	0	0	108	19	31
12.16472	12	10	14	112	102	95	112	106	119	0	0	108	19	31
12.16611	12	10	19	112	102	95	112	106	119	0	0	108	19	32
12.16750	12	10	24	112	102	94	112	106	119	0	0	108	19	32
12.16889	12	10	28	112	102	94	112	106	119	0	0	108	19	32
12.17028	12	10	33	112	102	94	112	106	119	0	0	108	19	32
12.17167	12	10	38	112	102	94	112	107	119	0	0	108	19	32
12.17306	12	10	43	112	102	94	112	107	119	0	0	108	19	32
12.17444	12	10	48	112	102	94	112	107	119	0	0	108	19	32
12.17583	12	10	53	112	102	94	112	107	119	0	0	108	19	32
12.17722	12	10	58	112	102	94	112	107	119	0	0	108	19	32
12.17861	12	10	63	112	102	94	112	107	119	0	0	108	19	32
12.18	12	10	68	112	102	94	112	107	119	0	0	108	19	32
12.18139	12	10	73	112	102	94	112	107	120	0	0	108	19	32
12.18278	12	10	78	112	102	94	111	107	120	0	0	108	19	32
12.18417	12	11	3	112	102	94	111	107	120	0	0	108	19	32
12.18556	12	11	8	112	102	94	111	107	120	0	0	107	19	32
12.18694	12	11	13	112	102	94	111	107	120	0	0	107	19	32
12.18833	12	11	18	112	102	94	111	107	120	0	0	107	19	32
12.18972	12	11	23	112	102	93	111	107	120	0	0	107	19	32

Flow meter calibration data.

12.19111	12	11	28	112	102	93	111	107	120	0	0	107	19	32
12.1925	12	11	33	112	102	93	111	107	120	0	0	107	19	32
12.19389	12	11	38	112	103	93	111	105	120	0	0	107	19	32
12.19528	12	11	43	112	103	93	111	109	119	0	0	107	19	32
12.19667	12	11	48	112	103	93	111	109	119	0	0	107	19	32
12.19806	12	11	53	112	103	93	111	109	119	0	0	107	19	32
12.19944	12	11	58	112	103	93	113	106	119	0	0	107	19	32
12.20083	12	12	3	112	103	93	113	106	119	0	0	107	19	32
12.20222	12	12	8	112	103	93	113	106	119	0	0	108	19	32
12.20361	12	12	13	112	103	93	113	106	119	0	0	108	19	32
12.205	12	12	18	112	103	93	113	106	119	0	0	108	19	31
12.20639	12	12	23	112	103	92	113	106	119	0	0	108	19	29
12.20778	12	12	28	112	103	92	113	106	119	0	0	108	19	25
12.20917	12	12	33	112	103	92	113	106	119	0	0	108	20	18
12.21056	12	12	38	112	103	92	113	106	119	0	0	108	21	13
12.21194	12	12	43	113	103	92	113	106	120	0	0	108	21	7
12.21333	12	12	48	113	103	92	113	106	120	0	0	108	22	3
12.21472	12	12	53	113	103	92	113	106	120	0	0	108	22	0
12.21611	12	12	58	113	103	92	112	106	120	0	0	108	22	0
12.2175	12	13	3	113	103	92	112	106	120	0	0	108	22	0
12.21889	12	13	8	113	103	92	112	106	120	0	0	107	22	0
12.22028	12	13	13	113	103	92	112	106	120	0	0	107	22	0
12.22167	12	13	18	113	103	92	112	106	120	0	0	107	22	0
12.22306	12	13	23	113	103	92	112	106	120	0	0	107	22	0
12.22444	12	13	28	113	103	92	112	106	120	0	0	107	22	0
12.22583	12	13	33	113	103	92	112	106	120	0	0	107	22	0
12.22722	12	13	38	113	102	92	112	106	120	0	0	107	22	0
12.22861	12	13	43	112	102	92	112	106	120	0	0	107	22	0
12.23	12	13	48	112	102	92	112	106	120	0	0	107	22	0
12.23139	12	13	53	112	102	92	112	106	120	0	0	107	22	1
12.23278	12	13	58	112	102	92	114	107	120	0	0	107	22	2
12.23417	12	14	3	112	102	92	114	107	120	0	0	107	22	4
12.23556	12	14	8	112	102	92	114	107	120	0	0	108	21	6
12.23694	12	14	13	112	102	92	114	107	120	0	0	108	21	8
12.23833	12	14	18	112	102	92	114	107	120	0	0	108	21	9
12.23972	12	14	23	112	102	95	114	107	120	0	0	108	21	11
12.24111	12	14	28	112	102	95	114	107	120	0	0	108	21	13
12.2425	12	14	33	112	102	95	114	107	120	0	0	108	21	15
12.24389	12	14	38	112	101	95	114	107	120	0	0	108	21	16
12.24528	12	14	43	113	101	95	114	107	120	0	0	108	21	18
12.24667	12	14	48	113	101	95	114	107	120	0	0	108	20	20
12.24806	12	14	53	113	101	95	109	107	120	0	0	108	20	22
12.24944	12	14	58	113	101	95	109	106	120	0	0	108	20	23
12.25083	12	15	3	113	101	95	109	106	120	0	0	108	20	25
12.25222	12	15	8	113	101	95	109	106	120	0	0	104	20	27
12.25361	12	15	13	113	101	95	109	106	120	0	0	104	20	29
12.255	12	15	18	113	101	95	109	106	120	0	0	104	20	30
12.25639	12	15	23	113	101	92	109	106	120	0	0	104	19	31
12.25778	12	15	28	113	101	92	109	106	120	0	0	104	19	32
12.25917	12	15	33	113	101	92	109	106	120	0	0	104	19	32
12.26056	12	15	38	113	101	92	109	106	120	0	0	104	19	32
12.26194	12	15	43	111	101	92	109	106	120	0	0	104	19	32
12.26333	12	15	48	111	101	92	109	106	120	0	0	104	19	32
12.26472	12	15	53	111	101	92	112	106	120	0	0	104	19	32
12.26611	12	15	58	111	101	92	112	107	120	0	0	104	19	32
12.2675	12	16	3	111	101	92	112	107	120	0	0	104	19	32
12.26889	12	16	8	111	101	92	112	107	120	0	0	106	19	32
12.27028	12	16	13	111	101	92	112	107	120	0	0	106	19	32
12.27167	12	16	18	111	101	92	112	107	120	0	0	106	19	32
12.27306	12	16	23	111	101	92	112	107	120	0	0	106	19	32
12.27444	12	16	28	111	101	92	112	107	120	0	0	106	19	32
12.27611	12	16	34	111	101	92	112	107	120	0	0	106	19	32
12.2775	12	16	39	113	102	92	112	107	120	0	0	106	19	32
12.27889	12	16	44	113	102	92	112	107	120	0	0	106	19	32
12.28028	12	16	49	113	102	92	112	107	120	0	0	106	19	32
12.28167	12	16	54	113	102	92	113	107	120	0	0	106	19	32
12.28306	12	16	59	113	102	92	113	105	120	0	0	106	19	32
12.28444	12	17	4	113	102	92	113	105	120	0	0	106	19	32
12.28583	12	17	9	113	102	92	113	105	120	0	0	106	19	32
12.28722	12	17	14	113	102	92	113	105	120	0	0	106	19	32
12.28861	12	17	19	113	102	92	113	105	120	0	0	106	19	32
12.29	12	17	24	113	102	91	113	105	120	0	0	106	19	32
12.29139	12	17	29	113	102	91	113	105	120	0	0	106	19	32
12.29278	12	17	34	113	102	91	113	105	120	0	0	106	19	32
12.29417	12	17	39	111	100	91	113	105	120	0	0	106	19	31
12.29556	12	17	44	111	100	91	113	105	120	0	0	106	19	26
12.29694	12	17	49	111	100	91	113	105	120	0	0	106	20	22
12.29833	12	17	54	111	100	91	112	105	120	0	0	104	20	15
12.29972	12	17	59	117	100	91	118	143	118	0	0	129	21	10

Flow meter calibration data.

12.30111	12	18	4	160	105	99	160	160	111	0	0	159	21	4
12.3025	12	18	9	166	123	106	160	160	111	0	0	159	22	1
12.30389	12	18	14	166	131	112	160	160	111	0	0	159	22	1
12.30528	12	18	19	166	136	117	166	160	111	0	0	159	22	1
12.30667	12	18	24	166	136	122	166	160	111	0	0	160	22	1
12.30806	12	18	29	166	142	122	166	164	109	0	0	166	22	1
12.30944	12	18	34	171	148	127	166	164	109	0	0	166	22	1
12.31083	12	18	39	171	148	127	166	164	109	0	0	166	22	1
12.31222	12	18	44	171	148	127	172	164	109	0	0	166	22	1
12.31361	12	18	49	171	153	127	172	164	109	0	0	166	22	1
12.315	12	18	54	171	153	127	172	164	109	0	0	166	22	1
12.31639	12	18	59	171	153	132	172	164	109	0	0	166	22	1
12.31778	12	19	4	171	153	132	172	164	109	0	0	166	22	1
12.31917	12	19	9	171	153	132	172	164	109	0	0	166	22	0
12.32056	12	19	14	171	153	132	172	164	109	0	0	166	22	0
12.32194	12	19	19	171	153	132	172	164	109	0	0	166	22	0
12.32333	12	19	24	171	153	132	172	164	109	0	0	166	22	0
12.32472	12	19	29	171	153	132	172	164	109	0	0	164	22	0
12.32611	12	19	34	172	153	132	172	164	109	0	0	164	22	0
12.3275	12	19	39	172	153	132	172	164	109	0	0	164	22	0
12.32889	12	19	44	172	156	132	172	164	109	0	0	164	22	0
12.33028	12	19	49	172	156	132	172	164	109	0	0	164	22	0
12.33167	12	19	54	172	156	132	172	164	109	0	0	164	22	0
12.33306	12	19	59	172	156	135	172	164	109	0	0	164	22	0
12.33444	12	20	4	172	156	135	172	164	109	0	0	164	22	0
12.33583	12	20	9	172	156	135	172	164	109	0	0	164	22	0
12.33722	12	20	14	172	156	135	172	164	109	0	0	164	22	0
12.33861	12	20	19	172	156	135	172	164	109	0	0	164	21	2
12.34	12	20	24	172	156	135	172	164	109	0	0	164	21	4
12.34139	12	20	29	172	156	135	172	164	109	0	0	164	21	6
12.34278	12	20	34	173	156	135	172	164	109	0	0	164	21	8
12.34417	12	20	39	173	156	135	172	164	109	0	0	164	21	10
12.34556	12	20	44	173	156	135	169	164	109	0	0	164	20	12
12.34694	12	20	49	173	157	135	169	164	109	0	0	164	20	14
12.34833	12	20	54	173	157	135	169	167	108	0	0	164	20	15
12.34972	12	20	59	173	157	135	169	164	108	0	0	164	20	18
12.35111	12	21	4	173	157	135	169	164	108	0	0	164	19	19
12.3525	12	21	9	173	157	135	169	164	108	0	0	164	19	22
12.35389	12	21	14	173	157	135	169	164	108	0	0	164	19	23
12.35528	12	21	19	173	157	135	169	164	108	0	0	164	19	25
12.35667	12	21	24	173	157	135	169	164	108	0	0	164	19	27
12.35806	12	21	29	173	157	135	169	164	108	0	0	164	18	29
12.35944	12	21	34	172	157	135	169	164	108	0	0	164	18	29
12.36083	12	21	39	172	157	135	169	164	108	0	0	164	18	29
12.36222	12	21	44	172	157	135	171	164	108	0	0	164	19	25
12.36361	12	21	49	172	157	135	171	164	108	0	0	164	20	19
12.365	12	21	54	172	157	135	171	164	108	0	0	164	20	15
12.36639	12	21	59	172	157	134	171	165	109	0	0	164	21	9
12.36778	12	22	4	172	157	134	171	165	109	0	0	164	21	6
12.36917	12	22	9	172	157	134	171	165	109	0	0	164	22	1
12.37056	12	22	14	172	157	134	171	165	109	0	0	164	22	1
12.37194	12	22	19	172	157	134	171	165	109	0	0	164	22	1
12.37333	12	22	24	172	157	134	171	165	109	0	0	164	22	1
12.37472	12	22	29	172	157	134	171	165	109	0	0	165	22	1
12.37583	12	22	33	171	157	134	171	165	109	0	0	165	22	1
12.37722	12	22	38	171	157	134	171	165	109	0	0	165	22	1
12.37861	12	22	43	171	157	134	173	165	109	0	0	165	22	1
12.38028	12	22	49	171	158	134	173	165	109	0	0	165	22	1
12.38167	12	22	54	171	158	134	173	165	109	0	0	165	22	1
12.38306	12	22	59	171	158	134	173	167	109	0	0	165	22	1
12.38444	12	23	4	171	158	134	173	167	109	0	0	165	22	1
12.38556	12	23	8	171	158	134	173	167	109	0	0	165	22	1
12.38694	12	23	13	171	158	134	173	167	109	0	0	165	22	0
12.38833	12	23	18	171	158	134	173	167	109	0	0	165	22	0
12.38972	12	23	23	171	158	134	173	167	109	0	0	165	22	0
12.39111	12	23	28	171	158	134	173	167	109	0	0	165	22	0
12.3925	12	23	33	172	158	134	173	167	109	0	0	165	22	0
12.39389	12	23	38	172	158	134	173	167	109	0	0	165	22	0
12.39528	12	23	43	172	158	134	172	164	109	0	0	165	22	0
12.39667	12	23	48	172	158	134	172	164	109	0	0	165	22	0
12.39806	12	23	53	172	158	134	172	164	109	0	0	165	22	0
12.39944	12	23	58	172	158	134	172	164	109	0	0	165	22	0
12.40083	12	24	3	172	158	134	172	164	109	0	0	165	22	0
12.40222	12	24	8	172	158	134	172	164	109	0	0	165	22	0
12.40361	12	24	13	172	158	134	172	164	109	0	0	165	22	0
12.405	12	24	18	172	158	134	172	164	109	0	0	165	22	0
12.40639	12	24	23	172	158	134	172	164	109	0	0	165	22	0
12.40778	12	24	28	172	158	134	172	167	109	0	0	166	22	0
12.40917	12	24	33	172	158	134	172	167	109	0	0	166	22	0

Flow meter calibration data.

12.41056	12	24	38	172	158	134	172	167	109	0	0	166	22	0
12.41194	12	24	43	172	158	134	174	167	109	0	0	166	22	1
12.41333	12	24	48	172	159	134	174	167	109	0	0	166	21	3
12.41472	12	24	53	172	159	134	174	167	109	0	0	166	21	5
12.41611	12	24	58	172	159	137	174	167	108	0	0	166	21	6
12.4175	12	25	3	172	159	137	174	167	108	0	0	166	21	9
12.41889	12	25	8	172	159	137	174	167	108	0	0	166	20	10
12.42028	12	25	13	172	159	137	174	167	108	0	0	166	20	13
12.42167	12	25	18	172	159	137	174	167	108	0	0	166	20	14
12.42306	12	25	23	172	159	137	174	167	108	0	0	166	20	16
12.42444	12	25	28	172	159	137	174	167	108	0	0	166	20	18
12.42583	12	25	33	174	159	137	174	167	108	0	0	166	19	20
12.42722	12	25	38	174	159	137	174	167	108	0	0	166	19	22
12.42861	12	25	43	174	159	137	173	167	108	0	0	166	19	24
12.43	12	25	48	174	159	137	173	167	108	0	0	166	19	26
12.43139	12	25	53	174	159	137	173	167	108	0	0	166	18	28
12.43278	12	25	58	174	159	137	173	167	108	0	0	166	18	29
12.43417	12	26	3	174	159	138	173	167	108	0	0	166	18	30
12.43556	12	26	8	174	159	138	173	167	108	0	0	166	18	31
12.43694	12	26	13	174	159	138	173	167	108	0	0	166	18	31
12.43833	12	26	18	174	159	138	173	167	108	0	0	166	18	32
12.43972	12	26	23	174	159	138	173	167	108	0	0	166	18	30
12.44111	12	26	28	174	159	138	173	164	108	0	0	166	19	25
12.4425	12	26	33	174	159	138	173	164	108	0	0	164	19	19
12.44389	12	26	38	173	159	138	173	167	108	0	0	164	20	15
12.44528	12	26	43	173	159	138	172	167	108	0	0	164	21	8
12.44667	12	26	48	173	158	138	172	167	108	0	0	164	21	4
12.44806	12	26	53	173	158	138	172	163	108	0	0	164	22	1
12.44944	12	26	58	173	158	138	172	163	109	0	0	164	22	1
12.45083	12	27	3	173	158	134	172	163	109	0	0	164	22	1
12.45222	12	27	8	173	158	134	172	166	109	0	0	164	22	1
12.45361	12	27	13	173	158	134	172	166	109	0	0	164	22	1
12.45528	12	27	19	173	158	134	172	166	109	0	0	164	22	1
12.45667	12	27	24	173	158	134	172	166	109	0	0	169	22	1
12.45806	12	27	29	181	158	134	187	199	103	0	0	199	22	1
12.45944	12	27	34	195	164	140	195	199	100	0	0	199	22	1
12.46083	12	27	39	195	170	140	195	199	99	0	0	199	22	1
12.46222	12	27	44	202	170	146	202	199	98	0	0	199	22	1
12.46361	12	27	49	202	176	151	202	199	98	0	0	199	22	1
12.465	12	27	54	202	176	151	202	199	98	0	0	198	22	0
12.46639	12	27	59	202	181	151	208	211	95	0	0	209	22	0
12.46778	12	28	4	209	181	157	208	211	94	0	0	209	22	0
12.46917	12	28	9	209	188	157	208	211	93	0	0	209	22	0
12.47056	12	28	14	215	188	157	215	211	93	0	0	209	22	0
12.47194	12	28	19	215	193	162	215	211	93	0	0	209	22	0
12.47333	12	28	24	215	193	162	215	211	93	0	0	209	22	0
12.47472	12	28	29	215	193	162	215	208	93	0	0	210	22	0
12.47611	12	28	34	215	193	162	215	216	91	0	0	216	22	0
12.4775	12	28	39	220	198	162	220	216	91	0	0	216	22	0
12.47889	12	28	44	220	198	168	220	216	90	0	0	216	22	0
12.48028	12	28	49	220	198	168	220	216	90	0	0	216	22	0
12.48167	12	28	54	220	198	168	220	216	90	0	0	216	22	0
12.48306	12	28	59	220	198	168	220	216	90	0	0	216	22	0
12.48444	12	29	4	220	198	168	220	216	90	0	0	216	22	0
12.48583	12	29	9	220	203	168	220	216	90	0	0	216	22	0
12.48722	12	29	14	220	203	173	220	216	90	0	0	216	22	0
12.48861	12	29	19	220	203	173	220	216	90	0	0	216	22	0
12.49	12	29	24	220	203	173	220	213	90	0	0	216	22	0
12.49139	12	29	29	220	203	173	220	213	90	0	0	216	22	0
12.49278	12	29	34	220	203	173	220	213	90	0	0	215	22	0
12.49417	12	29	39	223	203	173	223	213	90	0	0	215	22	0
12.49556	12	29	44	223	203	173	223	213	90	0	0	215	22	0
12.49694	12	29	49	223	203	173	223	216	90	0	0	215	22	0
12.49833	12	29	54	223	203	173	223	216	90	0	0	215	22	0
12.49972	12	29	59	223	203	173	223	216	89	0	0	215	22	0
12.50111	12	30	4	223	203	173	223	216	89	0	0	215	22	0
12.5025	12	30	9	223	204	173	223	216	89	0	0	215	22	0
12.50389	12	30	14	223	204	174	223	216	89	0	0	215	22	0
12.50528	12	30	19	223	204	174	223	216	89	0	0	215	22	0
12.50667	12	30	24	223	204	174	223	216	89	0	0	215	22	0
12.50806	12	30	29	223	204	174	223	216	89	0	0	215	22	0
12.50944	12	30	34	223	204	174	223	216	89	0	0	214	22	0
12.51083	12	30	39	224	204	174	223	216	89	0	0	214	22	0
12.51222	12	30	44	224	204	174	223	216	89	0	0	214	22	0
12.51361	12	30	49	224	204	174	223	215	89	0	0	214	22	0
12.515	12	30	54	224	204	174	223	215	89	0	0	214	22	0
12.51639	12	30	59	224	204	174	223	215	89	0	0	214	22	0
12.51778	12	31	4	224	204	174	223	215	89	0	0	214	22	0
12.51917	12	31	9	224	204	174	223	215	89	0	0	214	22	0

Flow meter calibration data.

12.52056	12	31	14	224	204	174	223	215	89	0	0	214	22	0
12.52194	12	31	19	224	204	174	223	215	89	0	0	214	22	0
12.52333	12	31	24	224	204	174	223	215	89	0	0	214	22	0
12.52472	12	31	29	224	204	174	223	215	89	0	0	214	22	0
12.52611	12	31	34	224	204	174	223	215	89	0	0	214	22	0
12.5275	12	31	39	224	204	174	223	215	89	0	0	214	22	0
12.52889	12	31	44	224	204	174	223	215	89	0	0	214	22	1
12.53028	12	31	49	224	204	174	223	215	89	0	0	214	21	3
12.53167	12	31	54	224	204	174	223	215	89	0	0	214	21	5
12.53306	12	31	59	224	204	174	223	215	89	0	0	214	21	7
12.53444	12	32	4	224	204	174	223	215	89	0	0	214	20	9
12.53583	12	32	9	224	203	174	223	215	89	0	0	214	20	11
12.53694	12	32	13	224	203	173	223	215	89	0	0	214	20	13
12.53833	12	32	18	224	203	173	223	215	89	0	0	214	19	15
12.53972	12	32	23	224	203	173	223	215	89	0	0	214	19	17
12.54111	12	32	28	224	203	173	223	215	89	0	0	214	19	19
12.5425	12	32	33	224	203	173	223	215	89	0	0	215	19	22
12.54389	12	32	38	222	203	173	222	215	89	0	0	215	18	23
12.54528	12	32	43	222	203	173	222	215	89	0	0	215	18	26
12.54667	12	32	48	222	203	173	222	215	89	0	0	215	18	27
12.54806	12	32	53	222	203	173	222	215	89	0	0	215	18	26
12.54944	12	32	58	222	203	173	222	212	89	0	0	215	19	23
12.55083	12	33	3	222	203	173	222	212	89	0	0	215	19	19
12.55222	12	33	8	222	204	173	222	212	89	0	0	215	20	14
12.55361	12	33	13	222	204	174	222	212	89	0	0	215	20	11
12.555	12	33	18	222	204	174	222	215	89	0	0	215	20	6
12.55639	12	33	23	222	204	174	222	215	89	0	0	215	21	2
12.55778	12	33	28	222	204	174	222	215	89	0	0	215	21	1
12.55917	12	33	33	222	204	174	222	215	89	0	0	214	21	1
12.56056	12	33	38	223	204	174	224	215	89	0	0	214	22	1
12.56194	12	33	43	223	204	174	224	215	89	0	0	214	22	1
12.56333	12	33	48	223	204	174	224	215	89	0	0	214	22	1
12.56472	12	33	53	223	204	174	224	215	89	0	0	214	22	1
12.56611	12	33	58	223	204	174	224	215	89	0	0	214	22	1
12.5675	12	34	3	223	204	174	224	215	89	0	0	214	22	1
12.56889	12	34	8	223	203	174	224	215	89	0	0	214	22	1
12.57028	12	34	13	223	203	172	224	212	89	0	0	214	22	1
12.57167	12	34	18	223	203	172	224	215	89	0	0	214	21	1
12.57306	12	34	23	223	203	172	224	215	89	0	0	214	21	3
12.57444	12	34	28	223	203	172	224	215	89	0	0	214	21	5
12.57583	12	34	33	223	203	172	224	215	89	0	0	215	21	7
12.57722	12	34	38	223	203	172	224	215	89	0	0	215	20	9
12.57861	12	34	43	223	203	172	224	215	89	0	0	215	20	11
12.58	12	34	48	223	203	172	224	215	89	0	0	215	20	14
12.58139	12	34	53	223	203	172	224	215	89	0	0	215	19	15
12.58278	12	34	58	223	203	172	224	215	89	0	0	215	19	18
12.58417	12	35	3	223	203	172	224	215	89	0	0	215	19	20
12.58556	12	35	8	223	204	172	224	215	89	0	0	215	19	22
12.58694	12	35	13	223	204	174	224	215	89	0	0	215	18	24
12.58833	12	35	18	223	204	174	224	213	89	0	0	215	18	26
12.58972	12	35	23	223	204	174	224	213	89	0	0	215	18	26
12.59111	12	35	28	223	204	174	224	216	87	0	0	189	19	25
12.5925	12	35	33	250	204	174	252	71	72	0	0	74	19	22
12.59389	12	35	38	261	211	179	258	71	67	0	0	74	19	19
12.59528	12	35	43	267	225	187	265	62	64	0	0	67	20	15
12.59667	12	35	48	273	231	192	272	61	63	0	0	60	20	12
12.59806	12	35	53	273	236	198	277	64	61	0	0	60	20	9
12.59944	12	35	58	273	236	198	277	61	61	0	0	60	21	7
12.60083	12	36	3	273	243	198	277	60	60	0	0	60	21	3
12.60222	12	36	8	273	243	204	277	60	60	0	0	60	21	1
12.60361	12	36	13	273	249	204	277	63	60	0	0	60	21	1
12.605	12	36	18	273	249	204	277	60	60	0	0	60	21	1
12.60639	12	36	23	279	249	204	277	58	59	0	0	60	22	1
12.60806	12	36	29	279	254	209	277	57	59	0	0	54	22	1
12.60944	12	36	34	279	254	209	277	63	59	0	0	63	22	1
12.61083	12	36	39	279	254	209	277	57	59	0	0	57	22	1
12.61222	12	36	44	279	254	209	277	66	59	0	0	64	22	1
12.61361	12	36	49	279	254	209	277	63	59	0	0	64	22	1
12.615	12	36	54	279	254	209	283	63	59	0	0	64	22	1
12.61639	12	36	59	279	254	209	283	58	59	0	0	58	22	1
12.61778	12	37	4	279	254	209	283	62	59	0	0	58	22	1
12.61917	12	37	9	279	254	209	283	62	59	0	0	58	22	0
12.62056	12	37	14	279	254	209	283	63	59	0	0	65	22	0
12.62194	12	37	19	279	254	209	283	59	59	0	0	59	22	0
12.62333	12	37	24	280	254	209	283	59	59	0	0	59	22	0
12.62472	12	37	29	280	256	212	283	56	58	0	0	59	22	0
12.62611	12	37	34	280	256	212	283	56	58	0	0	59	22	0
12.6275	12	37	39	280	256	212	283	62	58	0	0	59	22	0
12.62889	12	37	44	280	256	212	283	65	58	0	0	63	22	0

Flow meter calibration data.

12.63028	12	37	49	280	256	212	283	62	58	0	0	58	22	0
12.63167	12	37	54	280	256	212	284	63	58	0	0	62	22	0
12.63306	12	37	59	280	256	212	284	59	58	0	0	62	22	0
12.63444	12	38	4	280	256	212	284	59	58	0	0	56	22	0
12.63583	12	38	9	280	256	212	284	63	58	0	0	63	22	0
12.63722	12	38	14	280	256	212	284	59	58	0	0	63	22	0
12.63861	12	38	19	280	256	212	284	64	58	0	0	63	22	0
12.64	12	38	24	279	256	212	284	64	58	0	0	63	21	3
12.64139	12	38	29	279	256	212	284	58	58	0	0	57	21	5
12.64278	12	38	34	279	256	212	284	59	58	0	0	57	21	7
12.64417	12	38	39	279	256	212	284	59	58	0	0	57	20	9
12.64556	12	38	44	279	256	212	284	59	58	0	0	57	20	12
12.64694	12	38	49	279	256	212	284	63	58	0	0	63	20	14
12.64833	12	38	54	279	256	212	282	58	58	0	0	57	19	17
12.64972	12	38	59	279	256	212	282	58	58	0	0	62	19	19
12.65111	12	39	4	279	256	212	282	58	58	0	0	62	19	22
12.6525	12	39	9	279	256	212	282	58	58	0	0	57	18	24
12.65389	12	39	14	279	256	212	282	58	58	0	0	57	18	26
12.65528	12	39	19	279	256	212	282	60	58	0	0	57	18	26
12.65667	12	39	24	280	256	212	282	60	58	0	0	57	18	26
12.65806	12	39	29	280	256	211	282	60	58	0	0	57	19	25
12.65944	12	39	34	280	255	211	282	60	57	0	0	57	19	22
12.66083	12	39	39	280	255	211	282	56	57	0	0	53	19	19
12.66222	12	39	44	280	255	211	282	59	57	0	0	59	20	15
12.66333	12	39	48	280	255	211	282	62	57	0	0	59	20	12
12.66472	12	39	53	280	255	211	281	67	57	0	0	67	21	8
12.66611	12	39	58	280	255	211	281	64	57	0	0	67	21	5
12.6675	12	40	3	280	255	211	281	56	57	0	0	60	21	1
12.66889	12	40	8	280	255	211	281	56	57	0	0	56	21	1
12.67028	12	40	13	280	255	211	281	60	57	0	0	62	22	1
12.67167	12	40	18	280	255	211	281	65	57	0	0	62	22	1
12.67306	12	40	23	280	255	211	281	61	57	0	0	62	22	1
12.67444	12	40	28	280	255	212	281	62	57	0	0	62	22	1
12.67611	12	40	34	280	256	212	281	61	58	0	0	62	22	1
12.6775	12	40	39	280	256	212	281	61	58	0	0	62	22	1
12.67889	12	40	44	280	256	212	281	64	58	0	0	62	22	1
12.68028	12	40	49	280	256	212	281	60	58	0	0	62	22	1
12.68167	12	40	54	280	256	212	281	63	58	0	0	62	22	1
12.68306	12	40	59	280	256	212	281	60	58	0	0	62	22	1
12.68444	12	41	4	280	256	212	281	67	58	0	0	62	22	1
12.68583	12	41	9	280	256	212	281	63	58	0	0	63	22	0
12.68722	12	41	14	280	256	212	281	58	58	0	0	63	22	0
12.68861	12	41	19	280	256	212	281	61	58	0	0	63	22	0
12.69	12	41	24	279	256	212	281	58	58	0	0	63	22	0
12.69139	12	41	29	279	256	214	281	63	58	0	0	63	22	0
12.69278	12	41	34	279	257	214	281	63	58	0	0	63	22	0
12.69417	12	41	39	279	257	214	281	64	58	0	0	63	21	0
12.69556	12	41	44	279	257	214	281	61	58	0	0	63	21	2
12.69694	12	41	49	279	257	214	281	61	58	0	0	63	21	6
12.69833	12	41	54	279	257	214	283	65	58	0	0	63	20	7
12.69944	12	41	58	279	257	214	283	60	58	0	0	63	20	10
12.70083	12	42	3	279	257	214	283	60	58	0	0	63	20	11
12.70222	12	42	8	279	257	214	283	60	58	0	0	63	19	15
12.70361	12	42	13	279	257	214	283	60	58	0	0	61	19	17
12.705	12	42	18	279	257	214	283	60	58	0	0	61	19	19
12.70639	12	42	23	279	257	214	283	58	58	0	0	61	18	22
12.70778	12	42	28	279	257	214	283	58	58	0	0	61	18	24
12.70917	12	42	33	279	256	214	283	54	57	0	0	55	18	27
12.71056	12	42	38	279	256	214	283	61	57	0	0	61	18	28
12.71194	12	42	43	279	256	214	283	63	57	0	0	61	18	26
12.71333	12	42	48	279	256	214	283	59	57	0	0	61	18	28
12.71472	12	42	53	279	256	214	280	58	57	0	0	61	18	29
12.71611	12	42	58	279	256	214	280	58	57	0	0	61	18	30
12.7175	12	43	3	279	256	214	280	61	57	0	0	61	18	30
12.71889	12	43	8	279	256	214	280	59	57	0	0	61	18	31
12.72028	12	43	13	279	256	214	280	63	57	0	0	61	18	32
12.72167	12	43	18	279	256	214	280	59	57	0	0	61	18	32
12.72306	12	43	23	279	256	214	280	62	57	0	0	61	18	32
12.72444	12	43	28	279	256	216	280	59	57	0	0	55	18	32
12.72583	12	43	33	279	256	216	280	59	57	0	0	55	18	32
12.72722	12	43	38	279	256	216	280	57	57	0	0	55	18	32
12.72861	12	43	43	279	256	216	280	56	57	0	0	62	18	32
12.73	12	43	48	279	256	216	280	61	57	0	0	60	18	32
12.73139	12	43	53	279	256	216	278	60	57	0	0	60	18	32
12.73278	12	43	58	279	256	216	284	65	57	0	0	65	18	28
12.73417	12	44	3	279	256	216	284	61	57	0	0	57	19	24
12.73556	12	44	8	279	256	216	284	60	57	0	0	57	19	20
12.73694	12	44	13	279	256	216	284	62	57	0	0	63	20	17
12.73833	12	44	18	279	256	216	284	64	57	0	0	63	20	12

Flow meter calibration data.

12.73972	12	44	23	280	256	216	284	57	57	0	0	57	20	10
12.74111	12	44	28	280	256	215	284	57	57	0	0	57	21	6
12.7425	12	44	33	280	258	215	284	60	57	0	0	57	21	3
12.74389	12	44	38	280	258	215	278	60	57	0	0	57	21	1
12.74528	12	44	43	280	258	215	278	60	57	0	0	63	21	1
12.74667	12	44	48	280	258	215	278	58	57	0	0	63	22	1
12.74806	12	44	53	280	258	215	278	62	57	0	0	61	22	1
12.74944	12	44	58	280	258	215	284	62	57	0	0	61	22	1
12.75083	12	45	3	280	258	215	284	56	57	0	0	54	22	1
12.75222	12	45	8	280	258	215	284	56	57	0	0	54	22	1
12.75361	12	45	13	280	258	215	284	63	57	0	0	63	22	1
12.755	12	45	18	280	258	215	284	62	57	0	0	63	22	1
12.75667	12	45	24	280	258	215	284	62	57	0	0	63	22	1
12.75806	12	45	29	280	257	215	284	59	58	0	0	57	22	1
12.75944	12	45	34	280	257	215	284	62	58	0	0	57	22	1
12.76083	12	45	39	280	257	215	284	59	58	0	0	57	22	1
12.76222	12	45	44	280	257	215	284	59	58	0	0	57	22	1
12.76361	12	45	49	280	257	215	284	67	58	0	0	66	22	1
12.765	12	45	54	280	257	215	284	64	58	0	0	66	22	1
12.76639	12	45	59	280	257	215	283	60	58	0	0	58	22	1
12.76778	12	46	4	280	257	215	283	60	58	0	0	58	22	1
12.76917	12	46	9	280	257	215	283	59	58	0	0	58	22	1
12.77056	12	46	14	280	257	215	283	59	58	0	0	58	22	1
12.77194	12	46	19	280	257	215	283	66	58	0	0	66	22	1
12.77333	12	46	24	281	257	215	283	66	58	0	0	66	22	1
12.77472	12	46	29	281	257	215	283	70	58	0	0	66	22	1
12.77611	12	46	34	281	257	215	283	66	58	0	0	66	22	1
12.7775	12	46	39	281	257	215	283	62	58	0	0	60	22	1
12.77889	12	46	44	281	257	215	283	65	58	0	0	60	22	1
12.78028	12	46	49	281	257	215	283	61	58	0	0	60	22	1
12.78167	12	46	54	281	257	215	283	64	58	0	0	60	22	1
12.78306	12	46	59	281	257	215	280	64	58	0	0	60	22	1
12.78444	12	47	4	281	257	215	280	60	58	0	0	60	22	1
12.78583	12	47	9	281	257	215	280	65	58	0	0	60	22	1
12.78722	12	47	14	281	257	215	280	62	58	0	0	60	22	1
12.78861	12	47	19	281	257	215	280	58	58	0	0	60	22	1
12.79	12	47	24	283	257	215	280	63	58	0	0	67	22	1
12.79139	12	47	29	283	257	216	280	61	58	0	0	61	22	1
12.79278	12	47	34	283	257	216	280	62	58	0	0	61	22	1
12.79417	12	47	39	283	257	216	280	62	58	0	0	61	22	1
12.79556	12	47	44	283	257	216	280	58	58	0	0	61	22	1
12.79694	12	47	49	283	257	216	280	62	58	0	0	61	22	1
12.79833	12	47	54	283	257	216	280	58	58	0	0	61	22	1
12.79972	12	47	59	283	257	216	280	58	58	0	0	61	22	1
12.80111	12	48	4	283	257	216	280	61	58	0	0	61	22	1
12.8025	12	48	9	283	257	216	280	66	58	0	0	68	22	1
12.80389	12	48	14	283	257	216	280	63	58	0	0	60	22	1
12.80528	12	48	19	283	257	216	280	59	58	0	0	60	22	1
12.80667	12	48	24	281	257	216	280	62	58	0	0	60	22	1
12.80806	12	48	29	281	257	215	280	61	58	0	0	60	22	1
12.80945	12	48	33	281	257	215	280	59	58	0	0	59	22	1
12.81084	12	48	38	281	257	35	280	63	58	0	0	59	22	1
12.81223	12	48	43	281	257	3	280	60	58	0	0	59	22	1
12.81362	12	48	48	281	257	3	280	63	58	0	0	59	22	1
12.81501	12	48	53	281	257	3	280	57	58	0	0	59	22	1
12.81640	12	48	58	281	257	40	281	64	58	0	0	59	22	1
12.81779	12	49	3	281	257	17	281	60	58	0	0	65	22	1
12.81918	12	49	8	281	257	214	281	64	58	0	0	65	22	1
12.82057	12	49	13	281	257	214	281	64	58	0	0	65	22	1
12.82196	12	49	18	281	257	214	281	61	58	0	0	59	22	1
12.82335	12	49	23	280	257	214	281	58	58	0	0	59	22	1
12.82474	12	49	28	280	257	214	281	61	58	0	0	59	22	1
12.82613	12	49	33	280	259	214	281	61	58	0	0	59	22	1
12.82752	12	49	38	280	259	214	281	61	58	0	0	59	22	1
12.82891	12	49	43	280	259	214	281	61	58	0	0	57	22	1
12.83	12	49	48	280	259	214	281	60	58	0	0	60	22	1
12.83139	12	49	53	280	259	214	281	55	58	0	0	54	22	1
12.83278	12	49	58	280	259	214	280	58	58	0	0	60	22	1
12.83417	12	50	3	280	259	214	280	61	58	0	0	61	22	1
12.83556	12	50	8	280	259	213	280	61	58	0	0	61	22	1
12.83694	12	50	13	280	259	213	280	65	58	0	0	66	22	1
12.83833	12	50	18	280	259	213	280	62	58	0	0	58	22	1
12.83972	12	50	23	280	259	213	280	58	58	0	0	58	22	1
12.84111	12	50	28	280	259	213	280	69	58	0	0	63	22	1
12.8425	12	50	33	260	257	213	261	111	73	0	0	115	22	1
12.84389	12	50	38	234	234	196	233	119	88	0	0	122	22	1

Panel Temperature Data During Freezing

CRTF NET-80 99 POINT DATA FILE																														
TEST DATE	Time	Time	Time	1994 10.27 11 am	FT720	PF-001	PF-002	FT730	FT800	TEE16	TEE15	TEE14	TEE13	TEE12	TEE11	TEE10	TEE9	TEE8	TEE7	TEE6	TEE5	TEE4	TEE3	TEE2	TEE1	TEEH17	TEELH18	TEELH19		
Time	hour	min	sec		GPM	LV/min	LV/min	GPM	GPM	DEG F	DEG F	DEG F	DEG F	DEG F	DEG F	DEG F	DEG F	DEG F	DEG F	DEG F	DEG F	DEG F	DEG F	DEG F	DEG F	DEG F	DEG F	DEG F		
12	0	0	4		369	385	289	72	180	590	592	592	591	598	601	590	591	595	592	591	582	591	584	591	591	590	593	591	589	583
12	0	19			374	412	290	85	156	594	592	592	591	599	608	592	592	597	593	591	584	591	591	591	590	594	593	591	584	584
12	0	34			360	412	297	265	158	594	593	593	593	600	608	592	593	598	594	592	585	591	591	590	594	593	591	584	584	
12	0	49			331	341	282	321	196	594	593	596	593	600	608	592	597	598	594	591	584	591	591	590	593	594	592	584	584	
12	1	1			367	355	277	81	183	594	596	602	590	597	608	589	605	595	592	590	582	589	590	588	592	594	592	584	584	
12	1	1			390	336	279	81	154	592	594	597	590	599	608	589	602	595	592	590	582	589	590	588	592	594	592	584	584	
12	1	1			393	380	411	299	117	592	591	594	591	600	612	590	597	597	593	591	584	590	590	589	593	594	592	584	584	
12	1	1			380	346	285	141	144	592	593	594	593	601	622	591	593	598	593	591	584	591	591	590	594	592	584	584	584	
12	2	2			370	346	297	161	18	592	597	597	593	600	624	591	595	598	594	591	584	591	592	590	595	594	592	584	584	
12	2	2			376	354	299	5	2	594	595	596	594	598	614	593	595	597	594	591	580	591	591	590	594	592	584	584	584	
12	2	2			382	344	293	5	2	594	594	594	594	593	610	593	592	593	593	592	572	591	589	590	593	595	593	584	584	
12	2	2			376	354	299	5	2	594	591	589	589	583	605	590	591	590	590	590	566	589	586	588	590	595	593	586	586	
12	2	2			382	344	293	5	2	594	591	589	589	583	602	588	587	584	589	588	560	585	582	584	588	595	593	586	586	
12	2	3			382	369	286	5	2	594	591	589	589	583	607	584	585	580	587	584	554	583	580	581	585	595	593	586	586	
12	2	3			382	333	275	5	0	587	589	586	586	579	597	584	585	580	587	584	554	583	580	581	585	595	593	586	586	
12	2	3			388	363	302	6	0	587	588	583	582	574	593	581	582	571	580	578	542	577	572	575	579	585	593	585	585	
12	2	3			388	393	285	0	0	587	586	579	580	569	590	590	577	579	571	580	578	542	577	572	575	579	585	593	585	585
12	2	4			388	386	296	0	0	587	585	576	576	565	586	575	577	566	578	574	537	573	569	572	576	593	585	585	585	
12	2	4			388	353	306	0	0	581	583	572	573	561	582	572	573	562	574	571	532	571	566	568	573	594	593	585	585	
12	2	4			387	306	301	1	0	581	580	568	569	556	579	569	569	557	572	568	526	567	563	566	571	594	593	585	585	
12	2	4			387	310	275	29	132	581	580	566	567	553	576	565	566	562	569	565	521	565	559	564	566	594	593	584	584	
12	2	5			387	389	313	106	104	581	581	571	563	549	575	564	566	550	567	564	524	565	559	567	561	594	592	584	584	
12	2	5			382	382	307	158	127	569	572	571	569	560	569	568	567	564	570	569	557	567	568	568	569	590	587	583	583	
12	2	5			376	382	293	176	136	569	565	564	567	560	565	569	561	565	565	571	554	570	565	570	566	583	582	579	579	
12	2	5			376	320	287	176	145	569	561	561	576	568	564	577	561	574	572	578	557	578	568	577	571	578	578	575	575	
12	2	6			376	336	305	163	148	580	566	568	581	572	568	582	568	578	578	583	563	582	574	582	576	577	577	575	575	
12	2	6			376	360	299	157	161	580	570	572	584	575	563	584	574	581	585	568	584	579	585	581	577	577	578	578	578	
12	2	6			378	360	289	150	151	580	573	573	585	578	560	585	575	583	582	587	571	585	581	586	582	579	577	578	578	
12	2	6			378	285	286	150	154	580	583	583	586	578	562	585	580	583	584	587	572	585	581	586	584	580	578	579	579	
12	2	6			378	288	288	160	154	580	585	585	586	579	566	587	584	584	584	588	573	585	582	586	584	583	580	580	580	
12	2	7			378	269	303	160	154	586	585	585	586	579	574	587	584	584	585	588	573	587	582	587	585	584	582	581	581	
12	2	7			378	297	308	160	154	586	585	585	587	579	576	587	585	584	585	588	573	587	582	587	585	585	582	581	581	
12	2	7			376	289	308	160	154	586	585	585	587	579	578	587	585	584	585	588	573	587	582	587	585	585	582	583	583	
12	2	7			376	291	308	160	156	587	586	587	587	580	578	587	585	585	585	588	574	587	584	587	585	586	584	583	583	
12	2	8			376	344	283	160	156	587	586	587	587	588	580	578	588	585	585	586	589	574	587	584	588	586	584	584	584	
12	2	8			377	314	296	159	156	587	587	587	588	580	580	588	585	585	586	589	574	587	584	588	586	586	584	584	584	
12	2	8			377	347	295	159	156	587	587	587	588	580	580	588	585	585	586	589	574	587	584	588	586	587	585	584	584	
12	2	9			377	336	297	158	156	587	587	587	588	580	580	588	585	585	586	589	574	587	584	588	586	587	585	584	584	
12	2	9			377	376	304	164	153	588	587	587	588	580	580	588	585	585	586	589	574	587	584	588	586	587	585	584	584	
12	2	9			375	350	304	164	166	588	587	587	588	580	580	588	585	585	586	589	574	587	584	588	586	587	585	584	584	
12	2	9			375	342	288	158	166	588	587	587	588	580	579	588	586	585	586	589	574	587	584	588	586	587	585	584	584	
12	2	10			375	295	277	164	156	588	587	587	588	580	579	588	586	585	586	589	574	587	584	588	586	587	585	584	584	
12	2	10			375	305	294	158	166	588	587	587	588	580	578	588	586	585	586	589	573	587	584	588	586	587	585	584	584	
12	2	10			375	298	303	164	156	588	587	587	588	580	578	588	586	585	586	589	573	587	584	588	586	587	585	584	584	
12	2	10			375	293	302	164	166	588	587	587	588	580	578	588	586	585	586	589	573	587	584	588	586	587	585	583	583	
12	2	11			375	321	282	158	152	588	587	587	588	580	579	588	586	585	586	589	573	587	584	588	586	587	585	582	582	
12	2	11			375	318	301	159	156	587	587	587	588	580	579	588	586	585	586	589	574	587	584	588	586	587	585	583	583	
12	2	11			377	374	278	159	156	587	586	587	588	580	579	588	586	585	586	589	574	587	584	588	586	587	585	583	583	
12	2	11			377	336	307	130	74	587	586	587	588	579	575	588	586	584	586	589	568	587	582	588	586	587	585	583	583	
12	2	12			377	318	301	29	1	587	585	585	587	576	574	587	585	583	584	587	562	586	580	588	586	587	585	584	584	
12	2	12			55	305	4	90	1	584	583	582	586	573	574	586	582	579	582											

Panel Temperature Data During Freezing

Time hour	Time min	Time sec	FT720 GPM	PF-001 L/min	PF-002 L/min	FT730 GPM	FT800 GPM	TEE16 DEG F	TEE15 DEG F	TEE14 DEG F	TEE13 DEG F	TEE12 DEG F	TEE11 DEG F	TEE10 DEG F	TEE9 DEG F	TEE8 DEG F	TEE7 DEG F	TEE6 DEG F	TEES DEG F	TEE4 DEG F	TEE3 DEG F	TEE2 DEG F	TEE1 DEG F	TEEH17 DEG F	TEEH18 DEG F	TEEH19 DEG F
12	17	34	0	-4	0	1	0	560	556	546	553	537	543	547	538	534	536	548	503	539	535	533	549	567	562	556
12	17	48	0	-4	0	2	0	560	555	544	551	536	541	545	536	532	533	546	501	537	532	532	546	566	560	555
12	18	3	0	-4	0	7	0	560	553	542	550	535	539	544	534	531	532	544	499	536	530	530	545	565	559	554
12	18	18	0	-4	0	0	0	556	552	540	549	534	537	541	532	529	530	543	497	535	528	528	544	563	558	552
12	18	33	0	-4	0	2	0	556	551	538	546	533	536	539	529	528	527	541	496	532	525	526	543	561	556	552
12	18	48	0	-5	0	1	0	556	551	535	544	530	533	537	528	525	525	541	495	531	523	525	543	560	555	549
12	19	3	0	112	0	1	0	556	550	534	543	529	531	534	526	524	524	540	492	529	519	523	541	558	554	548
12	19	18	0	112	0	6	0	551	549	534	542	527	530	532	523	522	522	538	490	527	517	520	540	556	552	548
12	19	33	0	102	0	1	0	551	548	534	540	525	528	530	522	521	521	538	489	525	515	518	539	555	550	547
12	19	48	0	-3	0	0	0	551	547	533	540	523	526	528	520	518	518	538	485	524	511	517	538	554	549	546
12	20	3	0	28	0	2	0	551	546	532	540	523	525	526	519	517	517	536	485	523	509	516	537	553	548	543
12	20	18	0	85	0	2	0	545	544	531	539	521	524	525	518	516	515	535	484	520	506	513	534	552	546	542
12	20	33	0	67	0	2	0	545	543	531	539	521	523	524	515	515	514	535	481	519	504	511	533	551	544	541
12	20	48	0	60	0	6	0	545	542	531	538	520	521	524	514	514	512	533	481	517	501	510	532	549	542	540
12	21	3	0	70	0	1	0	545	541	530	537	519	520	523	514	512	510	532	480	516	499	508	530	548	541	537
12	21	18	0	70	0	7	0	540	539	529	536	517	520	521	513	511	509	531	480	513	497	506	529	547	539	536
12	21	34	0	75	0	7	0	540	538	527	533	516	519	520	512	510	508	529	479	512	494	505	526	546	538	535
12	21	49	0	82	0	0	0	540	537	526	532	515	518	519	510	510	507	527	478	511	493	502	525	545	535	533
12	22	4	0	54	0	5	0	540	536	525	531	514	517	519	510	508	505	526	476	509	491	501	524	543	534	532
12	22	19	0	54	0	5	0	536	533	524	530	513	516	517	509	507	504	523	475	509	489	500	521	542	533	530
12	22	34	0	-2	0	5	0	536	532	523	529	511	515	516	508	505	503	521	474	506	487	499	520	540	532	528
12	22	49	0	47	0	5	0	536	531	522	528	510	514	515	507	504	502	520	473	505	486	496	519	539	531	526
12	23	4	0	47	0	4	0	536	530	519	526	509	513	513	506	503	501	519	472	504	483	495	518	539	529	524
12	23	19	0	48	0	0	0	532	530	518	525	508	512	512	504	502	499	516	470	503	482	493	516	536	528	523
12	23	34	0	37	0	1	0	531	528	517	524	507	511	511	503	501	499	514	469	501	481	492	515	535	526	522
12	23	49	0	-3	0	1	0	531	527	514	522	505	510	510	502	499	496	514	468	500	480	491	514	533	525	521
12	24	4	0	33	0	2	0	531	525	513	519	503	507	507	500	497	495	512	467	499	477	488	513	531	523	520
12	24	19	0	41	0	1	0	531	523	512	518	502	506	506	499	496	494	510	465	497	476	487	510	530	522	519
12	24	34	0	-4	0	1	0	524	521	511	517	501	505	505	497	495	493	508	465	495	475	486	510	529	521	518
12	24	49	0	-4	0	1	0	524	520	510	516	500	504	504	496	494	491	508	462	494	474	484	509	528	520	517
12	25	3	0	-4	0	1	0	524	519	507	513	499	502	502	495	493	490	506	462	493	473	482	508	525	519	514
12	25	18	0	-4	0	7	0	524	517	507	513	497	501	500	494	491	489	505	461	492	471	481	507	524	517	514
12	25	33	0	-5	0	8	0	518	515	506	513	496	500	499	493	489	488	503	458	491	470	480	505	523	515	512
12	25	48	0	-5	0	2	0	518	514	505	511	495	499	499	491	489	487	502	458	489	469	478	504	522	514	511
12	26	3	0	-5	0	2	0	518	514	504	510	494	498	496	490	488	485	501	457	488	469	476	503	521	513	510
12	26	18	0	-5	0	0	0	518	513	502	509	493	497	495	489	487	484	500	456	487	468	475	501	519	512	509
12	26	33	0	-5	0	1	0	514	512	501	508	490	495	494	488	485	483	499	455	466	466	474	501	518	509	506
12	26	48	0	-5	0	1	0	514	511	500	507	489	494	493	487	484	482	497	453	485	465	473	498	517	508	505
12	27	3	0	-5	0	2	0	514	509	499	505	488	493	492	485	483	481	495	453	483	464	472	497	516	507	504
12	27	18	0	-5	0	8	0	514	508	497	504	487	492	490	484	482	479	495	451	482	463	471	496	514	506	503
12	27	33	0	-5	0	8	0	509	507	496	503	485	491	489	483	481	478	494	451	481	462	469	495	513	504	501
12	27	48	0	49	0	2	0	509	506	494	502	484	489	488	482	479	477	493	450	480	460	468	493	512	503	500
12	28	3	0	44	0	2	0	509	505	493	501	484	488	487	481	478	476	491	449	477	459	467	492	511	502	499
12	28	19	0	37	0	2	0	509	502	492	498	483	487	485	479	477	475	488	448	476	458	466	491	510	500	498
12	28	34	0	37	0	0	0	504	501	491	497	481	486	484	478	476	473	487	445	475	458	465	490	508	500	497
12	28	49	0	42	0	7	0	504	500	490	496	479	485	483	477	475	472	487	445	474	457	464	489	507	497	497
12	29	4	0	21	0	1	0	504	499	488	496	478	483	481	476	473	471	485	445	473	457	463	489	506	496	495
12	29	19	0	43	0	7	0	504	498	486	495	478	482	480	475	472	470	484	445	473	457	463	489	506	496	495
12	29	34	0	37	0	7	0	499	497	485	494	476	481	479	472	470	469	483	444	470	455	461	486	504	495	494
12	29	49	0	-4	0	2	0	499	495	484	492	475	479	478	472	470	469	482	444	469	455	460	484	502	492	492
12	30	5	0	-4	0	1	0	499	493	482	491	474	477	477	471	469	468	481	443	468	455	459	484	501	492	492
12	30	18	0	-4	0	1	0	499	493	482	491	473	476	475	470	468	466	480	443	467	454	459	483	500	490	491
12	30	33	0	-4	0	7	0	495	491	481	490	472	474	475	469	466	465	479	442	465	454	458	481	499	489	489
12	30	48	0	-4	0	2	0	495	489	480	489	470	473	474	467	466	465	478	441	464	454	458	480	498	489	488
12	31	3	0	-4	0	2	0	495	489	480	489	470	470	473	467	464	464	476	440	464	454	458	479	497	488	487
12	31	18	0	-4	0	7	0	495	488	479	488	468	469	472	466	463	464	476	437	463	454	458	478	495	487	487
12	31	34	0	35	0	6	0	492	486	478	486	467	467	472	465	462	463	475	436	462	454	457	478	494	485	486
12	31	49	0	-4	0	0	0	492	485	476	485	466	466	471	465	461										

Panel Temperature Data During Freezing

Time hour	Time min	Time sec	FT20 GPM	PF-001 Lv/min	PF-002 Lv/min	FT730 GPM	FT800 GPM	TEE16 DEG F	TEE15 DEG F	TEE14 DEG F	TEE13 DEG F	TEE12 DEG F	TEE11 DEG F	TEE10 DEG F	TEE9 DEG F	TEE8 DEG F	TEE7 DEG F	TEE6 DEG F	TEE5 DEG F	TEE4 DEG F	TEE3 DEG F	TEE2 DEG F	TEE1 DEG F	TEEUH17 DEG F	TEELH18 DEG F	TEELH19 DEG F
12	35	33	0	-5	0	6	0	474	469	457	469	447	452	460	453	448	457	462	415	454	444	449	462	486	473	477
12	35	48	0	-5	0	5	0	474	468	457	467	446	452	460	452	447	457	460	414	454	444	448	462	486	473	477
12	36	3	0	-5	0	1	0	469	467	456	466	445	451	459	452	445	457	459	413	453	443	446	462	485	472	477
12	36	18	0	-5	0	0	0	469	466	456	465	444	451	459	451	444	456	459	413	452	442	446	460	485	472	477
12	36	33	0	-5	0	6	0	469	465	455	464	443	450	459	450	443	454	459	411	452	441	445	459	485	472	476
12	36	48	0	-5	0	1	0	469	463	455	463	441	449	459	450	443	454	458	409	451	441	445	458	485	472	476
12	37	3	0	-5	0	1	0	464	462	454	463	440	449	459	449	442	453	458	408	450	439	444	458	485	472	476
12	37	18	0	-5	0	0	0	464	460	453	461	439	448	459	448	441	452	457	403	449	439	444	457	485	472	476
12	37	33	0	-5	0	1	0	464	459	451	460	438	448	457	448	439	451	457	404	449	438	443	456	485	472	475
12	37	48	0	-5	0	7	0	464	458	451	459	438	446	457	446	438	451	457	403	447	437	443	456	485	472	475
12	38	4	0	-5	0	7	0	457	457	450	459	437	445	456	445	438	450	456	402	447	437	442	456	486	472	475
12	38	19	0	-5	0	7	0	457	455	450	458	435	445	455	445	437	449	455	401	446	436	440	456	486	472	475
12	38	34	0	-5	0	1	0	457	455	448	458	434	444	454	444	436	449	454	401	445	436	440	455	486	472	476
12	38	49	0	-5	0	2	0	457	454	448	457	434	444	453	444	436	448	452	399	445	435	440	455	487	472	476
12	39	4	0	-5	0	2	0	453	454	447	455	433	443	453	443	435	447	451	397	444	435	439	455	487	473	476
12	39	19	0	-5	0	2	0	453	453	446	454	433	443	452	443	435	447	451	397	444	434	439	455	488	473	476
12	39	34	0	-5	0	2	0	453	453	446	453	432	443	452	442	434	445	449	395	444	434	438	455	488	473	476
12	39	49	0	-5	0	2	0	453	453	445	453	432	442	450	442	434	445	449	395	443	433	438	455	489	473	476
12	40	3	0	-5	0	2	0	452	452	445	452	431	442	450	440	432	444	449	394	442	432	437	455	489	473	476
12	40	18	0	-5	0	2	0	452	452	444	451	431	440	449	440	432	444	448	393	442	432	436	455	490	473	476
12	40	33	0	-5	0	0	0	452	452	444	450	429	440	449	440	431	444	448	392	442	430	436	455	490	473	476
12	40	48	0	-5	0	0	0	452	450	444	450	429	440	448	439	431	443	447	389	440	430	436	455	492	473	475
12	41	3	0	-5	0	7	0	452	450	442	450	428	439	448	439	430	443	445	387	440	429	435	455	492	473	475
12	41	18	0	-5	0	2	0	450	449	441	449	428	439	446	438	430	443	445	386	439	429	435	455	493	473	475
12	41	33	0	-5	0	7	0	450	448	441	448	427	438	446	438	429	442	444	385	439	429	435	454	493	473	475
12	41	48	0	-5	0	7	0	450	448	440	448	426	438	445	437	429	442	444	384	438	428	433	454	494	473	475
12	42	3	0	-5	0	1	0	450	447	440	446	426	437	445	437	428	441	443	382	438	427	433	454	494	474	475
12	42	18	0	-5	0	7	0	445	447	439	446	425	437	444	435	426	441	443	380	438	427	432	453	495	474	475
12	42	33	0	38	0	0	0	445	445	439	445	425	436	443	435	426	439	442	379	437	425	432	453	495	474	475
12	42	49	0	37	0	1	0	445	445	438	444	424	436	443	434	425	439	442	377	437	424	431	453	496	474	476
12	43	4	0	37	0	8	0	445	445	438	444	424	435	442	434	425	438	441	375	436	424	431	453	496	474	476
12	43	19	0	53	0	2	0	442	445	436	443	422	435	442	433	424	438	440	373	436	423	431	453	496	474	476
12	43	34	0	59	0	0	0	442	445	436	443	422	435	440	433	424	437	440	371	434	423	430	453	498	474	476
12	43	49	0	64	0	2	0	442	445	436	443	421	433	440	433	423	437	440	369	434	423	430	453	498	474	476
12	44	4	0	64	0	2	0	442	445	435	442	421	433	440	432	422	437	439	367	434	422	430	451	499	475	476
12	44	19	0	71	0	2	0	440	445	435	442	420	433	439	432	422	437	439	366	433	422	429	451	499	475	476
12	44	34	0	71	0	7	0	440	444	434	441	420	432	439	432	421	436	439	363	433	421	429	451	500	475	476
12	44	49	0	64	0	7	0	440	444	434	441	419	432	439	431	421	436	437	361	433	421	427	451	500	475	477
12	45	4	0	64	0	6	0	440	444	434	439	419	432	438	431	419	436	437	359	432	420	427	450	500	475	477
12	45	18	0	38	0	2	0	438	444	433	439	417	431	438	431	418	435	436	357	432	420	427	450	501	475	477
12	45	33	0	4	0	6	0	438	443	433	438	416	431	437	429	418	435	436	356	432	418	426	450	501	475	477
12	45	48	0	4	0	0	0	438	443	432	438	416	431	437	429	417	435	435	353	431	417	426	449	502	475	477
12	46	3	0	4	0	1	0	438	442	432	438	415	430	437	428	416	434	435	352	431	417	426	448	502	475	477
12	46	18	0	4	0	1	0	436	442	430	437	414	430	436	428	415	434	435	349	430	416	425	448	502	476	477
12	46	33	0	-5	0	0	0	436	442	430	437	414	429	436	427	415	433	434	347	430	416	425	447	504	476	477
12	46	48	0	-5	0	1	0	436	440	429	436	413	429	435	427	413	433	434	346	430	415	424	445	504	476	477
12	47	3	0	-5	0	1	0	436	440	429	436	411	427	435	427	411	431	433	343	428	414	424	445	504	476	477
12	47	18	0	-5	0	1	0	433	440	429	435	410	427	434	426	410	431	433	341	428	412	423	444	504	476	477
12	47	33	0	-5	0	0	0	433	439	428	435	409	426	434	425	409	431	432	338	427	411	423	443	504	476	477
12	47	48	0	-5	0	7	0	433	439	428	433	406	426	432	425	408	430	432	336	427	411	421	443	506	476	478
12	48	4	0	-5	0	1	0	433	439	427	433	407	425	432	424	407	430	432	334	426	410	421	442	506	476	478
12	48	19	0	-5	0	1	0	431	439	426	433	405	425	432	424	406	429	430	332	426	409	420	442	507	477	478
12	48	34	0	-5	0	1	0	431	438	426	432	405	424	431	423	404	429	430	331	425	407	420	441	507	477	478
12	48	49	0	-5	0	0	0	431	438	426	432	404	424	431	423	403	429	429	327	425	407	419	441	507	477	478
12	49	4	0	-5	0	2	0	431	438	425	432	403	423	430	421	402	428	429	326	424	406	419	441	508	477	478
12	49	19	0	-5	0	1	0	430	438	425	431	402	423	430	421	401	428	429	325	424	405	418	439	508	478	478
12	49	34	0	-5	0	0	0	430	437	424	431	401	421	430	420	400	427	427	324	422	404	417	439	508	478	478
12	49	49	0	-5	0	6	0	430	437	422	430	400	421	429	419	398	427	427								

Panel Temperature Data During Freezing

Time hour	Time min	Time sec	FT720 GPM	PF-001 L/min	PF-002 L/min	FT730 GPM	FT800 GPM	TEE16 DEG F	TEE15 DEG F	TEE14 DEG F	TEE13 DEG F	TEE12 DEG F	TEE11 DEG F	TEE10 DEG F	TEE9 DEG F	TEE8 DEG F	TEE7 DEG F	TEE6 DEG F	TEE5 DEG F	TEE4 DEG F	TEE3 DEG F	TEE2 DEG F	TEE1 DEG F	TEEH17 DEG F	TEEH18 DEG F	TEEH19 DEG F
12	53	34	0	-2	0	2	0	420	428	411	421	379	409	421	408	373	417	417	299	408	383	403	431	513	479	480
12	53	49	0	-2	0	0	0	417	428	409	421	377	408	420	405	372	417	415	295	407	382	401	431	514	479	480
12	54	4	0	-5	0	0	0	417	427	408	420	376	406	420	404	371	416	414	295	406	379	400	430	514	479	480
12	54	19	0	-5	0	1	0	417	427	407	420	374	406	419	402	369	416	414	295	405	378	399	430	514	479	480
12	54	34	0	-5	0	6	0	417	426	406	418	372	405	417	401	367	415	413	292	403	377	398	430	515	479	480
12	54	49	0	-5	0	6	0	414	426	406	418	371	404	417	400	366	413	412	292	402	376	396	429	515	479	480
12	55	4	0	31	0	2	0	414	425	405	417	369	403	416	399	364	413	411	291	401	373	395	429	515	479	480
12	55	19	0	38	0	2	0	414	423	404	416	368	402	415	398	362	412	409	290	400	372	394	428	515	479	480
12	55	33	0	-2	0	1	0	414	422	402	415	366	400	415	396	361	411	409	287	399	369	393	427	516	479	480
12	55	48	0	-2	0	6	0	408	422	401	415	364	399	414	394	360	410	408	286	397	368	392	427	516	479	480
12	56	3	0	-2	0	1	0	408	421	400	414	363	398	413	393	357	408	407	284	395	367	390	426	516	479	480
12	56	18	0	-2	0	1	0	408	421	398	412	361	395	412	391	356	408	406	283	394	365	389	425	516	479	480
12	56	33	0	-5	0	1	0	408	420	396	412	359	394	410	390	355	407	404	281	393	364	389	425	517	479	480
12	56	48	0	-5	0	1	0	403	419	395	411	358	393	409	389	354	406	403	280	391	362	388	424	517	480	481
12	57	3	0	-5	0	2	0	403	417	394	410	357	392	409	386	351	405	402	280	389	361	387	424	517	480	481
12	57	18	0	-5	0	2	0	403	417	393	409	355	391	408	385	351	403	401	278	388	360	385	423	517	480	481
12	57	33	0	-5	0	1	0	403	416	391	407	354	390	407	384	349	403	400	275	386	359	384	422	518	480	481
12	57	48	0	-5	0	2	0	399	416	389	407	353	388	407	383	348	402	398	275	385	357	383	422	518	480	482
12	58	3	0	-5	0	7	0	398	415	388	406	352	387	405	382	347	400	397	275	383	356	382	421	518	480	482
12	58	19	0	-5	0	1	0	398	414	387	405	350	386	404	379	346	399	396	272	382	355	382	419	518	480	482
12	58	34	0	-5	0	1	0	398	414	385	404	348	385	403	378	344	398	395	271	380	354	381	419	519	480	482
12	58	49	0	-5	0	6	0	393	412	383	403	347	384	402	377	343	397	393	270	379	351	379	418	519	480	482
12	59	4	0	-5	0	0	0	393	412	382	401	346	382	401	375	342	395	392	270	377	350	378	418	519	480	482
12	59	19	0	-5	0	7	0	393	411	380	400	344	381	399	373	341	393	390	269	375	349	378	417	520	480	482
12	59	34	0	-5	0	1	0	393	410	379	399	343	380	398	372	339	392	389	268	374	348	377	416	520	480	482
12	59	49	0	-5	0	1	0	386	409	377	398	342	379	397	371	338	390	387	265	373	346	376	416	520	481	483
13	0	4	0	-5	0	6	0	386	408	376	396	341	377	395	368	337	389	385	265	371	345	376	414	520	481	483
13	0	19	0	-5	0	5	0	386	406	374	395	340	376	394	367	336	388	384	263	369	344	375	413	521	481	483
13	0	34	0	-5	0	5	0	386	405	373	394	338	374	392	366	335	386	382	263	368	343	373	413	521	481	483
13	0	49	0	-5	0	5	0	379	404	371	392	337	373	391	365	334	386	382	262	367	342	372	412	521	481	483
13	1	4	0	-5	0	3	0	379	402	369	391	335	372	390	363	332	383	379	261	364	340	372	411	521	481	483
13	1	19	0	-5	0	3	0	379	401	368	389	334	370	387	362	331	382	378	260	363	339	371	410	521	481	483
13	1	34	0	-5	0	3	0	379	400	367	388	333	369	386	360	330	381	377	260	362	338	370	410	521	481	483
13	1	49	0	-5	0	3	0	373	399	366	387	331	368	385	359	329	379	375	256	361	337	370	408	521	481	483
13	2	4	0	-5	0	7	0	373	397	365	386	331	367	384	357	329	378	374	253	360	336	368	407	521	481	483
13	2	19	0	-5	0	0	0	373	396	363	385	330	367	383	356	328	377	373	254	358	335	368	406	522	481	483
13	2	33	0	-5	0	6	0	373	395	362	383	329	366	382	355	326	376	372	253	357	333	367	405	522	481	483
13	2	48	0	-5	0	2	0	368	393	361	382	328	364	380	354	325	375	369	252	356	332	366	404	522	481	484
13	3	3	0	-5	0	2	0	368	392	360	381	326	363	378	352	324	373	368	252	355	331	366	404	522	481	484
13	3	18	0	-5	0	7	0	368	391	358	380	325	362	377	351	323	372	367	252	354	330	375	402	523	481	484
13	3	33	0	-5	0	1	0	368	390	357	378	324	361	375	350	321	371	366	251	352	328	365	401	523	481	484
13	3	48	0	-5	0	1	0	363	389	356	377	323	360	374	349	321	370	364	250	351	327	364	400	523	482	485
13	4	3	0	-5	0	7	0	363	387	354	375	321	358	373	348	320	369	363	248	350	326	362	399	523	482	485
13	4	18	0	-5	0	1	0	363	385	352	373	320	357	372	346	319	367	362	248	347	326	362	397	524	482	485
13	4	33	0	-5	0	1	0	363	384	351	372	319	356	371	345	318	366	361	246	346	325	361	396	524	482	485
13	4	48	0	-5	0	6	0	357	382	350	371	318	355	368	344	317	365	360	245	345	322	361	394	524	482	485
13	5	3	0	-5	0	2	0	356	382	348	369	318	354	368	343	316	364	357	245	344	322	360	393	525	482	485
13	5	18	0	-5	0	0	0	356	379	347	368	316	353	366	341	314	363	356	243	343	321	359	391	525	482	485
13	5	33	0	-5	0	2	0	356	378	346	368	315	352	365	340	313	362	355	240	342	320	358	390	525	482	485
13	5	48	0	-5	0	0	0	356	377	344	367	314	351	363	339	312	360	353	240	341	318	358	389	525	482	485
13	6	3	0	-5	0	1	0	350	375	343	366	313	349	361	338	311	358	352	237	339	317	357	388	526	482	485
13	6	18	0	-5	0	1	0	350	375	342	364	313	348	360	337	311	357	351	236	338	316	357	387	526	482	485
13	6	34	0	-5	0	2	0	350	375	342	363	312	347	359	335	310	357	350	235	337	316	355	386	526	482	485
13	6	49	0	-5	0	1	0	350	373	341	362	310	347	358	334	308	356	349	233	336	315	355	384	526	482	485
13	7	4	0	-5	0	1	0	347	372	340	361	309	346	357	333	307	355	347	233	335	314	354	382	526	482	485
13	7	19	0	-5	0	0	0	347	371	338	359	309	345	355	332	307	354	346	233	333	312	354	381	526	482	485
13	7	34	0	-5	0	0	0	347	371	337	358	308	343	354	330	306	352	345	233	332	311	353	379	526	482	485
13	7	49	0	-5	0	2	0	347	370	336	357	307	343	353	329	305	351	344	233	332	310	353	378	52		

Panel Temperature Data During Freezing

Time hour	Time min	Time sec	FT720 GPM	PF-001 LV/min	PF-002 LV/min	FT730 GPM	FT800 GPM	TEE16 DEG F	TEE15 DEG F	TEE14 DEG F	TEE13 DEG F	TEE12 DEG F	TEE11 DEG F	TEE10 DEG F	TEE9 DEG F	TEE8 DEG F	TEE7 DEG F	TEE6 DEG F	TEE5 DEG F	TEE4 DEG F	TEE3 DEG F	TEE2 DEG F	TEE1 DEG F	TEEUH17 DEG F	TEELH18 DEG F	TEELH19 DEG F
13	11	33	0	-5	14	2	0	329	353	320	341	293	329	337	314	291	337	328	220	317	296	343	363	530	483	487
13	11	48	0	-5	1	2	0	329	352	319	340	291	328	336	312	290	335	327	219	315	295	343	362	530	483	487
13	12	3	0	-5	1	0	0	326	352	318	339	290	328	334	312	290	335	326	218	314	293	343	361	531	483	487
13	12	18	0	-5	1	2	0	326	351	317	337	290	326	333	311	289	334	326	215	313	292	342	359	531	484	487
13	12	33	0	-5	1	8	0	326	350	315	337	289	325	333	310	288	333	324	215	313	292	342	359	531	484	487
13	12	48	0	-5	0	1	0	326	350	315	336	288	324	332	309	286	332	323	215	312	291	341	358	531	484	487
13	13	3	0	-5	0	1	0	322	349	314	335	287	324	331	308	285	331	322	214	311	290	341	357	532	484	487
13	13	18	0	-5	0	0	0	322	347	313	334	287	323	330	306	285	330	321	214	309	289	340	356	532	484	488
13	13	33	0	-5	0	0	0	322	346	312	333	285	322	328	306	284	329	321	213	308	287	340	356	532	484	488
13	13	48	0	-5	0	1	0	322	345	311	331	284	320	327	305	283	329	319	212	307	286	339	354	532	484	488
13	14	3	0	-5	0	6	0	318	344	309	331	283	319	326	304	282	327	318	210	307	285	338	353	533	484	488
13	14	18	0	-5	0	0	0	318	342	309	330	282	319	326	303	280	326	317	210	306	285	337	352	533	484	488
13	14	33	0	-5	0	1	0	318	341	307	329	282	318	325	302	280	325	316	209	305	284	337	351	533	484	488
13	14	49	0	-5	0	1	0	318	342	308	329	282	318	325	300	279	325	316	206	303	283	337	351	533	484	488
13	15	4	0	-5	0	1	0	314	340	306	328	280	316	322	300	278	324	315	205	302	283	336	350	533	484	488
13	15	19	0	-5	0	1	0	314	340	306	326	279	316	321	299	278	322	313	205	302	281	336	349	533	484	489
13	15	34	0	-5	0	2	0	314	339	305	325	278	314	320	298	277	322	312	205	301	280	335	349	533	484	489
13	15	49	0	-5	0	8	0	314	339	303	325	278	314	320	298	276	321	312	205	300	279	335	347	533	484	489
13	16	4	0	-5	0	1	0	312	338	302	324	276	313	319	297	276	320	311	204	299	279	335	346	534	484	489
13	16	19	0	-5	0	1	0	312	338	302	323	276	312	318	296	274	320	310	203	299	278	333	346	534	484	489
13	16	34	0	-5	0	1	0	312	336	301	323	275	312	318	294	273	319	309	203	297	278	333	345	534	484	489
13	16	49	0	-5	0	1	0	312	336	300	321	274	311	316	294	273	319	309	202	296	277	333	345	534	484	489
13	17	4	0	-5	0	6	0	309	335	300	320	274	310	315	293	272	318	307	202	296	275	332	344	535	484	489
13	17	18	0	-5	0	0	0	309	334	299	319	273	310	315	292	272	316	306	202	295	274	332	344	535	484	489
13	17	33	0	-5	0	2	0	309	333	297	319	272	308	314	291	271	316	306	200	294	274	332	343	535	484	489
13	17	48	0	-5	0	1	0	309	333	296	318	272	307	313	291	270	315	305	200	293	273	331	343	535	484	489
13	18	3	0	-5	0	0	0	305	331	295	317	270	307	312	290	270	314	304	199	293	272	331	341	536	484	489
13	18	18	0	-5	0	6	0	305	330	295	317	269	306	312	288	268	313	304	198	291	272	331	341	536	485	489
13	18	33	0	-5	0	6	0	305	329	294	315	268	305	310	287	267	312	303	198	290	271	330	340	536	485	489
13	18	48	0	-5	0	0	0	305	328	293	314	268	305	309	286	266	312	301	197	289	270	330	340	536	485	489
13	19	3	0	-5	0	1	0	300	328	293	313	267	304	308	286	266	310	300	197	289	268	330	339	537	485	489
13	19	18	0	-5	0	1	0	300	327	291	313	266	302	308	285	265	310	300	196	288	268	329	339	537	485	489
13	19	33	0	-5	0	0	0	300	326	290	312	265	302	307	284	264	309	299	195	287	267	329	338	537	485	489
13	19	48	0	-5	0	2	0	300	325	290	311	265	301	306	283	264	308	298	192	286	266	329	338	537	485	489
13	20	3	0	-5	0	7	0	298	325	289	311	264	300	304	283	263	308	298	193	286	266	329	337	538	485	489
13	20	19	0	-5	0	7	0	298	325	288	309	262	300	304	281	261	307	297	192	285	265	327	337	538	485	490
13	20	34	0	-5	0	7	0	298	324	288	309	262	299	303	280	261	306	295	190	283	264	327	335	538	485	490
13	20	49	0	-5	0	2	0	298	324	287	308	261	299	302	280	260	306	294	192	282	262	326	334	538	485	490
13	21	4	0	-5	0	2	0	296	322	285	307	261	298	302	279	260	305	294	192	282	262	326	334	538	485	490
13	21	19	0	-5	0	5	0	296	322	284	307	260	296	301	278	259	303	293	190	281	261	326	334	538	485	490
13	21	34	0	-5	0	5	0	296	321	284	306	260	296	300	278	259	303	292	190	281	261	326	334	538	485	490
13	21	49	0	-5	0	5	0	296	321	283	304	259	295	300	277	258	302	292	189	280	260	326	333	538	485	490
13	22	4	0	-5	2	5	0	293	320	282	304	258	295	299	275	256	301	291	188	279	259	325	333	539	485	490
13	22	18	0	-5	38	5	0	293	319	281	303	256	294	297	274	256	301	289	188	279	259	325	332	539	486	490
13	22	33	0	-5	1	0	0	293	319	280	302	256	293	296	274	255	300	289	188	277	258	325	332	539	486	490
13	22	48	0	-5	1	1	0	293	317	280	302	255	292	296	273	254	299	288	185	276	256	325	331	539	486	490
13	23	3	0	-5	31	0	0	288	316	279	301	254	292	295	272	254	299	287	185	275	256	324	331	540	486	491
13	23	18	0	-5	2	2	0	288	316	277	300	254	290	294	272	253	297	287	185	275	255	324	331	540	486	491
13	23	33	0	-5	17	7	0	288	315	277	300	253	290	293	271	253	297	286	185	274	254	324	329	540	486	491
13	23	48	0	-5	1	1	0	288	314	276	299	253	289	293	269	252	296	285	185	273	254	324	329	540	486	491
13	24	3	0	-5	1	2	0	285	314	275	297	252	288	291	269	252	295	285	183	273	253	323	329	541	486	491
13	24	18	0	-5	17	8	0	285	314	275	297	251	288	291	268	250	295	283	183	272	252	323	328	541	486	491
13	24	33	0	-5	1	0	0	285	313	274	296	251	287	290	267	250	294	283	183	270	252	323	328	541	486	491
13	24	48	0	-5	1	0	0	285	313	274	296	250	287	289	267	249	294	282	182	270	250	323	328	541	486	491
13	25	3	0	-5	1	0	0	283	311	273	295	250	286	289	266	248	293	281	182	269	250	322	327	542	486	491
13	25	18	0	-5	1	0	0	283	311	271	295	249	286	288	266	248	293	281	181	269	249	322	327	542	486	492
13	25	33	0	-5	0	0	0	283	310	271	294	247	284	288	265	247	292	280	181	268	249	322	327	542	486	492
13	25	48	0	-5	0	2	0	283	310	270	292	247	284	287	263	247	291	280	180</							

Panel Temperature Data During Freezing

Time hour	Time min	Time sec	FT720 GPM	PF-001 LV/min	PF-002 LV/min	FT730 GPM	FT800 GPM	TEE16 DEG F	TEE15 DEG F	TEE14 DEG F	TEE13 DEG F	TEE12 DEG F	TEE11 DEG F	TEE10 DEG F	TEE9 DEG F	TEE8 DEG F	TEE7 DEG F	TEE6 DEG F	TEE5 DEG F	TEE4 DEG F	TEE3 DEG F	TEE2 DEG F	TEE1 DEG F	TEEH17 DEG F	TEELH18 DEG F	TEELH19 DEG F
13	29	33	0	-5	0	2	0	272	299	258	282	237	274	275	252	237	281	267	170	256	237	317	320	545	488	492
13	29	48	0	-5	0	1	0	272	299	258	282	236	273	274	251	236	280	267	170	256	236	317	320	545	488	492
13	30	3	0	-5	0	1	0	270	298	257	280	235	273	274	251	235	280	266	169	255	236	317	318	546	489	492
13	30	18	0	-5	0	1	0	270	298	256	280	235	271	273	250	235	279	266	169	254	235	317	318	546	489	492
13	30	34	0	-5	0	2	0	270	297	256	279	233	271	271	248	233	277	265	169	253	235	316	317	546	489	492
13	30	48	0	-5	0	2	0	270	297	255	278	233	270	271	248	233	277	265	169	253	235	316	317	546	489	492
13	31	4	0	-5	0	2	0	267	296	254	278	232	269	270	247	232	276	263	168	252	232	316	317	546	489	492
13	31	19	0	-5	0	2	0	267	294	254	277	231	269	269	246	231	275	263	168	250	232	315	316	546	490	493
13	31	34	0	-5	0	1	0	267	294	252	276	231	268	268	246	231	275	262	168	250	231	315	315	546	490	493
13	31	49	0	-5	0	1	0	267	293	251	276	230	267	268	245	230	274	261	167	249	230	315	315	546	490	493
13	32	4	0	-5	0	1	0	264	292	251	274	229	267	267	244	230	273	261	167	248	230	313	315	547	490	493
13	32	19	0	-5	0	2	0	264	292	250	273	229	265	266	244	229	273	259	162	248	229	313	314	547	490	493
13	32	34	0	-5	0	1	0	264	291	249	273	227	265	266	242	227	271	258	162	247	229	313	314	547	490	493
13	32	49	0	-5	0	1	0	264	291	249	272	226	264	265	241	227	271	258	162	246	228	312	313	547	490	493
13	33	4	0	-5	0	2	0	261	290	248	272	226	264	263	241	226	270	257	162	246	228	312	313	548	491	495
13	33	19	0	-5	0	1	0	261	290	247	271	226	263	263	240	226	270	257	163	244	226	312	311	548	491	495
13	33	33	0	-5	0	1	0	261	289	247	271	225	263	262	240	226	269	256	163	244	226	312	311	548	491	495
13	33	48	0	-5	0	7	0	261	289	246	270	225	262	262	239	225	269	255	162	243	225	311	310	548	491	496
13	34	3	0	-5	0	7	0	260	289	246	270	224	262	261	239	225	268	254	162	243	225	311	310	548	492	496
13	34	18	0	-5	0	1	0	260	288	244	268	224	261	261	238	224	268	254	162	243	224	311	309	548	492	496
13	34	33	0	-5	0	1	0	260	288	244	268	224	260	260	238	224	267	253	162	242	224	310	309	548	492	496
13	34	48	0	-5	0	1	0	260	286	243	267	223	260	260	237	223	267	253	161	241	223	310	308	548	492	497
13	35	3	0	-5	0	2	0	257	286	243	267	223	258	259	235	223	265	252	161	241	222	309	308	549	492	497
13	35	18	0	-5	0	7	0	257	285	242	266	222	258	257	235	222	265	251	160	240	222	309	307	549	492	497
13	35	33	0	-5	0	1	0	257	285	241	266	222	257	257	234	222	264	251	159	239	221	309	307	549	492	498
13	35	48	0	-5	0	0	0	257	284	241	265	220	257	256	234	221	263	249	159	238	219	308	305	549	493	498
13	36	3	0	-5	0	2	0	254	284	240	264	220	256	256	233	221	263	249	159	238	219	308	305	550	493	498
13	36	18	0	-5	0	0	0	254	283	240	264	219	256	255	232	221	262	249	158	238	219	308	304	550	493	499
13	36	34	0	-5	0	2	0	254	282	238	262	219	255	255	232	222	262	248	160	238	219	308	304	550	493	499
13	36	49	0	-5	0	0	0	254	282	237	262	218	255	254	231	222	262	249	164	239	221	309	304	550	494	499
13	37	4	0	-5	0	1	0	251	281	237	261	218	254	254	231	224	262	251	168	241	223	310	305	551	494	499
13	37	19	0	-5	0	1	0	251	281	236	261	217	254	254	231	227	263	253	173	244	225	311	306	551	494	501
13	37	34	0	-5	0	6	0	251	279	236	260	217	253	254	229	229	264	257	179	247	229	314	308	551	494	501
13	37	49	0	-5	0	5	0	251	279	235	260	217	253	254	229	232	265	261	184	251	233	315	309	551	495	502
13	38	4	0	-5	0	5	0	250	279	235	259	217	252	253	229	234	265	264	191	255	237	317	310	552	495	502
13	38	19	0	-5	0	5	0	250	278	234	259	216	252	253	229	237	267	267	196	258	239	318	311	552	495	502
13	38	34	0	-5	0	5	0	250	277	234	258	216	252	253	229	239	269	270	202	261	243	320	311	552	496	503
13	38	49	0	-5	0	0	0	250	277	232	258	216	250	253	229	241	270	274	208	265	245	321	312	552	496	503
13	39	4	0	-5	0	1	0	248	277	232	256	215	250	252	229	244	271	277	210	268	249	322	314	552	496	503
13	39	19	0	-5	0	2	0	248	276	231	256	215	249	252	229	246	272	280	216	272	251	323	315	552	497	504
13	39	34	0	-5	0	0	0	248	276	231	255	213	249	252	229	247	273	284	220	275	263	326	316	552	497	504

Panel Temperature Data During Freezing

CRTRF NET-90 99 POINT DATA				TEW18	TEW17	TEW16	TEW15	TEW14	TEW13	TEW12	TEW11	TEW10	TEW9	TEW8	TEW7	TEW6	TEW5	TEW4	TEW3	TEW2	TEW1	TEWU11	TEWLH20	TEWLH21	TE970	TE990	
TEST DATE	Time	Time	Time	DEG F	DEG F	DEG F	DEG F	DEG F	DEG F	DEG F	DEG F	DEG F	DEG F	DEG F	DEG F	DEG F	DEG F	DEG F	DEG F	DEG F	DEG F	DEG F	DEG F	DEG F	DEG F	DEG F	
Tue Jan 4 199	hour	min	sec																								
12	12	0	4	584	586	589	590	589	591	581	587	587	589	588	592	590	591	587	594	578	592	589	588	584	550	583	
12	12	0	19	581	584	587	590	585	590	577	583	583	589	583	593	591	592	582	595	572	592	589	590	584	549	595	
12	12	0	34	579	582	585	587	583	588	575	581	581	587	581	591	589	591	581	594	571	592	589	590	583	548	595	
12	12	0	49	579	581	585	586	585	587	577	582	583	585	583	589	587	589	584	592	575	590	589	590	583	548	596	
12	12	1	4	583	584	588	588	588	589	589	580	586	587	587	590	588	588	588	592	577	590	588	590	583	548	597	
12	12	1	19	583	585	589	590	588	590	579	586	585	589	586	592	590	590	585	594	575	592	588	589	583	545	597	
12	12	1	33	581	583	588	589	586	590	578	584	584	588	584	592	590	591	584	595	574	592	589	589	583	544	596	
12	12	1	49	581	582	587	588	587	589	579	584	585	588	585	591	590	590	585	594	574	593	589	590	583	544	596	
12	12	2	4	582	582	589	589	588	589	589	580	586	586	588	586	592	590	590	586	594	576	593	589	590	583	542	597
12	12	2	19	584	583	589	591	589	591	577	588	586	590	588	592	591	589	588	594	576	592	589	590	583	540	597	
12	12	2	34	581	577	588	590	588	590	566	586	586	589	587	591	590	585	587	593	571	592	589	590	584	536	596	
12	12	2	48	573	571	583	589	585	590	553	583	575	587	583	589	590	581	582	590	559	589	589	590	584	534	595	
12	12	3	3	585	567	577	587	580	587	538	579	570	584	578	587	587	576	576	587	549	586	589	589	584	534	595	
12	12	3	18	555	563	569	585	574	585	523	574	564	580	571	584	585	572	568	584	539	582	589	588	584	533	593	
12	12	3	33	545	559	562	581	568	583	508	568	557	573	563	581	582	567	560	581	531	579	589	588	584	533	593	
12	12	3	48	534	554	554	575	561	580	494	562	550	577	556	578	579	563	552	577	522	575	589	587	584	532	592	
12	12	4	3	625	552	545	575	555	578	481	557	542	569	548	574	577	559	544	576	514	573	589	587	583	531	592	
12	12	4	18	616	548	538	572	548	575	466	551	534	566	541	572	574	555	536	572	505	569	589	586	583	531	592	
12	12	4	33	507	546	530	569	541	572	453	546	526	563	533	568	572	551	528	569	496	567	589	586	583	529	592	
12	12	4	48	500	542	522	566	534	570	441	540	519	560	526	565	570	547	523	567	491	563	589	585	584	530	591	
12	12	5	3	538	549	556	563	568	566	544	566	574	555	572	582	566	543	583	565	571	560	586	585	584	530	591	
12	12	5	18	575	567	582	575	583	575	565	580	583	569	583	565	569	563	585	570	575	566	582	582	584	532	590	
12	12	5	33	580	573	587	582	586	581	570	585	587	579	587	572	579	575	589	581	579	579	580	577	584	533	573	
12	12	5	48	582	577	589	587	590	586	573	588	589	584	590	577	585	581	591	587	582	585	582	577	585	533	576	
12	12	6	3	584	580	590	589	591	588	574	589	590	587	591	579	587	583	592	590	582	587	584	578	586	535	580	
12	12	6	18	584	581	591	590	591	589	575	590	591	588	592	582	588	585	592	591	583	589	589	586	582	588	536	584
12	12	6	33	586	581	591	591	592	590	576	590	591	588	592	583	589	585	592	592	583	589	589	583	588	537	585	
12	12	6	48	586	582	591	591	592	590	576	590	591	589	592	584	589	586	592	592	583	590	590	585	589	538	586	
12	12	7	3	586	582	591	591	592	590	576	590	591	589	592	585	590	586	592	592	583	590	590	586	589	539	586	
12	12	7	18	586	582	592	591	592	591	576	590	591	589	592	585	590	586	592	592	583	590	590	586	590	540	587	
12	12	7	33	586	583	592	591	592	591	577	591	591	589	592	585	590	586	593	592	583	590	591	586	590	542	587	
12	12	7	48	586	583	592	592	592	591	577	591	591	589	592	585	590	586	592	592	583	590	591	586	590	542	588	
12	12	8	4	586	583	592	592	592	591	577	591	591	589	592	584	590	586	592	592	583	590	591	588	590	543	588	
12	12	8	19	586	583	592	592	592	591	576	591	591	589	592	584	590	586	593	592	583	590	591	588	590	543	588	
12	12	8	34	586	583	592	592	592	591	576	591	591	589	592	584	590	586	593	592	584	590	591	588	590	545	586	
12	12	8	49	586	583	592	592	592	591	577	591	591	589	592	584	590	586	592	592	583	590	591	588	591	546	587	
12	12	9	4	586	583	592	592	592	591	577	591	591	589	592	585	590	586	593	592	583	590	591	588	591	547	587	
12	12	9	19	586	583	592	591	592	591	576	591	591	589	592	584	590	586	593	592	583	590	591	588	591	548	587	
12	12	9	34	586	582	592	591	592	591	577	591	591	589	593	585	590	586	593	592	584	590	592	589	591	548	589	
12	12	9	49	586	582	592	591	592	591	576	591	591	590	593	585	590	586	593	593	583	590	592	588	591	548	589	
12	12	10	4	586	582	592	592	592	591	576	591	591	590	593	585	590	586	593	593	584	591	592	589	591	548	589	
12	12	10	19	586	582	592	592	592	591	577	591	591	590	593	585	590	586	593	593	584	591	592	589	591	549	589	
12	12	10	34	586	583	592	592	592	591	577	591	591	590	593	585	590	587	593	593	584	591	592	589	591	549	589	
12	12	10	48	586	583	592	592	592	591	577	591	592	590	593	584	590	586	593	593	584	591	592	589	591	549	589	
12	12	11	3	586	583	592	592	592	591	576	591	592	590	593	584	590	586	593	592	582	591	592	589	591	549	588	
12	12	11	18	586	583	593	592	593	591	577	591	592	590	593	584	590	586	593	593	583	591	592	589	591	549	588	
12	12	11	33	586	583	593	592	593	591	577	591	592	590	593	584	590	586	593	593	584	591	592	589	591	550	588	
12	12	11	48	585	581	593	592	592	591	575	591	591	589	593	583	590	584	593	593	582	591	592	589	591	548	588	
12	12	12	3	583	578	592	590	592	590	570	590	591	587	592	582	590	580	592	591	579	589	592	589	591	547	588	
12	12	12	18	580	574	590	589	590	590	561	588	588	585	590	581	588	575	591	589	575	587	592	588	591	542	588	
12	12	12	33	583	570	588	587	589	587	559	587	585	583	588	578	586	570	589	586	571	585	591	588	591	540	588	
12	12	12	48	582	567	585	585	587	585	552	585	584	581	585	576	584	566	586	583	565	582	591	587	590	537	588	
12	12	13	3	580	566	583	582	585	582	546	584	583	579	583	574	581	562	583	581	560	580	591	587	589	535	588	
12	12	13	18	580	564	581	579	582	580	541	582	580	575	590	572	578	558	579	578	557	578	591</					

Panel Temperature Data During Freezing

Time hour	Time min	Time sec	TEW18 DEG F	TEW17 DEG F	TEW16 DEG F	TEW15 DEG F	TEW14 DEG F	TEW13 DEG F	TEW12 DEG F	TEW11 DEG F	TEW10 DEG F	TEW9 DEG F	TEW8 DEG F	TEW7 DEG F	TEW6 DEG F	TEW5 DEG F	TEW4 DEG F	TEW3 DEG F	TEW2 DEG F	TEW1 DEG F	TEWU19 DEG F	TEWL20 DEG F	TEWL21 DEG F	TE970 DEG F	TE990 DEG F
12	17	34	560	545	558	560	549	557	513	551	548	542	537	539	551	527	542	552	509	534	574	559	556	521	586
12	17	48	557	542	557	558	547	555	511	549	546	540	535	537	550	526	540	550	507	533	573	558	555	520	586
12	18	3	556	541	556	557	546	553	509	547	545	538	534	535	549	524	537	548	505	532	572	557	554	520	586
12	18	18	555	540	555	555	544	552	507	545	544	536	532	534	547	522	534	546	503	530	571	556	553	519	586
12	18	33	554	538	554	554	543	550	507	543	543	534	530	532	546	521	531	545	502	529	570	554	552	519	586
12	18	48	553	538	553	553	541	550	505	541	541	533	528	530	545	519	528	544	499	526	568	553	550	518	587
12	19	3	551	535	552	551	539	548	504	540	540	532	526	529	544	517	525	543	499	525	567	552	548	518	587
12	19	18	550	535	549	549	538	547	502	538	538	530	525	527	543	515	522	541	495	523	566	551	547	517	587
12	19	33	548	533	548	548	535	545	500	536	537	529	523	525	542	514	520	540	494	522	565	549	546	516	587
12	19	48	547	533	547	546	534	543	498	535	535	527	522	523	541	513	517	538	492	519	564	547	544	516	587
12	20	3	547	532	546	545	533	541	497	533	534	524	520	522	540	511	514	535	491	518	562	546	543	515	587
12	20	18	546	531	545	543	531	540	496	532	533	523	519	520	539	510	512	532	489	516	561	545	541	515	586
12	20	33	544	529	543	543	529	539	496	531	530	522	517	518	538	508	510	530	487	514	560	543	540	515	586
12	20	48	542	528	542	542	527	538	494	530	528	520	515	517	536	507	508	527	486	512	558	541	538	514	585
12	21	3	541	527	540	542	525	537	493	528	526	519	514	515	535	506	506	524	484	511	557	539	537	512	584
12	21	18	539	526	538	541	524	536	492	527	524	517	513	514	533	504	504	522	483	509	555	538	536	511	584
12	21	34	538	524	537	541	522	534	491	526	523	515	511	512	532	502	502	520	481	508	554	537	533	510	583
12	21	49	537	523	536	540	520	533	491	525	522	514	510	510	530	501	501	517	479	507	553	534	532	510	583
12	22	4	536	522	535	538	519	532	489	524	521	513	508	509	528	499	499	515	478	504	552	533	531	510	583
12	22	19	535	521	534	537	518	531	488	523	519	511	507	507	527	498	498	513	476	503	550	532	530	509	583
12	22	34	532	520	531	536	517	530	486	522	519	510	506	505	524	497	496	511	474	502	549	531	529	508	583
12	22	49	531	519	530	535	516	528	485	521	518	509	505	504	523	495	494	509	473	501	548	530	528	508	583
12	23	4	530	517	529	534	515	527	484	520	517	507	504	502	521	494	493	507	473	499	547	528	526	507	584
12	23	19	529	516	528	533	513	525	483	519	515	507	503	500	520	492	492	505	471	497	546	527	525	507	584
12	23	34	528	515	527	532	511	525	482	518	513	505	501	499	518	491	490	503	469	496	544	526	524	507	584
12	23	49	526	514	524	531	510	524	481	517	512	504	500	498	517	490	489	502	468	495	544	525	523	506	584
12	24	4	525	511	523	530	509	523	479	515	510	503	499	496	516	489	488	500	467	493	542	523	521	506	584
12	24	19	523	510	523	529	507	522	478	514	510	502	498	494	514	489	487	499	465	492	540	522	520	505	584
12	24	34	522	509	522	527	506	520	477	513	508	500	496	493	513	487	485	498	464	492	539	520	518	503	584
12	24	49	521	508	521	526	504	519	476	512	507	499	495	491	512	486	484	496	463	490	538	519	517	503	584
12	25	3	521	507	518	525	503	517	475	511	505	498	494	490	510	484	483	495	463	488	537	518	516	502	583
12	25	18	518	505	517	523	501	516	473	510	504	497	493	489	509	483	482	493	461	486	535	517	515	502	582
12	25	33	517	504	516	522	501	514	473	509	503	495	492	487	507	482	480	491	460	484	534	515	514	501	582
12	25	48	515	503	515	521	500	514	471	507	503	494	491	486	506	480	479	490	458	482	533	514	512	500	581
12	26	3	514	502	514	520	499	512	471	506	502	493	489	485	505	479	478	489	457	481	532	512	511	500	580
12	26	18	513	501	512	518	498	511	469	505	501	492	489	483	503	478	477	487	457	480	531	511	510	499	580
12	26	33	512	498	511	517	497	510	468	504	500	490	488	482	502	478	477	486	456	479	530	510	509	497	580
12	26	48	511	497	510	516	495	508	467	503	498	489	486	481	501	476	476	484	455	478	529	509	508	497	580
12	27	3	511	496	509	515	495	507	465	502	496	488	485	480	500	475	475	483	454	477	527	508	508	497	580
12	27	18	508	495	508	514	494	506	464	500	495	487	484	478	499	473	474	482	453	476	526	506	507	497	580
12	27	33	508	493	506	513	493	505	463	499	495	486	483	477	497	472	473	481	453	475	526	505	506	497	581
12	27	48	507	493	505	511	491	503	462	498	495	485	482	476	496	472	472	470	452	473	525	504	506	496	581
12	28	3	505	491	504	510	490	502	460	487	484	484	481	475	495	471	471	478	451	472	524	503	505	495	582
12	28	19	505	490	503	509	489	501	458	485	483	482	480	474	494	469	470	477	451	471	523	502	503	495	582
12	28	34	504	489	502	508	488	500	456	485	481	481	479	472	492	469	469	475	451	470	522	500	502	494	581
12	28	49	503	488	501	506	488	499	457	493	490	480	478	471	491	467	468	474	450	469	522	498	502	494	581
12	29	4	502	487	501	505	487	497	456	492	489	479	477	470	490	466	468	473	450	467	520	497	501	493	581
12	29	19	500	485	499	504	486	496	455	491	489	478	476	469	488	464	467	472	449	466	519	496	500	493	581
12	29	34	499	484	498	503	485	495	454	490	489	476	475	468	487	463	466	470	449	465	518	495	499	492	579
12	29	49	499	483	497	502	484	494	453	489	487	475	475	467	486	462	465	469	449	465	517	493	498	491	579
12	30	5	498	482	496	501	483	493	453	488	485	474	474	466	485	461	465	468	448	464	516	492	495	491	578
12	30	18	497	481	495	500	482	493	452	487	485	473	473	465	484	460	464	467	448	462	514	491	495	490	578
12	30	33	496	479	495	499	482	491	450	486	484	472	472	464	483	459	464	466	448	462	513	490	495	489	577
12	30	48	494	478	493	498	481	490	450	485	484	470	471	463	481	458	463	466	448	461	513	490	494	489	577
12	31	3	493	477	492	497	480	490	449	484	483	470	471	461	480	457	463	465	448	461	512	489	494	488	577
12	31	18	492	477	491	496	479	489	448	483	483	469	470	461	480	457	462	464	448	460	511	487	492	488	577
12	31	34	492	476	490	494	478	487	447	483	481	467	469	460	479	456	462	463	448	460	510	486	491	487	577
12	31	49	491	475																					

Panel Temperature Data During Freezing

Time hour	Time min	Time sec	TEW18 DEG F	TEW17 DEG F	TEW16 DEG F	TEW15 DEG F	TEW14 DEG F	TEW13 DEG F	TEW12 DEG F	TEW11 DEG F	TEW10 DEG F	TEW9 DEG F	TEW8 DEG F	TEW7 DEG F	TEW6 DEG F	TEW5 DEG F	TEW4 DEG F	TEW3 DEG F	TEW2 DEG F	TEW1 DEG F	TEWU11 DEG F	TEWLH20 DEG F	TEWLH21 DEG F	TEG70 DEG F	TEG90 DEG F
12	35	33	473	460	477	476	470	469	421	472	471	456	463	450	463	447	458	457	447	453	498	475	484	476	574
12	35	48	472	459	476	475	469	488	420	471	471	455	463	449	463	445	458	457	447	451	497	475	484	476	574
12	36	3	471	457	476	473	469	466	419	471	471	454	462	449	461	444	458	456	447	451	497	474	484	475	574
12	36	18	470	456	475	471	468	464	419	470	471	454	462	448	460	444	458	456	447	450	497	474	484	475	575
12	36	33	467	454	475	469	467	463	415	470	470	453	462	448	460	441	458	455	447	450	497	474	483	474	575
12	36	48	467	452	474	468	467	461	414	469	470	452	462	447	459	440	457	454	447	450	496	474	483	474	575
12	37	3	465	450	474	466	466	460	413	468	470	451	461	446	459	439	457	453	447	449	496	474	483	474	575
12	37	18	465	450	474	464	466	460	409	467	469	450	461	446	458	438	457	452	445	449	496	474	483	474	576
12	37	33	464	448	474	462	465	459	409	466	469	450	461	446	458	437	457	451	445	448	496	474	483	473	576
12	37	48	463	446	473	461	465	459	409	466	468	449	460	445	457	436	457	450	444	447	496	474	482	473	575
12	38	4	462	445	473	459	464	458	406	465	467	448	460	444	456	435	457	450	441	447	496	474	482	472	575
12	38	19	461	444	473	459	464	457	405	464	467	447	460	444	455	434	457	449	439	445	495	474	482	470	574
12	38	34	461	443	472	458	464	457	404	463	467	447	460	443	454	434	457	448	438	445	495	473	482	470	574
12	38	49	458	440	472	458	464	456	403	463	466	446	460	443	454	433	457	448	436	444	494	473	482	470	573
12	39	4	458	439	472	457	464	455	402	462	466	445	460	442	453	432	456	447	434	443	494	473	482	469	573
12	39	19	457	439	471	456	464	455	401	461	465	445	460	442	452	431	456	447	433	443	493	473	481	469	572
12	39	34	455	437	471	456	464	454	400	460	465	444	460	441	452	430	456	446	432	442	493	473	481	469	572
12	39	49	455	436	471	455	463	453	399	459	465	443	460	441	451	430	456	445	431	442	493	473	481	468	571
12	40	3	452	434	469	454	462	453	398	459	464	443	459	440	450	429	456	445	431	441	493	473	481	467	571
12	40	18	452	433	469	453	462	452	396	458	464	442	459	440	450	429	456	445	430	441	492	473	481	467	571
12	40	33	450	432	469	453	461	451	394	458	463	442	458	440	449	428	456	444	428	440	492	474	481	466	571
12	40	48	449	431	468	452	461	451	391	457	463	441	459	439	449	427	456	443	429	440	492	474	482	466	572
12	41	3	448	430	468	451	461	450	389	457	462	441	459	438	448	427	456	443	427	439	492	474	482	465	572
12	41	18	446	430	468	451	461	449	388	456	462	440	459	438	448	426	456	443	427	439	492	474	482	465	572
12	41	33	446	428	467	450	460	448	387	456	462	439	459	438	447	425	456	442	426	439	492	474	482	464	572
12	41	48	445	428	467	449	460	448	385	455	461	439	459	437	446	424	456	441	425	439	493	474	483	464	573
12	42	3	444	427	467	449	460	447	384	454	461	439	459	437	446	423	456	441	425	438	493	474	483	464	573
12	42	18	443	426	466	448	460	447	382	453	461	438	458	436	445	422	456	441	424	438	493	474	483	464	572
12	42	33	442	425	466	447	460	446	381	453	461	437	458	436	445	421	456	440	424	436	493	474	483	462	572
12	42	48	440	425	466	447	461	446	378	452	461	437	458	435	444	420	456	440	422	436	493	474	483	462	571
12	43	4	440	424	466	446	461	445	377	452	461	436	458	435	444	419	456	439	422	435	493	474	483	461	571
12	43	19	438	424	465	445	461	445	375	451	460	436	458	434	443	418	455	438	421	435	493	474	483	461	570
12	43	34	437	422	465	445	460	444	373	450	460	435	457	434	443	417	455	436	420	434	493	474	483	461	570
12	43	49	437	421	465	444	460	444	371	450	460	435	457	433	442	416	455	438	419	433	493	474	482	459	569
12	44	4	434	420	464	444	460	443	369	449	459	434	456	433	442	415	455	437	418	433	493	474	482	459	568
12	44	19	434	419	463	443	460	443	367	449	459	434	455	433	441	415	455	437	417	433	493	474	482	459	568
12	44	34	433	418	461	443	459	442	365	448	458	433	454	432	441	414	455	436	416	433	493	474	482	458	568
12	44	49	433	417	460	442	459	442	363	448	458	433	453	432	440	413	455	436	415	432	493	475	483	458	568
12	45	4	432	416	459	441	459	441	361	447	458	432	453	431	440	412	455	435	415	432	493	475	483	458	569
12	45	18	431	416	458	441	458	441	358	447	457	432	452	431	439	411	454	435	414	432	494	475	483	457	569
12	45	33	430	414	457	441	458	440	357	446	457	431	451	430	439	410	454	435	413	431	494	475	483	457	569
12	45	48	430	413	457	440	457	440	355	446	456	431	450	430	439	409	454	434	412	431	495	475	484	456	569
12	46	3	428	413	457	439	457	439	351	445	455	431	449	430	438	408	453	434	412	431	495	475	484	456	569
12	46	18	428	412	455	439	457	439	350	445	455	430	449	429	438	407	452	433	410	431	495	475	484	456	570
12	46	33	427	411	454	438	456	438	347	444	455	430	448	429	437	406	451	433	409	430	496	475	485	455	570
12	46	48	426	410	454	438	456	438	345	444	454	429	447	428	437	405	450	433	408	430	496	476	485	454	569
12	47	3	425	410	453	437	455	438	343	444	453	429	447	428	436	403	448	432	407	429	496	476	485	454	569
12	47	18	424	408	453	437	455	437	340	443	452	428	446	427	436	402	447	431	407	428	496	476	485	452	568
12	47	33	422	407	452	436	454	437	338	443	451	427	445	426	436	400	445	431	405	428	497	476	485	452	567
12	47	48	422	406	451	436	453	436	335	442	450	427	444	426	435	399	444	430	403	427	497	476	485	451	567
12	48	4	421	405	450	435	453	436	332	442	449	427	444	425	435	397	443	429	403	426	497	476	486	450	566
12	48	19	420	403	449	435	452	435	330	441	448	426	443	424	434	396	442	429	401	426	497	476	487	450	566
12	48	34	419	402	448	434	452	435	328	441	447	425	442	424	434	395	442	428	400	425	498	476	487	450	565
12	48	49	417	402	448	434	451	435	324	440	447	425	442	423	433	393	441	428	399	425	498	477	487	449	565
12	49	4	416	401	446	433	451	434	322	440	446	424	441	423	433	392	440	427	398	424	499	477	488	448	565
12	49	19	416	400	446	433	450	434	321	440	445	424	441	422	432	391	439	426	396	424	500	477	488	448	565
12	49	34	415	399	445	432	449	433	319	439	444	423	440	421	432	389	439	426	396	423	500	477	489	447	565
12	49	49	414	397																					

Panel Temperature Data During Freezing

Time hour	Time min	Time sec	TEW18 DEG F	TEW17 DEG F	TEW16 DEG F	TEW15 DEG F	TEW14 DEG F	TEW13 DEG F	TEW12 DEG F	TEW11 DEG F	TEW10 DEG F	TEW9 DEG F	TEW8 DEG F	TEW7 DEG F	TEW6 DEG F	TEW5 DEG F	TEW4 DEG F	TEW3 DEG F	TEW2 DEG F	TEW1 DEG F	TEWU11 DEG F	TEWLH20 DEG F	TEWLH21 DEG F	TE970 DEG F	TE990 DEG F
12	53	34	396	376	435	424	440	425	290	433	433	411	431	406	424	361	429	413	370	410	506	479	497	440	562
12	53	49	395	373	435	424	440	424	288	432	433	409	431	404	424	359	428	412	369	409	507	480	498	439	562
12	54	4	392	372	434	423	440	424	286	432	432	409	430	403	423	357	428	411	367	407	507	480	498	439	562
12	54	19	391	370	434	422	439	423	284	432	432	408	430	402	423	356	427	410	365	406	508	480	499	438	562
12	54	34	390	368	433	421	439	422	282	431	431	406	429	401	422	354	427	409	363	405	508	480	500	438	563
12	54	49	389	367	433	421	438	422	281	431	431	406	429	400	422	353	426	408	363	404	509	481	500	438	563
12	55	4	388	366	431	420	437	421	280	431	430	404	428	398	421	351	425	407	361	403	509	481	501	438	564
12	55	19	386	364	431	420	437	420	279	430	429	403	427	396	420	349	425	405	360	402	510	481	501	437	564
12	55	33	385	362	431	419	437	419	277	430	429	402	427	395	419	347	424	404	358	401	510	481	501	437	563
12	55	48	384	361	430	418	436	419	276	430	428	400	426	393	418	345	423	403	356	398	511	481	502	437	563
12	56	3	381	359	430	417	436	418	274	429	427	399	425	392	418	344	422	401	355	397	511	481	502	437	562
12	56	18	380	357	429	417	435	417	272	429	427	398	424	390	417	342	421	400	352	396	511	481	502	436	562
12	56	33	378	355	429	416	435	416	271	428	426	396	424	389	416	341	420	398	351	395	511	481	502	436	561
12	56	48	377	354	428	415	435	416	270	428	426	394	423	387	415	340	419	397	349	393	512	482	503	435	560
12	57	3	377	351	427	414	434	415	269	427	425	393	422	386	415	338	419	396	348	391	512	482	503	434	560
12	57	18	373	350	427	413	434	414	267	427	424	392	421	384	414	337	417	394	347	390	513	482	503	434	559
12	57	33	372	349	425	412	434	413	265	427	424	390	421	382	413	335	417	392	345	388	513	482	503	434	559
12	57	48	372	348	425	412	433	412	265	426	423	389	420	381	412	334	415	391	343	387	513	482	503	433	559
12	58	3	371	347	424	410	433	411	263	426	422	387	419	379	411	333	415	390	341	386	513	482	503	433	559
12	58	19	368	345	423	410	432	411	261	425	421	386	418	378	410	331	414	389	340	385	514	483	504	432	559
12	58	34	367	344	423	408	432	410	260	425	421	384	418	376	409	330	413	387	339	385	514	483	504	432	559
12	58	49	366	343	422	407	431	408	259	424	420	383	417	375	408	329	412	386	338	384	515	483	505	432	559
12	59	4	365	342	420	406	431	407	258	424	419	382	416	373	407	328	411	385	337	383	515	483	505	432	559
12	59	19	362	339	420	404	430	406	257	423	418	380	414	371	405	326	410	383	335	381	516	484	506	431	560
12	59	34	361	338	419	403	430	405	255	423	417	379	414	371	404	325	409	382	334	380	516	484	506	431	560
12	59	49	360	336	418	402	429	404	254	422	416	377	413	369	403	324	408	381	334	379	517	484	507	431	560
13	0	4	359	335	418	401	429	403	253	421	416	376	412	368	402	323	407	379	332	379	517	484	507	431	560
13	0	19	357	334	417	399	428	401	252	421	415	375	411	366	400	321	406	378	331	378	517	484	507	430	560
13	0	34	356	333	415	398	428	401	251	420	414	373	410	365	399	320	405	377	330	377	517	484	507	428	560
13	0	49	355	332	414	396	428	399	250	420	413	372	408	363	397	319	403	376	329	375	518	484	508	428	559
13	1	4	355	330	414	395	427	398	248	419	412	371	407	362	396	318	402	374	327	374	518	484	508	427	558
13	1	19	352	330	413	394	427	397	248	418	411	369	406	361	395	317	401	373	327	373	519	484	508	427	558
13	1	34	350	327	412	392	426	396	247	418	410	368	405	359	393	316	400	372	325	372	519	484	508	426	557
13	1	49	351	327	411	391	426	394	244	417	409	367	404	358	392	315	398	370	324	371	519	485	508	425	557
13	2	4	349	326	409	390	425	393	243	416	408	366	402	357	390	313	396	369	323	370	519	485	508	425	556
13	2	19	348	324	408	388	425	392	243	416	407	365	401	356	389	313	395	368	322	370	520	485	509	425	556
13	2	33	346	323	407	387	424	390	241	415	405	363	400	355	388	312	394	367	320	368	520	485	509	425	556
13	2	48	345	322	406	386	424	389	241	414	404	362	398	353	386	310	393	366	319	368	521	485	509	425	556
13	3	3	344	321	404	384	423	387	240	413	403	361	397	352	385	310	391	365	319	367	521	485	509	424	556
13	3	18	343	319	403	383	422	386	239	413	402	360	395	351	383	308	390	364	318	366	522	486	510	423	556
13	3	33	341	318	402	381	421	384	238	412	401	359	394	350	382	307	388	363	318	366	522	486	510	423	556
13	3	48	340	317	401	380	421	383	237	411	399	358	392	349	381	307	387	362	317	365	522	486	511	423	557
13	4	3	339	317	400	379	420	381	235	410	398	356	391	347	379	306	385	360	315	365	522	486	511	423	557
13	4	18	339	316	397	377	419	380	235	409	397	355	389	346	378	304	384	359	314	364	523	487	511	422	555
13	4	33	337	315	396	376	419	378	233	409	395	354	388	345	377	304	383	358	313	363	523	487	511	422	560
13	4	48	337	313	395	375	418	377	233	408	393	353	386	344	375	303	381	357	312	362	524	487	512	421	567
13	5	3	335	312	392	373	417	375	232	406	392	351	385	342	374	301	380	356	311	362	524	487	512	421	567
13	5	18	334	311	391	372	416	374	230	406	390	351	383	341	372	300	378	355	310	360	524	487	512	422	574
13	5	33	333	310	390	371	416	373	228	405	389	349	381	340	371	299	376	353	309	359	524	487	512	422	576
13	5	48	333	310	389	370	415	372	228	404	387	348	380	339	370	298	375	352	308	359	524	487	512	423	577
13	6	3	330	309	386	369	414	370	226	402	385	347	378	338	369	297	373	352	308	358	524	487	512	423	579
13	6	18	329	308	385	367	413	369	226	401	384	346	377	337	367	296	372	350	306	357	524	487	512	424	580
13	6	34	329	306	384	366	412	368	224	400	382	345	376	336	366	295	370	348	305	357	525	487	512	424	580
13	6	49	328	305	381	365	411	366	223	399	380	344	374	335	365	294	368	348	304	356	525	487	512	425	581
13	7	4	326	305	380	364	410	365	222	397	379	343	373	334	363	292	367	347	303	356	526	488	512	425	582
13	7	19	326	304	379	362	409	364	222	397	377	342	371	333	362	292	366	346	302	354	526	488	512	426	582
13	7	34	325	303	378	361	408	362	221	395	376	341	370	332	361	291	365	345	301	354	527	488	513	426	583
13	7	49	324	302	375	360	407	361																	

Panel Temperature Data During Freezing

Time hour	Time min	Time sec	TEW18 DEG F	TEW17 DEG F	TEW16 DEG F	TEW15 DEG F	TEW14 DEG F	TEW13 DEG F	TEW12 DEG F	TEW11 DEG F	TEW10 DEG F	TEW9 DEG F	TEW8 DEG F	TEW7 DEG F	TEW6 DEG F	TEW5 DEG F	TEW4 DEG F	TEW3 DEG F	TEW2 DEG F	TEW1 DEG F	TEWU11 DEG F	TEWLH20 DEG F	TEWLH21 DEG F	TE070 DEG F	TE090 DEG F
13	11	33	311	288	355	343	387	343	207	375	352	326	350	316	343	275	345	330	289	345	531	490	515	428	585
13	11	48	309	287	354	342	385	342	206	374	350	325	349	315	342	274	344	328	289	344	532	490	515	428	586
13	12	3	308	287	352	341	384	341	205	373	349	324	347	315	341	273	343	328	287	344	532	490	515	428	586
13	12	18	307	286	351	340	382	340	203	372	348	323	346	314	340	273	341	327	287	343	533	490	515	428	587
13	12	33	306	285	350	339	381	339	203	371	346	322	345	313	339	272	340	326	286	343	533	490	515	428	587
13	12	48	305	284	349	338	380	337	202	369	345	321	344	312	338	271	339	326	286	343	534	490	515	430	588
13	13	3	305	284	347	337	378	336	201	368	344	320	343	311	337	270	338	325	285	343	534	490	515	430	588
13	13	18	305	282	346	336	377	335	201	367	342	319	341	310	336	269	337	324	284	341	534	491	516	430	589
13	13	33	303	282	345	335	375	334	200	366	341	318	341	309	335	268	336	323	284	341	534	491	516	430	589
13	13	48	303	281	344	334	374	333	200	365	340	318	339	308	334	267	334	322	284	341	535	491	516	430	589
13	14	3	302	280	343	333	373	332	199	363	338	317	338	307	333	265	333	321	283	339	535	491	516	430	589
13	14	18	301	280	342	332	371	331	198	363	337	316	337	306	332	264	332	320	283	339	535	491	515	430	589
13	14	33	300	279	340	332	370	330	197	361	336	315	336	305	331	264	331	319	281	338	535	491	515	430	589
13	14	49	299	278	339	330	368	329	195	360	334	314	334	305	330	263	329	318	280	338	536	491	515	429	588
13	15	4	298	277	337	330	367	328	194	359	333	313	334	304	329	262	328	317	280	337	536	491	515	429	588
13	15	19	297	276	336	328	366	328	194	358	332	312	332	303	328	261	326	316	279	337	536	491	515	429	588
13	15	34	296	276	335	328	364	327	194	357	331	312	331	302	327	260	325	315	279	336	536	491	515	429	588
13	15	49	296	274	334	327	363	325	193	356	330	311	330	301	326	259	324	315	278	336	537	492	515	429	588
13	16	4	296	274	333	326	362	325	192	355	329	310	329	300	325	259	324	314	278	335	537	492	515	429	589
13	16	19	295	273	332	325	361	324	191	354	327	309	328	299	324	258	323	313	277	335	537	492	516	429	589
13	16	34	294	272	330	324	359	323	191	353	326	308	327	299	323	257	322	312	277	335	537	492	516	429	590
13	16	49	294	272	330	323	358	322	190	352	325	308	326	298	322	256	321	312	276	335	538	492	516	429	590
13	17	4	293	271	329	322	357	321	190	351	324	307	325	297	321	256	320	311	276	334	538	492	516	429	591
13	17	18	292	270	328	321	355	320	189	350	322	306	324	296	321	255	319	311	276	334	539	493	516	430	591
13	17	33	291	270	327	320	354	319	189	349	322	305	323	295	320	255	318	310	276	334	539	493	516	430	591
13	17	48	291	268	325	319	353	318	188	348	320	304	322	294	319	254	317	309	275	334	540	493	517	430	592
13	18	3	289	268	324	319	352	317	187	347	319	303	321	293	318	253	317	308	275	333	540	493	517	430	592
13	18	18	288	267	324	318	350	316	187	346	318	303	320	293	317	252	316	308	274	333	540	493	517	430	592
13	18	33	288	265	323	317	349	315	185	344	317	302	319	292	316	252	315	307	274	332	540	493	517	430	592
13	18	48	287	265	322	316	348	314	185	344	316	301	318	291	316	251	314	306	273	332	541	493	517	430	592
13	19	3	287	264	320	315	347	314	185	343	315	300	317	290	315	250	313	305	272	331	541	493	517	429	592
13	19	18	286	264	319	314	346	313	184	342	314	300	316	290	314	249	312	304	273	331	541	493	517	429	591
13	19	33	283	263	318	314	345	312	182	341	313	299	315	289	313	248	311	303	272	330	541	493	517	429	591
13	19	48	283	263	317	313	344	311	181	340	312	298	314	288	312	247	309	303	272	330	541	493	517	429	591
13	20	3	283	262	316	312	343	310	181	339	310	297	313	287	312	246	308	302	271	330	541	493	517	429	590
13	20	19	282	261	315	311	341	309	180	338	309	296	312	286	310	246	307	300	271	330	541	493	517	429	590
13	20	34	282	261	315	310	340	309	179	337	308	296	311	285	310	245	306	300	271	329	542	493	517	429	591
13	20	49	281	259	314	310	339	308	180	336	308	295	310	285	309	244	305	299	270	329	542	493	517	429	591
13	21	4	280	259	312	309	338	307	179	335	306	294	309	284	308	243	305	299	270	329	543	493	517	429	592
13	21	19	279	259	311	308	337	306	179	334	306	293	308	283	307	243	304	298	270	329	543	493	517	429	592
13	21	34	279	257	310	307	336	305	178	334	305	293	308	282	306	242	303	298	270	329	544	494	518	429	593
13	21	49	278	257	310	306	335	304	178	333	304	292	306	281	306	241	302	297	270	329	544	494	518	429	594
13	22	4	278	257	309	306	334	303	177	332	303	291	306	281	305	240	302	296	269	328	544	494	518	430	595
13	22	18	277	256	308	305	333	302	177	331	302	291	305	280	304	240	300	296	269	328	544	494	518	430	595
13	22	33	277	255	308	304	332	302	176	330	301	290	304	279	303	239	299	295	269	328	545	494	518	429	595
13	22	48	276	255	306	303	331	301	175	329	300	289	303	278	303	238	299	294	268	328	545	494	518	429	595
13	23	3	275	254	305	303	330	300	174	328	299	288	302	277	302	238	298	293	268	328	545	494	518	429	595
13	23	18	275	254	304	302	329	299	174	328	298	287	301	277	301	237	297	293	268	327	545	494	518	429	594
13	23	33	273	253	303	301	328	299	174	327	297	287	300	276	300	236	296	292	268	327	546	494	518	429	594
13	23	48	273	252	303	300	327	298	174	326	296	286	299	275	300	236	295	291	268	327	546	494	518	429	593
13	24	3	272	252	302	300	326	297	173	325	295	285	299	275	299	235	294	290	268	326	546	494	518	428	593
13	24	18	271	250	301	299	325	296	172	324	294	285	297	274	298	234	293	290	267	326	546	494	518	428	593
13	24	33	271	250	300	298	325	296	172	323	294	284	297	273	297	233	293	289	267	326	547	495	518	429	593
13	24	48	270	248	298	297	324	295	171	322	293	283	296	272	296	233	292	289	267	326	547	495	518	429	593
13	25	3	269	248	298	297	322	294	170	321	291	282	295	272	296	232	291	288	268	326	547	495	518	429	594
13	25	18	268	247	297	296	321	293	170	321	291	282	294	271	295	231	290	287	267	326	547	495	518	429	594
13	25	33	268	247	296	295	320	292	169	320	290	281	294	270	294	231	290	287	267	325	548	495	518	429	594
13	25	48	267	246																					

Panel Temperature Data During Freezing

Time hour	Time min	Time sec	TEW18 DEG F	TEW17 DEG F	TEW16 DEG F	TEW15 DEG F	TEW14 DEG F	TEW13 DEG F	TEW12 DEG F	TEW11 DEG F	TEW10 DEG F	TEW9 DEG F	TEW8 DEG F	TEW7 DEG F	TEW6 DEG F	TEW5 DEG F	TEW4 DEG F	TEW3 DEG F	TEW2 DEG F	TEW1 DEG F	TEWU11 DEG F	TEWLH20 DEG F	TEWLH21 DEG F	TE970 DEG F	TE990 DEG F
13	29	33	258	236	283	283	307	280	160	307	278	270	279	259	282	221	275	276	265	322	552	499	519	433	563
13	29	48	256	236	282	283	306	279	160	307	278	269	279	258	281	220	274	275	265	322	552	499	518	433	563
13	30	3	255	235	281	282	305	278	159	306	275	268	278	257	281	219	274	275	265	322	552	499	518	433	563
13	30	18	255	235	279	281	304	278	158	305	274	267	277	256	280	218	273	274	265	322	553	499	518	434	563
13	30	34	254	234	279	280	303	277	158	304	273	267	276	256	279	218	272	273	266	321	553	500	518	434	564
13	30	48	254	234	279	280	302	276	158	304	272	266	276	255	278	218	272	273	265	321	554	500	519	434	564
13	31	4	254	233	277	279	301	275	157	303	271	265	275	254	278	217	271	272	265	321	554	500	519	434	564
13	31	19	253	233	276	278	300	274	156	302	270	265	274	253	277	217	270	272	265	321	555	500	519	434	564
13	31	34	253	232	276	278	300	273	156	301	269	264	273	253	276	216	269	271	265	320	555	500	519	434	563
13	31	49	252	232	275	277	299	273	155	301	268	263	272	252	275	216	269	270	265	320	555	500	519	434	563
13	32	4	252	232	275	276	298	272	155	300	268	263	271	251	275	215	268	269	265	319	555	500	519	434	562
13	32	19	252	230	274	276	297	272	153	299	267	262	270	251	274	214	267	269	263	319	555	500	519	434	562
13	32	34	250	230	273	275	296	271	153	298	266	261	270	250	273	213	266	268	263	318	555	500	519	434	561
13	32	49	250	229	271	274	296	270	153	298	265	260	269	249	272	212	264	267	263	318	556	500	519	434	560
13	33	4	250	229	271	273	295	270	152	297	264	260	268	249	272	212	264	266	262	316	558	501	519	434	560
13	33	19	249	228	270	273	294	269	153	296	264	259	267	248	271	211	263	266	262	316	556	501	520	434	559
13	33	33	249	228	269	272	293	268	152	295	263	259	266	247	270	211	262	266	262	316	556	501	520	434	559
13	33	48	248	227	269	272	293	267	152	295	262	258	265	247	270	210	262	265	261	316	557	501	520	434	560
13	34	3	246	227	268	271	292	267	151	294	261	257	265	246	269	210	261	264	260	315	557	502	520	434	560
13	34	18	246	226	266	270	291	266	151	293	261	256	264	245	268	209	260	264	260	315	557	502	521	434	560
13	34	33	246	226	265	270	290	265	151	292	260	256	263	244	268	209	260	264	260	315	557	502	521	434	561
13	34	48	246	225	265	269	290	264	151	292	259	256	263	244	267	208	259	263	260	315	558	503	521	435	562
13	35	3	245	225	264	268	289	264	151	291	258	255	262	243	266	208	259	263	259	314	558	503	521	435	562
13	35	18	245	223	264	267	288	263	150	290	258	254	261	243	266	207	258	262	259	314	559	503	522	435	564
13	35	33	244	223	263	267	287	262	150	290	257	254	261	242	265	206	257	262	258	313	559	505	522	435	564
13	35	48	244	223	263	266	287	262	150	289	256	253	260	241	264	206	256	261	258	313	559	505	523	435	564
13	36	3	244	223	262	266	286	261	149	289	256	253	259	241	264	205	256	260	257	313	559	505	523	435	564
13	36	18	243	223	262	265	285	260	149	288	255	252	258	240	263	205	255	260	256	313	560	505	523	434	564
13	36	34	243	221	261	264	284	260	149	287	255	252	259	241	264	206	255	260	256	312	560	506	523	434	564
13	36	49	243	221	259	264	284	259	149	287	254	252	259	242	264	208	256	262	257	313	560	506	523	434	563
13	37	4	242	220	259	263	283	259	149	286	254	251	260	244	265	210	258	264	258	314	560	506	523	434	563
13	37	19	240	219	258	263	283	258	149	286	254	252	261	246	266	213	259	266	259	316	560	507	523	434	563
13	37	34	240	219	257	262	282	257	149	285	254	252	262	249	267	216	261	268	259	317	560	507	523	434	563
13	37	49	239	219	257	261	281	257	149	284	254	252	264	252	269	221	263	270	261	318	561	508	524	434	562
13	38	4	239	218	256	261	280	256	148	284	254	252	265	255	271	224	265	273	262	319	561	509	524	434	562
13	38	19	238	218	256	260	279	255	148	283	254	252	267	258	273	228	267	275	262	322	561	509	524	434	563
13	38	34	238	216	255	259	279	255	148	283	254	252	268	262	275	232	269	278	263	323	562	509	525	434	563
13	38	49	238	216	254	259	278	254	148	282	254	253	270	264	277	235	271	280	264	324	562	510	525	434	564
13	39	4	237	215	253	258	277	254	148	282	255	253	272	268	279	239	273	282	265	325	562	511	525	434	565
13	39	19	237	215	251	258	276	253	148	281	255	254	274	271	281	242	275	284	265	328	562	511	525	434	565
13	39	34	236	214	251	256	275	252	147	280	255	253	276	274	283	246	277	287	266	329	563	513	526	434	566

Checkvalve Cycling Data

CRTF NET-90 99 POINT DATA FILE									
TEST DATE: Wed Dec 15 1993 7:39:18 am									
Time	Time	Time	FT720	PF-001	FT730	FT800	PT710	PP-001	PT720
hour	min	sec	Lt/min	Lt/min	Lt/min	Lt/min	PSIG	PSIG	PSIG
7	40	3	0	56	4	0	-2	-2	-1
7	40	18	0	68	4	0	-2	-2	-1
7	40	33	0	67	3	0	-2	-2	-1
7	40	48	0	61	3	0	-2	-2	-1
7	46	3	0	58	5	0	-2	-2	-1
7	46	6	0	58	5	0	-2	-2	-1
7	46	10	0	58	5	0	-2	-2	-1
7	46	13	0	58	5	0	-2	-2	-1
7	46	16	0	58	5	0	-2	-2	-1
7	46	19	0	58	5	0	-2	-2	-1
7	46	22	0	60	5	0	-2	-2	-1
7	46	25	0	55	5	0	-2	-2	-1
7	46	28	0	69	5	0	-2	-2	-1
7	46	31	0	62	5	0	-2	-2	-1
7	46	34	0	56	5	0	-2	-2	-1
7	46	38	0	56	5	0	-2	-2	-1
7	46	41	0	61	5	0	-2	-2	-1
7	46	44	0	61	5	0	-2	-2	-1
7	46	47	0	61	5	0	-2	-2	-1
7	46	50	0	61	5	0	-2	-2	-1
7	46	53	0	61	1	0	-2	-2	-1
7	46	56	0	68	1	0	-2	-2	-1
7	46	59	0	59	1	0	-2	-2	-1
7	47	2	0	59	1	0	-2	-2	-1
7	47	6	0	66	7	0	-2	-2	-1
7	47	9	0	66	1	0	-2	-2	-1
7	47	12	0	66	1	0	-2	-2	-1
7	47	15	0	66	1	0	-2	-2	-1
7	47	18	0	55	8	0	-2	-2	-1
7	47	21	0	69	2	0	-2	-2	-1
7	47	34	0	76	6	0	-2	-2	-1
7	47	49	0	64	5	0	-2	-2	-1
7	48	4	0	68	5	0	-2	-2	-1
7	48	19	0	58	5	0	-2	-2	-1
7	48	34	0	71	5	0	-2	-2	-1
7	48	49	0	68	1	0	-2	-2	-1
7	49	4	0	53	7	0	-2	-2	-1
7	49	19	0	50	7	0	-2	-2	-1
7	49	34	0	61	2	0	-2	-2	-1
7	49	49	0	56	2	0	-2	-2	-1
7	50	4	0	56	2	0	-2	-2	-1
7	50	18	0	56	2	0	-2	-2	-1
7	50	33	0	56	7	0	-2	-2	-1
7	50	48	0	51	2	0	-2	-2	-1
7	51	3	0	50	1	0	-2	-2	-1
7	51	18	0	50	8	0	-2	-2	-1
7	51	33	0	45	7	0	-2	-2	-1
7	51	48	0	45	0	0	-2	-2	-1
7	52	3	0	51	2	0	-2	-2	-1
7	52	18	0	51	2	0	-2	-2	-1
7	52	33	0	56	7	0	-2	-2	-1
7	52	48	0	56	7	0	-2	-2	-1
7	53	3	0	56	5	0	-2	-2	-1
7	53	19	0	51	5	0	-2	-2	-1
7	53	34	0	55	5	0	-2	-2	-1
7	53	49	0	52	5	0	-2	-2	-1
7	54	4	0	52	1	0	-2	-2	-1
7	54	19	-1	52	5	0	-2	-2	-1
7	54	34	-1	52	5	0	-2	-2	-1
7	54	49	-1	50	5	0	-2	-2	-1
7	55	4	-1	50	5	0	-2	-2	-1
7	55	19	0	55	1	0	-2	-2	-1
7	55	33	214	322	2	0	106	83	-1
7	55	49	320	309	2	0	111	103	-1
7	56	3	320	303	2	0	110	103	-1
7	56	18	392	367	225	0	46	33	0
7	56	33	403	385	192	0	62	49	2
7	56	48	397	379	186	0	64	50	4
7	57	3	392	378	173	0	66	52	6

Checkvalve Cycling Data

Time hour	Time min	Time sec	FT720 Lt/min	PF-001 Lt/min	FT730 Lt/min	FT800 Lt/min	PT710 PSIG	PP-001 PSIG	PT720 PSIG
7	57	18	386	361	162	0	68	53	10
7	57	33	386	373	148	0	71	57	14
7	57	48	387	302	5	0	68	55	15
7	58	3	387	289	5	0	68	55	15
7	58	18	387	336	5	0	68	55	15
7	58	34	387	352	5	0	68	55	15
7	58	49	74	335	77	0	-3	16	13
7	59	4	4	-4	4	0	-6	31	10
7	59	19	4	-4	4	0	-6	31	9
7	59	34	4	-4	4	0	-6	30	9
7	59	49	4	-4	4	0	-6	30	8
8	0	4	0	-5	0	0	-6	30	8
8	0	19	0	-5	1	0	-6	30	8
8	0	33	0	-5	6	0	-6	30	7
8	0	48	0	-5	6	0	-6	30	7
8	1	3	0	-5	1	0	-6	30	6
8	1	18	0	-5	2	0	-6	30	6
8	1	33	0	-5	7	0	-6	30	6
8	1	48	0	-5	7	0	-6	30	5
8	2	3	0	-5	1	0	-6	30	5
8	2	18	0	-5	0	0	-6	30	5
8	2	33	0	-5	0	0	-6	30	4
8	2	48	0	-5	1	0	-6	29	4
8	3	3	0	-5	1	0	-6	29	4
8	3	18	0	-5	1	0	-6	29	4
8	3	34	0	-5	0	0	-6	29	3
8	3	49	0	-5	6	0	-6	28	3
8	4	4	0	-5	7	0	-6	28	3
8	4	19	0	-5	1	0	-6	28	3
8	4	34	0	-5	7	0	-6	28	2
8	4	49	0	-5	7	0	-6	28	2
8	5	4	0	-5	1	0	-6	28	2
8	5	19	0	-5	1	0	-6	28	2
8	5	33	0	-5	0	0	-6	28	2
8	5	48	0	-5	0	0	-6	27	1
8	6	3	3	-5	6	0	-6	5	0
8	6	18	399	-5	221	0	56	49	0
8	6	33	399	388	188	0	63	51	2
8	6	48	393	359	183	0	64	51	5
8	7	3	393	366	171	0	66	53	8
8	7	18	387	367	159	0	69	55	12
8	7	33	360	358	30	0	67	55	16
8	7	48	387	361	4	0	68	55	15
8	8	4	387	382	4	0	68	55	15
8	8	19	387	382	4	0	68	55	15
8	8	34	387	347	4	0	68	55	15
8	8	49	387	320	6	0	68	55	15
8	9	4	387	359	5	0	68	55	15
8	9	19	387	371	5	0	68	55	15
8	9	34	387	309	5	0	68	55	15
8	9	49	386	361	5	0	68	55	15
8	10	4	386	352	6	0	68	55	15
8	10	19	386	370	6	0	68	55	15
8	10	34	386	352	2	0	68	55	15
8	10	49	386	361	1	0	68	55	15
8	11	4	386	364	1	0	68	55	15
8	11	19	386	349	1	0	68	55	15
8	11	33	386	355	1	0	68	54	15
8	11	48	386	384	1	0	68	54	15
8	12	3	386	383	0	0	68	54	15
8	12	18	386	381	2	0	68	54	15
8	12	33	386	373	6	0	68	55	15
8	12	48	387	352	1	0	68	55	15
8	13	3	387	411	1	0	68	55	15
8	13	18	387	399	1	0	68	55	15
8	13	33	387	360	1	0	68	55	15
8	13	48	386	401	0	0	68	55	15
8	14	4	386	359	0	0	68	55	15
8	14	19	386	355	2	0	68	55	15
8	14	34	386	385	1	0	68	55	15
8	14	49	386	383	2	0	68	55	15

Checkvalve Cycling Data

Time	Time	Time	FT220	PF-001	FT730	FT800	PT710	PP-001	PT720
hour	min	sec	Lt/min	Lt/min	Lt/min	Lt/min	PSIG	PSIG	PSIG
8	15	4	386	362	6	0	68	55	15
8	15	19	386	390	2	0	68	55	15
8	15	34	387	378	2	0	68	55	15
8	15	49	387	383	5	0	68	55	15
8	16	4	387	370	0	0	68	55	15
8	16	19	387	398	1	0	68	55	15
8	16	33	387	349	1	0	68	55	15
8	16	48	388	351	1	0	68	55	15
8	17	3	388	353	1	0	68	55	15
8	17	18	388	364	1	0	68	55	15
8	17	33	388	364	1	0	68	55	15
8	17	48	387	360	2	0	68	55	15
8	18	3	387	352	2	0	68	55	15
8	18	18	387	358	1	0	68	55	15
8	18	33	387	325	1	0	68	55	15
8	18	48	387	360	1	0	68	55	15
8	19	4	387	378	1	0	68	55	15
8	19	19	387	342	1	0	68	55	15
8	19	34	388	340	7	0	68	55	15
8	19	49	388	342	7	0	68	55	15
8	20	4	388	365	6	0	68	55	15
8	20	19	388	314	7	0	68	55	15
8	20	34	388	322	1	0	68	54	15
8	20	49	388	385	2	0	68	54	15
8	21	4	388	364	2	0	68	54	15
8	21	19	388	356	2	0	68	54	15
8	21	34	388	386	1	0	68	55	15
8	21	48	387	372	7	0	68	55	15
8	22	3	387	359	1	0	68	55	15
8	22	18	387	398	2	0	68	55	15
8	22	33	387	354	1	0	68	55	15
8	22	48	386	357	6	0	68	55	15
8	23	3	386	378	1	0	68	55	15
8	23	18	386	359	1	0	68	55	15
8	23	33	386	335	2	0	68	55	15
8	23	48	388	366	2	0	68	55	15
8	24	3	388	382	0	0	68	55	15
8	24	18	388	337	2	0	68	55	15
8	24	34	388	348	2	0	68	55	15
8	24	49	388	383	2	0	68	55	15
8	25	4	388	350	2	0	68	55	15
8	25	19	388	354	2	0	68	55	15
8	25	34	388	325	0	0	68	55	15
8	25	49	387	371	2	0	68	55	15
8	26	4	387	374	2	0	68	55	15
8	26	19	387	403	1	0	68	55	15
8	26	34	386	362	1	0	68	55	15
8	26	49	386	376	1	0	68	55	15
8	27	4	386	402	2	0	68	55	15
8	27	19	386	354	1	0	68	55	15
8	27	33	386	367	2	0	68	55	15
8	27	48	387	366	5	0	68	55	15
8	28	3	387	379	5	0	68	55	15
8	28	18	387	335	5	0	68	55	15
8	28	33	387	375	5	0	68	54	15
8	28	48	387	337	8	0	68	54	15
8	29	3	387	361	2	0	68	54	15
8	29	18	387	303	2	0	68	54	15
8	29	33	387	371	2	0	68	55	15
8	29	48	388	338	0	0	68	55	15
8	30	4	388	375	7	0	68	55	15
8	30	19	388	401	1	0	68	53	15
8	30	34	389	357	7	0	68	53	15
8	30	49	389	363	2	0	68	53	15
8	31	4	389	379	6	0	68	43	15
8	31	19	1	-3	4	0	-6	38	17
8	31	34	1	-3	4	0	-6	38	16
8	31	49	1	-3	4	0	-6	38	14
8	32	3	1	-3	4	0	-6	36	14
8	32	18	0	-5	6	0	-6	36	13
8	32	33	0	-5	7	0	-6	36	12

Checkvalve Cycling Data

Time hour	Time min	Time sec	FT720 Lt/min	PF-001 Lt/min	FT730 Lt/min	FT800 Lt/min	PT710 PSIG	PP-001 PSIG	PT720 PSIG
8	32	48	0	-5	2	0	-6	36	11
8	33	3	0	-5	6	0	-6	35	11
8	33	18	0	-5	7	0	-6	35	10
8	33	33	0	-5	0	0	-6	35	10
8	33	48	0	-5	7	0	-6	35	9
8	34	3	0	-5	1	0	-6	35	9
8	34	18	6	-5	1	0	-6	35	8
8	34	34	6	-5	2	0	-6	35	8
8	34	49	1	-5	7	0	-6	35	7
8	35	4	1	-5	1	0	-6	33	7
8	35	19	6	-5	2	0	-6	33	6
8	35	34	1	-5	2	0	-6	33	6
8	35	49	1	-5	2	0	-6	32	5
8	36	4	6	-5	1	0	-6	32	5
8	36	19	0	-5	1	0	-6	32	5
8	36	34	0	-5	2	0	-6	30	5
8	36	49	0	-5	8	0	-6	30	4
8	37	3	0	-5	0	0	-6	30	4
8	37	18	0	-5	1	0	-6	30	4
8	37	33	0	-5	1	0	-6	29	3
8	37	48	0	-5	0	0	-6	29	3
8	38	3	0	-5	1	0	-6	29	3
8	38	18	0	-5	2	0	-6	29	3
8	38	33	0	-5	2	0	-6	27	2
8	38	48	0	-5	2	0	-6	27	2
8	39	3	0	-5	1	0	-6	27	2
8	39	18	0	-5	2	0	-6	27	2
8	39	34	0	-5	2	0	-6	26	2
8	39	49	19	-5	9	0	-6	19	1
8	40	4	253	-5	203	0	58	50	0
8	40	19	400	358	195	0	62	52	2
8	40	34	394	380	184	0	65	52	5
8	40	49	394	348	172	0	67	52	8
8	41	4	388	355	160	0	69	55	12
8	41	19	382	351	45	0	68	55	16
8	41	34	382	365	7	0	68	55	16
8	41	49	382	365	1	0	68	55	15
8	42	4	388	367	1	0	68	55	15
8	42	19	388	354	2	0	68	55	15
8	42	34	388	364	2	0	68	55	15
8	42	48	388	380	2	0	68	55	15
8	43	3	388	350	2	0	68	55	15
8	43	18	388	373	2	0	68	55	15
8	43	33	388	349	1	0	68	55	15
8	43	48	388	352	2	0	68	55	15
8	44	3	386	355	7	0	68	55	15
8	44	18	386	399	5	0	68	55	15
8	44	33	386	307	0	0	68	55	15
8	44	48	386	356	7	0	68	55	15
8	45	3	387	379	7	0	68	55	15
8	45	19	387	376	7	0	68	55	15
8	45	34	387	386	1	0	68	55	15
8	45	49	387	354	2	0	68	55	15
8	46	4	386	335	2	0	68	55	15
8	46	19	386	393	2	0	68	55	15
8	46	34	386	333	0	0	68	55	15
8	46	49	386	333	1	0	68	55	15
8	47	4	387	344	7	0	68	55	15
8	47	19	387	397	2	0	68	55	15
8	47	33	387	340	0	0	68	55	15
8	47	48	387	366	1	0	68	55	15
8	48	3	385	374	0	0	68	55	15
8	48	18	385	336	2	0	68	55	15
8	48	33	385	353	1	0	68	55	15
8	48	48	385	394	2	0	68	55	15
8	49	3	389	381	4	0	68	55	15
8	49	18	389	343	4	0	68	55	15
8	49	33	389	361	4	0	68	55	15
8	49	48	389	376	4	0	68	55	15
8	50	3	387	355	2	0	68	55	15
8	50	18	387	338	2	0	68	55	15

Checkvalve Cycling Data

Time	Time	Time	FT720	PF-001	FT730	FT800	PT710	PP-001	PT720
hour	min	sec	Lt/min	Lt/min	Lt/min	Lt/min	PSIG	PSIG	PSIG
8	50	34	387	301	2	0	68	55	15
8	50	49	387	386	2	0	68	55	15
8	51	4	386	347	2	0	68	55	15
8	51	19	386	366	1	0	68	55	15
8	51	34	386	303	2	0	68	55	15
8	51	49	386	359	2	0	68	55	15
8	52	4	388	341	7	0	68	55	15
8	52	19	388	347	2	0	68	55	15
8	52	33	388	370	2	0	68	55	15
8	52	48	388	343	1	0	68	55	15
8	53	3	387	369	1	0	68	55	15
8	53	18	387	337	6	0	68	55	15
8	53	33	387	365	2	0	68	55	15
8	53	48	387	378	5	0	68	55	15
8	54	3	389	368	0	0	68	55	15
8	54	18	389	353	2	0	68	55	15
8	54	33	389	343	7	0	68	55	15
8	54	48	389	337	1	0	68	55	15
8	55	4	386	356	1	0	68	55	15
8	55	19	386	372	7	0	68	55	15
8	55	34	386	357	7	0	68	55	15
8	55	49	386	405	6	0	68	55	15
8	56	4	387	368	0	0	68	55	15
8	56	19	387	362	4	0	68	55	15
8	56	34	387	388	4	0	68	55	15
8	56	48	387	377	4	0	68	55	15
8	57	3	386	369	4	0	68	55	15
8	57	18	386	349	0	0	68	55	15
8	57	33	386	376	0	0	68	55	15
8	57	48	386	355	1	0	68	55	15
8	58	3	389	358	2	0	68	55	15
8	58	18	389	408	0	0	68	55	15
8	58	33	389	359	2	0	68	55	15
8	58	48	389	366	0	0	68	55	15
8	59	3	388	365	2	0	68	55	15
8	59	18	388	355	2	0	68	55	15
8	59	33	389	369	7	0	68	55	15
8	59	49	389	331	6	0	68	55	15
9	0	4	389	379	2	0	68	55	15
9	0	19	389	395	1	0	68	55	15
9	0	34	385	354	6	0	68	55	15
9	0	49	385	370	6	0	68	55	15
9	1	4	385	356	7	0	68	55	15
9	1	19	385	367	4	0	68	55	15
9	1	33	388	373	4	0	68	55	15
9	1	48	388	351	4	0	68	55	15
9	2	3	388	396	4	0	68	55	15
9	2	18	388	343	0	0	68	55	15
9	2	33	387	329	1	0	68	55	15
9	2	48	387	365	2	0	67	55	15
9	3	5	387	376	2	0	68	55	15
9	3	18	387	345	2	0	68	55	15
9	3	33	388	373	2	0	68	55	15
9	3	48	388	313	2	0	68	55	15
9	4	3	388	377	7	0	68	55	15
9	4	18	388	384	2	0	68	55	15
9	4	34	386	386	6	0	68	55	15
9	4	49	386	317	1	0	68	55	15
9	5	4	363	365	54	0	70	60	15
9	5	19	1	-3	5	0	-6	38	16
9	5	34	1	-3	5	0	-6	38	15
9	5	49	1	-3	5	0	-6	38	14
9	6	4	1	-3	5	0	-6	36	13
9	6	19	0	-5	0	0	-6	36	12
9	6	33	0	-5	2	0	-6	36	12
9	6	48	0	-5	6	0	-6	36	11
9	7	3	6	-5	0	0	-6	35	11
9	7	18	1	-5	1	0	-6	35	10
9	7	33	7	-5	2	0	-6	35	10
9	7	48	7	-5	8	0	-6	35	9
9	8	3	12	-5	6	0	-6	35	9

Checkvalve Cycling Data

Time hour	Time min	Time sec	FT720 L/min	PF-001 L/min	FT730 L/min	FT800 L/min	PT710 PSIG	PP-001 PSIG	PT720 PSIG	
9	8	18	9	-5	0	0	0	-6	35	8
9	8	33	4	-5	0	0	0	-6	35	7
9	8	48	4	-5	0	0	0	-6	35	7
9	9	4	4	-5	0	0	0	-6	33	6
9	9	19	4	-5	0	0	0	-6	33	6
9	9	34	4	-5	0	0	0	-6	33	6
9	9	49	0	-5	1	0	0	-6	32	5
9	10	4	0	-5	1	0	0	-6	32	5
9	10	19	0	-5	2	0	0	-6	32	5
9	10	34	0	-5	2	0	0	-6	30	4
9	10	49	0	-5	2	0	0	-6	30	4
9	11	4	0	-5	1	0	0	-6	30	4
9	11	18	0	-5	7	0	0	-6	29	4
9	11	34	2	-5	2	0	0	-6	29	3
9	11	48	2	-5	6	0	0	-6	29	3
9	12	3	2	-5	6	0	0	-6	29	3
9	12	18	2	-5	7	0	0	-6	27	3
9	12	33	0	-5	1	0	0	-6	27	2
9	12	48	0	-5	1	0	0	-6	27	2
9	13	3	0	-5	4	0	0	-6	27	2
9	13	18	0	-5	4	0	0	-6	26	2
9	13	33	0	-5	4	0	0	-6	26	2
9	13	48	5	-5	10	0	0	-6	12	0
9	14	3	396	118	194	0	62	52	52	1
9	14	18	397	367	189	0	63	52	52	3
9	14	33	391	363	177	0	65	52	52	6
9	14	48	391	366	165	0	68	54	54	10
9	15	3	385	360	153	0	70	57	57	14
9	15	19	387	355	4	0	68	55	55	16
9	15	34	387	367	4	0	68	55	55	15
9	15	49	387	354	4	0	68	55	55	15
9	16	4	387	367	4	0	68	55	55	15
9	16	19	385	362	5	0	68	55	55	15
9	16	34	385	341	0	0	68	55	55	15
9	16	49	385	406	4	0	68	55	55	15
9	17	4	385	355	4	0	68	55	55	15
9	17	18	386	326	4	0	68	55	55	15
9	17	33	386	365	4	0	68	55	55	15
9	17	48	386	353	2	0	68	55	55	15
9	18	3	386	381	2	0	68	55	55	15
9	18	18	386	324	2	0	68	55	55	15
9	18	33	386	322	2	0	68	55	55	15
9	18	48	386	363	5	0	68	55	55	15
9	19	3	386	352	7	0	68	55	55	15
9	19	18	386	394	1	0	68	55	55	15
9	19	33	386	387	7	0	68	55	55	15
9	19	48	386	345	1	0	68	55	55	15
9	20	3	386	340	1	0	68	55	55	15
9	20	19	387	407	1	0	68	55	55	15
9	20	34	387	386	0	0	68	55	55	15
9	20	49	387	368	8	0	68	55	55	15
9	21	4	387	355	2	0	68	55	55	15
9	21	19	387	363	6	0	68	55	55	15
9	21	34	387	411	6	0	68	55	55	15
9	21	49	387	393	0	0	68	55	55	15
9	22	4	387	348	1	0	68	55	55	15
9	22	19	387	361	0	0	68	55	55	15
9	22	34	387	361	1	0	68	55	55	15
9	22	48	387	359	2	0	68	55	55	15
9	23	3	387	372	0	0	68	55	55	15
9	23	18	386	338	8	0	68	55	55	15
9	23	33	386	365	2	0	68	55	55	15
9	23	48	386	333	2	0	67	55	55	15
9	24	3	386	380	6	0	68	55	55	15
9	24	18	387	308	6	0	68	55	55	15
9	24	33	387	366	1	0	68	55	55	15
9	24	48	387	328	1	0	68	55	55	15
9	25	3	387	391	8	0	68	55	55	15
9	25	18	388	362	2	0	68	55	55	15
9	25	34	388	325	1	0	68	55	55	15
9	25	49	388	349	8	0	67	55	55	15

Checkvalve Cycling Data

Time	Time	Time	FT720	PF-001	FT730	FT800	PT710	PP-001	PT720
hour	min	sec	Lt/min	Lt/min	Lt/min	Lt/min	PSIG	PSIG	PSIG
9	26	4	388	336	4	0	68	55	15
9	26	19	387	372	4	0	68	55	15
9	26	34	387	362	4	0	68	55	15
9	26	49	387	392	4	0	68	55	15
9	27	3	387	371	8	0	68	55	15
9	27	18	384	296	1	0	68	55	15
9	27	33	384	320	6	0	68	55	15
9	27	48	384	369	1	0	68	55	15
9	28	3	384	370	2	0	68	55	15
9	28	18	387	372	0	0	68	55	15
9	28	33	387	353	6	0	68	55	15
9	28	48	387	342	7	0	68	55	15
9	29	3	387	354	1	0	68	55	15
9	29	18	388	366	1	0	68	55	15
9	29	33	388	360	1	0	68	55	15
9	29	48	388	374	6	0	68	55	15
9	30	4	388	330	0	0	68	55	15
9	30	19	387	345	2	0	68	55	15
9	30	34	387	380	7	0	67	55	15
9	30	49	387	349	1	0	68	55	15
9	31	4	387	371	1	0	68	55	15
9	31	19	388	385	2	0	68	55	15
9	31	34	388	352	7	0	68	55	15
9	31	49	388	351	0	0	68	55	15
9	32	4	388	325	1	0	68	55	15
9	32	19	387	359	7	0	68	55	15
9	32	34	387	365	2	0	68	55	15
9	32	48	387	354	2	0	68	55	15
9	33	3	387	343	7	0	68	55	15
9	33	18	385	316	2	0	68	55	15
9	33	33	385	344	1	0	68	55	15
9	33	48	385	287	1	0	68	55	15
9	34	3	385	334	1	0	68	55	15
9	34	18	385	352	1	0	67	55	15
9	34	33	385	351	6	0	68	55	15
9	34	48	385	345	7	0	68	55	15
9	35	4	385	334	7	0	68	55	15
9	35	19	386	401	2	0	68	55	15
9	35	34	386	346	6	0	68	55	15
9	35	49	391	361	1	0	68	55	15
9	36	4	385	381	1	0	68	55	15
9	36	19	385	309	1	0	68	55	15
9	36	34	385	392	1	0	68	55	15
9	36	49	385	336	1	0	68	55	15
9	37	4	388	331	1	0	67	55	15
9	37	19	388	368	1	0	68	55	15
9	37	33	388	314	8	0	68	55	15
9	37	48	388	343	8	0	68	55	15
9	38	3	388	361	2	0	68	55	15
9	38	18	388	360	2	0	68	55	15
9	38	35	388	364	6	0	68	55	15
9	38	48	388	372	0	0	68	55	15
9	39	3	377	315	7	0	78	69	15
9	39	18	3	2	3	0	-6	36	15
9	39	33	3	-4	3	0	-6	36	14
9	39	48	3	-4	3	0	-6	36	13
9	40	3	3	-4	3	0	-6	36	12
9	40	19	0	-5	4	0	-6	35	12
9	40	34	0	-5	4	0	-6	35	11
9	40	49	0	-5	4	0	-6	35	11
9	41	4	0	-5	4	0	-6	35	10
9	41	19	0	-5	2	0	-6	35	10
9	41	34	0	-5	2	0	-6	35	9
9	41	49	0	-5	0	0	-6	35	9

Thermal Shock Data for Components

CRTF NET-90 99 POINT DATA FILE				Check	4"	6"
TEST DATE: Tue May 3 1994 8:52:37				valve	flange	flange
Time	Time	Time	FT720	TEPL-5	TEPL-8	TEPL-12
hour	min	sec	Lt/min	DEG F	DEG F	DEG F
8	53	3	0	72	69	92
8	53	18	0	72	69	92
8	53	33	0	72	69	92
8	53	48	0	72	70	92
8	54	3	0	72	70	92
8	54	19	0	72	70	92
8	54	34	0	72	70	92
8	54	49	0	71	68	91
8	55	4	0	71	68	91
8	55	19	0	71	68	91
8	55	34	0	71	68	91
8	55	49	0	72	70	92
8	56	4	0	72	70	92
8	56	18	0	72	70	92
8	56	33	0	72	70	92
8	56	48	0	72	69	92
8	57	3	0	72	69	92
8	57	18	323	72	69	92
8	57	33	355	134	69	92
8	57	48	361	223	80	98
8	58	3	361	279	105	122
8	58	18	361	329	154	145
8	58	33	361	367	191	168
8	58	48	360	391	241	193
8	59	3	360	415	283	228
8	59	18	360	438	320	265
8	59	33	360	451	344	288
8	59	49	360	461	367	311
9	0	4	360	472	390	336
9	0	19	360	484	402	347
9	0	34	360	496	414	372
9	0	49	361	507	425	384
9	1	4	361	507	425	384
9	1	19	361	518	437	395
9	1	34	361	518	448	407
9	1	49	359	530	448	407
9	2	3	359	530	448	418
9	2	18	359	541	461	418
9	2	33	359	541	461	429
9	2	48	359	541	461	429
9	3	3	359	552	472	441
9	3	18	359	552	472	441
9	3	33	359	552	472	441
9	3	48	357	552	472	441
9	4	3	357	561	482	452
9	4	18	357	561	482	452
9	4	33	357	561	482	452
9	4	49	361	561	482	461

Thermal Shock Data for Components

Time hour	Time min	Time sec	FT720 Lt/min	TEPL-5 DEG F	TEPL-8 DEG F	TEPL-12 DEG F
9	5	4	361	568	492	461
9	5	19	361	568	492	461
9	5	34	361	568	492	461
9	5	49	359	568	492	472
9	6	4	359	572	500	472
9	6	19	359	572	500	472
9	6	34	359	572	500	472
9	6	48	358	572	500	479
9	7	3	358	575	505	479
9	7	18	358	575	505	479
9	7	33	358	575	505	479
9	7	48	358	575	505	488
9	8	3	358	575	512	488
9	8	18	358	578	512	488
9	8	33	358	578	512	488
9	8	48	359	578	512	495
9	9	3	359	578	516	495
9	9	19	359	579	516	495
9	9	34	359	579	516	495
9	9	49	360	579	516	502
9	10	4	360	579	523	502
9	10	19	360	581	523	502
9	10	34	360	581	523	502
9	10	49	359	581	523	507
9	11	3	359	581	526	507
9	11	18	359	581	526	507
9	11	33	359	581	526	507
9	11	48	358	581	526	507
9	12	3	358	581	530	512
9	12	18	358	583	530	512
9	12	33	358	583	530	512
9	12	48	358	583	530	512
9	13	3	358	583	535	518
9	13	19	358	584	535	518
9	13	34	358	584	535	518
9	13	49	358	584	535	518
9	14	4	358	584	537	522
9	14	19	358	584	537	522
9	14	34	358	584	537	522
9	14	49	358	584	537	522
9	15	4	358	584	542	526
9	15	18	358	586	542	526
9	15	33	358	586	542	526
9	15	48	357	586	542	526
9	16	3	357	586	544	530
9	16	18	357	585	544	530
9	16	33	357	585	544	530
9	16	48	357	585	544	530
9	17	3	357	585	548	533
9	17	18	357	586	548	533

Thermal Shock Data for Components

Time hour	Time min	Time sec	FT720 Lt/min	TEPL-5 DEG F	TEPL-8 DEG F	TEPL-12 DEG F
9	17	33	357	586	548	533
9	17	49	358	586	548	533
9	18	4	358	586	551	537
9	18	19	358	587	551	537
9	18	34	358	587	551	537
9	18	49	358	587	551	537
9	19	4	358	587	552	540
9	19	18	358	587	552	540
9	19	33	358	587	552	540
9	19	48	358	587	552	540
9	20	3	358	587	556	543
9	20	18	358	588	556	543
9	20	33	358	588	556	543
9	20	48	359	588	556	543
9	21	4	359	588	557	545
9	21	19	359	588	557	545
9	21	34	359	588	557	545
9	21	49	360	588	557	545
9	22	4	360	588	557	548
9	22	19	360	590	561	548
9	22	34	360	590	561	548
9	22	49	357	590	561	548
9	23	4	357	590	561	550
9	23	19	357	590	562	550
9	23	34	357	590	562	550
9	23	49	357	590	562	550
9	24	3	357	590	562	552
9	24	18	357	591	564	552
9	24	33	357	591	564	552
9	24	48	357	591	564	552
9	25	3	357	591	564	555
9	25	18	357	591	567	555
9	25	33	357	591	567	555
9	25	48	357	591	567	555
9	26	3	357	591	567	556
9	26	19	357	591	567	556
9	26	34	357	591	567	556
9	26	49	357	591	567	556
9	27	4	357	591	567	558
9	27	19	357	591	570	558
9	27	34	357	593	570	558
9	27	48	356	593	570	558
9	28	3	356	593	570	560
9	28	18	356	593	570	560
9	28	33	356	592	570	560
9	28	48	358	592	570	560

Data for Slow Cool Down of Components with Fan Simulating Nightly Cool Down.

				Check 4"flg 6"flg							
				Time	Z 521	Z 522	Z 523	Z 524	Z 525		
OCT20,1993	12:28:20	12	28	20	12.5	583	585	585	582	575	DEG F
OCT20,1993	12:43:20	12	43	20	12.7	586	588	588	586	581	DEG F
OCT20,1993	12:58:20	12	58	20	13.0	592	594	594	591	586	DEG F
OCT20,1993	13:13:20	13	13	20	13.2	574	582	579	581	575	DEG F
OCT20,1993	13:28:20	13	28	20	13.5	572	566	559	561	560	DEG F
OCT20,1993	13:43:20	13	43	20	13.7	584	550	539	543	546	DEG F
OCT20,1993	13:58:20	13	58	20	14.0	586	533	519	526	532	DEG F
OCT20,1993	14:13:20	14	13	20	14.2	579	518	501	506	524	DEG F
OCT20,1993	14:28:20	14	28	20	14.5	589	502	482	487	505	DEG F
OCT20,1993	14:43:20	14	43	20	14.7	570	486	462	466	485	DEG F
OCT20,1993	14:58:20	14	58	20	15.0	591	469	444	449	474	DEG F
OCT20,1993	15:13:20	15	13	20	15.2	567	454	424	432	456	DEG F
OCT20,1993	15:28:20	15	28	20	15.5	585	437	406	415	438	DEG F
OCT20,1993	15:43:20	15	43	20	15.7	569	423	390	399	429	DEG F
OCT20,1993	15:58:20	15	58	20	16.0	575	408	374	384	412	DEG F
OCT20,1993	16:13:20	16	13	20	16.2	572	393	358	370	396	DEG F
OCT20,1993	16:28:20	16	28	20	16.5	564	378	343	358	390	DEG F
OCT20,1993	16:43:20	16	43	20	16.7	575	364	330	345	372	DEG F
OCT20,1993	16:58:20	16	58	20	17.0	565	350	317	332	360	DEG F
OCT20,1993	17:13:20	17	13	20	17.2	573	339	304	322	355	DEG F
OCT20,1993	17:28:20	17	28	20	17.5	554	327	292	311	339	DEG F
OCT20,1993	17:43:20	17	43	20	17.7	575	315	282	301	334	DEG F
OCT20,1993	17:58:20	17	58	20	18.0	553	304	272	291	323	DEG F
OCT20,1993	18:13:20	18	13	20	18.2	572	294	261	282	310	DEG F
OCT20,1993	18:28:20	18	28	20	18.5	551	283	252	273	308	DEG F
OCT20,1993	18:43:20	18	43	20	18.7	571	273	243	265	296	DEG F
OCT20,1993	18:58:20	18	58	20	19.0	549	264	235	256	287	DEG F
OCT20,1993	19:13:20	19	13	20	19.2	570	255	227	248	284	DEG F
OCT20,1993	19:28:20	19	28	20	19.5	547	247	218	241	271	DEG F
OCT20,1993	19:43:20	19	43	20	19.7	569	239	212	234	269	DEG F
OCT20,1993	19:58:20	19	58	20	20.0	547	232	205	227	261	DEG F
OCT20,1993	20:13:20	20	13	20	20.2	568	224	198	221	250	DEG F
OCT20,1993	20:28:20	20	28	20	20.5	546	218	192	215	250	DEG F
OCT20,1993	20:43:20	20	43	20	20.7	567	211	186	209	242	DEG F
OCT20,1993	20:58:20	20	58	20	21.0	545	205	181	204	234	DEG F
OCT20,1993	21:13:20	21	13	20	21.2	565	199	176	199	234	DEG F
OCT20,1993	21:28:20	21	28	20	21.5	542	194	171	194	224	DEG F
OCT20,1993	21:43:20	21	43	20	21.7	563	188	166	189	223	DEG F
OCT20,1993	21:58:20	21	58	20	22.0	547	183	162	185	217	DEG F
OCT20,1993	22:13:20	22	13	20	22.2	562	179	157	181	208	DEG F
OCT20,1993	22:28:20	22	28	20	22.5	544	174	153	177	211	DEG F
OCT20,1993	22:43:20	22	43	20	22.7	567	170	149	172	203	DEG F
OCT20,1993	22:58:20	22	58	20	23.0	541	165	144	168	198	DEG F
OCT20,1993	23:13:20	23	13	20	23.2	564	162	142	166	199	DEG F
OCT20,1993	23:28:20	23	28	20	23.5	538	159	139	162	190	DEG F
OCT20,1993	23:43:20	23	43	20	23.7	563	155	135	159	192	DEG F
OCT20,1993	23:58:20	23	58	20	24.0	539	151	132	156	187	DEG F

Data for Slow Heat Up of Components with Two Heat Trace Circuits.

Heatup With Two Circuits			
	CheckV	4"Flange	6"flange
Time,hr	TEPL-4	TEPL-8	TEPL-10
0.	104.8205	104.8205	104.8205
0.4135	137.351	169.8815	148.1945
0.827	202.412	281.931	238.557
1.2405	245.786	354.221	289.16
1.654	285.5455	401.2095	354.221
2.0675	325.305	433.74	397.595
2.481	383.137	484.343	444.5835
2.8945	379.5225	469.885	448.198
3.308	404.824	502.4155	495.1865
3.7215	415.6675	502.4155	495.1865
4.135	422.8965	506.03	502.4155
4.5485	433.74	516.8735	516.8735
4.962	448.198	527.717	527.717
5.3755	459.0415	538.5605	538.5605
5.789	451.8125	520.488	520.488

Unlimited Distribution

Attn: Tom Tracey
6922 S. Adams Way
Littleton, CO 80122

Advanced Thermal Systems
Attn: Dave Gorman
7600 East Arapahoe Road, Suite 215
Englewood, CO 80112

Advanced Thermal Systems
Attn: Robert Thomas
7600 East Arapahoe Road, Suite 215
Englewood, CO 80112

Arizona Public Service Co.
Attn: Scott McLellan
P.O. Box 53999
MS 1424
Phoenix, AZ 85072-3999

Arizona State University
Attn: Paul Russell
College of Engineering
Tempe, AZ 85287

Battelle Pacific Northwest Laboratory
Attn: K. Drumheller
P.O. Box 999
Richland, WA 99352

Bechtel Group, Inc.
Attn: Madanjit Singh
50 Beale Street
45/4/C27
P.O. Box 193965
San Francisco, CA 94119-3965

Bechtel National, Inc.
Attn: Pat DeLaquil
50 Beale Street
50/15 D8
P.O. Box 193965
San Francisco, CA 94119-3965

Bechtel National, Inc.
Attn: William Gould
50 Beale Street
45/4/C27
P.O. Box 193965
San Francisco, CA 94119-3965

Bechtel National, Inc.
Attn: Bruce Kelly
50 Beale Street
45/4/C27
P.O. Box 193965
San Francisco, CA 94119-3965

Bechtel National, Inc.
Attn: Lorne Marjerison
50 Beale Street
45/4/C27
P.O. Box 193965
San Francisco, CA 94119-3965

Bechtel National, Inc.
Attn: S. Nickovich
50 Beale Street
50/15 D8
P.O. Box 193965
San Francisco, CA 94119-3965

Bechtel National, Inc.
Attn: Brock Parsens
50 Beale Street
45/4/C27
P.O. Box 193965
San Francisco, CA 94119-3965

Bechtel National, Inc.
Attn: Alex Zavoico
50 Beale Street
45/4/C27
P.O. Box 193965
San Francisco, CA 94119-3965

Bureau of Reclamation
Attn: Stanley Hightower
Code D-3710
P.O. Box 205007
Denver, CO 80225

California Energy Commission
Attn: Alec Jenkins
Energy Technology Development Div. R&D
Office
1516 9th Street
MS-43
Sacramento, CA 95814-5512

California Polytechnic State University
Attn: William B. Stine
Department of Mechanical Engineering
3801 West Temple Avenue
Pomona, CA 91768-4062

Carrizo Solar Corporation
Attn: Mike Elliston
P.O. Box 10239
1011-C Sawmill Road NW
Albuquerque, NM 87184-0239

Carrizo Solar Corporation
Attn: John Kusianovich
P.O. Box 10239
1011-C Sawmill Road NW
Albuquerque, NM 87184-0239

Central and Southwest Services
Attn: E.L. Gastineau
1616 Woodall Rogers Freeway
MS 7RES
Dallas, TX 75202

Centro Investigaciones Energeticas
Attn: M. Macias
Medioambientales y Technologicas
Instituto de Energias Renovables
Avda. Complutense, 22
28040 Madrid, SPAIN

Centro Investigaciones Energeticas
Attn: M. Romero
Medioambientales y Technologicas
Instituto de Energias Renovables
Avda. Complutense, 22
28040 Madrid, SPAIN

Conservation and Renewable Energy System
Attn: Ben Wolff
6918 N.E. Fourth Plain Blvd., Suite B
Vancouver, WA 98661

DEO Enterprises
Attn: Dave Ochenreider
P.O. Box 2110
Helendale, CA 92342

DLR
Attn: Reiner Buck
Pfaffenwaldring 38-40
7000 Stuttgart 80, GERMANY

Dynatherm Corporation
Attn: D. Wolf
1 Beaver Court
P.O. Box 398
Cockeysville, MD 21030

Electric Power Research Institute
Attn: Doug Morris
P.O. Box 10412
3412 Hillview Avenue
Palo Alto, CA 94303

Electric Power Research Institute
Attn: J. Schaeffer
P.O. Box 10412
3412 Hillview Avenue
Palo Alto, CA 94303

Flachglas Solartechnik GmbH
Attn: M. Geyer
Theodor-Heuss-Ring 1
5000 Koln 1, GERMANY

Florida Solar Energy Center
Attn: Library
300 State Road, Suite 401
Cape Canaveral, FL 32920-4099

Fricker Consulting
Attn: Hans Fricker
Breitest. 22
CH 8544 Rickenbach, SWITZERLAND

Attn: R. Hollis
41100 Highway 395
Boron, CA 93516

Georgia Power Co.
Attn: W. Rosskist
7 Solar Circle
Shenandoah, GA 30265

Lawrence Berkeley Laboratory
Attn: Arlon Hunt
University of California
MS 90-2024
One Cyclotron Road
Berkeley, CA 94720

Idaho Power
Attn: John Carstensen
P.O. Box 70
Boise, ID 83707

Los Alamos National Laboratory
Attn: M. Merrigan
P.O. Box 1663
MS-E13
Los Alamos, NM 87545

Idaho Power
Attn: Jerry Young
P.O. Box 70
Boise, ID 83707

Los Angeles Dept. of Water and Power
Attn: David Anderson
Alternate Energy Systems
111 North Hope Street, Rm. 661A
Los Angeles, CA 90012

Institute of Gas Technology
Attn: Library
34245 State Street
Chicago, IL 60616

Los Angeles Dept. of Water and Power
Attn: Daryl Yonamine
Alternate Energy Systems
111 North Hope Street, Rm. 661A
Los Angeles, CA 90012

Dick Holl
1938A Avenida Del Oro
Oceanside, CA 92056

McDonnell-Douglas Astronautics Co.
Attn: Bob Drubka
5301 Bolsa Avenue
Huntington Beach, CA 92647-2048

Jet Propulsion Laboratory
Attn: M. Alper
4800 Oak Grove Drive
Pasadena, CA 91109

McDonnell-Douglas Astronautics Co.
Attn: J. Rogan
5301 Bolsa Avenue
Huntington Beach, CA 92647

Kearney & Associates
Attn: David W. Kearney
14022 Condessa Drive
Del Mar, CA 92014

McDonnell-Douglas Astronautics Co.
Attn: D. Steinmeyer (3)
5301 Bolsa Avenue
Huntington Beach, CA 92647

KJC Operating Company
Attn: Gilbert Cohen
41100 Highway 395
Boron, CA 93516

KJC Operating Company

National Renewable Energy Laboratory
Attn: Mark Bohn
1617 Cole Blvd.
Golden, CO 80401-3393

Nevada Power Co.
Attn: Mark Shank
P.O. Box 230
Las Vegas, NV 89151

National Renewable Energy Laboratory
Attn: Gary Jorgensen
1617 Cole Blvd.
Golden, CO 80401-3393

Northern Research & Engineering Corp.
Attn: James B. Kesseli
39 Olympia Avenue
Woburn, MA 01801-2073

National Renewable Energy Laboratory
Attn: A. Lewandowski
1617 Cole Blvd.
Golden, CO 80401-3393

Pacific Gas and Electric Co.
Attn: Chris Haslund (2)
3400 Crow Canyon Road
San Ramon, CA 94583

National Renewable Energy Laboratory
Attn: L.M. Murphy
1617 Cole Blvd.
Golden, CO 80401-3393

Pacific Power
Attn: Stephen Schuck
Park and Elizabeth Streets
GPO Box 5257
Sydney
New South Wales, 2001 AUSTRALIA

National Renewable Energy Laboratory
Attn: Hank Price
1617 Cole Blvd.
Golden, CO 80401-3393

PacifiCorp
Attn: Ian Andrews
Utah Power
1407 West North Temple
Salt Lake City, UT 84140-0001

National Renewable Energy Laboratory
Attn: Tim Wendelin
1617 Cole Blvd.
Golden, CO 80401-3393

Power Kinetics, Inc.
Attn: W.E. Rogers
415 River Street
Troy, NY 12180-2822

National Renewable Energy Laboratory
Attn: Tom Williams
1617 Cole Blvd.
Golden, CO 80401-3393

Renewable Energy Training Institute
Attn: Kevin Porter
122 C St. NW, Suite 520
Washington, DC 20001

Nevada Power Co.
Attn: Doug Bailey
P.O. Box 230
Las Vegas, NV 89151

Research International
Attn: E. Saaski
18706 142nd Avenue, NE
Woodinville, WA 98072

Nevada Power Co.
Attn: Eric Dominguez
P.O. Box 230
Las Vegas, NV 89151

Rockwell International Corp.
Attn: William Bigelow
Energy Technology Engineering Center
P.O. Box 1449
Canoga Park, CA 91304

Rockwell International Corp.
Attn: Tom M. Griffin
P.O. Box 582808
Tulsa, OK 74158

Rockwell International Corp.
Attn: R. LeChevalier
Energy Technology Engineering Center
P.O. Box 1449
Canoga Park, CA 91304

Rockwell International Corp.
Attn: Bob Litwin
Rocketdyne Division
P.O. Box 7922
6633 Canoga Avenue
MS SA70
Canoga Park, CA 91309-7922

Rockwell International Corp.
Attn: Mark Marko
Rocketdyne Division
P.O. Box 7922
6633 Canoga Avenue
MS SA70
Canoga Park, CA 91309-7922

Rockwell International Corp.
Attn: W. Marlatt
Rocketdyne Division
P.O. Box 7922
6633 Canoga Avenue
Canoga Park, CA 91309-7922

Rockwell International Corp.
Attn: Bob Musica
Energy Technology Engineering Center
P.O. Box 1449
Canoga Park, CA 91304

Rockwell International Corp.
Attn: Ron Pauckert
Rocketdyne Division
P.O. Box 7922
6633 Canoga Avenue
MS SA70
Canoga Park, CA 91309-7922

Sacramento Municipal Utility District
Attn: Bud Beebe
Generation Systems Planning
Power Systems Dept.
6201 'S' St.
P.O. Box 15830
Sacramento, CA 95852-1830

Sacramento Municipal Utility District
Attn: Don Osborne
Generation Systems Planning
Power Systems Dept.
6201 'S' St.
P.O. Box 15830
Sacramento, CA 95852-1830

Sacramento Municipal Utility District
Attn: R. Wichert
Generation Systems Planning
Power Systems Dept.
6201 'S' St.
P.O. Box 15830
Sacramento, CA 95852-1830

Salt River Project
Attn: Bob Hess
Research and Development
P.O. Box 52025
Phoenix, AZ 85072-2025

Salt River Project
Attn: Ernie Palomino
Research and Development
P.O. Box 52025
Phoenix, AZ 85072-2025

Schlaich, Bergermann & Partner
Attn: W. Schiel
Hohenzollernstr. 1
D-7000 Stuttgart 1, GERMANY

Science Applications International Corp.
Attn: Kelly Beninga
15000 W. 6th Avenue
Suite 202
Golden, CO 80401

Solar Energy Industries Association
Attn: Scott Sklar
122 C Street., NW
4th Floor
Washington, DC 20001-2109

Science Applications International Corp.
Attn: Bill Bruninga
15000 W. 6th Avenue
Suite 202
Golden, CO 80401

Solar Kinetics, Inc.
Attn: Gus Hutchinson
10635 King William Drive
P.O. Box 540636
Dallas, TX 75354-0636

Science Applications International Corp.
Attn: Barry L. Butler
Room 2043, M/S C2J
10260 Campus Point Dr.
San Diego, CA 92121

Solar Kinetics, Inc.
Attn: D. White
10635 King William Drive
P.O. Box 540636
Dallas, TX 75354-0636

Science Applications International Corp.
Attn: Roger L. Davenport
15000 W. 6th Avenue
Suite 202
Division 448
Golden, CO 80401

South Coast AQMD
Attn: Ranji George
21865 Copley Drive
Diamond Bar, CA 91765

Science Applications International Corp.
Attn: Neil Otto
10260 Campus Point Dr.
Mail Stop 32
San Diego, CA 92121

Southern California Edison Co.
Attn: Amy Brown
P.O. Box 800
2244 Walnut Grove Avenue
Rosemead, CA 91770

Solar Energy Industries Association
Attn: Linda Ladas
122 C Street, NW
4th Floor
Washington, DC 20001-2109

Southern California Edison Co.
Attn: Donald Brundage
P.O. Box 800
2131 Walnut Grove Avenue
Rosemead, CA 91770

Solar Energy Industries Association
Attn: Ken Sheinkopf
122 C Street, NW
4th Floor
Washington, DC 20001-2109

Southern California Edison Co.
Attn: Irving Katter
P.O. Box 800
2244 Walnut Grove Avenue
Rosemead, CA 91770

Southern California Edison Co.
Attn: Chuck Lopez
P.O. Box 800
Rosemead, CA 91770

Southern California Edison Co.
Attn: Hugh Reilly
P.O. Box 800, G01
2244 Walnut Grove Avenue
Rosemead, CA 91770

U.S. Department of Energy
Attn: R. (Bud) Annan (2)
Code EE-13
Forrestal Building
1000 Independence Ave. SW
Washington, DC 20585

Southern California Edison Co.
Attn: Mark Skowronski
P.O. Box 800
2244 Walnut Grove Avenue
Rosemead, CA 91770

U.S. Department of Energy
Attn: Gary Burch (5)
Code EE-132
Forrestal Building
1000 Independence Avenue, SW
Washington, DC 20585

Southern California Edison Co.
Attn: Paul Sutherland
P.O. Box 800
2131 Walnut Grove Avenue
Rosemead, CA 91770

U.S. Department of Energy
Attn: R. Hughey
San Francisco Operations Office
1333 Broadway
Oakland, CA 94612

Southern California Edison Co.
Attn: Roy Takekawa
37000 Santa Fe Road
Daggett, CA 92327

U.S. Department of Energy
Attn: Bob Martin
Golden Field Office
1617 Cole Boulevard
Golden, CO 80401

Sunpower, Inc.
Attn: W. Beale
6 Byard Street
Athens, OH 45701

U.S. Department of Energy
Attn: John Meeker
Golden Field Office
1617 Cole Boulevard
Golden, CO 80401

Technology Properties Limited
Attn: Janet Neal
4010 Moorpark Avenue, Suite 215
San Jose, CA 95117

U.S. Department of Energy
Attn: D.A. Sanchez (2)
Albuquerque Operations Office
P.O. Box 5400
Albuquerque, NM 87115

The Solar Letter
Attn: Allan L. Frank
9124 Bradford Road
Silver Spring, MD 20901-4918

Union of Concerned Scientists
Attn: Donald Aitken
20100 Skyline Boulevard
Woodside, CA 94062

U.S. Department of Energy
Attn: Dan Alpert
2140 L Street, #709
Washington, DC 20037-1530

University of Houston
Attn: James Richardson (2)
Solar Energy Laboratory
4800 Calhoun Road
Houston, TX 77704

University of Houston
Attn: Lorin Vant-Hull (2)
Energy Laboratory 5505
4800 Calhoun Road
Houston, TX 77704

University of Minnesota
Attn: E.A. Fletcher
1111 Church Street, SE
Dept. of Mech. Engr.
Minneapolis, MN 55455

Zomeworks
Attn: Steve Baer
1011A Sawmill Road, NW
Albuquerque, NM 87104

Internal Distribution:

MS 0100 Document Proc. for DOE/OSTI, 7613-2 (2)
MS 0619 G.C. Claycomb, 13416
MS 0619 Technical Publications, 12613
MS 0702 D.E. Arvizu, 6200
MS 0703 R.B. Diver, 6216
MS 0703 L.R. Evans, 6216
MS 0703 S.A. Jones, 6216
MS 0703 G.J. Kolb, 6216
MS 0703 F. Lippke, 6216
MS 0703 T.R. Mancini, 6216
MS 0703 J.E. Pacheco, 6216
MS 0703 M.R. Prairie, 6216
MS 0703 C.E. Tyner, 6216
MS 0704 P.C. Klimas, 6201
MS 0724 D.L. Hartley, 6000
MS 0753 C.P. Cameron, 6218
MS 0753 M.E. Ralph, 6218
MS 0835 R.E. Hogan, Jr., 1513
MS 0835 V.J. Romero, 1513
MS 0835 R.D. Skocypec, 1513
MS 0899 Technical Library, 13414 (5)
MS 0980 G.S. Phipps, 9225
MS 1127 J.M. Chavez, 6215
MS 1127 S.R. Dunkin, 6215
MS 1127 R.M. Edgar, 6215
MS 1127 C.M. Ghanbari, 6215
MS 1127 J.W. Grossman, 6215
MS 1127 R.M. Houser, 6215
MS 1127 D.W. Johnson, 6215
MS 1127 J.J. Kelton, 6215
MS 1127 W.J. Kolb, 6215
MS 1127 Library, 6215 (5)
MS 1127 A.R. Mahoney, 6215
MS 1127 K.S. Rawlinson, 6215
MS 1127 E.E. Rush, 6215
MS 1127 R.K. Tucker, 6215
MS 9018 Central Technical Files, 8523-2